WILD HERITAGE

January 18, 2023

Objection Reviewing Officer
USDA Forest Service, Southwest Region
333 Broadway SE, Albuquerque, NM 87102
Submitted via email to: objections-southwestern-regional-office@usda.gov

Re: Objection to Santa Fe Mountains Landscape Resiliency Project Draft Decision and Finding of No Significant Impact

To the Objection Reviewing Officer,

On behalf of Wild Heritage, a Project of the Earth Island Institute, we file this objection to the U.S. Forest Service's December 2022 draft decision notice ("Draft DN") finding of no significant impact ("FONSI") and Final Environmental Assessment ("Final EA") for the Santa Fe Mountains Landscape Resiliency Project (SFMLRP) on the Espanola and the Pecos-Las Vegas Ranger Districts of the Santa Fe National Forest. Our objection is related to the Forest Service's selected Alternative 2, the Proposed Action, that includes expansive and damaging mechanical and manual "thinning" treatments that lack proper analysis. The project area covers 50,566 acres, 38,680 acres of which are designated for such treatments over 10 years, including 18,000 acres of thinning, 38,000 acres of prescribed burning (every 5-10 years) and 680 acres of riparian restoration. The responsible official is Acting Santa Fe National Forest Supervisor, James Duran. This objection covers issues raised previously in our July 2019 scoping comments that were either ignored or inappropriately dismissed.

As required by 36 C.F.R. § 218.8(d) the Lead Objector is: Dr. Dominick A. DellaSala (dominick@wild-heritage.org; 541-621-7223), Chief Scientist, Wild Heritage; a Project of the Earth Island Institute, 2150 Allston Way, Suite 460, Berkeley, CA, 94704. In addition, the 2012 Forest Planning Rule requires that the Forest Service use the best available science in decision making. However, the agency continues to routinely dismiss science that disagrees with their desired project outcomes and by selectively citing research that supports project actions. Determining what is "best" science needs to be based on a range of alternatives, an expansive view of the literature including studies that demonstrate treatment limitations, and a transparent and rationale decision making process, which the agency in this case has not demonstrated. We identify 3 major SFMLRP omissions and 6 suggested resolutions to remedy the deficiencies noted in our objection.

Wild Heritage
A Project of Earth Island Institute
PO Box 9451 Berkeley, CA 94709 ▪ (510) 862-5359 ▪ www.wild-heritage.org

1. FAILURE TO SUFFICIENTLY ANALYZE LIMITATIONS OF VEGETATION TREATMENTS IN RELATION TO CLIMATE CHANGE

In our scoping comments on the SFMLRP and related comments on the Draft EIS for the Santa Fe Land Management Plan and Draft Environmental Impact Assessment (DEIS), we commented on the inadequacies of the agency's climate change analysis and remedial climate measures, particularly whether vegetation treatments involving thinning and prescribed fire would even work in a rapidly changing climate where large fires are driven mainly by top-down global climate influences (high temperatures, droughts, winds).

For instance, we state in our 2019 scoping comments: "The effectiveness of proposed treatments is highly uncertain because of the likelihood that the region's fire regimes will increasingly shift to large and more intense burns due primarily to climate change (Abatzoglou and Williams 2017) and the extremely low odds that thinned sites will encounter a fire when fuels are lowest (Schoennagel et al. 2017)."

Additionally, new information is now available demonstrating the ineffectiveness of prescribed fire in regions experiencing top-down climate drivers of fire behavior governing reburns (Solander et al. 2023). Like the other researchers cited above, Solander et al. (2023) noted that prescribed fire is ineffective under extreme fire weather (drought, high temperatures, wind) and that treatments should prioritize the WUI to protect homes.

As it turned out, the failure of the Forest Service to sufficiently plan for and address limitations of its prescribed fire program in a changing climate proved costly to local communities in the Hermit's Peak Fire and the Chief's admission of under-estimating global climate influences.

On April 2022, the Forest Service released its Gallinas-Las Dispensas Prescribed Fire Declared Wildfire Review Santa Fe National Forest, Southwestern Region. Specifically, the Chief's Review of the Hermit's Peak Fire illustrates the agency's abject neglect for climate change effects on wildfire behavior and the inability of prescribed fire to reduce fire-line intensity under extreme fire-weather, which has been increasing due to climate change effects in this region.

"Climate change is leading to conditions on the ground we have never encountered. We know these conditions are leading to more frequent and intense wildfires. Drought, extreme weather, wind conditions and unpredictable weather changes are challenging our ability to use prescribed fire as a tool to combat destructive fires. This spring in New Mexico, a pile burn of hazardous logs that started in January, smoldered underground for months, persisting through multiple snowstorms and freezing temperatures, before resurfacing as a wildfire. That type of event was nearly unheard of until recently in the century-plus of experience the Forest Service has in working on these landscapes. Fires are outpacing our models and, as the final report notes, we need to better understand how megadrought and climate change are affecting our actions on the ground. We must learn from this event and

Wild Heritage
A Project of Earth Island Institute
PO Box 9451 Berkeley, CA 94709 ▪ (510) 862-5359 ▪ www.wild-heritage.org

ensure our decision-making processes, tools, and procedures reflect these changed conditions."

The report further states (p. 3) – "*….a post-prescribed fire analysis of fuel and weather revealed that the implementation was occurring under much drier conditions than were recognized. Persistent drought, limited overwinter precipitation, less than average snowpack, fine fuel accumulation—post mechanical treatment, and increased heavy fuel loading after fireline preparation all contributed to increasing the risk of fire escape."*

And

"*Competing obligations limit the ability of the workforce to prioritize and focus on prescribed fire projects. Increasing agency goals for prescribed fire treatments and, in this case, expectations from the forest, district and the Burn Boss to begin catching-up after 2 years of delays due to government shutdowns, a global pandemic, and Mexican Spotted Owl regulations have led to unrealistic expectations. These expectations, coupled with the opportunity to implement during a narrow window when the crew was available, smoke dispersion was good and the prescribed fire area was forecasted to be in prescription, led to acceptance of unforeseen risk."*

And

"*Traditional monsoon precipitation was significantly below the historic average in 2019 and 2020 during the planning and preparation phase of the Gallinas Watershed Project leading up to the Las Dispensas Prescribed Fire. In the summer of 2021, a monsoon did bring some short-term benefits. However, overall precipitation for the season was near to below average for the northern New Mexico mountains. Nevertheless, there was an increase in late season fine fuels growth that cured in the fall and early winter coincident with seasonal dormancy. Overall, these fine fuels remained upright and available to burn because the few light snow events that occurred failed to compact them. According to the Drought Mitigation Center's Drought Monitor product, which represents long-term impacts, both the magnitude and spatial extent of drought improved beginning in July and August 2021 due to the monsoon precipitation. They slightly improved from the highest drought category "Exceptional, D4" to "Extreme, D3". This trend continued through fall, winter and spring during the time leading up to the prescribed fire. Despite the limited improvement to the drought conditions, anomalous dryness continued in the fall and then transitioned to a second consecutive winter (Double Dip) La Niña cycle that strengthened in the spring."*

Thus, the lack of planning for climate change in prescribed burns demonstrates that the agency ignored public comment calling into question its treatments because of climate associated risks. Those risks were incredibly costly and the agency continues to plan poorly for climate-related increases in wildfire spread rates and acres burning. Because climate is now the top down driver of large fires, the agency has unrealistic expectations about treatment efficacy.

2. FAILURE TO APPROPRIATELY ANALYZE THE IMPACT OF CARBON EMISSIONS FROM EXTENSIVE VEGETATION TREATMENTS

In our July 9, 2019 scoping comments, we note:

"*A stated intent of the SFLMRP is to provide for resilience to climate change yet there is no analysis of project-related emissions from tree clearing and road improvements. Notably, emissions from wildfires are typically much lower than landscape-level logging projects aimed at reducing wildfires (e.g., see Mitchell et al. 2009, Campbell et al. 2016, Law et al. 2018 as examples of appropriate methodologies). Actions that minimize emissions should be compared in CO_2 equivalents, including the social cost of carbon[1]. Project alternatives should then be selected with the lowest emissions."*

Since the submission of our comments and the completion of the SFLMRP Environmental Assessment, CEQ issued Interim Guidance effective immediately related to "National Environmental Policy Act Guidance on Consideration of Greenhouse Gas Emissions and Climate Change" (CEQ-2022-0005).

The guidance provides a standardized approach for estimating project-related emissions and represents new information that was not analyzed in the SFLMRP. Specifically, CEQ interim guidance notes:

"*Recommending that agencies provide additional context for GHG emissions, including through the use of the best available social cost of GHG (SC-GHG) estimates, to translate climate impacts into the more accessible metric of dollars, allow decision makers and the public to make comparisons, help evaluate the significance of an action's climate change effects, and better understand the tradeoffs associated with an action and its alternatives;*
 Discussing methods to appropriately analyze reasonably foreseeable direct, indirect, and cumulative GHG emissions;"

CEQ guidance is directly relevant to our comments that were dismissed by the SFLMRP in claiming that their project emissions were negligible based a flawed estimate that lacks standardization and social cost of carbon from which a range of alternatives could have been provided along with a preferred option that chooses an option with the least emissions and lowest social cost of carbon. Therefore, the SFLMRP did not use the best available science to estimate nor reduce project-related emissions in the interim CEQ guidelines now available.

"*Advising agencies to use the best available information and science when*

[1]See https://19january2017snapshot.epa.gov/climatechange/social-cost-carbon .html

assessing the potential future state of the affected environment in NEPA analyses and providing up to date examples of existing sources of scientific information (CEQ).

And

"*Outlining unique considerations for agencies analyzing biogenic carbon dioxide sources and carbon stocks associated with land and resource management actions under NEPA.*

No life cycle analysis of carbon stocks or effects of fuel treatments on them was provided by the SFLMRP as noted below.

3. FAILURE TO ANALYZE CARBON STOCKS AND IMPORTANCE OF PROTECTING MATURE/OLD GROWTH FORESTS FROM FUEL TREATMENTS

In our scoping comments, we identified major deficiencies in the SFLMRP analysis of mature and old-growth forests in the project area. The lack of an ecological definition of mature in the SFLMRP makes those forests vulnerable to inappropriate treatments. Most notably, the SFLMRP did not consider the president's Executive Order 14072 that came out on Earth Day (April 22 2021) directing federal agencies to define and inventory *mature* (emphasis added) and old-growth forests for conservation purposes.

Because no such definition or analysis was provided in the SFLMRP, the project is inconsistent with the conservation purposes for mature forests as directed by EO 14072.

Importantly, new information is now available from which mature forests can be readily defined and mapped based on spatially derived forest proxies (DellaSala et al. 2022) and the minimum age and size of larger trees and their importance in carbon sequestration and storage (Birdsey et al. 2023).

Figure 1 shows the distribution of mature and old-growth forests in SFLMRP and vicinity. Notably, the SFLMRP lacks such an analysis needed to properly inform the public about cumulative impacts in both **mature** and old growth and not just old growth and to comply with President Biden's EO 14072 that calls on federal agencies to conserve these forests. The EO needs to be factored into project decisions but it was not for the SFLMRP that was issued before the order and therefore needs to be updated.

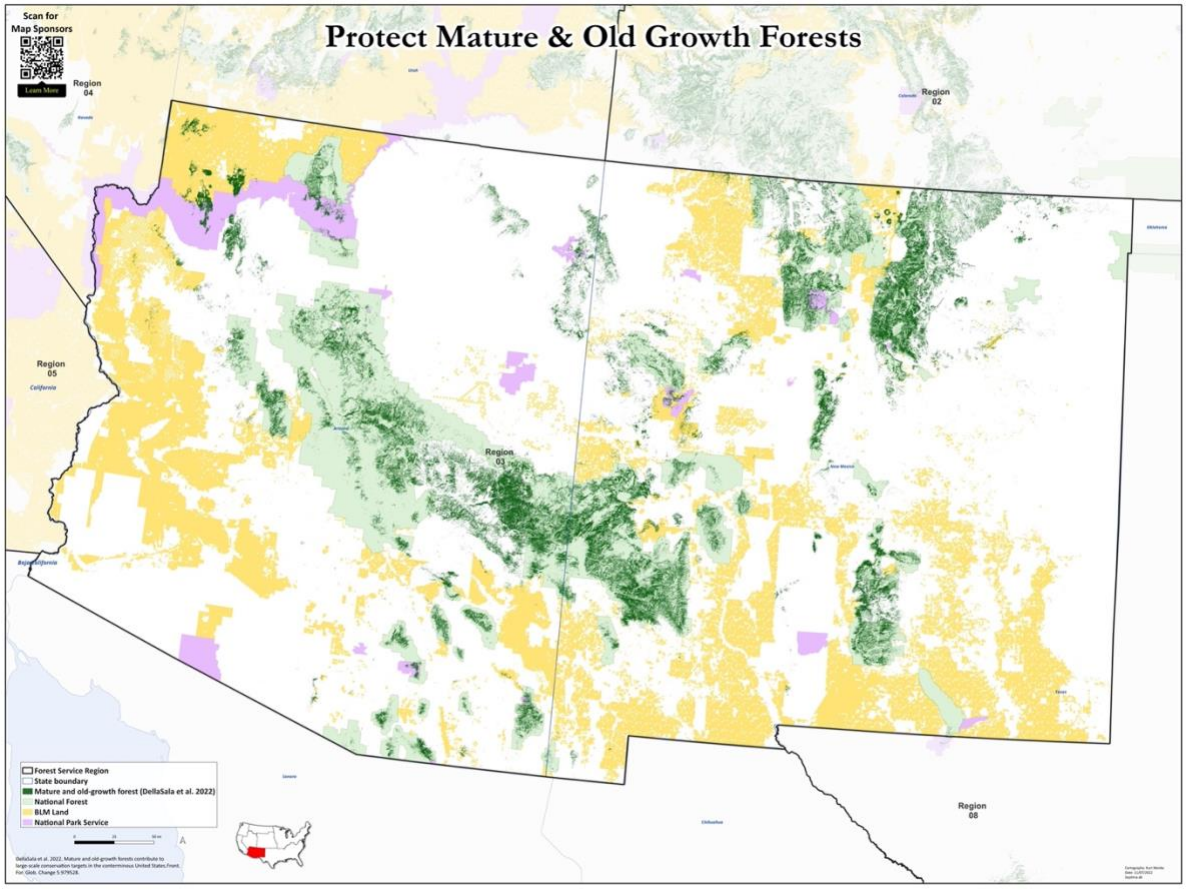

Figure 1. Spatially explicit location of mature and old-growth forests (dark green) in the project vicinity based on three proxies that define structural maturity (DellaSala et al. 2022). Note the clustering in the project area (center).

Birdsey et al. (2023) used FIA plot data for 11 national forests in the lower 48 states including those dominated by frequent-fire return intervals associated with dry pine and dry mixed conifer forest sites. A total of 849 FIA plots were sampled in the four Arizona National Forests, for instance (Coconino, Prescott, Tonto, Sitgreaves). Based on culmination of net primary productivity, dry forests on the Arizona sites were considered mature at 75 years or when trees had a 12-inch dbh. The 12-in dbh maturity threshold is <16-in dbh cap typically used in fuel treatments on the Santa Fe National Forest, meaning the agency is killing mature trees in definance of the president's executive order. The killing of large trees on the SFLMRP is also inconsistent with CEQ guidance mentioned above given the Forest Service did not use best science to examine and then choose an alternative with the least emissions, particularly since large trees are being "thinned" at the 12-16 in dbh level and those large trees store the bulk of above ground living biomass and associated carbon (Birdsey et al. 2023).

In addition, as the forests on the SFLMRP mature over time, the canopy naturally will close some and a complex understory will develop along with the emergence of coarse-woody debris and dead standing trees (snags). That process of when maturity occurs based on site conditions,

climatic factors, and natural disturbances is missing from the SFLMRP despite our request to protect mature forests and thus it is impossible for the public to assess impacts to mature forests that will occur in the project area despite the presidential directive.

SUGGESTED RESOLUTION

In our objection, we have identified sufficient deficiencies remaining in the SFLMRP that reflect a lack of attention to best available science, were ignored based on our prior scoping comments, or were not analyzed because of new relevant information that has arisen science the project's EA was published.

We request that the SLMRP:

(1) Include studies by researchers that do not support large-scale thinning and prescribed fire.
(2) Conduct a spatially explicit and field-based inventory of mature forests to assess carbon stock value and comply with the presidential order 14072.
(3) As part of the inventory, ground verify the location of mature forests as, for instance, as identified in Figure 1 to pin-point location for conservation purposes and EO compliance.
(4) A mature forest inventory needs to incorporate the methodology of Birdsey et al. (2023) to assess carbon stock value of larger trees and base maturity approaches on trees sizes where carbon accumulation is maximized plus additional factors such as coarse woody debris, snags, closed canopy conditions etc. Mature forests need to be protected from mechanical treatments unless such treatments result in recruitment of large snags (by killing live trees) to be left on site or felled and tipped into streams for aquatic restoration.
(5) A detailed carbon life cycle analysis is needed to comply with the CEQ interim guidance on minimizing carbon emissions from project-specific actions. Life cycle analysis must follow best available science and be specific to the project actions and onsite emissions relative to alternatives, rather than flat out dismissing emissions as nationally or globally insignificant. Hudiburg et al. (2019) and Harmon (2019) provide exemplary methods in this regard.
(6) A careful and best available science analysis of project treatments and limitations in relation to climate change is urgently needed and best handled via a project-specific EIS.

Sincerely,

Dominick A. DellaSala, Ph. D
Chief Scientist

Wild Heritage
A Project of Earth Island Institute
PO Box 9451 Berkeley, CA 94709 ▪ (510) 862-5359 ▪ www.wild-heritage.org

Impact of anthropogenic climate change on wildfire across western US forests

John T. Abatzoglou[a,1] and A. Park Williams[b]

[a]Department of Geography, University of Idaho, Moscow, ID 83844; and [b]Lamont–Doherty Earth Observatory, Columbia University, Palisades, NY 10964

Edited by Monica G. Turner, University of Wisconsin–Madison, Madison, WI, and approved July 28, 2016 (received for review May 5, 2016)

Increased forest fire activity across the western continental United States (US) in recent decades has likely been enabled by a number of factors, including the legacy of fire suppression and human settlement, natural climate variability, and human-caused climate change. We use modeled climate projections to estimate the contribution of anthropogenic climate change to observed increases in eight fuel aridity metrics and forest fire area across the western United States. Anthropogenic increases in temperature and vapor pressure deficit significantly enhanced fuel aridity across western US forests over the past several decades and, during 2000–2015, contributed to 75% more forested area experiencing high (>1 σ) fire-season fuel aridity and an average of nine additional days per year of high fire potential. Anthropogenic climate change accounted for ∼55% of observed increases in fuel aridity from 1979 to 2015 across western US forests, highlighting both anthropogenic climate change and natural climate variability as important contributors to increased wildfire potential in recent decades. We estimate that human-caused climate change contributed to an additional 4.2 million ha of forest fire area during 1984–2015, nearly doubling the forest fire area expected in its absence. Natural climate variability will continue to alternate between modulating and compounding anthropogenic increases in fuel aridity, but anthropogenic climate change has emerged as a driver of increased forest fire activity and should continue to do so while fuels are not limiting.

wildfire | climate change | attribution | forests

Widespread increases in fire activity, including area burned (1, 2), number of large fires (3), and fire-season length (4, 5), have been documented across the western United States (US) and in other temperate and high-latitude ecosystems over the past half century (6, 7). Increased fire activity across western US forests has coincided with climatic conditions more conducive to wildfire (2–4, 8). The strong interannual correlation between forest fire activity and fire-season fuel aridity, as well as observed increases in vapor pressure deficit (VPD) (9), fire danger indices (10), and climatic water deficit (CWD) (11) over the past several decades, present a compelling argument that climate change has contributed to the recent increases in fire activity. Previous studies have implicated anthropogenic climate change (ACC) as a contributor to observed and projected increases in fire activity globally and in the western United States (12–19), yet no studies have quantified the degree to which ACC has contributed to observed increases in fire activity in western US forests.

Changes in fire activity due to climate, and ACC therein, are modulated by the co-occurrence of changes in land management and human activity that influence fuels, ignition, and suppression. The legacy of twentieth century fire suppression across western continental US forests contributed to increased fuel loads and fire potential in many locations (20, 21), potentially increasing the sensitivity of area burned to climate variability and change in recent decades (22). Climate influences wildfire potential primarily by modulating fuel abundance in fuel-limited environments, and by modulating fuel aridity in flammability-limited environments (1, 23, 24). We constrain our attention to climate processes that promote fuel aridity that encompass fire behavior characteristics of landscape ignitability, flammability, and fire spread via fuel desiccation in primarily flammability-limited western US forests by considering eight fuel aridity metrics that have well-established direct interannual relationships with burned area in this region (1, 8, 24, 25). Four metrics were calculated from monthly data for 1948–2015: (*i*) reference potential evapotranspiration (ETo), (*ii*) VPD, (*iii*) CWD, and (*iv*) Palmer drought severity index (PDSI). The other four metrics are daily fire danger indices calculated for 1979–2015: (*v*) fire weather index (FWI) from the Canadian forest fire danger rating system, (*vi*) energy release component (ERC) from the US national fire danger rating system, (*vii*) McArthur forest fire danger index (FFDI), and (*viii*) Keetch–Byram drought index (KBDI). These metrics are further described in the *Materials and Methods* and *Supporting Information*. Fuel aridity has been a dominant driver of regional and subregional interannual variability in forest fire area across the western US in recent decades (2, 8, 22, 25). This study capitalizes on these relationships and specifically seeks to determine the portions of the observed increase in fuel aridity and area burned across western US forests attributable to anthropogenic climate change.

The interannual variability of all eight fuel aridity metrics averaged over the forested lands of the western US correlated significantly ($R^2 = 0.57$–0.76, $P < 0.0001$; Table S1) with the logarithm of annual western US forest area burned for 1984–2015, derived from the Monitoring Trends in Burn Severity product for 1984–2014 and the Moderate Resolution Imaging Spectroradiometer (MODIS) for 2015 (*Supporting Information*). The record of standardized fuel aridity averaged across the eight metrics (hereafter, all-metric mean) accounts for 76% of the variance in the burned-area record, with significant increases in both records for 1984–2015 (Fig. 1). Correlation between fuel aridity and forest fire area remains highly significant ($R^2 = 0.72$, all-metric mean) after removing the linear-least squares trends for each time series for 1984–2015, supporting the mechanistic relationship between fuel aridity and

Significance

Increased forest fire activity across the western United States in recent decades has contributed to widespread forest mortality, carbon emissions, periods of degraded air quality, and substantial fire suppression expenditures. Although numerous factors aided the recent rise in fire activity, observed warming and drying have significantly increased fire-season fuel aridity, fostering a more favorable fire environment across forested systems. We demonstrate that human-caused climate change caused over half of the documented increases in fuel aridity since the 1970s and doubled the cumulative forest fire area since 1984. This analysis suggests that anthropogenic climate change will continue to chronically enhance the potential for western US forest fire activity while fuels are not limiting.

Author contributions: J.T.A. and A.P.W. designed research, performed research, contributed new reagents/analytic tools, analyzed data, and wrote the paper.

The authors declare no conflict of interest.

This article is a PNAS Direct Submission.

See Commentary on page 11649.

[1]To whom correspondence should be addressed. Email: jabatzoglou@uidaho.edu.

This article contains supporting information online at www.pnas.org/lookup/suppl/doi:10.1073/pnas.1607171113/-/DCSupplemental.

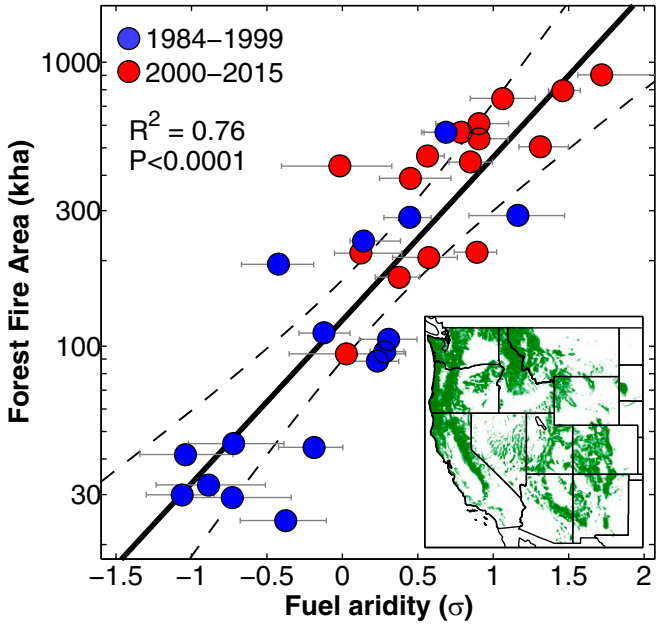

Fig. 1. Annual western continental US forest fire area versus fuel aridity: 1984–2015. Regression of burned area on the mean of eight fuel aridity metrics. Gray bars bound interquartile values among the metrics. Dashed lines bounding the regression line represent 95% confidence bounds, expanded to account for lag-1 temporal autocorrelation and to bound the confidence range for the lowest correlating aridity metric. The two 16-y periods are distinguished to highlight their 3.3-fold difference in total forest fire area. *Inset* shows the distribution of forested land across the western US in green.

forest fire area. It follows that co-occurring increases in fuel aridity and forest fire area over multiple decades would also be mechanistically related.

We quantify the influence of ACC using the Coupled Model Intercomparison Project, Phase 5 (CMIP5) multimodel mean changes in temperature and vapor pressure following Williams et al. (26) (Fig. S1; *Methods*). This approach defines the ACC signal for any given location as the multimodel mean (27 CMIP5 models) 50-y low-pass-filtered record of monthly temperature and vapor pressure anomalies relative to a 1901 baseline. Other anthropogenic effects on variables such as precipitation, wind, or solar radiation may have also contributed to changes in fuel aridity but anthropogenic contributions to these variables during our study period are less certain (22). We evaluate differences between fuel aridity metrics computed with the observational record and those computed with observations that exclude the ACC signal to determine the contribution of ACC to fuel aridity. To exclude the ACC signal, we subtract the ACC signal from daily and monthly temperature and vapor pressure, leaving all other variables unchanged and preserving the temporal variability of observations. The contribution of ACC to changes in fuel aridity is shown for the entire western United States; however, we constrain the focus of our attribution and analysis to forested environments of the western US (Fig. 1, *Inset*; *Methods*).

Anthropogenic increases in temperature and VPD contributed to a standardized (σ) increase in all-metric mean fuel aridity averaged for forested regions of +0.6 σ (range of +0.3 σ to +1.1 σ across all eight metrics) for 2000–2015 (Fig. 2). We found similar results with reanalysis products (all-metric mean fuel aridity increase of +0.6 σ for two reanalysis datasets considered; *Methods*), suggesting robustness of the results to structural uncertainty in observational products (Figs. S2–S4 and Table S2). The largest anthropogenic increases in standardized fuel aridity were present across the intermountain western United States, due in part to larger modeled warming rates relative to more maritime areas (27). Among aridity metrics, the largest increases tied to the ACC signal were for VPD and ETo because the interannual variability of these variables is primarily driven by temperature for much of the study area (28). By contrast, PDSI and ERC showed more subdued ACC driven increases in fuel aridity because these metrics are more heavily influenced by precipitation variability.

Fuel aridity averaged across western US forested areas showed a significant increase over the past three decades, with a linear trend of +1.2 σ (95% confidence: 0.42–2.0 σ) in the all-metric mean for 1979–2015 (Fig. 3*A*, *Top* and Table S1). The all-metric mean ACC contribution since 1901 was +0.10 σ by 1979 and +0.71 σ by 2015. The annual area of forested lands with high fuel aridity (>1 σ) increased significantly during 1948–2015, most notably since 1979 (Fig. 3*A*, *Bottom*). The observed mean annual areal extent of forested land with high aridity during 2000–2015 was 75% larger for the all-metric mean (+27% to +143% range across metrics) than was the case where the ACC signal was excluded.

Significant positive trends in fuel aridity for 1979–2015 across forested lands were observed for all metrics (Fig. 3*B* and Table S1). Positive trends in fuel aridity remain after excluding the ACC signal, but the remaining trend was only significant for ERC. Anthropogenic forcing accounted for 55% of the observed positive trend in the all-metric mean fuel aridity during 1979–2015, including at least two-thirds of the observed increase in ETo, VPD, and FWI, and less than a third of the observed increase in ERC and PDSI. No significant trends were observed for monthly fuel aridity metrics from 1948–1978.

The duration of the fire-weather season increased significantly across western US forests (+41%, 26 d for the all-metric mean) during 1979–2015, similar to prior results (10) (Fig. 4*A* and Table S2). Our analysis shows that ACC accounts for ~54% of the increase in fire-weather season length in the all-metric mean (15–79% for individual metrics). An increase of 17.0 d per year of high fire potential was observed for 1979–2015 in the all-metric mean (11.7–28.4 d increase for individual metrics), over twice the rate of increase calculated from metrics that excluded the ACC signal (Fig. 4*B* and Table S2). This translates to an average of an additional 9 d (7.8–12.0 d) per year of high fire potential during 2000–2015 due to ACC.

Given the strong relationship between fuel aridity and annual western US forest fire area, and the detectable impact of ACC on fuel aridity, we use the regression relationship in Fig. 1 to model

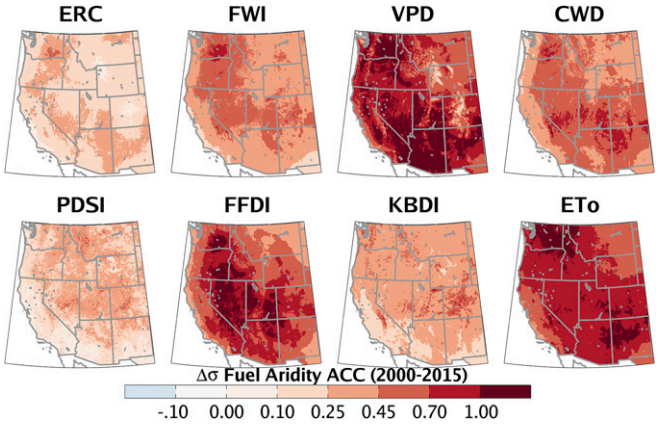

Fig. 2. Standardized change in each of the eight fuel aridity metrics due to ACC. The influence of ACC on fuel aridity during 2000–2015 is shown by the difference between standardized fuel aridity metrics calculated from observations and those calculated from observations excluding the ACC signal. The sign of PDSI is reversed for consistency with other aridity measures.

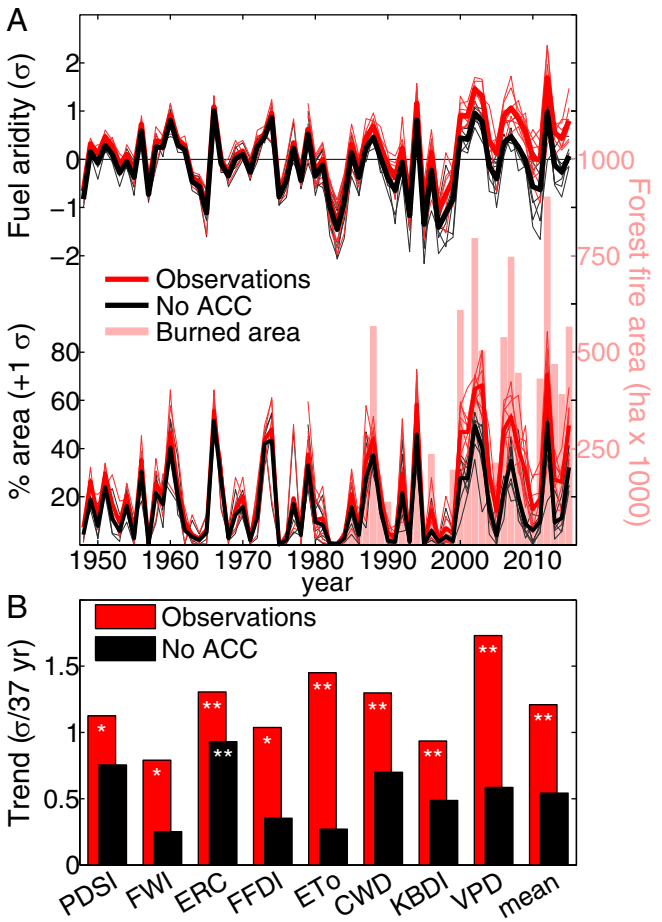

Fig. 3. Evolution and trends in western US forest fuel aridity metrics over the past several decades. (*A*) Time series of (*Upper*) standardized annual fuel aridity metrics and (*Lower*) percent of forest area with standardized fuel aridity exceeding one SD. Red lines show observations and black lines show records after exclusion of the ACC signal. Only the four monthly metrics extend back to 1948. Daily fire danger indices begin in 1979. Bold lines indicate averages across fuel aridity metrics. Bars in the background of *A* show annual forested area burned during 1984–2015 for visual comparison with fuel aridity. (*B*) Linear trends in the standardized fuel aridity metrics during 1979–2015 for (red) observations and (black) records excluding the ACC signal (differences attributed to ACC). Asterisks indicate positive trends at the (*) 95% and (**) 99% significance levels.

the contribution of ACC on western US forest fire area for the past three decades (Fig. 5 and Fig. S5). ACC-driven increases in fuel aridity are estimated to have added ∼4.2 million ha (95% confidence: 2.7–6.5 million ha) of western US forest fire area during 1984–2015, similar to the combined areas of Massachusetts and Connecticut, accounting for nearly half of the total modeled burned area derived from the all-metric mean fuel aridity. Repeating this calculation for individual fuel aridity metrics yields ACC contributions of 1.9–4.9 million ha, but most individual fuel aridity metrics had weaker correlations with burned area and thus may be less appropriate proxies for attributing burned area. The effect of the ACC forcing on fuel aridity increased during this period, contributing ∼5.0 (95% confidence: 4.2–5.9) times more burned area in 2000–2015 than in 1984–1999 (Fig. 5*B*). During 2000–2015, the ACC-forced burned area likely exceeded the burned area expected in the absence of ACC (Fig. 5*B*). A more conservative method that uses the relationship between detrended records of burned area and fuel aridity (2) still indicates a substantial impact of ACC on total burned area, with a 19% (95% confidence: 12–24%) reduction in the proportion of total burned area attributable to ACC (Fig. S5).

Our attribution explicitly assumes that anthropogenic increases in fuel aridity are additive to the wildfire extent that would have arisen from natural climate variability during 1984–2015. Because the influence of fuel aridity on burned area is exponential, the influence of a given ACC forcing is larger in an already arid fire season such as 2012 (Fig. 5*A* and Fig. S5*C*). Anthropogenic increases in fuel aridity are expected to continue to have their most prominent impacts when superimposed on naturally occurring extreme climate anomalies. Although numerous studies have projected changes in burned area over the twenty-first century due to ACC, we are unaware of other studies that have attempted to quantify the contribution of ACC to recent forested burned area over the western United States. The near doubling of forested burned area we attribute to ACC exceeds changes in burned area projected by some modeling efforts to occur by the mid-twenty-first century (29, 30), but is proportionally consistent with mid-twenty-first century increases in burned area projected by other modeling efforts (17, 31–33).

Beyond anthropogenic climatic changes, several additional factors have caused increases in fuel aridity and forest fire area since the 1970s. The lack of fuel aridity trends during 1948–1978 and persistence of positive trends during 1979–2015 even after removing the ACC signal implicates natural multidecadal climate variability as an important factor that buffered anthropogenic

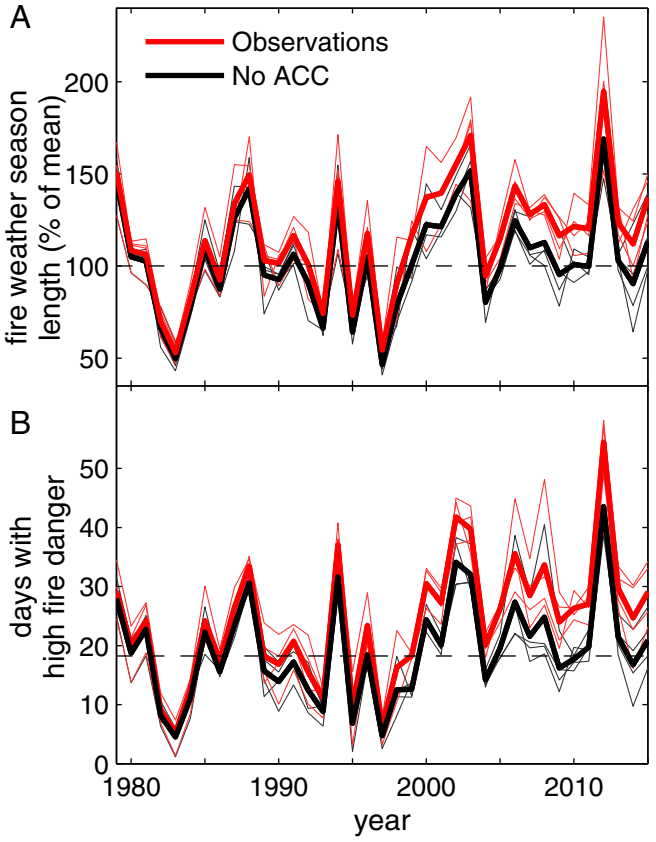

Fig. 4. Changes in fire-weather season length and number of high fire danger days. Time series of mean western US forest (*A*) fire-weather season length and (*B*) number of days per year when daily fire danger indices exceeded the 95th percentile. Baseline period: 1981–2010 using observational records that exclude the ACC signal. Red lines show the observed record, and black lines show the record that excludes the ACC signal. Bold lines show the average signal expressed across fuel aridity metrics.

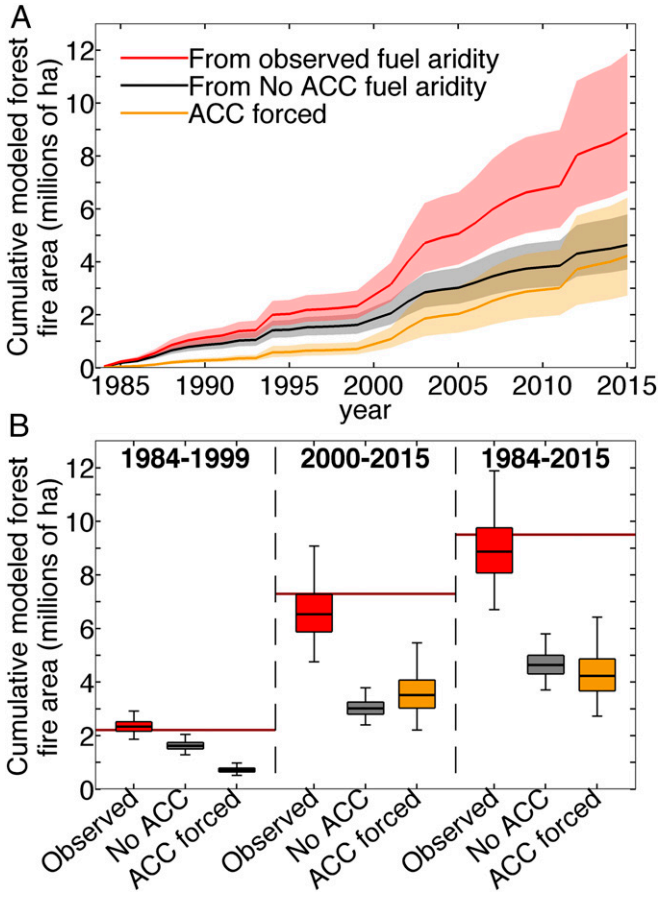

Fig. 5. Attribution of western US forest fire area to ACC. Cumulative forest fire area estimated from the (red) observed all-metric mean record of fuel aridity and (black) the fuel aridity record after exclusion of ACC (No ACC). The (orange) difference is the forest fire area forced by anthropogenic increases in fuel aridity. Bold lines in *A* and horizontal lines within box plots in *B* indicate mean estimated values (regression values in Fig. 1). Boxes in *B* bound 50% confidence intervals. Shaded areas in *A* and whiskers in *B* bound 95% confidence intervals. Dark red horizontal lines in *B* indicate observed forest fire area during each period.

effects during 1948–1978 and compounded anthropogenic effects during 1979–2015. During 1979–2015, for example, observed Mar–Sep vapor pressure decreased significantly across many US forest areas, in marked contrast to modeled anthropogenic increases (Fig. S6) (34). Significant declines in spring (Mar–May) precipitation in the southwestern United States and summer (Jun–Sep) precipitation throughout parts of the northwestern United States during 1979–2015 (Fig. S7 *A* and *B*) hastened increases in fire-season fuel aridity, consistent with observed increases in the number of consecutive dry days across the region (10). Natural climate variability, including a shift toward the cold phase of the interdecadal Pacific Oscillation (35), was likely the dominant driver of observed regional precipitation trends (36) (Fig. S7 *B* and *D*).

Our quantification of the ACC contribution to observed increases in forest fire activity in the western United States adds to the limited number of climate change attribution studies on wildfire to date (37). Previous attribution efforts have been restricted to a single GCM and biophysical variable (14, 16). We complement these studies by demonstrating the influence of ACC derived from an ensemble of GCMs on several biophysical metrics that exhibit strong links to forest fire area. However, our attribution effort only considers ACC to manifest as trends in mean climate conditions, which may be conservative because climate models also project anthropogenic increases in the temporal variability of climate and drought in the western United States (34, 38, 39). In focusing exclusively on the direct impacts of ACC on fuel aridity, we do not address several other pathways by which ACC may have affected wildfire activity. For example, the fuel aridity metrics that we used may not adequately capture the role of mountain snow hydrology on soil moisture. Nor do we account for the influence of climate change on lightning activity, which may increase with warming (40). We also do not account for how fire risk may be affected by changes in biomass/fuel due to increases in atmospheric CO_2 (41), drought-induced vegetation mortality (42), or insect outbreaks (43).

Additionally, we treat the impact of ACC on fire as independent from the effects of fire management (e.g., suppression and wildland fire use policies), ignitions, land cover (e.g., exurban development), and vegetation changes beyond the degree to which they modulate the relationship between fuel aridity and forest fire area. These factors have likely added to the area burned across the western US forests and potentially amplified the sensitivity of wildfire activity to climate variability and change in recent decades (2, 22, 24, 44). Such confounding influences, along with nonlinear relationships between burned area and its drivers (e.g., Fig. 1), contribute uncertainty to our empirical attribution of regional burned area to ACC. Our approach depends on the strong observed regional relationship between burned area and fuel aridity at the large regional scale of the western United States, so the quantitative results of this attribution effort are not necessarily applicable at finer spatial scales, for individual fires, or to changes in nonforested areas. Dynamical vegetation models with embedded fire models show emerging promise as tools to diagnose the impacts of a richer set of processes than those considered here (41, 45) and could be used in tandem with empirical approaches (46, 47) to better understand contributions of observed and projected ACC to changes in regional fire activity. However, dynamic models of vegetation, human activities, and fire are not without their own lengthy list of caveats (2). Given the strong empirical relationship between fuel aridity and wildfire activity identified here and in other studies (1, 2, 4, 8), and substantial increases in western US fuel aridity and fire-weather season length in recent decades, it appears clear from empirical data alone that increased fuel aridity, which is a robustly modeled result of ACC, is the proximal driver of the observed increases in western US forest fire area over the past few decades.

Conclusions

Since the 1970s, human-caused increases in temperature and vapor pressure deficit have enhanced fuel aridity across western continental US forests, accounting for approximately over half of the observed increases in fuel aridity during this period. These anthropogenic increases in fuel aridity approximately doubled the western US forest fire area beyond that expected from natural climate variability alone during 1984–2015. The growing ACC influence on fuel aridity is projected to increasingly promote wildfire potential across western US forests in the coming decades and pose threats to ecosystems, the carbon budget, human health, and fire suppression budgets (13, 48) that will collectively encourage the development of fire-resilient landscapes (49). Although fuel limitations are likely to eventually arise due to increased fire activity (17), this process has not yet substantially disrupted the relationship between western US forest fire area and aridity. We expect anthropogenic climate change and associated increases in fuel aridity to impose an increasingly dominant and detectable effect on western US forest fire area in the coming decades while fuels remain abundant.

Methods

We focus on climate variables that directly affect fuel moisture over forested areas of the western continental United States, where fire activity tends to be flammability-limited rather than fuel- or ignition-limited (1) (study region shown in Fig. 1, *Inset*). There are a variety of climate-based metrics that have been used as proxies for fuel aridity, yet there is no universally preferred metric across different vegetation types (24). We consider eight frequently used fuel aridity metrics that correlate well with fire activity variables, including annual burned area (Fig. 1 and Table S1), in western US forests.

Fuel aridity metrics are calculated from daily surface meteorological data (50) on a 1/24° grid for 1979–2015 for the western United States (west of 103°W). Although we calculated metrics across the entire western United States, we focus on forested lands defined by the climax succession vegetation stages of "forest" or "woodland" in the Environmental Site Potential product of LANDFIRE (landfire.gov). Forested 1/24° grid cells are defined by at least 50% forest coverage aggregated from LANDFIRE. We extended the aridity metrics calculated at the monthly timescale (ETo, VPD, CWD, and PDSI) back to 1948 using monthly anomalies relative to a common 1981–2010 period from the dataset developed by the Parameterized Regression on Independent Slopes Model group (51) for temperature, precipitation, and vapor pressure, and by bilinearly interpolating NCEP–NCAR reanalysis for wind speed and surface solar radiation. We aggregated data to annualized time series of mean May–Sep daily FWI, KBDI, ERC, and FFDI; Mar–Sep VPD and ETo; Jun–Aug PDSI; and Jan–Dec CWD. We also calculated the aridity metrics strictly from ERA-INTERIM and NCEP–NCAR reanalysis products for 1979–2015 covering the satellite era (*Supporting Information*).

Days per year of high fire potential are quantified by daily fire danger indices (ERC, FWI, FFDI, and KBDI) that exceed the 95th percentile threshold defined during 1981–2010 from observations after removing the ACC signal. Observational studies have shown that fire growth preferentially occurs during high fire danger periods (52, 53). We also calculate the fire weather season length for the four daily fire danger indices following previous studies (10).

The ACC signal is obtained from ensemble members taken from 27 CMIP5 global climate models (GCMs) regridded to a common 1° resolution for 1850–2005 using historical forcing experiments and for 2006–2099 using the Representative Concentration Pathway (RCP) 8.5 emissions scenario (Table S3 and *Supporting Information*). These GCMs were selected based on availability of monthly outputs for maximum and minimum daily temperature (T_{max} and T_{min}, respectively), specific humidity (*huss*), and surface pressure. Saturation vapor pressure (e_s), vapor pressure (e), and VPD were calculated using standard methods (*Supporting Information*). A variety of approaches exist to estimate the ACC signal (26). We define the anthropogenic signals in T_{max}, T_{min}, e, e_s, VPD, and relative humidity by a 50-y low-pass-filter time series (using a 10-point Butterworth filter) averaged across the 27 GCMs using the following methodology: For each GCM, variable, month, and grid cell, we converted each annual time series to anomalies relative to a 1901–2000 baseline. We averaged annual anomalies across all realizations (model runs) for each GCM and calculated a single 50-y low-pass-filter annual time series for each of the 12 mo for 1850–2099. We averaged each month's low-pass-filtered time series across the 27 GCMs and additively adjusted so that all smoothed records pass through zero in 1901. The resultant ACC signal represents the CMIP5 modeled anthropogenic impact since 1901 for each variable, grid cell, and month (*Supporting Information*).

We bilinearly interpolated the 1° CMIP5 multimodel mean 50-y low-pass time series to the 1/24° spatial resolution of the observations and subtracted the ACC signal from the observed daily and monthly time series. We consider the remaining records after subtraction of the ACC signal to indicate climate records that are free of anthropogenic trends (26).

Annual variations in fuel aridity metrics are presented as standardized anomalies (σ) to accommodate differences across geography and metrics. All fuel aridity metrics are standardized using the mean and SD from 1981 to 2010 for observations that excluded the ACC signal. Although the selection of a reference period can bias results (54), our findings were similar when using the full 1979–2015 time period or the observed data (without removal of ACC) for the reference period. The influence of anthropogenic forcing on fuel aridity metrics is quantified as the difference between metrics calculated with observations and those calculated with observations that excluded the ACC signal. Area-weighted standardized anomalies and the spatial extent of western US forested land that experienced high (>1 σ) aridity are computed for each aridity metric. Annualized burned area as well as aggregated fuel aridity metrics calculated with data from ref. 50 and the two reanalysis products are provided in Datasets S1–S3.

We use the regression relationship between the annual western US forest fire area and the all-metric mean fuel aridity index in Fig. 1 to estimate the forcing of anthropogenic increases in fuel aridity on forest fire area during 1984–2015. Uncertainties in the regression relationship due to imperfect correlation and temporal autocorrelation are propagated as estimated confidence bounds on the anthropogenic forcing of forest fire area. This approach was repeated using a more conservative definition of the regression relationship, where we removed the linear least squares trend for 1984–2015 from both the area burned and fuel aridity time series before regression to reduce the possibility of spurious correlation due to common but unrelated trends (Fig. S5). Statistical significance of all linear trends and correlations reported in this study are assessed using both Spearman's rank and Kendall's tau statistics. Trends are considered significant if both tests yield $P < 0.05$.

ACKNOWLEDGMENTS. We thank J. Mankin, B. Osborn, and two reviewers for helpful comments on the manuscript and coauthors of ref. 26 for help developing the empirical attribution framework. A.P.W. was funded by Columbia University's Center for Climate and Life and by the Lamont-Doherty Earth Observatory (Lamont contribution 8048). J.T.A. was supported by funding from National Aeronautics and Space Administration Terrestrial Ecology Program under Award NNX14AJ14G, and the National Science Foundation Hazards Science, Engineering and Education for Sustainability (SEES) Program under Award 1520873.

1. Littell JS, McKenzie D, Peterson DL, Westerling AL (2009) Climate and wildfire area burned in western U.S. ecoprovinces, 1916-2003. *Ecol Appl* 19(4):1003–1021.
2. Williams AP, Abatzoglou JT (2016) Recent advances and remaining uncertainties in resolving past and future climate effects on global fire activity. *Curr Clim Chang Reports* 2:1–14.
3. Dennison P, Brewer S, Arnold J, Moritz M (2014) Large wildfire trends in the western United States, 1984–2011. *Geophys Res Lett* 41:2928–2933.
4. Westerling AL, Hidalgo HG, Cayan DR, Swetnam TW (2006) Warming and earlier spring increase western U.S. forest wildfire activity. *Science* 313(5789):940–943.
5. Westerling AL (2016) Increasing western US forest wildfire activity: Sensitivity to changes in the timing of spring. *Philos Trans R Soc B Biol Sci* 371(1696):20150178.
6. Kasischke ES, Turetsky MR (2006) Recent changes in the fire regime across the North American boreal region - Spatial and temporal patterns of burning across Canada and Alaska. *Geophys Res Lett* 33(9):L09703.
7. Kelly R, et al. (2013) Recent burning of boreal forests exceeds fire regime limits of the past 10,000 years. *Proc Natl Acad Sci USA* 110(32):13055–13060.
8. Abatzoglou JT, Kolden CA (2013) Relationships between climate and macroscale area burned in the western United States. *Int J Wildland Fire* 22(7):1003–1020.
9. Seager R, et al. (2015) Climatology, variability, and trends in the U.S. vapor pressure deficit, an important fire-related meteorological quantity. *J Appl Meteorol Climatol* 54(6):1121–1141.
10. Jolly WM, et al. (2015) Climate-induced variations in global wildfire danger from 1979 to 2013. *Nat Commun* 6:7537.
11. Dobrowski SZ, et al. (2013) The climate velocity of the contiguous United States during the 20th century. *Glob Change Biol* 19(1):241–251.
12. Flannigan MD, Krawchuk MA, de Groot WJ, Wotton BM, Gowman LM (2009) Implications of changing climate for global wildland fire. *Int J Wildland Fire* 18(5):483–507.
13. Flannigan M, et al. (2013) Global wildland fire season severity in the 21st century. *For Ecol Manage* 294:54–61.
14. Yoon J, Kravitz B, Rasch P (2015) Extreme fire season in California: A glimpse into the future? *Bull Am Meteorol Soc* 96:S5–S9.
15. Barbero R, Abatzoglou JT, Larkin NK, Kolden CA, Stocks B (2015) Climate change presents increased potential for very large fires in the contiguous United States. *Int J Wildland Fire* 24(7):892–899.
16. Gillett NP, Weaver AJ, Zwiers FW, Flannigan MD (2004) Detecting the effect of climate change on Canadian forest fires. *Geophys Res Lett* 31(18):L18211.
17. Westerling AL, Turner MG, Smithwick EAH, Romme WH, Ryan MG (2011) Continued warming could transform Greater Yellowstone fire regimes by mid-21st century. *Proc Natl Acad Sci USA* 108(32):13165–13170.
18. Krawchuk MA, Moritz MA, Parisien MA, Van Dorn J, Hayhoe K (2009) Global pyrogeography: The current and future distribution of wildfire. *PLoS One* 4(4):e5102.
19. Moritz MA, et al. (2012) Climate change and disruptions to global fire activity. *Ecosphere* 3(6):1–22.
20. Marlon JR, et al. (2012) Long-term perspective on wildfires in the western USA. *Proc Natl Acad Sci USA* 109(9):E535–E543.
21. Parks SA, et al. (2015) Wildland fire deficit and surplus in the western United States, 1984–2012. *Ecosphere* 6(12):1–13.
22. Higuera PE, Abatzoglou JT, Littell JS, Morgan P (2015) The changing strength and nature of fire–climate relationships in the northern Rocky Mountains, U.S.A., 1902-2008. *PLoS One* 10(6):e0127563.
23. Pausas JG, Ribeiro E (2013) The global fire–productivity relationship. *Glob Ecol Biogeogr* 22(6):728–736.
24. Littell JS, Peterson DL, Riley KL, Liu Y, Luce CH (2016) A review of the relationships between drought and forest fire in the United States. *Glob Change Biol* 22(7): 2353–2369.

25. Williams AP, et al. (2015) Correlations between components of the water balance and burned area reveal new insights for predicting forest fire area in the southwest United States. *Int J Wildland Fire* 24(1):14–26.
26. Williams AP, et al. (2015) Contribution of anthropogenic warming to California drought during 2012–2014. *Geophys Res Lett* 42(16):6819–6828.
27. Sheffield J, et al. (2013) North American Climate in CMIP5 experiments. Part I: Evaluation of historical simulations of continental and regional climatology. *J Clim* 26(23): 9209–9245.
28. Hobbins MT (2016) The variability of ASCE standardized reference evapotranspiration: A rigorous, CONUS-wide decomposition and attribution. *Trans Am Soc Agric Biol Eng* 59(2):561–576.
29. Mann ML, et al. (2016) Incorporating anthropogenic influences into fire probability models: Effects of human activity and climate change on fire activity in California. *PLoS One* 11(4):e0153589.
30. Yue X, Mickley LJ, Logan JA, Kaplan JO (2013) Ensemble projections of wildfire activity and carbonaceous aerosol concentrations over the western United States in the mid-21st century. *Atmos Environ (1994)* 77:767–780.
31. Pechony O, Shindell DT (2010) Driving forces of global wildfires over the past millennium and the forthcoming century. *Proc Natl Acad Sci USA* 107(45):19167–19170.
32. Littell JS, et al. (2010) Forest ecosystems, disturbance, and climatic change in Washington State, USA. *Clim Change* 102(1-2):129–158.
33. Rogers BM, et al. (2011) Impacts of climate change on fire regimes and carbon stocks of the U.S. Pacific Northwest. *J Geophys Res Biogeosci* 116(G3):G03037.
34. Williams AP, et al. (2014) Causes and implications of extreme atmospheric moisture demand during the record-breaking 2011 wildfire season in the southwestern United States. *J Appl Meteorol Climatol* 53(12):2671–2684.
35. Dong B, Dai A (2015) The influence of the Interdecadal Pacific Oscillation on temperature and precipitation over the globe. *Clim Dyn* 45(9-10):2667–2681.
36. Deser C, Knutti R, Solomon S, Phillips AS (2012) Communication of the role of natural variability in future North American climate. *Nat Clim Chang* 2(11):775–779.
37. National Academies of Sciences, Engineering, and Medicine (2016) *Attribution of Extreme Weather Events in the Context of Climate Change* (The National Academies Press, Washington, DC).
38. Swain DL, Horton DE, Singh D, Diffenbaugh NS (2016) Trends in atmospheric patterns conducive to seasonal precipitation and temperature extremes in California. *Sci Adv* 2(4):e1501344.
39. Polade SD, Pierce DW, Cayan DR, Gershunov A, Dettinger MD (2014) The key role of dry days in changing regional climate and precipitation regimes. *Sci Rep* 4:4364.
40. Romps DM, Seeley JT, Vollaro D, Molinari J (2014) Climate change. Projected increase in lightning strikes in the United States due to global warming. *Science* 346(6211): 851–854.
41. Knorr W, Jiang L, Arneth A (2016) Climate, CO_2 and human population impacts on global wildfire emissions. *Biogeosciences* 13(1):267–282.
42. Williams AP, et al. (2013) Temperature as a potent driver of regional forest drought stress and tree mortality. *Nat Clim Chang* 3(3):292–297.
43. Hart SJ, Schoennagel T, Veblen TT, Chapman TB (2015) Area burned in the western United States is unaffected by recent mountain pine beetle outbreaks. *Proc Natl Acad Sci USA* 112(14):4375–4380.
44. Van Wagtendonk JW (2007) The history and evolution of wildland fire use. *Fire Ecol* 3(2):3–17.
45. Bowman DMJS, Murphy BP, Williamson GJ, Cochrane MA (2014) Pyrogeographic models, feedbacks and the future of global fire regimes. *Glob Ecol Biogeogr* 23(7): 821–824.
46. Parisien M-A, et al. (2014) An analysis of controls on fire activity in boreal Canada: Comparing models built with different temporal resolutions. *Ecol Appl* 24(6):1341–1356.
47. Krawchuk MA, Moritz MA (2014) Burning issues: Statistical analyses of global fire data to inform assessments of environmental change. *Environmetrics* 25(6):472–481.
48. Millar CI, Stephenson NL (2015) Temperate forest health in an era of emerging megadisturbance. *Science* 349(6250):823–826.
49. Smith AMS, et al. (2016) The science of firescapes: Achieving fire-resilient communities. *Bioscience* 66(2):130–146.
50. Abatzoglou JT (2013) Development of gridded surface meteorological data for ecological applications and modelling. *Int J Climatol* 33(1):121–131.
51. Daly C, et al. (2008) Physiographically sensitive mapping of climatological temperature and precipitation across the conterminous United States. *Int J Climatol* 28(15): 2031–2064.
52. Stavros EN, Abatzoglou J, Larkin NK, McKenzie D, Steel EA (2014) Climate and very large wildland fires in the contiguous Western USA. *Int J Wildland Fire* 23(7):899–914.
53. Riley KL, Abatzoglou JT, Grenfell IC, Klene AE, Heinsch FA (2013) The relationship of large fire occurrence with drought and fire danger indices in the western USA, 1984–2008: The role of temporal scale. *Int J Wildland Fire* 22(7):894–909.
54. Sippel S, et al. (2015) Quantifying changes in climate variability and extremes: Pitfalls and their overcoming. *Geophys Res Lett* 42(22):9990–9998.
55. Littell JS, Gwozdz RB (2011) Climatic water balance and regional fire years in the Pacific Northwest, USA: linking regional climate and fire at landscape scales. *The Landscape Ecology of Fire* (Springer, Dordrecht, The Netherlands), pp 117–139.
56. Morton DC, et al. (2013) Satellite-based assessment of climate controls on US burned area. *Biogeosciences* 10(1):247–260.
57. Stocks BJ, et al. (1989) Canadian forest fire danger rating system: An overview. *For Chron* 65(4):258–265.
58. Westerling AL, Gershunov A, Brown TJ, Cayan DR, Dettinger MD (2003) Climate and wildfire in the western United States. *Bull Am Meteorol Soc* 84(5):595–604.
59. Flannigan MD, et al. (2016) Fuel moisture sensitivity to temperature and precipitation: Climate change implications. *Clim Change* 134(1-2):59–71.
60. Flannigan MD, Van Wagner CE (1991) Climate change and wildfire in Canada. *Can J Res* 21(1):66–72.
61. Dowdy AJ, Mills GA, Finkele K, de Groot W (2010) Index sensitivity analysis applied to the Canadian Forest Fire Weather Index and the McArthur Forest Fire Danger Index. *Meteorol Appl* 17(3):298–312.
62. Mitchell KE, et al. (2004) The multi-institution North American Land Data Assimilation System (NLDAS): Utilizing multiple GCIP products and partners in a continental distributed hydrological modeling system. *J Geophys Res Atmos* 109(D7):D07S90.
63. Allen RG, Pereira LS, Raes D, Smith M (1998) Crop evapotranspiration-Guidelines for computing crop water requirements-FAO Irrigation and drainage paper 56. *FAO, Rome* 300(9):D05109.
64. Willmott CJ, Rowe CM, Mintz Y (1985) Climatology of the terrestrial seasonal water cycle. *J Climatol* 5(6):589–606.
65. Andrews PL, Loftsgaarden DO, Bradshaw LS (2003) Evaluation of fire danger rating indexes using logistic regression and percentile analysis. *Int J Wildland Fire* 12(2): 213–226.
66. Cohen JE, Deeming JD (1985) The National Fire-Danger Rating System: basic equations. *Gen Tech Rep*:16.
67. McArthur AG (1967) *Fire behaviour in eucalypt forests* (Forestry and Timber Bureau Leaflet 107).
68. Griffiths D (1999) Improved formula for the drought factor in McArthur's Forest Fire Danger Meter. *Aust For* 62(3):202–206.
69. Wallace JM, Hobbs PV (2006) *Atmospheric Science: An Introductory Survey* (Academic, Amsterdam), 2nd Ed.
70. Eidenshink JC, et al. (2007) A project for monitoring trends in burn severity. *Fire Ecol* 3(1):3–21.
71. Roy DP, Boschetti L, Justice CO, Ju J (2008) The collection 5 MODIS burned area product—Global evaluation by comparison with the MODIS active fire product. *Remote Sens Environ* 112(9):3690–3707.
72. van Vuuren DP, et al. (2011) The representative concentration pathways: An overview. *Clim Change* 109(1):5–31.

frontiers | Frontiers in Forests and Global Change

TYPE Original Research
PUBLISHED 06 January 2023
DOI 10.3389/ffgc.2022.1074508

OPEN ACCESS

EDITED BY
Alfredo Di Filippo,
University of Tuscia, Italy

REVIEWED BY
Roel Brienen,
University of Leeds, United Kingdom
Jeffrey Stenzel,
University of California, Merced,
United States

*CORRESPONDENCE
Richard A. Birdsey
✉ rbirdsey@woodwellclimate.org

SPECIALTY SECTION
This article was submitted to
Forest Management,
a section of the journal
Frontiers in Forests and Global Change

RECEIVED 19 October 2022
ACCEPTED 15 December 2022
PUBLISHED 06 January 2023

CITATION
Birdsey RA, DellaSala DA, Walker WS, Gorelik SR, Rose G and Ramírez CE (2023) Assessing carbon stocks and accumulation potential of mature forests and larger trees in U.S. federal lands.
Front. For. Glob. Change 5:1074508.
doi: 10.3389/ffgc.2022.1074508

Assessing carbon stocks and accumulation potential of mature forests and larger trees in U.S. federal lands

Richard A. Birdsey[1]*, Dominick A. DellaSala[2], Wayne S. Walker[1], Seth R. Gorelik[1], Garett Rose[3] and Carolyn E. Ramírez[3]

[1]Woodwell Climate Research Center, Falmouth, MA, United States, [2]The Wild Heritage, A Project of Earth Island Institute, Berkeley, CA, United States, [3]Natural Resources Defense Council, Inc., Washington, DC, United States

Mature and old-growth forests (collectively "mature") and larger trees are important carbon sinks that are declining worldwide. Information on the carbon value of mature forests and larger trees in the United States has policy relevance for complying with President Joe Biden's Executive Order 14072 directing federal agencies to define and conduct an inventory of them for conservation purposes. Specific metrics related to maturity can help land managers define and maintain present and future carbon stocks at the tree and forest stand level, while making an important contribution to the nation's goal of net-zero greenhouse gas emissions by 2050. We present a systematic method to define and assess the status of mature forests and larger trees on federal lands in the United States that if protected from logging could maintain substantial carbon stocks and accumulation potential, along with myriad climate and ecological co-benefits. We based the onset of forest maturity on the age at which a forest stand achieves peak net primary productivity. We based our definition of larger trees on the median tree diameter associated with the tree age that defines the beginning of stand maturity to provide a practical way for managers to identify larger trees that could be protected in different forest ecosystems. The average age of peak net primary productivity ranged from 35 to 75 years, with some specific forest types extending this range. Typical diameter thresholds that separate smaller from larger trees ranged from 4 to 18 inches (10–46 cm) among individual forest types, with larger diameter thresholds found in the Western forests. In assessing these maturity metrics, we found that the unprotected carbon stock in larger trees in mature stands ranged from 36 to 68% of the total carbon in all trees in a representative selection of 11 National Forests. The unprotected annual carbon accumulation in live

above-ground biomass of larger trees in mature stands ranged from 12 to 60% of the total accumulation in all trees. The potential impact of avoiding emissions from harvesting large trees in mature forests is thus significant and would require a policy shift to include protection of carbon stocks and future carbon accumulation as an additional land management objective on federal forest lands.

KEYWORDS

carbon stock, climate change, large trees, mature forests, national forest lands

1. Introduction

Nature-based climate solutions are needed to meet anticipated national targets associated with the Paris Climate Agreement which establishes a global framework to avoid dangerous climate change by limiting warming to less than 2°C (United Nations, 2015). In the United States, the Biden administration announced a "roadmap" for nature-based solutions during the COP27 climate summit (White House, 2022a). Reducing carbon dioxide (CO_2) emissions and increasing CO_2 removals from the atmosphere using forests are considered to be the most significant of terrestrial natural climate solutions globally and in the U.S. (Griscom et al., 2017; Fargione et al., 2018).

Protecting mature forests to achieve their potential to reduce greenhouse gases is controversial in part because it restricts logging (Law and Harmon, 2011; Moomaw et al., 2020). Forests in the later stages of seral development (mature and old-growth, DellaSala et al., 2022a) and the large trees within them (Stephenson et al., 2014; Mildrexler et al., 2020) play an outsized role in the accumulation and long-term storage of atmospheric carbon, and consequently enabling their protection where lacking has been recognized as an effective nature-based climate solution (Griscom et al., 2017). Notably, President Joe Biden issued an executive order (White House, 2022b) recognizing the climate value of mature and old-growth forests and directed federal officials to define and inventory them on Federal lands and develop policies for their conservation. Thus, providing techniques for defining when forests qualify as mature and quantifying their relative carbon content and storage potential has high policy relevance.

This undertaking supports the nation's goal of achieving net-zero greenhouse gas emissions by 2050 and to conserve 30% of the nation's land by 2030 (White House, 2021). Protecting older, larger trees and mature forests would also help reverse the global degradation of older forests that have diverse ecological values (Lindenmayer et al., 2012), and facilitate the continued growth of mid-sized trees toward maturity (Moomaw et al., 2019). Mature forests provide refugia for many imperiled species (Buotte et al., 2020; DellaSala et al., 2022a), store disproportionate amounts of above-ground carbon in forests (Stephenson et al., 2014; Lutz et al., 2018; Mildrexler et al., 2020), and historically constitute a large volume of valuable timber (Johnson and Swanson, 2009). These values often conflict with one another resulting in contentious policy debates about land management objectives and best practices, particularly on federal lands in the U.S. where much of the remaining mature forest area resides according to national forest inventory data (Bolsinger and Waddell, 1993; DellaSala et al., 2022a). Recent studies of land values reveal that the importance of mature forests for ecosystem integrity and non-timber ecosystem services far exceeds their value for timber products (Watson et al., 2018; Gilhen-Baker et al., 2022).

Some researchers argue that it is necessary to log larger trees in fire-suppressed forests in the western U.S. to restore fire regimes, reduce biomass, and minimize emissions from wildfires (Kirschbaum, 2003; Hessburg et al., 2020; Johnston et al., 2021). However, these assertions have been challenged (Stephenson et al., 2014; Lutz et al., 2018; Mildrexler et al., 2020; DellaSala et al., 2022b) in part because removing larger trees from forests having high carbon stocks creates a significant "carbon debt" that can take decades or centuries to repay (Moomaw et al., 2019; Law et al., 2022).

It follows that our objectives are to (1) present an approach to defining larger trees and mature forests on federal lands; (2) estimate the current carbon stock and annual carbon accumulation in larger trees in mature forests across a representative selection of national forests, and (3) estimate the carbon stock and accumulation left unprotected by current binding designations.

We do not identify the proportion of mature forest area and carbon stocks that could be classified more specifically as "old growth." Defining old-growth in a consistent way across the diversity of temperate forests is challenging since existing definitions are based on structural, successional, and biogeochemical factors that are unique for individual forest types and researcher's interests (Wirth et al., 2009). Our characterization of mature forests has ecological and policy relevance for restoring old-growth characteristics over

time, pursuant to the presidential executive order as well (DellaSala et al., 2022a). Thus, we determined that this paper would be more broadly focused on mature forests rather than old-growth forests.

2. Materials and methods

2.1. Approach

Our approach requires addressing two components: (1) individual trees referred to as the "larger" trees in a forest; and (2) mature forest stand development represented by stand age. This method for identifying larger trees in mature stands—and the related assessment of above-ground live carbon stocks and annual carbon accumulation—is intended to be broadly applicable and readily implementable independent of how mature stands are defined. We settled on defining stand maturity with respect to the age of maximum Net Primary Productivity (NPP), which is estimated as the annual net quantity of carbon removed from the atmosphere and stored in biomass (see section 2.2 for definitions of key terms). NPP was calculated by combining 4 terms: Annual accumulation of live biomass, annual mortality of above-ground and below-ground biomass, foliage turnover to soil, and fine root turnover in soil (He et al., 2012). Live biomass and annual mortality were estimated from the Forest Inventory and Analysis (FIA) database. Foliage and fine root turnover were estimated using maps of leaf area index (LAI) and forest age to derive LAI-age relationships for different forest types. These relationships were then used to derive foliage and fine root turnover estimates using species-specific trait data (He et al., 2012).

This is a particularly appropriate approach to maturity in the context of how forests help temper climate change. Our integrating method of associating the median tree diameter with age is intended to be applicable to other definitions of stand maturity, including simple ones applied across the landscape without regard to specific stand characteristics, for example a uniform age cutoff.

2.2. Key definitions and data source

Net Primary Productivity (NPP)—The difference between the amount of carbon produced through photosynthesis and the amount of energy that is used for respiration. Estimate is based on the net increment of tree and understory biomass, leaf production, and fine root turnover (He et al., 2012).

Biomass—The carbon stored in live trees greater than 1 inch (2.54 cm) diameter at breast height (dbh), including stump, bole, bark, branches, and foliage.

Carbon stock—The carbon stored in live biomass at a point in time, unless otherwise defined to include additional ecosystem components, in units of megagrams (Mg) or teragrams (Tg) of carbon (C).

Carbon accumulation—The net change in carbon stock of live tree biomass over a period of time, in units of megagrams (Mg) or teragrams (Tg) of carbon (C), per hectare (ha^{-1}) and/or or per year (yr^{-1}).

Metric ton—In the literature, the term metric ton (Mt or tonne) is often used instead of megagram.

Definitions of other terms commonly used in this paper are included in the **supplementary material**.

To apply our method to each national forest, recent FIA data collected by the U.S. Forest Service were queried using the EVALIDator online query system (USDA Forest Service, 2022). The sampling approach and estimation methods of forest inventory variables in the FIA database follow documented procedures (**Supplementary material**; Bechtold and Patterson, 2005). Our analysis is focused on above-ground carbon in live-trees, though some representative data are also presented about all ecosystem C pools to show the full potential of protecting carbon stocks on selected national forests.

2.3. Study area

The study area includes 11 individual national forests or small groups of national forests in the conterminous U.S. (**Table 1** and **Figure 1**), selected to represent the geographic diversity of U.S. forests and to have at least one forest in each USFS region. Forests with similar characteristics within a region were grouped if preliminary analysis determined that there were insufficient sample data to develop the biomass distributions for a single forest by main forest types.

2.4. Defining larger trees and mature forests

We combine two key indicators—stand age and tree diameter—in a way that could be used by land managers to assess maturity for informing management practices, in contrast to basing maturity and management on either tree diameter or stand age alone as in some previous studies (Mildrexler et al., 2020; Johnston et al., 2021). Mature forests are defined as stands with ages exceeding that at which accumulation of carbon in biomass peaks as indicated by NPP. We considered FIA sample plots to represent stands of relatively uniform condition. The sampled areas and trees are partitioned into uniform domains during field sampling and data processing if more than one stand condition falls within the sampling area. For this study, a new term "Culmination of Net Primary Productivity" (CNPP) is used to describe the age at which NPP reaches a maximum carbon accumulation rate. Physiologically, peak productivity occurs approximately at the age when the growing space in the

TABLE 1 National Forests, sampling dates, and number of sample plots used in our study.

National Forest	FIA sampling dates	Number of sample plots
Gifford Pinchot, WA	2008–2019	626
Malheur, OR	2011–2019	758
Black Hills, SD	2013–2019	348
Chequamegon-Nicolet, WI	2013–2019	559
Green Mountain, VT and White Mountain, NH	2013–2019	580
Appalachian National Forests[1]	2013–2020	982
White River, CO	2010–2019	291
Flathead, MT	2010–2019	341
Arizona National Forests[2]	2010–2019	849
Central California National Forests[3]	2011–2019	410
Arkansas National Forests[4]	2017–2021	427

[1]Pisgah (NC), Nantahala (NC), Cherokee (TN), Monongahela (WV), Jefferson (VA), George Washington (VA).
[2]Coconino, Prescott, Tonto, Sitgreaves, AZ.
[3]Eldorado, Stanislaus, and Sierra, CA.
[4]Oachita, Ozark-St. Francis, AR.

ecosystem is fully covered by leaf area—i.e., tree canopy closure reaches 100%. After this age, NPP either stays constant or declines gradually, depending on tree species composition, and other environmental factors such as nutrient availability (Kutsch et al., 2009; He et al., 2012). Previous analyses of FIA data indicate that peak NPP occurs at a relatively young stage of stand succession, roughly 25—50 years following stand establishment (**Figure 2**; He et al., 2012; Dugan et al., 2017; Birdsey et al., 2019). Foresters have a similar metric, referred to as the "culmination of mean annual increment" (CMAI), that is based on estimated net volume increment (i.e., volume growth minus mortality) as a function of age, rather than net productivity as a function of age, which is more relevant to assessing forests potential to reduce greenhouse gases. CMAI is calculated in the same way as CNPP, except that the mean annual increment variable is net volume increment instead of net primary productivity.

Larger trees are then defined as having a diameter at breast height (dbh) that is equal to or greater than the median diameter in forest stands at or near the age of stand-level CNPP. A range of ages around the age of CNPP, taken to be the CNPP age plus or minus one age class (30-year bin size), was used in order to have sufficient FIA sampling plots (generally 100 or more) to develop a tree diameter distribution for individual forest types. Then the median diameter of the distribution is used as the lower diameter threshold of maturity for the population of trees in the CNPP age class.

Our approach involves clustering (post-stratifying) sample plots by forest type and stand age class, and individual sample trees by tree diameter class, and then calculating estimates for the clusters (populations) as groups. Because most clusters include a wide distribution of tree diameters, there can be larger trees present in stands having ages below CNPP age, and *vice versa*, stands with ages above CNPP age can have trees with diameters below the lower diameter limit. The definitions of mature stands and associated larger trees in this study is conceptually consistent with stages of maturity derived from classifying FIA sample plots (Stanke et al., 2020; USDA Forest Service, 2022) and from an approach involving spatial data (DellaSala et al., 2022a). **Table 2** compares the terminology and approaches of each.

To estimate the area of mature stands based on sample plot characterization, we used the FIA stand-size variable coded as "large diameter" (column 2 of **Table 2**) because our method is not based on stand-scale variables alone but rather a crosswalk

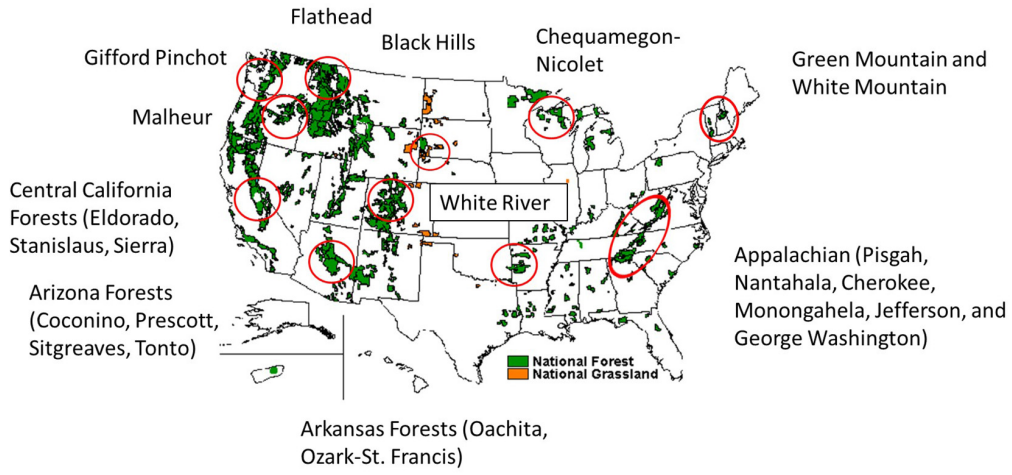

FIGURE 1
Approximate locations of 11 National Forests in our study area.

of stand and tree population variables. Large diameter stands are defined by FIA as those with more than 50 percent of the stocking in medium and large diameter trees, and with the stocking of large diameter trees equal to or greater than the stocking of medium and small diameter trees.

2.5. Estimation of carbon stock and accumulation in living biomass

We used the age-to-diameter crosswalk to estimate live above-ground carbon stocks and annual carbon accumulation for larger trees in forests above the CNPP threshold. We focused on live above-ground biomass since it is typically the largest of the C pools (except for soil in some cases) and is the most dynamic in terms of how carbon stocks and accumulation change with age or tree size (Domke et al., 2021). The estimated carbon in biomass of trees or stands is taken directly from the FIA database and is based on measurements of dbh and height. The current standard FIA approach to estimating biomass from tree measurements uses the component ratio method (Woodall et al., 2011). Unless stated otherwise, we use the term "carbon" to refer to carbon in live-tree biomass, not the carbon in all ecosystem carbon pools. Live-tree biomass includes the main stem or bole of the tree, rough or rotten sections of the bole, tree bark, branches, and leaves.

Estimation of the carbon accumulation rate is based on remeasurement of the same grid of sample points and trees at intervals ranging from 5 to 10 years depending on the state, with generally shorter remeasurement cycles in the eastern U.S. compared with the western U.S. (Table 1). Carbon in live-tree biomass was estimated at the beginning and end of the time period, and carbon accumulation was calculated as change in carbon over the period divided by the number of years.

The uncertainty of estimates of carbon stock and carbon accumulation was taken directly from the FIA data retrieval system that reports sampling error with 67% confidence, which we multiplied by 1.96 to report estimates with 95% confidence. These uncertainty estimates do not include the uncertainty of using biomass equations to estimate

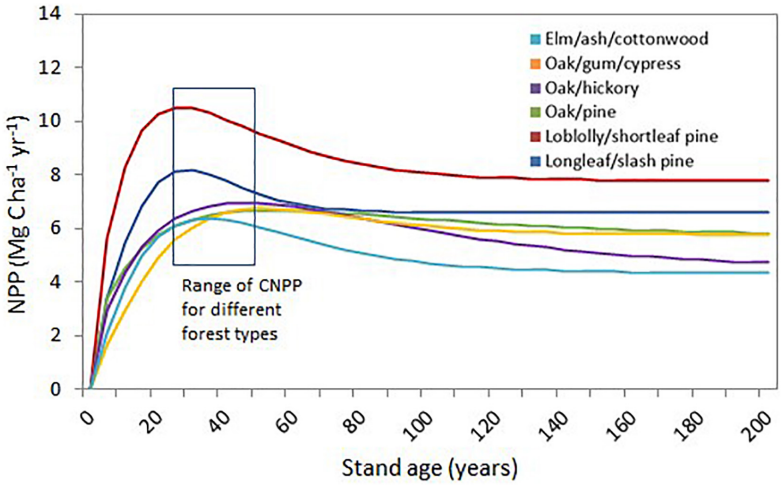

FIGURE 2
Net primary productivity (NPP) for selected forest types in the South (He et al., 2012). Culmination of NPP (CNPP) occurs at the stand age having the greatest annual increment rate, typically at or just after the tree canopy closes. Younger stands are those with ages less than CNPP. Older stands have ages greater than CNPP. CNPP is highly variable among forest types and geographic regions—in this example, from ages 23 to 45. The He et al. (2012) paper includes detailed uncertainty analyses of these and other NPP curves.

TABLE 2 Successional stages of forest maturity or stand structure as defined by several studies.

Maturity or structural stage	FIA stand-size[1]	Stanke et al. (2020)[1]	DellaSala et al. (2022a)[2]	This study[3]
1	Small diameter	Pole	Young	Young
2	Medium diameter	Mature	Intermediate	Mature
3	Large diameter	Late	Mature/Old-growth	

Classifications across the rows are similar but not identical.
[1]Stand structural stage is classified based on the relative basal area of canopy stems in various size classes.
[2]Forest maturity model based on three spatial data layers of forest cover, height, and above-ground living biomass for all landownerships.
[3]Based on culmination of net primary productivity (CNPP) and median stand diameter at CNPP. Late succession or old-growth not distinguished from mature.

tree carbon from diameter and height measurements or from wood density.

2.6. Domains and filters

We filtered the data to include only sample plots that were classified in the database as belonging to the national forest or group of forests being analyzed. For estimating CNPP, we screened out sample plots if they showed evidence of logging or natural disturbance. The remaining "undisturbed" stands, however, could still include some tree mortality and loss of live biomass associated with aging and succession, or small-scale disturbances. All plots including those disturbed or harvested were included in final estimates of the carbon stock and accumulation for the whole forest or for reserved and unreserved areas within the National Forest. Reserved and unreserved areas were defined by the FIA database variable "reserved class." The classification of reserved is not the same as land defined as "protected" by the USGS GAP analysis project (USGS, 2019). Reserved land is withdrawn by law(s) prohibiting the management of land for the production of wood products, though tree harvesting may occur to support other management objectives. We use the classification "unreserved" as a proxy for forest areas that are lacking protection from timber harvest, while acknowledging that this definition of unreserved land may not be consistent with other definitions of unprotected land.

2.7. Model outputs

Estimates of carbon stock and accumulation are presented separately for reserved and unreserved forest areas since the target for future management policies may focus on carbon stocks of older forests in areas that could be logged in the future. Some additional details regarding definitions and calculation protocols are available in the **Supplementary material**.

3. Results

3.1. National forest characteristics

Individual forests and groups of forests range in forest area from about 0.4 to 2.0 million hectares (M ha), and the total area of all forests analyzed is about 8.9 M ha (**Table 3**). The carbon stock in above-ground biomass ranges from 9 to 113 million megagrams (Mg). There is a wide range of average C density, with the lowest amount of 21 Mg ha^{-1} in Arizona National Forests, and the highest amount of 166 Mg ha^{-1} in the Gifford Pinchot National Forest in Washington. The total carbon in the forest ecosystems, which includes above- and below-ground biomass, dead wood, litter, and soil, is from 2 to 5 times the amount of carbon in above-ground biomass alone (Domke et al., 2021). All but one of the national forests studied (the Black Hills National Forest in South Dakota) experienced an increase in above-ground carbon over the

TABLE 3 Biomass carbon stock and accumulation for all live-trees greater than 1 inch (2.54 cm), for each National Forest or group of forests studied.

National Forest	Total forest area (ha)	Total biomass C stock (Mg)	Total biomass C accumulation[1] (Mg yr^{-1})	Average C density (Mg ha^{-1})	Average C accumulation[2] (Mg $ha^{-1}yr^{-1}$)
Gifford Pinchot	508,502	84,233,113	878,348	166	1.73
Malheur	584,951	23,566,550	234,124	40	0.40
Black Hills	394,508	9,130,825	−32,622	23	−0.08
Chequamegon-Nicolet	583,050	30,777,312	607,023	53	1.04
Green and White Mountains	478,285	35,572,874	299,164	74	0.63
Appalachian Forests	1,216,520	112,798,380	1,122,302	93	0.92
White River	685,869	30,887,524	N/D	45	N/D
Flathead	906,902	39,688,676	N/D	44	N/D
Arizona Forests	2,083,049	43,194,094	N/D	21	N/D
Central California Forests	996,197	86,238,281	125,730	87	0.13
Arkansas Forests	454,986	64,714,071	1,498,668	142	3.29
Total	8,892,819	560,801,700	4,732,737	63	0.91

[1]Change in carbon stock over approximately the last 10 years.
[2]Average of national forests with available growth data from FIA database.
"N/D" means data were not available.

10.3389/ffgc.2022.1074508

remeasurement period, ranging from 0.13 (Central California) to 3.29 (Arkansas) Mg $ha^{-1}yr^{-1}$. All of the national forests were affected by disturbances—the most common being fire, insects and logging—though the areas and mix of disturbance types that occurred and the areas undisturbed are highly variable among the forests (**Supplementary Table 1**). Natural disturbances can result in significant tree mortality and transfer of carbon from live to dead trees, and gradual net emissions over several decades especially if the disturbances are of high severity (Birdsey et al., 2019). In the case of logging disturbances, emissions are significant both in the near term and over time, even when accounting for the amount of carbon in the harvested live trees that is initially transferred to the long-term harvested wood product pool (Hudiburg et al., 2019).

3.2. Culmination of net primary productivity and diameter limits

The estimated CNPP ages range from 35 to 75 years among the 11 National Forests with an average age of 50 years (**Table 4**) and are highly variable by forest type within each forest (**Supplementary Table 2**). Productivity at CNPP ranges from <1.0 to about 4.0 MgC $ha^{-1}yr^{-1}$, which is higher than the average productivity among all age classes since it represents the peak value. Typically, the productivity values after CNPP age decline at a variable rate by region and forest type (**Figure 2**). The estimates of CNPP age may be affected by sparse data points for some age classes, different stand disturbance histories, and other factors that influence tree growth rates over time such as climate and topography. In this study, the age at CNPP is used to define the lower age threshold for mature forests.

Determining the age threshold associated with CNPP involves examining the distribution of biomass by diameter (dbh) class for the stand-age class window around the age of CNPP. In most cases, there is a clearly defined peak of biomass at the median diameter of the distribution (**Supplementary Figure 1**). Because of the diversity of stand conditions associated with CNPP across the landscape, as well as uneven aged stand conditions, there are rather wide distributions of tree sizes associated with any particular CNPP (**Supplementary Figure 1**). Since the FIA stand-age data we used were compiled into diameter classes of 2 inches (5 cm), we used the upper end of the range to define the diameter threshold. Typically, there is more carbon stored in the population of trees with diameters at and near the diameter at CNPP, though these trees can grow to much larger sizes as indicated by the upper end of the diameter distributions. For the national forests in this study, the diameter limits ranged from a low of 4 inches (10 cm) for Douglas-fir in the Flathead National Forest to a high of 18 inches (46 cm) for two forest types in the Central California National Forests (**Supplementary Table 2**). Combining CNPP with median diameter in a cross-tabulation results in identifying the carbon stocks in larger trees in mature forests for each national forest, highlighted in yellow in the example table (**Supplementary Table 3**).

TABLE 4 Average age and tree diameter at culmination of net primary production (CNPP), all forest types combined on 11 National Forests in our study area.

National Forest	Average CNPP age (Years)	Diameter threshold (Inches/cm)
Gifford Pinchot	45	13/33
Malheur	45	12/30
Black Hills	75	14/36
Chequamegon-Nicolet	45	9/23
Green and White Mountains	35	12/30
Appalachian Forests	35	11/28
White River	55	6/15
Flathead	45	8/20
Arizona Forests	75	12/30
Central California Forests	50	16/41
Arkansas Forests	40	10/25
Average of all Forests	50	11/28

Tree diameters represent the lower age bound of mature forests (i.e., age at CNPP). Detailed ages and tree diameters by forest type are shown in supplementary Table 2.

3.3. Comparison of CNPP and CMAI

Evaluation of forest inventory data indicated that CNPP and CMAI occur at about the same age (**Supplementary Figure 2**). Some older studies based on different data, mainly from volume growth and yield studies, associate CMAI with a greater age (e.g., McArdle, 1930). This difference is likely caused by several factors such as management intensity, temporal changes in productivity from environmental changes, and sampling protocols.

3.4. Carbon stocks and accumulation of larger trees in mature stands

The total C stock and C accumulation of larger trees in stands older than age at CNPP compared with all trees and stands is highly variable among the different forests analyzed (**Table 5**). Likewise, sampling errors are highly variable, reflecting the total areas classified as mature and therefore the number of FIA sample plots therein. Sampling errors for C accumulation estimates are significantly higher than for C stocks, mainly because the variability of accumulation rates among sample plots is higher than the variability of stock estimates.

TABLE 5 Estimated area, carbon stock, carbon accumulation, and sampling errors for larger trees in mature stands within individual National Forests based on most recent forest inventory data (Table 1).

National Forest	Area (ha)	C Stock (Mg)	C stock sampling error[1] (%)	Net C accumulation (Mg yr^{-1})	Net C accumulation sampling error[1] (%)	C stock[2] (% of total NF)	Net C accumulation[2] (% of total NF)
Gifford Pinchot	440,005	68,148,420	5.5	380,998	22.7	80.9	43.4
Malheur	471,439	16,886,265	7.1	165,949	19.1	71.7	70.9
Black Hills	215,379	3,711,144	14.6	−15,167	82.2	40.6	−46.5
Chequamegon-Nicolet	303,176	20,625,499	6.9	281,034	11.9	67.0	46.3
Green and White Mountains	301,884	15,786,690	7.9	60,593	141.7	44.4	20.3
Appalachian	1,033,833	83,571,980	6.2	675,970	15.3	74.1	60.2
White River	390,370	26,038,059	13.1	N/D	N/D	84.3	N/D
Flathead	507,053	27,841,625	13.6	N/D	N/D	70.2	N/D
Arizona National Forests	1,738,672	36,254,717	11.2	N/D	N/D	83.9	N/D
Central California National Forests	821,991	65,973,313	8.8	−66,370	52.2	76.5	−52.8
Arkansas National Forests	384,972	41,808,132	6.3	619,759	13.5	64.6	41.4
Total/mean	6,608,774	406,645,844	[redacted]	2,102,766	[redacted]	72.5	44.4

[1]With 95% confidence.

[2]Calculated by dividing values by those in Table 3. The percentages of carbon stocks and accumulation of larger trees in mature stands compared with all forests are also shown (last 2 columns). Larger trees in mature stands are the subset of the forest population composed of trees greater than the median dbh associated with CNPP in stands greater than CNPP age (Figure 2). Areas of mature forests estimated by a proxy variable "stand-size class" from FIA (see methods).

"N/D" means data were not available.

10.3389/ffgc.2022.1074508

Of the 11 forests, the C stock of larger trees in mature stands ranged from 41 to 84 percent of the total C stock of the forests, whereas C accumulation ranged from −53 to 71 percent of the total C accumulation. This difference between changes in C stock and C accumulation reflects several underlying causes: (1) younger forests can have higher NPP rates than mature forests as illustrated in **Figure 2**; (2) increasing mortality as forests grow older because some trees die from overcrowding or insects and diseases; and (3) disturbances such as severe wildfire that kill significant numbers of trees can reduce NPP, in some cases to a negative number.

3.5. Carbon stocks and accumulation in mature stands and larger trees in unreserved forest areas

The methodology described above can be further refined to separate out unreserved areas that could be designated for protection of carbon stocks and accumulation on national forest lands. In the 11 forests analyzed, unreserved C stocks of larger trees from all tree species in mature stands ranged from 36 to 69 percent of total C stocks (**Table 6** and **Supplementary Table 4**). Unreserved C accumulation of such trees in mature forests ranged from 12 to 60 percent of total C accumulation, not including the Black Hills national forest where the unreserved C accumulation was negative because of logging and natural disturbances (primarily insects). Typically, one or a few species comprise the main part of unprotected stocks and accumulation. Generally, the percentage of unreserved C accumulation is less than the percentage of unreserved C stock because the growth rates of mature forests are somewhat lower than younger forests.

3.6. Potential protected carbon stocks with variable diameter and age limits

The final stage of the analysis estimated the amount of C in unreserved areas above variable diameter and age limits for logging (**Supplementary Table 5**). These data further illustrate the functionality and flexibility of the age to diameter association that we developed for policy makers and land managers. The impact of selecting either the diameter limit or the age limit, or both, is highly dependent on the distribution of the estimated C stocks by these factors. For example, the diameter limit for Gifford Pinchot at a stand age of 80 years (20 inches; 51 cm dbh) would protect 57% of the total above-ground C, and the age limit of 80 years would protect 79% of the total above-ground C. In contrast, the diameter limit for Chequamegon–Nicolet at a stand age of 80 years (13 inches; 33 cm dbh) would protect only 27% of the total above-ground C, and the age limit of 80 years would protect only 48% of the total above-ground C. Each of the studied forests has a unique pattern of unreserved C based on diameter or age limits.

4. Discussion

4.1. Summary of results

The average age of maximum carbon accumulation (CNPP) ranged from 35 to 75 years for all forest types combined (**Table 4**), and the ranges were wider for individual forest types (**Supplementary Table 2**). Many factors contribute to determining the CNPP age (e.g., tree species, competition, site productivity, and climate). The lowest CNPP ages were estimated for the eastern forests in the southern and northern Appalachian regions, while the highest CNPP ages were found in the West. Typical diameter thresholds that separate smaller from larger trees (based on CNPP age) ranged from 6 to 16 inches (15–41 cm), with larger diameter thresholds found in the Western forests. The unprotected carbon stock of larger trees in mature stands ranged from 4 to 74 million MgC (**Table 6**), representing between 36.0 and 68.3 percent of the total carbon in the forest biomass. Forests with the highest percentage of unprotected carbon stock in larger trees in mature forest stands included Gifford Pinchot, Malheur, Chequamegon–Nicolet, and Appalachian National Forests. The unprotected carbon accumulation of larger trees in mature stands ranged widely from 11.5 to 60.2 percent of the total carbon accumulation in biomass, with one forest (Black Hills) showing a reduction in biomass.

4.2. Diameter and age thresholds

Our approach to establishing mature forest definitions and diameter thresholds for larger trees is rooted in a crosswalk of stand age and tree diameter that integrates two variables used to describe mature forests and trees. Both tree diameter and stand age have been used independently in the past to identify the lower bounds of maturity and provide guidance for on-the-ground tree and forest management decision rules (Mildrexler et al., 2020; Johnston et al., 2021). The two variables complement each other because although age is a good indicator of stand maturity, it can sometimes be difficult to determine a precise stand age in the field especially for stands of multi-aged trees, whereas tree diameter is an easily and accurately measured variable in any forestry operation. While our approach lacks complexity, it can form the foundation for more detailed analyses needed to guide on-the-ground management decisions.

Our approach is based on the application of FIA data, a standard source of detailed field inventory data for all forests of the U.S. that is readily available to the public and continuously updated. There are sufficient sample plots to evaluate most

TABLE 6 Carbon stocks and accumulation in larger trees in mature stands in unreserved forest areas, all forest types, within 11 National Forests in our study.

National Forest	Unreserved C stock		Unreserved C increment	
	Mg	% of total C[1]	Mg yr^{-1}	% of total C increment[1]
Gifford Pinchot	57,074,409	67.8	378,553	43.1
Malheur	16,103,923	68.3	108,878	53.7
Black Hills	3,625,966	39.7	−22,597	−69.3
Chequamegon-Nicolet	19,949,333	64.8	271,540	44.7
Green and White Mountains	12,794,081	36.0	60,821	20.3
Appalachian	74,359,965	65.9	675,969	60.2
White River	17,767,821	57.5	N/D	N/D
Flathead	18,383,736	46.3	N/D	N/D
Arizona National Forests	23,540,573	54.5	N/D	N/D
Central California National Forests	51,225,061	59.4	14,483	11.5
Arkansas National Forests	40,184,951	62.1	747,726	49.9
Total	335,009,819	59.7	2,235,373	47.2

[1]Calculated by dividing values by those in Table 3. Percentages of total forest C stock and accumulation are included. Detailed estimates by forest type are in supplementary Table 4.

National Forests individually or in groups, and different forests or regions can be compared or aggregated using consistent and high-quality data. Furthermore, FIA data have become a standard for many other forest analysis tools and greenhouse gas registries (Hoover et al., 2014), so consistency across platforms is also feasible. Finally, there are developments underway to integrate FIA-based ground data analysis with other approaches based on remote sensing and mapping to support policy and land management (Dugan et al., 2017; Harris et al., 2021; Hurtt et al., 2022), which is the objective of future research building directly on this study and related work (DellaSala et al., 2022a).

Moreover, using CNPP as the threshold for stand maturity is an extension of and a refinement on prior work. The concept of CNPP is closely related to CMAI, which has been used for many decades to describe the point at which tree volume increment is greatest in the maturation of a forest stand for assessing return on investment in forestry operations (e.g., Assmann, 1970; Curtis, 1994) but more recently has been proposed as a way to identify the minimum age of ecosystem maturity for protection efforts (Kerr, 2020). Published CMAI estimates are often derived from managed forests and plantations, which limits their applicability to low-intensity management regimes. Also, CNPP is more closely related than volume to the carbon variables of interest (C and CO_2) for analyses of climate mitigation potential by the forest sector to reduce emissions or remove atmospheric CO_2. Considering the uncertainties of establishing the exact age for forests that did not originate as tree plantations, CNPP and CMAI often occur at similar ages in the life of forests, that is, at or very near the age of crown closure and the onset of tree physiological maturity (Burns and Honkala, 1990; Groover, 2017).

4.3. Uncertainty and data limitations

Most forests or groups of forests studied had sufficient sample plots to keep uncertainty of carbon estimates (described in methods) within 15% of the estimated values (**Tables 1**, **5**). In contrast, the uncertainties of carbon accumulation estimates were significantly larger and more variable, ranging from 13 to 142% of the estimated values (**Table 5**). Although the same number of sample plots were available for both estimates, the variability of C accumulation estimates was much higher in some cases, most likely because C accumulation has higher interannual variability if affected by natural disturbances, tree mortality, and tree growth rates that can vary from year to year. Although the reported uncertainty is related to sample size and variability of the tree populations studied, there is additional uncertainty associated with the biomass models used to estimate above-ground biomass carbon. The error of biomass models typically ranges from about 10–15% for large forest areas, with 95% confidence (US Environmental Protection Agency, 2021).

Our ecosystem C estimates only include above-ground live biomass in trees greater than one-inch (2.4 cm) dbh. C pools in standing and down dead wood, understory vegetation including tree seedlings, litter on the forest floor, and soil C account for significantly more C that could double or quadruple the amount of estimated C stock depending on the geographic location of the forest and other land characteristics such as physiography and soil depth (Domke et al., 2021; US Environmental Protection Agency, 2021). Above-ground live biomass is typically the most dynamic of the C pools in forests, though in some cases, particularly related to logging and natural

disturbance, the dead wood and litter C pools may change significantly over short periods of time (Domke et al., 2021).

Forest age is an important variable used to estimate when NPP reaches a maximum value (CNPP) above which forests are considered mature. However, forest age (or time since disturbance) can be difficult to determine especially for uneven- or multi-aged forests and is based on coring trees and counting tree rings from just a few sample trees on a sample plot in the FIA sampling protocol. It is likely that the sample trees that are cored do not represent the population of larger and older trees on a sample plot, meaning that the assigned age could be biased to younger ages (Stevens et al., 2016). In some cases, the NPP curve is rather flat at and around the age of CNPP, making it difficult to identify the precise age associated with CNPP. Despite these issues, age is an easily understood metric that is closely related to forest maturity, and the approach of identifying the median diameter associated with CNPP using a 30-year window of age classes helps to mask the uncertainty of using age as a critical step in the methodology.

4.4. Policy and management implications

Recent policy goals target "net zero" emissions for all sectors by 2050 to arrest the global climate emergency. Since net zero cannot be achieved by reducing fossil fuel emissions alone (United Nations, 2015; Griscom et al., 2017), the potential of nature-based climate solutions to contribute to this larger goal is the subject of legislation and executive orders in the U.S. The approach and methodology developed here are designed to inform policy makers about federally managed mature forests and their large and vulnerable C stocks and high rates of accumulation of carbon from the atmosphere. Some recent legislation and executive orders specifically call for increased analysis of the current and potential role of mature forests and large trees (White House, 2021, 2022b; U.S. Congress, 2022). The approach and methods presented here provide options for policy makers to consider as the specific land management rules are implemented by agencies for national forest lands.

Our study further corroborates that large areas of mature federal forests are significant carbon sinks that lack protection. Results indicate that 10 of the 11 forests analyzed were carbon sinks over the last decade or so, with the largest sinks occurring in the Eastern U.S. Forests with less disturbance and/or younger age-class distributions had greater increases in above-ground carbon per area than forests with higher rates of disturbance and/or older age-class distributions. These observations reflect multiple factors: the past history of management, trends in incidence and severity of recent natural disturbances and logging, and the inherent age at which the productivity of different forest types begins to level-off or decline. We also note an important distinction that rates of carbon accumulation tend to be higher in younger forests while the largest amounts of stored carbon are found in mature forests. Protecting these carbon sinks and avoiding losses of carbon from logging would require a policy shift to focus more on the potential role of federal forests in climate mitigation (DellaSala et al., 2022a). Such a shift requires considering how both natural disturbances (exacerbated by climate change) and harvesting are emitting carbon stored in larger trees across federal forest lands. In this context, it is notable that national and regional estimates of emissions from logging (direct plus lifecycle emissions) are 5–10 times greater than direct emissions from natural disturbances (wildfire, insects, and wind combined) (Harris et al., 2016; Law et al., 2018).

For operational land management practices, it is often easier to apply a diameter limit in timber operations by species than an age limit by forest type, because as noted previously it can be challenging to determine a precise stand age, whereas measuring tree diameter is simple and accurate [although see DellaSala et al. (2022a) for an alternate approach to stand maturity without age or dbh determinations]. The diameter limits derived here are based on stand age at CNPP and so have that element of maturity embedded in their determination. And, as noted, this approach can be used regardless of the age selected. For some forest types, stand level characterization is obscured by their frequent association with selective logging and/or natural disturbances like wildfire, making larger trees the more appropriate component for defining maturity.

The results presented here by region and forest type reveal that there is a wide variation in CNPP age and associated tree diameters reflecting variation in forest type/composition, climate, competition for resources and soil moisture, disturbance dynamics, site productivity, and geographic region. This variability needs to be considered in developing policies and management practices. It is also important to consider risks of loss to stored C from natural disturbances, and other values of forests that are tied to land management objectives, which may or may not be compatible with increasing C stocks and accumulation.

We developed an approach to assess mature forests and their current carbon stock and accumulation benefits, and applied the methods to 11 different case studies of individual or groups of National Forests that can inform implementing the president's executive order. This method can be applied regardless of how mature stands are defined (e.g., it is readily applicable to age thresholds above CNPP). And this ground-based estimation approach can be linked with remote sensing and mapping approaches (e.g., DellaSala et al., 2022a) to provide a geographic view of forest maturity as well as protected status beyond the reserved/unreserved designation available in the FIA database.

This work can also be extended to more clearly identify that subset of mature forests that are truly old-growth, and estimate the associated carbon stocks and accumulation. As forests get older, they tend to have very large and increasing carbon stocks, making them especially valuable as carbon reserves (DellaSala et al., 2022a; Law et al., 2022). Even when threatened by natural disturbances or climate change, there is substantial evidence that old-growth forests can continue to maintain or increase carbon stocks (Stephenson et al., 2014; Law et al., 2018; Lesmeister et al., 2021; Begović et al., 2022). Building upon our definition of mature forests, future research could further inform management decisions by more clearly and consistently identifying those mature forests that are truly old-growth or that potentially could become old-growth, and estimating their carbon stocks and accumulation.

5. Conclusion

Our study presents a framework for in-depth analysis and management of larger trees and mature forests on federal lands. The integration of basic data about stand age, tree diameter, biomass carbon dynamics, and reserved status comprises the main elements of the methodology. After applying the methods to 11 national forests, we found that the unprotected carbon stock in larger trees in mature stands ranged from 36 to 68% of the total carbon in tree biomass. The unprotected annual carbon accumulation in tree biomass of larger trees in mature stands ranged from 12 to 60% of the total accumulation in all trees. The potential climate impact of avoiding emissions from logging larger trees and mature forests is thus significant. Key discussion points focused on uncertainty, policy implications, and land management practices. This work is highly relevant to emerging policies regarding climate change, nature-based climate solutions, and mature forests including the role of larger trees.

Data availability statement

Publicly available datasets were analyzed in this study. This data can be found here: https://www.fia.fs.usda.gov/tools-data/.

Author contributions

RB led the research along with GR and DD. All authors contributed to the writing.

Funding

This work was funded by a grant from the Natural Resources Defense Council Inc., and ongoing financial support from the Woodwell Climate Research Center.

Conflict of interest

GR and CR were employed by Natural Resources Defense Council, Inc.

The remaining authors declare that the research was conducted in the absence of any commercial or financial relationships that could be construed as a potential conflict of interest.

Publisher's note

Supplementary material

The Supplementary Material for this article can be found online at: https://www.frontiersin.org/articles/10.3389/ffgc.2022.1074508/full#supplementary-material

References

Assmann, E. (1970). *The principles of forest yield study*. Oxford: Pergamon Press, 504.

Bechtold, W. A., and Patterson, P. L. (Eds.) (2005). *The enhanced forest inventory and analysis program - national sampling design and estimation procedures*. Asheville, NC: U.S. Department of Agriculture, Forest Service, Southern Research Station, 85. doi: 10.2737/SRS-GTR-80

Begović, K., Schurman, J. S., Svitok, M., Pavlin, J., Langbehn, T., Svobodová, K., et al. (2022). Large old trees increase growth under shifting climatic constraints: Aligning tree longevity and individual growth dynamics in primary mountain spruce forests. *Glob. Change Biol.* 29, 143–164. doi: 10.1111/gcb.16461

Birdsey, R. A., Dugan, A. J., Healey, S. P., Dante-Wood, K., Zhang, F., Mo, G., et al. (2019). *Assessment of the influence of disturbance, management activities, and environmental factors on carbon stocks of U.S. National Forests. Gen. Tech. Rep. RMRS-GTR-402*. Fort Collins, CO: U.S. Department of Agriculture, Forest Service, Rocky Mountain Research Station, 116. doi: 10.2737/RMRS-GTR-402

Bolsinger, C. L., and Waddell, K. L. (1993). *Area of old-growth forests in California, Oregon, and Washington. Res. Bull. PNW-RB-197*. Portland, OR: U.S. Department of Agriculture, Forest Service, Pacific Northwest Research Station, 26.

Buotte, P. C., Law, B. E., Ripple, W. J., and Berner, L. T. (2020). Carbon sequestration and biodiversity co-benefits of preserving forests

in the western United States. *Ecol. Appl.* 30:e02039. doi: 10.1002/eap.2039

Burns, R. M., and Honkala, B. H. (1990). "Silvics of North America," in *Conifers*, Vol. 1. Washington, DC: U.S.D.A. Forest Service Agriculture Handbook 654.

Curtis, R. O. (1994). *Some simulation estimates of mean annual increment of Douglas-fir: Results, limitations, and implications for management. Res. Pap. PNW-RP-471*. Portland, OR: U.S. Department of Agriculture, Forest Service, Pacific Northwest Research Station, 27.

DellaSala, D. A., Mackey, B., Norman, P., Campbell, C., Comer, P. J., Kormos, C. F., et al. (2022a). Mature and old-growth forests contribute to large-scale conservation targets in the conterminous USA. *Front. For. Glob. Change* 28:979528. doi: 10.3389/ffgc.2022.979528

DellaSala, D. A., Baker, B. C., Hanson, C. T., Ruediger, L., and Baker, W. (2022b). Have Western USA fire suppression and megafire active management approaches become a contemporary Sisyphus? *Biol. Conserv.* 268:109499. doi: 10.1016/j.biocon.2022.109499

Domke, G. M., Walters, B. F., Nowak, D. J., Smith, J. E., Nichols, M. C., Ogle, S. M., et al. (2021). *Greenhouse gas emissions and removals from forest land, woodlands, and urban trees in the United States, 1990–2019. Resource Update FS–307*. Madison, WI: U.S. Department of Agriculture, Forest Service, Northern Research Station, 5. doi: 10.2737/FS-RU-307

Dugan, A. J., Birdsey, R., Healey, S. P., Pan, Y., Zhang, F., Mo, G., et al. (2017). Forest sector carbon analyses support land management planning and projects: Assessing the influence of anthropogenic and natural factors. *Clim. Change* 144, 207–220. doi: 10.1007/s10584-017-2038-5

Fargione, J. E., Bassett, S., Boucher, T., Bridgham, S. D., Conant, R. T., Cook-Patton, S. C., et al. (2018). Natural climate solutions for the United States. *Sci. Adv.* 4:eaat1869. doi: 10.1126/sciadv.aat1869

Gilhen-Baker, M., Giovanni, R., Beresford-Kroeger, D., and Roviello, V. (2022). Old growth forests and large old trees as critical organisms connecting ecosystems and human health. A review. *Environ. Chem. Lett.* 20, 1529–1538.

Griscom, B. W., Adams, J., Ellis, P. W., Houghton, R. A., Lomax, G., Miteva, D. A., et al. (2017). Natural climate solutions. *Proc. Natl. Acad. Sci. U.S.A.* 114, 11645–11650. doi: 10.1073/pnas.1710465114

Groover, A. (2017). *Age-related changes in tree growth and physiology*. Chichester: John Wiley & Sons, Ltd. doi: 10.1002/9780470015902.a0023924

Harris, N. L., Gibbs, D. A., Baccini, A., Birdsey, R. A., de Bruin, S., Farina, M., et al. (2021). Global maps of twenty-first century forest carbon fluxes. *Nat. Clim. Change* 11, 234–240. doi: 10.1038/s41558-020-00976-6

Harris, N. L., Hagen, S. C., Saatchi, S. S., Pearson, T. R. H., Woodall, C. W., Domke, G. M., et al. (2016). Attribution of net carbon change by disturbance type across forest lands of the conterminous United States. *Carbon Balance Manag.* 11:24. doi: 10.1186/s13021-016-0066-5

He, L., Chen, J. M., Pan, Y., Birdsey, R., and Kattge, J. (2012). Relationships between net primary productivity and forest stand age in U.S. forests. *Glob. Biogeochem. Cycles* 26:GB3009. doi: 10.1029/2010GB003942

Hessburg, P. F., Charnley, S., Kendra, L., White, E. M., Singleton, P. H., Peterson, D. W., et al. (2020). *The 1994 eastside screens–large tree harvest limit: Synthesis of science relevant to forest planning 25 years later. Gen. Tech. Rep. PNW-GTR-990*. Portland, OR: U.S. Department of Agriculture, Forest Service, Pacific Northwest Research Station, 114.

Hoover, C., Birdsey, R., Goines, R., Lahm, P., Marland, G., Nowak, D., et al. (2014). "Chapter 6: Quantifying greenhouse gas sources and sinks in managed forest systems," in *Quantifying greenhouse gas fluxes in agriculture and forestry: Methods for entity-scale inventory. Technical bulletin number 1939*, eds. M. Eve, D. Pape, M. Flugge, R. Steele, D. Man, M. Riley-Gilbert, et al. (Washington, DC: U.S. Department of Agriculture, Office of the Chief Economist), 606.

Hudiburg, T., Law, B. E., Stenzel, J., Harmon, M., and Moomaw, W. (2019). Meeting regional GHG reduction targets requires accounting for all forest sector emissions. *Environ. Res. Lett.* 14:095005. doi: 10.1088/1748-9326/ab28bb

Hurtt, G. C., Andrews, A., Bowman, K., Brown, M. E., Chatterjee, A., Escobar, V., et al. (2022). The NASA carbon monitoring system phase 2 synthesis: Scope, findings, gaps and recommended next steps. *Environ. Res. Lett.* 17:063010. doi: 10.1088/1748-9326/ac7407

Johnson, K. N., and Swanson, F. J. (2009). "Historical context of old-growth forests in the Pacific Northwest–policy, practices, and competing worldviews," in *Old growth in a new world: A Pacific Northwest icon reexamined*, eds. T. A. Spies and S. L. Duncan (Washington, DC: Island Press), 12–28.

Johnston, J. D., Greenler, S. M., Miller, B. A., Reilly, M. J., Lindsay, A. A., and Dunn, C. J. (2021). Diameter limits impede restoration of historical conditions in dry mixed-conifer forests of eastern Oregon, USA. *Ecosphere* 12:e03394. doi: 10.1002/ecs2.3394

Kerr, A. (2020). *Defining the minimum age of a mature forest in either legislation or regulation*. Ashland, OR: The Larch Company, 13.

Kirschbaum, M. U. F. (2003). To sink or burn? A discussion of the potential contributions of forests to greenhouse gas balances through storing carbon or providing biofuels. *Biomass Bioener.* 24, 297–310.

Kutsch, W. L., Wirth, C., Kattge, J., and Nollert, S. (2009). "Ecophysiological characteristics of mature trees and stands–Consequences for old-growth forest productivity," in *Old-growth forests*, eds. C. Wirth, G. Gleixner, and M. Heimann (Berlin: Springer), 57–79. doi: 10.1007/978-3-540-92706-8_4

Law, B. E., and Harmon, M. E. (2011). Forest sector carbon management, measurement and verification, and discussion of policy related to climate change. *Carbon Manage.* 2, 73–84. doi: 10.4155/cmt.10.40

Law, B. E., Hudiburg, T. W., Berner, L. T., Kent, J. J., Buotte, P. C., and Harmon, M. (2018). Land use strategies to mitigate climate change in carbon dense temperate forests. *Proc. Nat. Acad. Sci. U.S.A.* 115, 3663–3668. doi: 10.1073/pnas.1720064115

Law, B. E., Moomaw, W. R., Hudiburg, T. W., Schlesinger, W. H., Sterman, J. D., and Woodwell, G. M. (2022). Creating strategic reserves to protect forest carbon and reduce biodiversity losses in the United States. *Land* 11:721. doi: 10.3390/land11050721

Lesmeister, D. B., Davis, R. J., Sovern, S. G., and Yang, Z. (2021). Northern spotted owl nesting forests as fire refugia: A 30-year synthesis of large wildfires. *Fire Ecol.* 17:32. doi: 10.1186/s42408-021-00118-z

Lindenmayer, D. B., Laurance, W. F., and Franklin, J. F. (2012). Global decline in large old trees. *Science* 338, 1305–1306.

Lutz, J. A., Furniss, T. J., Johnson, D. J., Davies, S. J., Allen, D., Alonso, A., et al. (2018). Global importance of large-diameter trees. *Glob. Ecol. Biogeogr.* 2018, 849–864. doi: 10.1111/geb.12747

McArdle, R. E. (1930). *The yield of Douglas fir in the Pacific Northwest. Technical bulletin No. 201*. Washington, DC: U.S. Department of Agriculture.

Mildrexler, D. J., Berner, L. T., Law, B. E., Birdsey, R. A., and Moomaw, W. R. (2020). Large trees dominate carbon storage in forests east of the cascade crest in the United States Pacific Northwest. *Front. For. Glob. Change* 3:594274. doi: 10.3389/ffgc.2020.594274

Moomaw, W. R., Law, B. E., and Goetz, S. J. (2020). Focus on the role of forests and soils in meeting climate change mitigation goals: Summary Environ. *Res. Lett.* 15:045009.

Moomaw, W. R., Masino, S. A., and Faison, E. K. (2019). Intact forests in the United States: Proforestation mitigates climate change and serves the greatest good. *Front. For. Glob. Change* 2:27. doi: 10.3389/ffgc.2019.00027

Stanke, H., Finley, A. O., Weed, A. S., Walters, B. F., and Domke, G. M. (2020). rFIA: An R package for estimation of forest attributes with the US Forest Inventory and Analysis database. *Environ. Model. Softw.* 127:104664. doi: 10.1016/j.envsoft.2020.104664

Stephenson, N. L., Das, A. J., Condit, R., Russo, S. E., Baker, P. J., Beckman, N. G., et al. (2014). Rate of tree carbon accumulation increases continuously with tree size. *Nature* 507, 90–93. doi: 10.1038/nature12914

Stevens, J. T., Safford, H. D., North, M. P., Fried, J. S., Gray, A. N., Brown, P. M., et al. (2016). Average stand age from forest inventory plots does not describe historical fire regimes in ponderosa pine and mixed-conifer forests of western North America. *PLoS One* 11:e0147688. doi: 10.1371/journal.pone.0147688

U.S. Congress (2022). *Public law no: 117-169. Inflation reduction act of 2022*. Washington, DC: U.S. Congress.

United Nations (2015). "Framework convention on climate change," in *Proceedings of the 21st conference of the parties adoption of the Paris agreement*, (Paris: United Nations).

US Environmental Protection Agency (2021). *Inventory of U.S. Greenhouse gas emissions and sinks: 1990–2019. EPA 430-R-21-005*. Washington, DC: US Environmental Protection Agency.

USDA Forest Service (2022). *EVALIDator user guide*. Washington, DC: USDA Forest Service.

USGS (2019). *GAP analysis project protected areas, PAD-US vision*. Reston, VA: USGS.

Watson, J. E. M., Evans, T., Venter, O., Williams, B., Tulloch, A., Stewart, C., et al. (2018). The exceptional value of intact forest ecosystems. *Nat. Ecol. Evol.* 2, 599–610. doi: 10.1038/s41559-018-0490-x

White House (2021). *Executive order 14008–tackling the climate crisis at home and abroad*. Washington, DC: White House.

White House (2022a). *Fact sheet: Biden-Harris administration announces roadmap for nature-based solutions to fight climate change, strengthen communities, and support local economies*. Washington, DC: White House.

White House (2022b). *Executive order 14072–strengthening the Nation's forests, communities, and local economies*. Washington, DC: White House.

Wirth, C., Messier, C., Bergeron, Y., Frank, D., and Fankhänel, A. (2009). "Old-growth forest definitions: A pragmatic view," in *Old-growth forests. ecological studies*, Vol. 207, eds. C. Wirth, G. Gleixner, and M. Heimann (Berlin: Springer). doi: 10.1007/978-3-540-92706-8_2

Woodall, C. W., Heath, L. S., Domke, G. M., and Nichols, M. C. (2011). *Methods and equations for estimating aboveground volume, biomass, and carbon for trees in the U.S. forest inventory, 2010. GTR NRS-88*. Newtown Square, PA: U.S. Department of Agriculture, Forest Service, Northern Research Station, 30.

JOURNAL OF GEOPHYSICAL RESEARCH, VOL. 112, G04014, doi:10.1029/2007JG000451, 2007

Pyrogenic carbon emission from a large wildfire in Oregon, United States

John Campbell,[1] Dan Donato,[1] David Azuma,[2] and Beverly Law[1]

Received 21 March 2007; revised 1 September 2007; accepted 25 September 2007; published 27 December 2007.

[1] We used a ground-based approach to compute the pyrogenic carbon emissions from the Biscuit Fire, an exceptionally large wildfire, which in 2002 burned over 200,000 ha of mixed conifer forest in southwestern Oregon. A combination of federal inventory data and supplementary ground measurements afforded the estimation of preburn densities for 25 separate carbon pools at 180 independent locations in the burn area. Average combustion factors for each of these pools were then compiled from the postburn assessment of thousands of individual trees, shrubs, and parcels of surface and ground fuel. Combustion factors were highest for litter, duff, and foliage, lowest for live woody pools. Combustion factors also increased with burn severity as independently assessed from remote imagery, endorsing the use of such imagery in scaling emissions to fire area. We estimate the total pyrogenic carbon emissions from the Biscuit Fire to be between 3.5 and 4.4 Tg C (17 and 22 Mg C ha^{-1}) depending on uncertainty in our ability to estimate preburn litter pools and mineral soil combustion with a central estimate of 3.8 Tg C (19 Mg C ha^{-1}). We estimate that this flux is approximately 16 times the annual net ecosystem production of this landscape prior to the wildfire and may have reduced mean net biome production across the state of Oregon by nearly half in the year 2002.

Citation: Campbell, J., D. Donato, D. Azuma, and B. Law (2007), Pyrogenic carbon emission from a large wildfire in Oregon, United States, *J. Geophys. Res.*, *112*, G04014, doi:10.1029/2007JG000451.

1. Introduction

[2] Efforts to quantify carbon exchange between terrestrial vegetation and the atmosphere have typically focused on patterns of photosynthesis and respiration. While complex in nature, basic mechanistic understanding of physiology and soil processes has been used in models to predict vegetation responses over broad spatial and temporal domains. In contrast, pyrogenic releases of carbon from vegetation to the atmosphere, while physically simple, are inherently stochastic and therefore not typically included in most process-based models [*Schimel and Baker*, 2002; *Arora and Boer*, 2005].

[3] This deficiency in global vegetation modeling was made apparent following the El Niño of 1997–1998 when an anomalous two-fold increase in global atmospheric CO_2 enrichment was attributed to pyrogenic emissions from Southeast Asian wildfires [*Page et al.*, 2002; *van der Werf et al.*, 2004]. Interest in this phenomenon, combined with advances in remote detection of wildfire [*Lentile et al.*, 2006], concerns over fuel-driven increases in fire frequency and severity in the western United States [*Schoennagel et al.*, 2004], and possible feedbacks between global warming and wildfire frequency [*Westerling et al.*, 2006] has resulted in a number of large-scale, bottom-up efforts to quantify pyrogenic emissions from Africa [*Barbosa et al.*, 1999], Alaska [*French et al.*, 2002; *Kasischke and Bruhwiler*, 2002; *French et al.*, 2004], Siberia [*Soja et al.*, 2004], China [*Lü et al.*, 2006], and North America [*Wiedinmyer et al.*, 2006]. All of these studies use the same general measure-and-multiply approach popularized by *Seiler and Crutzen* [1980], where pyrogenic emissions are calculated as the product of four parameters: area burned, fuel density (biomass per unit area), combustion factor (fraction of biomass consumed by fire), and emission factor (mass of a given chemical species released per mass of fuel consumed). For the most part, the area affected by fire can be accurately assessed either remotely or from inventories and there is general agreement on the emission factors for carbon and other airborne pollutants. However, while most studies recognize the need to vary the inputs of fuel density by vegetation type and the combustion factors by fire severity, the ground data needed to parameterize these functions has been deeply lacking. This is especially true for combustion factors that are compiled from a limited source of widely varying data [see *Peterson and Sandberg*, 1988; *Soja et al.*, 2004; *Wiedinmyer et al.*, 2006] and simple assumptions on how these factors vary with respect to an operationally defined fire severity classification. To improve our regional and global estimates of pyrogenic emissions, it is necessary to improve the specificity and accuracy of our

[1]Department of Forest Science, Oregon State University, Corvallis, Oregon, USA.
[2]Forest Sciences Laboratory, U.S. Forest Service, Portland, Oregon, USA.

0148-0227/07/2007JG000451$09.00

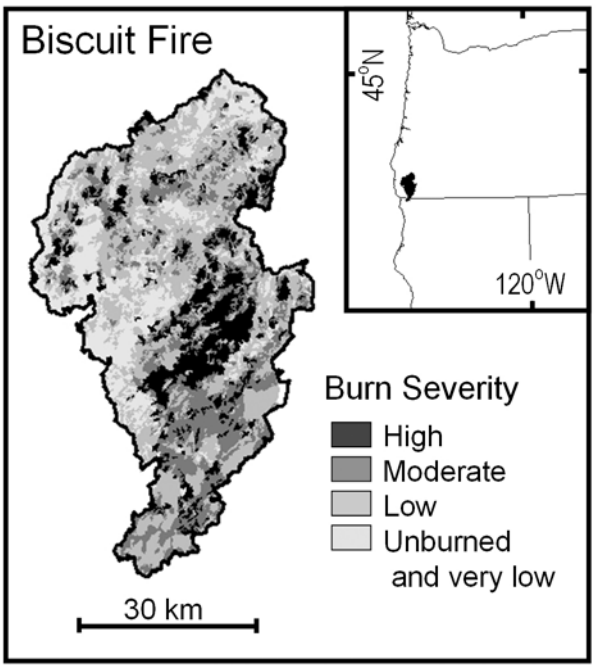

Figure 1. The Biscuit Fire. The Biscuit Fire burned at a mix of severities over 200,000 ha of forest in the Siskiyou Mountains of southwestern Oregon and northern California in the summer of 2002 making it the largest contiguous wildfire in Oregon history. The severity classes shown are those of the remotely derived 2002 BAER classification.

estimates of fuel density and combustion factors beyond what is generally available [*Houghton et al.*, 2000], especially for temperate ecosystems where quantification of fire effects lags behind that of boreal systems.

[4] In this study we consider an exceptionally large wildfire, the Biscuit Fire, which in 2002 burned over 200,000 ha of mixed conifer forest in southwestern Oregon. Carbon emissions from a fire this large are likely to contribute sizably to the annual carbon budget of the region [*Law et al.*, 2004]. Accurate quantification of this flux has been limited by our understanding of the amount of fuel present and the fraction actually combusted. Conveniently, however, the Biscuit perimeter encompassed 180 systematically located U.S. Department of Agriculture (USDA) Forest Service inventory plots. Structural measurements made on these plots before and after the fire, combined with biomass measurements on additional plots, now afford an assessment of preburn fuel density and combustion factors across a combination of forest types, ages, and burn severities unprecedented for a single fire.

[5] Our objectives were to: (1) Determine combustion factors (as a probability distribution) for each of 25 different forest carbon pools representing different fuel types. (2) Assess variation in the above combustion factors as a function of remotely sensed burn severity. (3) Combine the combustion factors with estimates of preburn fuel densities and burn area by severity to estimate fire-wide pyrogenic carbon emission. (4) Assess the utility of federal inventory plots as a method of compiling much needed fuel density and combustion factors. Results are then considered in the context of regional carbon fluxes over time for the same forest and throughout the region in the year of the fire.

2. Methods

2.1. Study Sites

[6] The Biscuit Fire burned at a mix of severities across 200,000 ha of forest in the Siskiyou Mountains of southwestern Oregon and northern California in the summer of 2002, making it the largest contiguous wildfire on record for Oregon (see Figures 1 and 2). The Siskiyou Mountains are characterized by a variety of forest types from Douglas-fir/western hemlock/bigleaf maple communities on mesic sites, to Douglas-fir/tanoak on drier sites, to Jeffrey pine on ultramafic substrates [see *Whittaker*, 1960].

[7] Within the perimeter of the Biscuit Fire there are 180 regularly spaced permanent federal inventory plots (i.e., systematic sample design). In these one-hectare plots (referred to hence forth as inventory plots), metrics to quantify biomass, composition, and various structural attributes have been collected in approximate 10-year intervals since 1970 [see *USDA*, 1995]. The most recent measurements before the Biscuit Fire were made between 1993 and 1997. A 2003–2004 measurement cycle in the years following the fire was then conducted in which additional metrics quantifying fire effects were collected [see *USDA*, 2003].

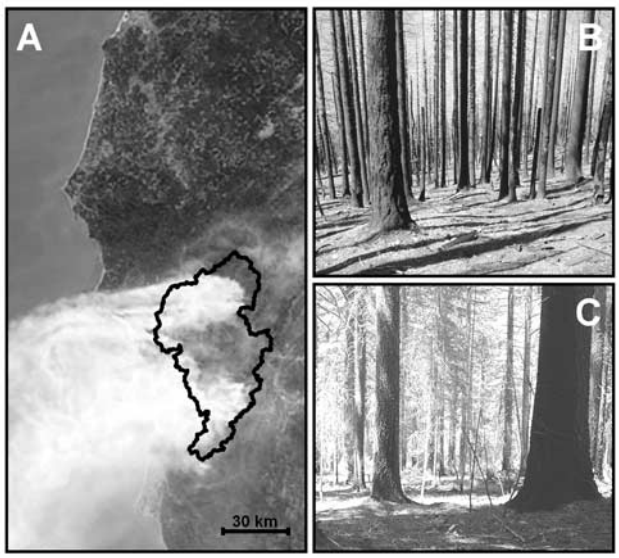

Figure 2. Images from the Biscuit Fire showing (a) the smoke plume drifting over the Pacific Ocean, (b) a forest stand which burned at high severity, and (c) a forest stand which burned at low severity. The black line on Figure 2a denotes the final perimeter of the fire. Even in the most severely burned stands in the Biscuit, where mortality reached 100% and fine surface fuels were completely combusted, tree boles and fine branches remained largely intact. Typical low severity burn in the Biscuit was characterized by bole scorching, minimal canopy mortality, and partial consumption of understory vegetation and ground fuels. Photo for Figure 2a provided by NASA Visible Earth (http://visibleearth.nasa.gov/); photos for Figures 2b and 2c courtesy of Joe Fontaine and Dan Donato.

[8] While data from the inventory plots provided detailed measurements of fire effects on the boles and crowns of most trees, as well as most detritus pools, they did not include fire effects on coarse woody detritus and smaller woody stems killed in the fire. To assess the effects of the Biscuit Fire on these carbon pools, we made pertinent measurements (see below) in 2004 on 54 additional one-hectare plots (referred to hence forth as supplementary plots) randomly located within 54 independent forest stands deliberately distributed across burn severities, including areas unaffected by fire.

2.2. Pyrogenic Emissions

[9] Following the approach of *Seiler and Crutzen* [1980], pyrogenic carbon emissions from the Biscuit Fire were computed according to equation (1):

$$PE = \sum_{i=1,j=1}^{n} A_i\left(D_{ij} \cdot CF_{ij}\right) \quad (1)$$

where PE is pyrogenic emission in mass of carbon, A is the area affected by burn severity class i, D is the preburn carbon density in mass per unit area of carbon pool j averaged across plots of burn severity i, and CF (hence forth referred to as combustion factor) is the fraction of preburn carbon pool j combusted in burn severity class i. In this study we recognize four burn severities: high, moderate, low, and unburned/very low; and 25 separate carbon pools separated by tissue type, growth form, size class, and mortality status.

2.3. Pool-Specific Combustion Factors

[10] The methods for calculating combustion factors specific to various carbon pools are shown in Table 1. We used two basic approaches for arriving upon combustion factors: (1) a back-calculation method where combustion factors are calculated solely from postburn measurements of charring and perceived loss of foliage and branches, and (2) a before-and-after method where combustion factors are calculated as the difference between preburn and postburn mass. As a general rule, the combustion factor of large carbon pools and those that experience low fractional combustion (i.e., live stem wood) are more precisely assessed using the back-calculation method since the sampling error associated with before-and-after comparisons would result in unacceptably low signal-to-noise ratios. Conversely, the combustion factor of smaller carbon pools and those that experience high fractional combustion (i.e., fine woody debris and surface litter) are more precisely assessed using the before-and-after method since postburn measurements reveal little regarding the preburn pool size.

[11] For each separate carbon pool, combustion factors were assessed at the finest possible scale (see Table 1). For instance, since the impacts of fire on foliage, bark, and stem wood were measured separately on each tree, combustion factors for these pools were computed separately for each tree. When measurements represented plot-level average responses (e.g., downed wood), combustion factors were computed at the plot level.

[12] Unlike tissue combustion in larger trees, much of the losses in smaller trees (<7 cm DBH; diameter at 1.37 m above ground) occurs as a result of complete tree combustion. To quantify the incidence of complete combustion of small diameter trees, the frequency of small conifers was compared between burned and unburned plots. The apparent deficit of small diameter trees in burned plots was attributed to complete combustion (see Table 1). Similarly, we investigated the need to account for complete combustion of stumps and other coarse woody detritus, which was not assessed in the postburn inventory. However, despite anecdotal evidence of complete combustion of stumps and logs, there was no detectable difference in these pools between burned and unburned plots; consequently carbon losses due to their complete combustion are believed to be trivial.

2.4. Preburn Carbon Density

[13] Preburn carbon density for each recognized carbon pool was computed for each inventory plot using preburn survey data and a combination of allometric scaling equations appropriate for species in the region. Tree bole mass was estimated with species- and site-specific allometric equations relating stem diameter to volume and species-specific wood density values [*van Tuyl et al.*, 2005]. Foliage and bark mass were estimated directly from species- and site-specific allometric equations [*Means et al.*, 1994]. The mass of downed woody detritus was computed from line intercept data using geometric scaling and species-specific wood density values [*Harmon and Sexton*, 1996]. Biomass of small hardwoods (including shrubs) was determined using allometric equations derived empirically from tissue harvests made in the region of the Biscuit Fire: stem mass in g = 2203(1 − exp(−0.0002(shrub volume in dm^3))); foliage mass in g = 6498(1 − exp(−0.0001(shrub volume in dm^3))). Ocular estimates of total grass and forb coverage was converted to biomass using 4.0 g m^{-2}, which is the average mass per unit coverage reported for common local species [*Means et al.*, 1994].

[14] Because litter and duff masses were not recorded on the inventory plots prior to the fire, it was necessary to estimate preburn masses for these pools from samples collected in 2004 from locations distributed throughout the Biscuit area but unaffected by fire. Recognizing that these preburn carbon pools varied across the forests affected by the Biscuit, we originally set out to collect unburned litter and duff samples from a variety of cover types and apply these cover type-specific masses to each inventory plot according to the plot's location on a cover type map. However, upon collecting these samples it became apparent that both inaccuracies in the cover type map and variability in forest floor (soil O-horizon) depth within forest type were leading to false accuracy. Considering this, we decided to aggregate forest types on the Biscuit into the two most distinct classes: (1) low biomass forests growing on ultramafic (serpentine) substrates, and (2) higher biomass forests growing on nonultramafic substrates. Sampling involved the collection of six-inch-diameter parcels of forest floor from 8 to 32 points from each of 43 independent plots distributed throughout the Biscuit perimeter (11 in ultramafic sites, 32 in nonultramafic sites). Samples were dried, separated into duff and litter, and produced four separate values: 1691 and 993 g m^{-2} for litter and duff on ultramafic substrates, respectively; 2000 and 1399 g m^{-2} for litter and

Table 1. Methods and Decision Rules for Computing Combustion Factors for Various Carbon Pools[a]

Carbon Pool	Method for Deriving Combustion Factor	Sample Size and Source
Foliage (large live trees)	The fraction of foliage reported missing from each tree via ocular estimate was equated to the fraction combusted and then corrected to account for foliage killed and dropped but not combusted based on postburn measurements of new litter accumulation.	13,000 trees in inventory plots
Branch (large live trees)	The fraction of branch and twigs reported missing from each tree via ocular estimate in the inventory records was equated to the fraction combusted.	13,000 trees in inventory plots
Bark (large live trees)	Computed for each tree as the product of: fraction of bole surface charred (derived from fire scar measurements), fraction of bark depth charred (determined through supplementary measurements to average 0.29 independent of fire severity), and fraction of mass loss resulting from charring (assumed to be 0.9, 0.5, 0.4 for high, moderate, and low severity plots, respectively crudely extrapolated from *Czimczik et al.* [2002] and assuming a maximum bark temperature of 500°C).	13,000 trees in inventory plots
Bole (large live trees)	No bole wood consumption was reported in either the inventory or supplementary plots for these larger live trees. Therefore, combustion was assumed to be negligible.	not applicable
Bole, bark, branch, and foliage (small live conifers)	Based on a comparison of density and size class distribution between burned and unburned plots, complete combustion of all tissues was determined to occur at a frequency of 0.6, 0.6, and 0.4 for high, moderate, and low severity plots, respectively. Bark, branch, and foliage loss for trees not fully combusted was assumed to be equal to that of larger trees.	430 trees in supplementary plots
Bole, bark, branch, and foliage (small live hardwoods)	Tissue combustion was determined for each stem as the difference between postburn volume (computed allometricly from basal diameter and stem height) and preburn volume (extrapolated allometricly from postburn basal diameter).	480 trees in supplementary plots
Bole, bark, branch, (standing dead trees)	Tissue combustion was computed by the same methods used for live trees except that in cases where bark was absent surface char was assessed as wood rather than bark combustion. Field records of char depth, while variable, indicate no difference between live and dead trees.	1,200 trees in inventory plots
Downed dead wood (large)	A lack of data on char severity for large downed wood prevented direct assessment. Instead the combustion factors for large downed wood was assumed to be twice that of standing dead wood.	not applicable
Downed dead wood (medium and small)	Fraction combusted was determined for each plot as the difference between preburn and postburn debris volume (determined line intercept transects).	180 inventory plots
Litter (O_i-horizon, including leaf litter and woody fragments <0.51 cm diameter)	Computed occular estimates of burn effects on 13.5m2 plots as $(a + 0.5b)/c$ where, a is the sum area of all sublitter surfaces indicating total litter combustion (light and deeply charred duff, mineral soil and rock), b is the area over which litter was reported as lightly charred, and c is total area believed to be covered by litter prior to the fire (the sum of all surfaces covered by uncharred litter, lightly charred litter, and all sublitter surfaces showing some charring).	720 inventory subplots
Duff (O_e and O_a - horizon)	Computed from postburn surveys with the same equation used for litter substituting duff char values for that of litter and referring only to subduff layers as indicators of duff loss.	720 inventory subplots
Mineral soil (A and B - horizon including fine roots to 10 cm)	Combustion of mineral soil C was assessed only when postburn surveys reported either a deeply charred mineral surface (in which case all C in the top 4 cm of soil was presumed combusted) or a moderately charred mineral surface (in which case all C in the top 2 cm of soil was presumed combusted).	720 inventory subplots

[a]Large refers to >7.62 cm DBH for trees and fragment diameter for dead wood; Small refers to <7.62 cm DBH for trees and fragment diameter for dead wood. Sample size refers to the number of independent events assessed across the fire. For details regarding postfire samplinmg procedures, see *USDA* [2003].

duff on nonultramafic substrates, respectively. To verify our estimates of preburn litter and duff were reasonable, we compared our numbers to modeled estimates using the FCCS national fuel bed map and associated fuel loadings [*Sandberg et al.*, 2001; *Ottmar et al.*, 2007] (http://www.fs.fed.us/pnw/fera/fccs). As shown in Table 2, differences in cover type partitioning between that of our study and that of the FCCS do not permit comparisons at scales smaller then the entire fire. When comparing values across the entire Biscuit, our values for duff mass were lower than that of FCCS and our values for litter mass were higher than that of FCCS suggesting a discrepancy in the operational definition of litter and duff between the two methodologies. However, the sum of litter and duff (i.e., forest floor) is in general agreement between the two approaches with the FCCS predicting only 30% more mass fire wide than we estimated from our sampling.

[15] A considerable portion of the Biscuit reburned the 38,000-hectare 1987 Silver Fire, introducing the possibility that fuel masses were different for these parts of the Biscuit. However, the pre-Biscuit inventory was conducted between 1993 and 1997, 6–11 a after the Silver Fire; thus most such differences were implicitly accounted for in the inventory plot data. As for litter and duff masses, which were not

Table 2. A Comparison of Modeled Forest Floor Mass to That Measured for This Study

Forest Cover Type	Fraction of Biscuit Area	Preburn C Pool, kg C ha^{-1}		
		Litter	Duff	Total Forest Floor[a]
Modeled from FCCS database[b]				
(2) W.hemlock/W.redcedar/Douglas-fir	0.53	4000	21075	25075
(7) Douglas-fir/Sugar pine/Tanoak	0.15	1277	21523	22800
(28) Ponderosa pine savanna	0.09	986	4078	5064
(38) Douglas-fir/Madrone/Tanoak	0.09	3193	8291	11484
(10,24,47,48,52,53,59) All others	0.14	2426	38596	41022
All combined and weighted by class	1.00	2989	19663	22652
From field measurements in this study				
Forest on nonultramafic substrates	0.72	10001	6993	16994
Forest on ultramafic substrates	0.28	8455	4966	13421
All combined and weighted by class	1.00	9562	6417	15979

[a]The sum of litter amd duff.
[b]Number codes correspond to mapped FCCS fuel bed types.

measured in the pre-Biscuit inventory and were derived from our supplementary sampling, the absence of unreburned Silver Fire area prohibited direct sampling of this condition to assess forest floor masses in those stands prior to reburning. We addressed this issue by collecting forest floor samples from the nearby Galice Fire, which burned the same year as the Silver Fire but did not reburn in the Biscuit. Litter and duff masses in the Galice were not discernibly different from those collected from unburned sites, suggesting that the forest floor in the Silver area had recovered to preburn levels by the time the Biscuit burned.

[16] An estimate of the carbon present in the top 10 cm of mineral soil throughout the area affected by the Biscuit was based on a rock-free soil carbon fraction of 0.10, a rock-free soil bulk density of 0.89 g cm^{-3}, a fine root mass of 0.01 g cm^{-3}, (determined from 96 soil cores taken on 3 unburned plots) and a rock fraction of 0.50 by volume chosen to represent both the typical and highly skeletal substrates present in the Siskiyou mountains. We assumed the carbon content of all pools to be 0.50 by mass (a standard approximation) except for the litter and duff pools which we assumed to be 0.40 (based on Dumas combustion of 36 field samples producing an average of 0.40 and a standard deviation of 0.08).

2.5. Binning of Data by Burn Severity

[17] To assess carbon combustion as a function of burn severity, each of the study plots was classified as one of four burn severities (e.g., high, moderate, low, or unburned/very low) based on an overlay of the Biscuit BAER (Burned Area Emergency Rehabilitation) fire severity map. The levels of severity in the BAER map were based on classification of the differenced normalized burn ratio (dNBR), a widely used index of burn severity derived from Landsat data [*Miller and Yool*, 2002; *van Wagtendonk et al.*, 2004; *Key and Benson*, 2005]. dNBR is a measure of prefire to postfire change in the ratio of near- to short-wave infrared spectral reflectance [*Key and Benson*, 2005]. BAER assessments are used by federal land management agencies for remediation reconnaissance and are independent of any of the measurements used to compute combustion in this study. Then each of the approximately 60,000 separate combustion computations made for individual trees, plots of ground cover, or debris transects were binned by the burn severity of the plot in which the record was taken and averaged to produce the values CF_{ij} in equation (1). This approach allowed us to assess the ability of BAER severity classification to detect within-fire variability in the combustion of various carbon pools and therefore the utility of BAER severity in scaling combustion factors for other fires. Similarly, to account for possible interaction between preburn carbon density and subsequent burn severity, the preburn carbon densities of each for each plot were averaged by BAER severity classification to produce the values *Dij* in equation (1). Finally, the total area affected by each burn severity class in the Biscuit Fire perimeter (value A_i in equation (1)) was determined from the BAER severity map to be 32, 46, 84, and 41 thousand ha for the high, moderate, low, and unburned/very low severities, respectively. While several different burn severity maps are available for the Biscuit, we chose BAER because it is among the most readily available and widely used burn severity classification for wildfires in the western United States.

3. Results

3.1. Combustion Factors

[18] The combustion factors estimated for each carbon pool and burn severity class are shown in Table 3. Discrepancies between mean and median values indicate a right skew in the event probability in high severity plots and a left skew in the lower severity plots. In other words, while combustion scales to the landscape according to the average of that experienced by individual trees or specified patches of litter, most individuals in low severity plots are affected by fire to a much lesser degree than the average of individuals located in low severity plots. Conversely, most individuals in high severity plots are affected by fire to a much greater degree than the average of individuals located in high severity.

[19] Nearly all 25 carbon pools show a monotonic increase in combustion factor as burn severity increases from the unburned-very low class through to the high severity class (Table 3). Such a consistent trend for ground, surface, and canopy fuels is an endorsement of the BAER severity classification for distinguishing the fraction of carbon combusted from different pools. Such trends are especially clear in the highly combustible ground and surface pools such as litter and fine woody detritus. This relationship between remotely assessed fire severity and ground and

Table 3. Average (and Median) Combustion Factors by Carbon Pool and Burn Severity

Forest Carbon Pool (Fuel Type)	Combustion Factor[a]							
	High Severity		Moderate Severity		Low Severity		Unburned and Very-Low Severity	
Foliage								
Large conifers	0.69	(0.98)	0.27	(0.01)	0.08	(0.00)	0.02	(0.00)
Large hardwoods	0.58	(0.87)	0.29	(0.00)	0.12	(0.00)	0.03	(0.00)
Small conifers	0.89	(1.00)	0.76	(1.00)	0.44	(0.07)	0.01	(0.00)
Small hardwoods	1.00	(1.00)	0.80	(1.00)	0.50	(0.00)	0.00	(0.00)
Grass and forbs	1.00	(1.00)	0.76	(0.88)	0.75	(0.87)	0.70	(0.83)
Branch								
Large conifers	0.05	(0.08)	0.02	(0.00)	0.00	(0.00)	0.00	(0.00)
Large hardwoods	0.05	(0.06)	0.02	(0.00)	0.01	(0.00)	0.00	(0.00)
Small conifers	0.64	(1.00)	0.69	(1.00)	0.41	(0.00)	0.00	(0.00)
Small hardwoods	0.79	(0.81)	0.63	(0.65)	0.40	(0.41)	0.00	(0.00)
Bark								
Large conifers	0.20	(0.26)	0.06	(0.03)	0.03	(0.01)	0.01	(0.01)
Large hardwoods	0.22	(0.26)	0.11	(0.15)	0.03	(0.00)	0.01	(0.00)
Small conifers	0.70	(1.00)	0.70	(1.00)	0.42	(0.05)	0.01	(0.01)
Small hardwoods	0.79	(0.81)	0.63	(0.65)	0.40	(0.41)	0.00	(0.00)
Bole								
Large conifers	0.00	(0.00)	0.00	(0.00)	0.00	(0.00)	0.00	(0.00)
Large hardwoods	0.00	(0.00)	0.00	(0.00)	0.00	(0.00)	0.00	(0.00)
Small conifers	0.61	(1.00)	0.68	(1.00)	0.40	(0.00)	0.00	(0.00)
Small hardwoods	0.79	(0.81)	0.63	(0.65)	0.40	(0.41)	0.00	(0.00)
Dead wood								
Large standing	0.12	(0.07)	0.04	(0.03)	0.02	(0.01)	0.02	(0.00)
Small standing	0.61	(1.00)	0.68	(1.00)	0.40	(0.00)	0.00	(0.00)
Large downed	0.24	(0.14)	0.08	(0.06)	0.04	(0.02)	0.04	(0.01)
Medium downed	0.79	(1.00)	0.73	(0.83)	0.67	(0.76)	0.62	(0.67)
Small downed	0.78	(0.83)	0.58	(0.62)	0.61	(0.70)	0.62	(0.69)
Forest floor and soil[b]								
Litter	1.00	(1.00)	0.76	(0.88)	0.75	(0.87)	0.70	(0.83)
Duff	0.99	(0.99)	0.51	(0.64)	0.54	(0.75)	0.44	(0.50)
Soil to10 cm	0.08	(0.05)	0.04	(0.01)	0.04	(0.01)	0.02	(0.00)

[a]Fraction of preburn mass lost to combustion.
[b]Litter is O_i horizon, duff is O_e and O_a horizon, soil is all mineral soil to a depth of 10 cm including fine roots. For live trees, small is <7.62 cm DBH; large is >7.62 cm DBH. For dead wood, small is 0.51–2.54 cm, medium is 2.54–7.62 cm, and large is >7.62 cm diameter.

surface fuel combustion was not a foregone conclusion, as fire effects on the ground can often be decoupled from fire effects in the canopy [*Pyne et al.*, 1996; *van Wagner*, 1977]. While litter, duff, and small woody detritus combustion was lowest in the unburned-very low severity plots, the fact that the values still average 60% combustion indicate just how prevalent surface fire was across all of the Biscuit Fire. Field records confirm that, of the 41 inventory plots that were remotely classified as unburned-very low, only two showed no sign of surface fire.

[20] Combustion factors also varied expectedly among carbon pools. Pools with larger surface to volume ratios (e.g., foliage, small stems, and litter) showed consistently higher combustion factors than those with lower surface to volume ratios (e.g., large tree boles). This is consistent with most fire behavior models which equate fuel fragment size inversely to their propensity for desiccation and combustibility [*Reinhardt et al.*, 1997].

3.2. Preburn Carbon Pools

[21] Preburn carbon mass for each pool and burn severity class is shown in Table 4. As is the case with most mature forest landscapes, biomass is concentrated in the largest trees. Differences in biomass among burn severities reflect the tendency for stands with more small trees and fewer large trees to burn at higher severity, a finding consistent with that of *Azuma et al.* [2004]. Notably, this trend is reversed for dead wood in that higher severity plots had consistently lower amounts of coarse woody detritus prior to the fire. To aid in comparison with other wildfire research [e.g., *Ottmar et al.*, 2007], preburn carbon pools were also summarized according to conventional fuel categorization and expressed in total dry mass per unit area along with corresponding combustion factors in Table 5.

3.3. Total Pyrogenic Emissions and Sources

[22] Using equation (1) to combine the combustion factors of Table 3, the preburn carbon pools of Table 4, and the area exposed to each burn severity class (see methods above) yields a Biscuit-wide pyrogenic emission of 3.8 Tg C. Here, the two largest sources of pyrogenic emissions were both from the forest floor. As shown in Table 6, 31% of the total pyrogenic emissions arose from combustion of the litter layer and another 26% arose from combustion of the underlying duff and mineral soil layers. The next largest source was the combustion of dead wood which contributed 19% to total emissions. The relative contribution of different pools to total emissions was largely the same when carbon losses were computed separately by burn severity class, with the litter and duff pools being the largest contributors. However, as burn severity decreases there is a slight shift in major combustion sources from the canopy

Table 4. Average Carbon Density by Forest Carbon Pool and Burn Severity[a]

	Carbon Density, kg C ha^{-1}				
Forest Carbon Pool	High Severity	Moderate Severity	Low Severity	Unburned Very Low Severity	All Burn Severities
Foliage					
Large conifers	2853	3045	3397	3670	3242
Large hardwoods	1152	234	1594	3813	1698
Small conifers	1172	3272	1746	1260	1863
Small hardwoods	378	397	431	461	417
Grass and forbs	3	2	2	3	2
Branch					
Large conifers	11421	6725	9886	11399	9858
Large hardwoods	2759	565	3964	10113	4350
Small conifers	105	117	2152	64	609
Small hardwoods	505	432	831	549	579
Bark					
Large conifers	8759	7279	12171	16587	11199
Large hardwoods	2779	565	4053	10694	4523
Small conifers	99	89	2148	52	597
Small hardwoods	18	115	67	76	69
Bole					
Large conifers	40650	38509	65120	85396	57419
Large hardwoods	19331	3991	28727	70943	30748
Small conifers	347	365	236	202	288
Small hardwoods	188	1127	711	772	700
Dead wood					
Large standing	6791	2877	7338	6701	5927
Small standing	869	554	2148	2998	1642
Large downed	6179	9003	12145	7201	9324
Medium downed	1388	1422	1933	2196	1798
Small downed	1055	1414	1499	2028	1543
Forest floor and soil					
Litter	9228	9096	9743	9929	9499
Duff	5979	5806	6655	6898	6335
Soil and roots to 10 cm	45500	45500	45500	45500	45500

[a]Values are the average of 26, 41, 66, and 43 inventory plots for high, moderate, low, and unburned-very low severity study plots, respectively, except that one Biscuit-wide value was used for soil and roots. For live trees, small is <7.62 cm DBH; large is >7.62 cm DBH. For dead wood, small is 0.51–2.54 cm, medium is 2.54–7.62 cm, and large is >7.62 cm diameter. Litter is O_i horizon; duff is O_e and O_a horizon.

to the ground and surface, reflecting the shift in fire behavior from a crown fire (which in most cases included ground and surface combustion as well) to a surface fire.

3.4. Uncertainty Assessment

[23] The sources of uncertainty in our estimates of pyrogenic emissions range from measurement uncertainty in the field, to sampling error at both the plot and landscape level, to the various quantitative assumptions regarding allometric scaling of preburn carbon pools and mass losses, to decision rules regarding the partitioning of carbon pools. Considering the difficulty in estimating combustion of subsurface carbon and that 65% of the total fire-wide carbon emissions may come from the combustion of litter, duff, and mineral soil carbon, we contend that most of the uncertainty in our estimate of total pyrogenic emissions arises from uncertainty in combustion of these pools.

[24] In the case of litter and duff, we are reasonably confident that our sample means for preburn mass for both that of ultramafic and nonultramafic substrates approach the true Biscuit-area means. Likely, most of the uncertainty arises from the assumption that combustion factors for litter

Table 5. Preburn Fuel Mass and Combustion Factors by Alternative Convention[a]

		Combustion Factor (Fraction Combusted)			
Fuel Category	Fuel Mass, Mg dry mass ha^{-1}	High Severity	Moderate Severity	Low Severity	Unburned Very Low Severity
Trees	263.2	0.08	0.07	0.03	0.00
Snags	15.7	0.18	0.14	0.11	0.01
Shrubs	3.7	0.86	0.66	0.42	0.00
Nonwoody fuel	<0.1	1.00	0.76	0.75	0.70
1 h surface fuels	6.1	1.00	0.76	0.75	0.70
10 h surface fuels	3.1	0.24	0.08	0.04	0.04
100 h surface fuels	3.6	0.79	0.73	0.67	0.62
1000+ h surface fuels	18.6	0.78	0.58	0.61	0.62
Litter	13.0	1.00	0.76	0.75	0.70
Duff	12.8	0.99	0.51	0.54	0.44

[a]Shrubs include all hardwoods <7.6 cm DBH; unlike elsewhere in paper, here litter excludes all woody fragments. Other categories follow the FCCS fuel category definitions.

Table 6. Pyrogenic Carbon Emissions by Carbon Pool and Burn Severity Class

	Combusted Carbon, Mg ha^{-1}				
Forest Carbon Pool	High Severity	Moderate Severity	Low Severity	Unburned Very Low Severity	Fire-Wide[a] Combustion, Tg C
Litter	7.4	5.5	5.8	5.4	1.00–1.24
Duff, soil and roots	8.3	4.2	4.6	3.5	0.79–1.48
Dead wood	4.8	3.1	3.7	2.9	0.72
Live wood and bark	4.1	2.1	3.0	0.4	0.49
Live foliage	4.1	3.7	1.4	0.2	0.43
Total	28.6	18.6	18.6	12.4	3.83

[a]Calculated by weighting the emissions from each burn class by the area of that burn class over the fire perimeter. Ranges shown for litter, duff, and soil reflect uncertainty in parameter estimates as described in text.

and duff computed for each of the 180 plots did not covary with the actual preburn litter and mass. For instance, if conditions were such that ground fuel consumption was moisture-limited, more litter and duff masses may equate to lower fractional combustion due to greater moisture retention. Conversely, if conditions were such that ground fuel consumption was continuity-limited rather than moisture-limited, lower litter and duff masses may equate to lower fractional combustion.

[25] While our estimate of preburn mineral soil carbon (including roots) was crudely based on samples from only three study plots, by far the most uncertain parameter was the presumed depth to which all carbon was combusted below exposed mineral surfaces identified in the inventory data as either ''moderately'' or ''deeply'' charred. Our best estimate of 2.0 and 4.0 cm, respectively, was based on the assumption that surface temperatures during the Biscuit in some cases exceeded 700°C (Bormann, personal communication), that soil temperatures during fire attenuate rapidly with depth, and that soil carbon begins to combust at 100°C [*Agee*, 1993]. However, it is also reasonable to believe that soil carbon could have completely combusted to depths of up to 5 cm or that complete combustion never exceeded 2 cm.

[26] To quantify the potential uncertainty stemming from assumptions regarding litter, duff, and mineral soil combustion, we computed an alternative maximum and minimum value for total pyrogenic emissions across the Biscuit. An alternative maximum value of 4.4 Tg was arrived upon by matching the higher litter and duff combustion factors to higher preburn litter and duff masses (i.e., a positive interaction effect), and assigning deep maximum soil C consumption depths of 3 cm and 5 cm for mineral surfaces identified as moderately and deeply charred, respectively. Similarly, an alternative minimum value of 3.5 Tg was arrived upon by matching the higher litter and duff combustion factors to lower preburn litter and duff masses (i.e., a negative interaction effect), and assigning shallow maximum soil C consumption depths of 1 cm and 2 cm for mineral surfaces identified as moderately and deeply charred, respectively. The litter and duff component of the analysis was performed by first identifying the percentile of each combustion record from the entire distribution, then multiplying each litter and duff combustion record by a preburn mass selected from the same percentile of its distribution (for maximum value), and finally multiplying each litter and duff combustion record by a preburn mass selected from the reverse percentile (100-x) of the preburn mass distribution (for minimum value).

[27] Because the combustion data come from a regular sampling scheme, and because the severity map was used only to bin (not measure) combustion factors, the particular burn severity classification used to bin the plots has little influence on our estimate of fire-wide emissions. The effect of burn severity classification on the estimate of fire-wide emissions arises only from potential covariance between burn severity and preburn carbon density. To investigate this source of uncertainty, we computed an alternative estimate of fire-wide emissions using all the same combustion data but treating all plots as a single burn severity class (equation (1) without the i designation). The resulting estimate of fire-wide pyrogenic emissions was different by only 10%. Because any alternative severity classification would likely have more in common with the BAER classification than no classification at all, it is reasonable to assume that the use of an alternative severity classification would result in a discrepancy in total pyrogenic emissions much smaller than 10%.

4. Discussion

4.1. Comparisons With Other Studies

[28] Overall, the combustion factors reported here for litter and duff (0.70–1.00 for litter and 0.40–1.00 for duff depending on fire severity) are similar to those reported or used by others modeling fire emissions. *Wiedinmyer et al.* [2006] used litter combustion factors of 0.8 to 0.9 depending on tree cover when modeling combustion across North America, *Soja et al.* [2004] used litter combustion factors of 0.2 to 1.0 depending on fire severity when modeling combustion across Siberia, and *Michalek et al.* [2000] used combined litter and humus combustion factors of 0.2 to 0.9 depending on fire severity when modeling combustion for a black spruce forest in Alaska.

[29] Our combustion factors for tree stems (<0.01–0.03 for stems >7.6 cm DBH and <0.01–0.71 for stems <7.6 cm DBH, depending on fire severity) are somewhat lower than values commonly used by modelers. *Wiedinmyer et al.* [2006] used a woody fuel combustion factor of 0.30 when modeling high severity combustion across North America, *Soja et al.* [2004] used a tree combustion factor of 0.30 when modeling high severity combustion across Siberia, and *Lü et al.* [2006] used a tree combustion factor of 0.10 for temperate forests of China. While the definition of woody fuel varies among these studies, the application of these combustion factors to the Biscuit Fire would lead to a large overestimation of pyrogenic emissions, in part because a significant portion of the biomass is in large trees that experience very little wood combustion. Notably, the com-

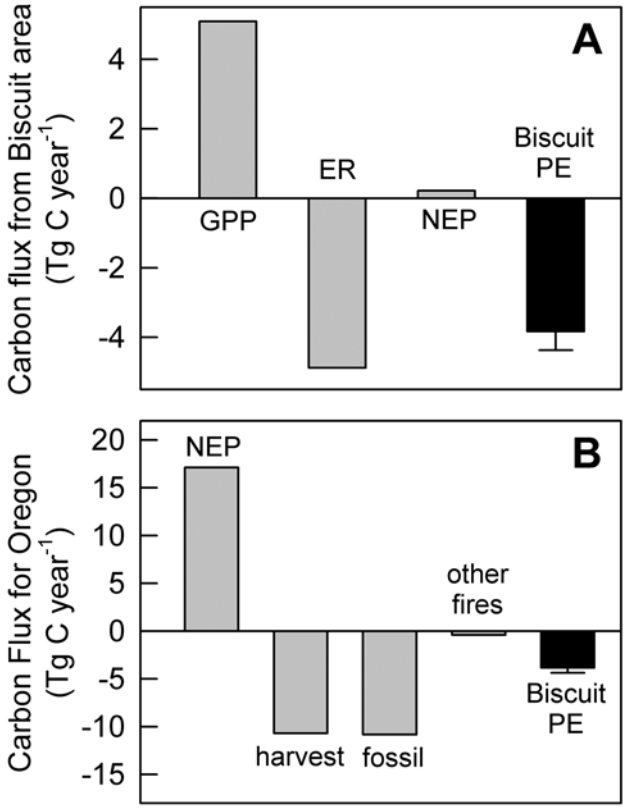

Figure 3. Pyrogenic carbon emissions from the 2002 Biscuit Fire (PE) compared with simulated ecosystem fluxes from (a) the forest present prior to the fire and (b) simulated biome fluxes across Oregon. GPP is Gross Ecosystem Production, NEP is Net Ecosystem Production, ER is total Ecosystem Respiration, and harvest is the sum of both forest product and crop removals. Data for all grey bars are from simulations by *Turner et al.* [2007] averaging the years 1996–2000 except fossil emissions which represent 2000 values from *Blasing et al.* [2004]. Error bar on Biscuit PE covers the upper alternative estimate described in this study.

bustion factors we report here for high severity fire are very similar to those reported for western Washington state, United States, by *Fahnestock and Agee* [1983], who, using no more than expert knowledge, estimated combustion factors to be 0.05, 0.10, 0.75, 0.30, and 0.80 for stems, branches, understory vegetation, dead wood, and forest floor, respectively, in high-severity wildfire.

[30] The latest AP-42, a document used by the U.S. Environmental Protection Agency in estimating air pollution, reports values for fuel loading (mass of fuel typically consumed by wildfire) of 135 and 40 Mg ha^{-1} for Oregon and California forests, respectively. Applying the former of these two values to the Biscuit would yield a total pyrogenic emission of about 14 Tg C (four times that reported in this study). However, applying the latter of these two values to the Biscuit would yield a total pyrogenic emission of about 4 Tg C (just outside our upper estimate). The discrepancy between values for Oregon and California can be traced to *Yamate* [1973], who first compiled fuel loading values for forests of the United States from what were regionally different approaches to estimating forest fuels.

4.2. Utility of Inventory Data

[31] Only through the use of federal inventory data were we able to assess pool-specific carbon losses over an area as large and diverse as that affected by the Biscuit Fire. The addition of fire-related measurements to the normal suite of inventory metrics was done primarily to predict delayed mortality, validate fire behavior models, and monitor the effects of fire on soil. These measurements also proved very useful in making estimates of pyrogenic emissions. The largest limitation to the inventory data used in this study is the absence of preburn litter and duff mass. While one can, as we did, use cover type to assign each plot a regional average value, only by matching observations of combustion to preburn measurements made at the same location can one confidently account for interactions that may exist between preburn mass and the subsequent combustion factor. The addition of litter and duff depth to the standard inventory protocol would go a long way toward improving our ability to estimate carbon losses.

[32] The second most valuable addition to inventory measurement with respect to pyrogenic emissions would be to extend the measurement of dead trees to include those less than 7.6 cm DBH. As determined from data collected in our supplementary plots, a great deal of the mortality and combustion occurred in this smaller size class. If the purpose of postburn inventory is to be expanded to include estimates of pyrogenic emissions of carbon or any another chemical species, it would be highly recommended to modify federal inventory protocols to include assessment of the smaller fire-killed trees. As interest grows in monitoring the effects of and recovery from fire in forests of the western United States, it is likely that federal inventory data will be increasingly relied upon.

4.3. Regional Significance of Biscuit Emissions

[33] One way to consider the importance of pyrogenic emissions from the Biscuit Fire is to compare it to fluxes from the same parcel of ground prior to the fire. As illustrated in Figure 3a, the estimated 3.8 Tg of C released as a result of combustion during the fire is nearly equal to the annual gross primary production, and approximately 18 times the annual net ecosystem production, simulated for an equal area of forest in the same Klamath-Siskiyou ecoregion (data from simulations by *Turner et al.* [2007]). Clearly pyrogenic emissions from a disturbance of this magnitude are an important part of any forest carbon budget. Nevertheless, one must realize that over 60% of the combustion comes from litter, foliage, and small downed wood, all of which are believed to have mean residence times of 10–20 years [*Law et al.*, 2001]. While some fraction of the combusted surface fuels would, without fire, find its way into long-term soil carbon pools, a sizable fraction of the pyrogenic emissions may be thought of as being destined for biogenic emission (i.e., through decay) within 1 to 2 decades with or without fire. Moreover, the proportion of these higher turn-over pools that is combusted should equate to a subsequent reduction in the heterotrophic respiration of these pools until they become recharged by new litter and branch fall. Conversely, carbon pools with

longer residence times, such as the stems of larger trees, contributed proportionally less to the pyrogenic emissions.

[34] Preliminary calculations suggest that the biomass killed but not combusted by the Biscuit Fire approaches 11 Tg C. As this material decays, the protracted biogenic emissions initiated by the Biscuit Fire should eventually exceed the one-time pyrogenic emission. However, considering that the majority of this fire mortality is in the form of large tree boles, uncertainties in the aerial decay rates of fire-killed trees, the rates at which these trees fall to the ground, and any decompositional effects of charring make it difficult to predict just how this biogenic loss will play out.

[35] Another way to consider the importance of pyrogenic emissions from the Biscuit Fire is to compare this one-time flux to regional fluxes in the same year. As illustrated in Figure 3b, the 3.8 Tg C estimated to have been released by the Biscuit Fire in this study is equal to approximately one third of the 10.8 Tg C reported to be released annually through fossil fuel burning in Oregon [*Blasing et al.*, 2004]. Furthermore, our estimate pyrogenic emission from the Biscuit Fire reduces estimates of Net Biome Production in Oregon (Net Ecosystem Production minus timber and crop harvest removals minus average fire emissions) in 2002 by more than half from 6.2 to 2.4 according process simulations made by *Turner et al.* [2007].

4.4. Future Research

[36] In this paper we estimate the pyrogenic carbon emissions from a particularly large fire in Oregon primarily for the purpose of determining the significance of this historical disturbance event to the carbon balance of the region, but also to explore the utility of federal inventory to do so. Undoubtedly, the most reliable way to extend these computations to future wildfires in the region would be to conduct similar ground measurements on these fires. However, the vast majority of fires in the western United States do not burn large enough to affect an appropriately large number of inventory plots that cover a range of variability in severity and preburn carbon pools. So, in the short term, combustion factors reported here could be applied to other Oregon fires with the assumption that they would be more accurate than other literature values that are derived largely from boreal fires. The observation that BAER severity classification consistently ranked the combustion factors of nearly all 24 preburn carbon pools (Table 3) suggests that it, as well as other classifications derived from remote imagery, may scale combustion factors across fires on comparable forests with acceptable accuracy. Only additional ground studies will be able to confirm this.

[37] One important direction for future work is to better quantify combustive losses from litter, duff, and mineral soil, as this was a primary source of uncertainty in our computations. Especially valuable would be repeated measures of litter and duff mass at the same sample points before and after a fire, as only these studies would reveal any covariance between preburn mass and fraction combusted (a potentially important interactive term not accounted for in equation (1)). Quantifying carbon combustion from mineral soil poses its own challenges. In a meta analysis including eight forest wildfire studies, *Johnson and Curtis* [2001] found substantial variability in the impacts of wildfire on A-horizon carbon content with an overall tendency for this pool to increase following wildfire, which was attributed to additions of charcoal and hydrophobic organic matter. The potential for wildfire to enrich soil carbon, combined with uncertainty surrounding postburn erosion and the sampling error ubiquitous to soil carbon quantification, unfortunately renders the before-after approach for assessing carbon combustion from mineral soil less tractable than it is for litter and duff. For these reasons the mechanistic modeling of soil carbon combustion from fire temperature (as done very crudely in this study) holds more promise than empirical approaches quantifying pyrogenic emissions from forest soils.

[38] Fine scale estimates of fuel loads, fuel consumption, and carbon production across the continental United States, Hawaii and Alaska continue to be improved by the FCCS (Fuel Characteristic Classification System) and fire behavior modles such as Consume 3.0 [*Sandberg et al.*, 2001; *Ottmar et al.*, 2007] (http://www.fs.fed.eu/pnw/fera/research/smoke). Future efforts to assess pyrogenic losses will likely be carried out through the use of process-based fire behavior models parameterized with these or similar fuel load layers, and driven by the sort of high precision remote imagery that can measure the intensity and duration of surface energy flux during the course of a wildfire [*Riggan et al.*, 2004]. These sophisticated approaches will still require independent estimates of fuel consumption like those that can be provided by prefire and postfire inventory.

[39] **Acknowledgments.** This project was supported in part by the North American Carbon Program, grants from the U.S. Department of Energy Biological and Environmental Research Terrestrial Carbon Program (award DE-FG02-04ER63917), and the U.S. Environmental Protection Agency NCER-STAR program (grant R-82830901-0). Data sources included the U.S. Forest Service PNW-FIA program.

References

Agee, J. K. (1993), *Fire Ecology of Pacific Northwest Forests*, Island Press, Washington, D. C.

Arora, V. K., and G. J. Boer (2005), Fire as an interactive component of dynamic vegetation models, *J. Geophys. Res.*, *110*, G02008, doi:10.1029/2005JG000042.

Azuma, D. L., J. D. Donnegan, and D. Gedney (2004), Southwest Oregon Biscuit Fire: An analysis of forest resources and fire severity, *Res. Pap. PNW-RP-560*, U.S. Dep. of Agric., For. Serv., Pac. Northwest Res. Stn., Portland, Oreg.

Barbosa, P. M., D. Stroppiana, and J. Gregoire (1999), An assessment of vegetation fire in Africa (1981–1991): Burned areas, burned biomass, and atmospheric emissions, *Global Biogeochem. Cycles*, *13*, 933–950.

Blasing, T., C. Broniak, and G. Marland (2004), Estimates of annual fossil-fuel CO_2 emitted for each state in the U.S.A. and the District of Columbia for each year from 1960 through 2001, Oak Ridge Natl. Lab., U.S. Dep. of Energy, Oak Ridge, Tenn. (Available at http://gcmd.nasa.gov/records/GCMD_CDIAC_TRENDS_CO2USA.html)

Czimczik, C. I., C. M. Preston, M. W. Schmidt, R. A. Werner, and E. D. Schulze (2002), Effects of charring on mass, organic carbon, and stable carbon isotope composition of wood, *Org. Chem.*, *33*, 1207–1223.

Fahnestock, G. R., and J. K. Agee (1983), Biomass consumption and smoke production by prehistoric and modern forest fires in western Washington, *J. For.*, *81*, 653–657.

French, N. H. F., E. S. Kasischke, and D. G. Williams (2002), Variability in the emission of carbon-based trace gases from wildfire in the Alaskan boreal forest, *J. Geophys. Res.*, *107*, 8151, doi:10.1029/2001JD000480 [printed *108*(D1), 2003].

French, N. H. F., P. Goovaerts, and E. S. Kasischke (2004), Uncertainty in estimating carbon emissions from boreal forest fires, *J. Geophys. Res.*, *109*, D14S08, doi:10.1029/2003JD003635.

Harmon, M. E., and J. Sexton (1996), Guidelines for measurement of woody detritus in forest ecosystems, *Rep. 20*, U.S. Long Term Ecol. Res. Network Off., Univ. of Wash., Seattle.

Houghton, R. A., J. L. Hackler, and K. T. Lawrence (2000), Changes in the terrestrial carbon storage in the United States. 2: The roll of fire and fire management, *Global Ecol. Biogeogr.*, *9*, 145–170.

Johnson, D. W., and P. S. Curtis (2001), Effects of forest management on soil C and N storage: Meta analysis, *For. Ecol. Manage.*, *140*, 227–238.

Kasischke, E. S., and L. P. Bruhwiler (2002), Emissions of carbon dioxide, carbon monoxide, and methane from boreal forest fires in 1998, *J. Geophys. Res.*, *107*, 8146, doi:10.1029/2001JD000461 [printed *108*(D1), 2003].

Key, C. H., and N. C. Benson (2005), Landscape Assessment (LA): Sampling and analysis methods, *USDA For. Serv. Gen. Tech. Rep. RMRS-GTR-164-CD*, U.S. Dep. of Agric., Ogden, Utah.

Law, B. E., P. Thornton, J. Irvine, S. van Tuyl, and P. Anthoni (2001), Carbon storage and fluxes in ponderosa pine forests at different developmental stages, *Global Change Biol.*, *7*, 755–777.

Law, B. E., D. Turner, J. L. Campbell, O. J. Sun, S. van Tuyl, W. D. Ritts, and W. B. Cohen (2004), Disturbances and climate effects on carbon stocks and fluxes across western Oregon, USA, *Global Change Biol.*, *10*, 1429–1444.

Lentile, L. B., Z. A. Holden, A. M. S. Smith, M. J. Falkowski, A. T. Hudak, P. Morgan, S. A. Lewis, P. E. Gessler, and N. C. Benson (2006), Remote sensing techniques to assess active fire characteristics and post-fire effects, *Int. J. Wildland Fire*, *15*, 319–345.

Lü, A., H. Tian, M. Liu, J. Liu, and J. M. Melillo (2006), Spatial and temporal patterns of carbon emissions from forest fires in China from 1950 to 2000, *J. Geophys. Res.*, *111*, D05313, doi:10.1029/2005JD006198.

Means, J. E., H. A. Hansen, G. J. Koerper, P. B. Alaback, and M. W. Klopsch (1994), Software for computing plant biomass: BIOPAK users guide, *Gen. Tech. Rep. PNW-GRT-340*, U.S. Dep. of Agric., For. Serv., Pac. Northwest Res. Stn., Portland, Oreg.

Michalek, J. L., N. French, E. Kasischke, R. Johnson, and J. Colwell (2000), Using Landsat™ data to estimate carbon release from burned biomass in an Alaskan spruce complex, *Int. J. Remote Sens.*, *21*, 323–338.

Miller, J. D., and S. R. Yool (2002), Mapping forest post-fire canopy consumption in several overstory types using multi-temporal Landsat™ and ETM data, *Remote Sens. Environ.*, *82*, 481–496.

Ottmar, R., D. Sandberg, C. Riccardi, and S. Prichard (2007), An overview of the Fuel Characteristic Classification System–Quantifying, classifying, and creating fuelbeds for resource planning, *Can. J. For. Res.*, in press.

Page, S. E., F. Siegert, J. O. Rieley, H. V. Boehm, A. Jayak, and S. Limink (2002), The amount of carbon released from peat and forest fires in Indonesia during 1997, *Nature*, *420*, 61–65.

Peterson, J. L., and D. V. Sandberg (1988), A national PM_{10} emissions inventory approach for wildland fires and prescribed fires, in *Transactions PM-10 Implementation of Standards: An APCA/EPA International Specialty Conference*, edited by C. V. Mathai and D. H. Stonefield, pp. 353–371, Air Pollut. Control Assoc., Pittsburgh, Pa.

Pyne, S. J., P. L. Andrews, and R. D. Laven (1996), *Introduction to Wildland Fire*, 2nd ed., John Wiley, Hoboken, N. J.

Reinhardt, E., R. Keane, and J. Brown (1997), First Order Fire Effects Module: FOFEM 4.0, User's Guide, *Gen. Tech. Rep. INT-GTR-344*, U.S. Dep. of Agric., For. Serv., Intermountain Res. Stn., Ogden, Utah.

Riggan, P. J., R. G. Tissell, R. N. Lockwood, J. A. Brass, J. A. R. Pereira, H. S. Miranda, A. C. Miranda, T. Campos, and R. Higgins (2004), Remote measurements of energy and carbon flux from wildfires in Brazil, *Ecol. Appl.*, *14*, 855–872.

Sandberg, D. A., R. D. Ottmar, and G. H. Cushon (2001), Characterizing fuels in the 21st century, *Int. J. Wildland Fire*, *10*, 381–387.

Schimel, D., and D. Baker (2002), The wildfire factor, *Nature*, *420*, 29–30.

Schoennagel, T., T. V. Veblen, and W. H. Romme (2004), The interaction of fire, fuels, and climate across Rock Mountain forests, *BioScience*, *54*, 661–676.

Seiler, S. W., and P. J. Crutzen (1980), Estimates of gross and net fluxes of carbon between the biosphere and the atmosphere, *Clim. Change*, *2*, 207–247.

Soja, A. J., W. R. Cofer, H. H. Shugart, A. I. Sukhinin, P. W. Stackhouse Jr., D. J. McRae, and S. G. Conard (2004), Estimating fire emissions and disparities in boreal Siberia (1998–2002), *J. Geophys. Res.*, *109*, D14S06, doi:10.1029/2004JD004570.

Turner, D. P., W. D. Ritts, B. E. Law, W. B. Cohen, Z. Yang, T. Hudiburg, J. L. Campbell, and M. Duane (2007), Scaling net ecosystem production and net biome production over a heterogeneous region in the western United States, *Biogeosciences*, *4*, 597–612.

U.S. Department of Agriculture (USDA) (1995), Current vegetation survey, natural resource inventory, Pacific Northwest Region, version 1.5, 82 pp., For. Serv., Pac. Northwest Res. Stn., Portland, Oreg.

U.S. Department of Agriculture (USDA) (2003), Annual inventory 2003 field guide supplement: Fire effects and recovery, 28 pp., For. Serv., Pac. Northwest Res. Stn., Portland, Oreg.

van der Werf, G. R., J. T. Randerson, G. J. Collatz, L. Giglio, P. S. Kasibhatla, A. F. Arellano, S. C. Olson, and E. S. Kasischke (2004), Continental-scale partitioning of fire emissions during the 1997 to 2001 El Niño/La Niña period, *Science*, *303*, 73–76.

van Tuyl, S., B. E. Law, D. P. Turner, and A. Gitelman (2005), Variability in net ecosystem production and carbon storage in biomass across forests: An assessment integrating data from forest inventories, intensive sites, and remote sensing, *For. Ecol. Manage.*, *209*, 273–291.

van Wagner, C. (1977), Conditions for the start and spread of crown fire, *Can. J. For. Res.*, *7*, 23–24.

van Wagtendonk, J. W., R. R. Root, and C. H. Key (2004), Comparison of AVIRIS and Landsat ETM+ detection capabilities for burn severity, *Remote Sens. Environ.*, *92*, 397–408.

Westerling, A. L., H. G. Hidalgo, D. R. Cayan, and T. W. Swetnam (2006), Warming and earlier spring increases western U.S. forest wildfire activity, *Science*, *313*, 940–943.

Whittaker, R. H. (1960), Vegetation of the Siskiyou Mountains, Oregon and California, *Ecol. Monogr.*, *30*, 279–338.

Wiedinmyer, C., B. Quayle, C. Geron, A. Belote, D. McKenzie, X. Zhang, S. O'Neill, and K. K. Wynne (2006), Estimating emissions from fires in North America for air quality modeling, *Atmos. Environ.*, *40*, 3419–3432.

Yamate, G. (1973), Development of emission factors for estimating atmospheric emissions from forest fires, *EPA-450/3-73-009*, U.S. Environ. Prot. Agency, Research Triangle Park, N. C.

D. Azuma, Forest Sciences Laboratory, U.S. Forest Service, Portland, OR 97208, USA.

J. Campbell, D. Donato, and B. Law, Department of Forest Science, Oregon State University, Corvallis, OR 97331, USA. (john.campbell@oregonstate.edu)

frontiers | Frontiers in Forests and Global Change

TYPE Original Research
PUBLISHED 28 September 2022
DOI 10.3389/ffgc.2022.979528

OPEN ACCESS

EDITED BY
Thomas J. Dean,
Louisiana State University,
United States

REVIEWED BY
Don Waller,
University of Wisconsin System,
United States
Kristin DeMarco,
Louisiana State University,
United States

*CORRESPONDENCE
Dominick A. DellaSala
dominick@wild-heritage.org

SPECIALTY SECTION
This article was submitted to Forest Management, a section of the journal Frontiers in Forests and Global Change

RECEIVED 27 June 2022
ACCEPTED 09 September 2022
PUBLISHED 28 September 2022

CITATION
DellaSala DA, Mackey B, Norman P, Campbell C, Comer PJ, Kormos CF, Keith H and Rogers B (2022) Mature and old-growth forests contribute to large-scale conservation targets in the conterminous United States. *Front. For. Glob. Change* 5:979528. doi: 10.3389/ffgc.2022.979528

Mature and old-growth forests contribute to large-scale conservation targets in the conterminous United States

Dominick A. DellaSala[1]*, Brendan Mackey[2], Patrick Norman[2], Carly Campbell[2], Patrick J. Comer[3], Cyril F. Kormos[1], Heather Keith[2] and Brendan Rogers[4]

[1]Wild Heritage, A Project of Earth Island Institute, Berkeley, CA, United States, [2]Griffith Climate Action Beacon, Griffith University, Queensland, AU, United States, [3]NatureServe, Boulder, CO, United States, [4]Woodwell Climate Research Center, Falmouth, MA, United States

Mature and old-growth forests (MOG) of the conterminous United States collectively support exceptional levels of biodiversity but have declined substantially from logging and development. National-scale proposals to protect 30 and 50% of all lands and waters are useful in assessing MOG conservation targets given the precarious status of these forests. We present the first coast to coast spatially explicit MOG assessment based on three structural development measures—canopy height, canopy cover, and above-ground living biomass to assess relative maturity. MOG were displayed by major forest types (n = 22), landownerships (federal, state, private, and tribal), and Gap Analysis Project (GAP) management status overlaid on the NatureServe's Red-listed Ecosystems and species, above-ground living biomass, and drinking water source areas. MOG total ~67.2 M ha (35.9%) of all forest structural classes and were scattered across 8 regions with most in western regions. All federal lands combined represented the greatest (35%) concentrations of MOG, ~92% of which is on national forest lands with ~9% on Bureau of Land Management (BLM) and ~3% on national park lands (totals do not sum to 100% due to minor mapping errors in the datasets). MOG on national forest lands supported the highest concentration of conservation values. However, national forests and BLM lands did not meet lower bound (30%) targets with only ~24% of MOG in GAP1,2 (5.9 M ha) protection status. The vast majority (76%, 20.8 M ha) of MOG on federal lands that store 10.64 Gt CO_2 (e) are vulnerable to logging (GAP3). If federal MOG are logged over a decade, and half their carbon stock emitted, there would be an estimated 0.5 ppm increase in atmospheric CO_2 by 2030, which is equivalent to ~9% of United States total annual emissions. We recommend upper bound (100%) protection of federal MOG, including elevating the conservation status of Inventoried Roadless Areas. This would avoid substantial CO_2 emissions while allowing ongoing carbon sequestration

to act as natural climate solutions to aid compliance with the Paris Climate Agreement and presidential executive orders on MOG and 30% of all lands and waters in protection by 2030. On non-federal lands, which have fewer MOG, regulatory improvements and conservation incentives are needed.

KEYWORDS

United States, mature forests, biodiversity, carbon, drinking water

Introduction

Forest conservation in the United States has for decades centered on protection and ecological restoration of forests in the later stages of stand structural development because of their irreplaceable biodiversity and ecosystem services (e.g., Davis, 1996; Strittholt et al., 2006). Terms like primary forest, late-successional forest, mature forest, old-growth forest, and ancient forest are routinely used, sometimes interchangeably (Mackey et al., 2014). However, verifiable metrics for national-scale inventory and conservation target setting for these forests are lacking.

Precisely when a forest is considered to be in the later structural development is typically based on several diagnostic features such as the age, height, and diameter-at-breast height (dbh) of the dominant-codominant trees; canopy and understory complexity (vertical and horizontal layering); large standing dead (snags) and down trees (logs); and large trees with broken and highly branched tops. These structural characteristics vary among regions, major forest types, and site conditions (e.g., productive vs. slow growing sites). In particular, gap-phase dynamics, the result of tree death (singular or in cohorts), and blow-down along edges and exposed ridgelines, are important drivers of structural development in later forest development stages. When gaps are formed, the resultant increased light and nutrient levels release suppressed trees to fill the gaps over time (e.g., in the eastern forests, Davis, 1996; Pacific Northwest, Franklin and Van Pelt, 2004; Spies, 2004). The lack of severe stand-level disturbances over extended periods allows trees to acquire impressive stature and old ages associated with increasing biological complexity.

Old-growth forests (the most structurally advanced stage) generally have exceptional levels of biodiversity compared to logged forests (the least structurally advanced) (Luyssaert et al., 2008; Keith et al., 2009; Lindenmayer et al., 2012, 2014; Cannon et al., 2022). However, because of the timber value of older trees they are declining globally (Lindenmayer et al., 2012, 2014; Mackey et al., 2014). The loss of old-growth forests is coupled with changes to the global climate (Lawrence et al., 2022), reducing opportunities for natural climate solutions (Griscom et al., 2017; Moomaw et al., 2019). In the United States, conservation importance of old-growth forests has been recognized in every forested region, including Alaska (DellaSala, 2011; Orians and Schoen, 2012; Vynne et al., 2021; DellaSala et al., 2022), Pacific Northwest (Strittholt et al., 2006; Krankina et al., 2014), West (Rockies, Pacific Southwest, Southwest collectively: Kauffman et al., 1992, 2007), Central (Shifley et al., 1995), Great Lakes (Alverson et al., 1994; Carleton, 2003), Southeast (Hanberry et al., 2018), and Northeast (Davis, 1996; Leak and Yamasaki, 2012; Ducey et al., 2013).

Old-growth forest importance can also be described along a spatial gradient from individual trees within a stand to their context within watersheds and landscapes. At the tree level, the largest trees in old-growth forests may represent just 1% of all stems yet store at least 40% of the above-ground carbon as carbon stock increases with tree size as trees age (Stephenson et al., 2014; Lutz et al., 2018; Mildrexler et al., 2020). At the stand level, old-growth forests store 35 to 70% more carbon, including in the soils, compared to logged stands (Keith et al., 2009; Mackey et al., 2014; Mayer et al., 2020). Old-growth forest stands may also act as a natural buffer against extreme climate conditions (De Frenne et al., 2013; DellaSala et al., 2015; Frey et al., 2016; Betts et al., 2017). At the watershed level, old-growth forests maintain hydrological cycles (Perry and Jones, 2016; Crampe et al., 2021). In the Pacific Northwest, old-growth forests may function as fire refugia in large wildfire complexes (Lesmeister et al., 2021).

Aside from select portions of the West, most old-growth forests in the conterminous United States were eliminated decades-centuries ago as logging and development proceeded from east to west coast. What remains is largely on federal lands where the government has untapped policy options for stepped-up conservation. Some of the remaining old-growth forests on national forest land are within Inventoried Roadless Areas (IRAs) that are at least 2,000 ha. Road building and most forms of logging are prohibited within IRAs but only administratively and not by an act of Congress, meaning protections are not inviolate or permanent (i.e., classified as GAP3 multiple use management). Importantly, significant portions of eastern forests are approaching maturity (100 + years, Gunn et al., 2013). As mature forests with advanced structure recover from historical logging, they could develop old-growth characteristics within just a few decades.

Primary and old-growth forests generally have received increased attention internationally as natural climate solutions (DellaSala et al., 2020; IUCN, 2020; Law et al., 2021),

including from policy makers[1] (e.g., March 22, 2022) and conservation non-governmental organizations (NGOs) in the United States[2]; [3] (accessed May 15, 2022). Article 5.1 of the Paris Climate Agreement calls on governments to protect and enhance "carbon sinks and reservoirs," while Article 21 of the UNFCCC COP26 Glasgow Climate Pact emphasizes "the importance of protecting, conserving and restoring nature and ecosystems, including forests... to achieve the long-term global goal of the Convention by acting as sinks and reservoirs of greenhouse gases and protecting biodiversity..." (UNFCCC, 2021). Furthermore, the United States was one of 140 nations at COP26 that pledged to end forest degradation and deforestation by 2030 (United Nations Climate Change, 2021). Also, the Summary for Policy Makers (SPM.D.4) in the Intergovernmental Panel on Climate Change [IPCC] (2022) report mentions safeguarding biodiversity and ecosystem integrity as fundamental to climate resilient developments. Attention to mature and old-growth forests can inform implementation of these policy commitments.

Large-scale conservation proposals for all land and waters have increasingly relied on 30 percent (i.e., 30% protected by 2030 or 30 × 30; Dinerstein et al., 2019; Carroll and Noss, 2021; Carroll and Ray, 2021; Law et al., 2021, 2022; One Earth Global Safety Net[4]; accessed May 28, 2022) and 50 percent (Half Earth) protection targets that involve triage approaches (Noss et al., 2012; Wilson, 2016). Large-scale target setting also has policy relevance, as exemplified by President Joe Biden's January 2021 executive order directing federal agencies to develop 30 × 30 targets for all lands and waters in the United States (White House, 2021). An April 2022 executive order from the President also directed federal agencies to inventory and assess threats to both mature and old-growth forests nationwide for possible protections (White House, 2022). Moreover, regionally specific proposals, such as the 79M ha of proposed protected areas in a five state area (OR, WA, ID, MT, and WY; Bader, 2000), a portion of which includes congressionally proposed wilderness additions in the Northern Rockies Ecosystem Protection Act (S.1276), have not assessed the amount of mature and old-growth forests nor its management status (i.e., how much protection is needed?). In all cases, it is vital that these forests are clearly defined, assessed, and mapped at multiple spatial scales (regional to national) to advise decision makers and NGOs on how best to meet climate and biodiversity policies and conservation targets.

Our objectives are to examine the contribution of mature and old-growth forests in the conterminous United States to: (1) conservation of at-risk forest ecosystems and species based on IUCN Red List criteria (Comer et al., 2022); (2) source catchments for drinking water (Mack et al., 2022); and (3) above-ground living biomass (Harris et al., 2021). We also applied conservation target setting developed for continental scale assessments to determine the contribution these forests could make to 30% (i.e., 30 × 30, Dinerstein et al., 2019) (lower bound), 50% (i.e., Half Earth; Noss et al., 2012; Wilson, 2016) (mid bound), and 100% (upper bound) protections. For our study, we are using estimates of forest structure that correlate with stand development collectively referred to as mature-old growth forests (MOG) to capture both the mature stage that is approaching old growth condition and the most advanced old growth stage as well. We also consider old growth a subset of primary forest defined as any forest stage lacking commercial logging or other industrial-scale developments that impairs ecosystem functions (Mackey et al., 2014). To our knowledge, this is the first comprehensive and spatially explicit assessment of MOG in the conterminous United States.

Materials and methods

Forest structure mapping

We mapped the relative level of forest structural maturity using three published spatial data sets that include forest canopy cover, canopy height, and above-ground living biomass derived from modeled satellite data (**Table 1**). These data were stratified by United States Ecoregions Level III (n = 28) (Omernik and Griffith, 2014) and Forest Types Groups (n = 85) (Ruefenacht et al., 2008) to account for the influences of variation in life history traits governing tree longevity and local environmental conditions on plant growth and ecosystem processes, as well as differing human and natural disturbance regimes. We used field measurements of canopy height and biomass from the Forest Inventory and Analysis plot database (FIA, 2022) to compare with our modeled forest maturity map and to aid in the interpretation of the map. We used a time series of available spatial data to examine the extent to which forests that were mapped as relatively less structurally advanced coincided with the footprints of severe natural disturbances. Further details on the methodology are provided in the Supplementary.

Expert workshops

A series of regional zoom workshops were conducted from September to November 2021 to consult with ecological and forest conservation experts (Supplementary). In total, 40 experts attended with each workshop focused on a major forested region within their region of interest. Key workshop objectives are listed in the Supplementary, including using participants to provide feedback on the initial modeling results for fine tuning. Expert consensus was that the appropriate level of forest

1 https://ktvz.b-cdn.net/2022/02/2022-02-17-DOI-and-USDA-Old-Growth.pdf

2 https://www.climate-forests.org/

3 https://forestcarboncoalition.org/

4 https://www.oneearth.org/the-global-safety-net-a-blueprint-to-save-critical-ecosystems-and-stabilize-the-earths-climate/

ecosystem classification was the 28 Forest Types Groups—which comprise aggregations of more finely defined forest types—spatially modeled from FIA inventory plot data at a 250-m pixel resolution (Ruefenacht et al., 2008) and for Level III ecoregions (Omernik and Griffith, 2014).

Spatial analysis

The three spatial structural data layers of forest cover, canopy height, and above-ground living biomass were made available for the conterminous United States (**Table 1**). Spatial analyses were undertaken using Google Earth Engine (Gorelick et al., 2017). As the three data layers were generated using the Global Land Analysis and Discovery's (GLAD) Landsat Analysis Ready Data (ARD), they shared the same 30-m pixel resolution.

An overview of the workflow to create a seamless conterminous-United States wide spatial data layer of relative forest maturity is provided in **Figure 1**. This included creating a spatial vector file of each Forest Type Group for each Level III Ecoregion. Spatial data layers were generated based on spatial coverage for the Forest Type Groups found in each Level III Ecoregion, resulting in a total of 782 unique combinations. For each pixel, we quantified quartile values for the three structural variables (canopy cover, canopy height, and biomass) within each of the 782 combinations. A score was then calculated for each pixel as follows: (a) the lowest quartile value for each metric was given a score of 0 and the highest a score of 3; then (b) the three metric scores were summed giving a range in possible values from 0 (lowest quartile for the three variables) to 9 (highest quartile for the three variables), representing 10 ordinal forest maturity classes. Based on expert feedback, we then produced a simplified structural class map by classifying pixels with a score of 0 as "indeterminant, those with scores of 1–3 as "Young," scores 4–6 "Intermediate" and scores of 7–9 as "Mature." Using a global spatial data set (Petersen et al., 2016), we analyzed the modeled forest maturity map to identify how much of each maturity class was plantation rather than naturally regenerating forest and excluded plantations from analysis.

Calibration analysis

We used FIA plot data as an independent data source for calibration off the modeled forest maturity structure map. Of the three variables, only canopy height could be used for validation as the input biomass layer used FIA biomass data. The spatial units of analysis (SUA) for comparison with the FIA plot data were generated from the intersection of the map of 85 United States Ecoregion Level III with the maps of the 28 Forest Type Groups. Those SUAs were analyzed for which there were at least 10 FIA plots for each of the three FIA Structural Stage Classification levels (Pole, Mature, Late) (n = 41). For each of these 41 SUAs, we calculated aggregate statistics from the quartiles and median values for canopy height and biomass from a random sample of pixels within each of the three modeled structure levels (Young, Intermediate, MOG) with 1.5–5% of pixels sampled. Further details are provided in the Supplementary.

Land ownership and gap analysis project status

The extent and management status of MOG was assessed using spatial data provided by government agencies. We used the forest ownership dataset produced by Sass et al. (2020) for the USDA Forest Service based on 2017 data. Each ownership

TABLE 1 Details for the spatial data layers used in the forest maturity modeling and the attribution and validation analyses.

Layer	Description	Data type and scale/resolution	Calibration data/validation approach	Source
Tree canopy cover	Percent tree canopy cover where trees defined as all vegetation taller than 5 m. forest extent in the year 2000 similarly to Hansen et al., that is, any 30-m Landsat pixel that met a tree canopy threshold of at least 30% with trees taller than 5 m.	Raster (30 m)	Training data to relate to the Landsat metrics were derived from very high resolution image interpretation methods	Hansen et al. (2013) updated to 2010 (GLAD)
Forest height	Forest canopy height	Raster (30 m)	Vegetation structure data collected using airborne lidar instruments (ALS) and GEDI field plots	Potapov et al., 2021
Forest biomass	Modeled estimates of above-ground living biomass	Raster (30 m)	Based on machine learning of satellite band ratios, plot measurements of biomass, and environmental variables	Harris et al., 2021
Ecoregions (Levels III)	Areas of similar ecosystems	vector data layer (at or above 1:24,000 scale)	Field verification trips across 30 United States	Omernik and Griffith, 2014
Forest Type Groups	Aggregation of forest types into 28 categories	Raster (250 m)	Spatial distribution models based on correlations between FIA inventory plot data (2022) and spatial environmental data layers	Ruefenacht et al., 2008

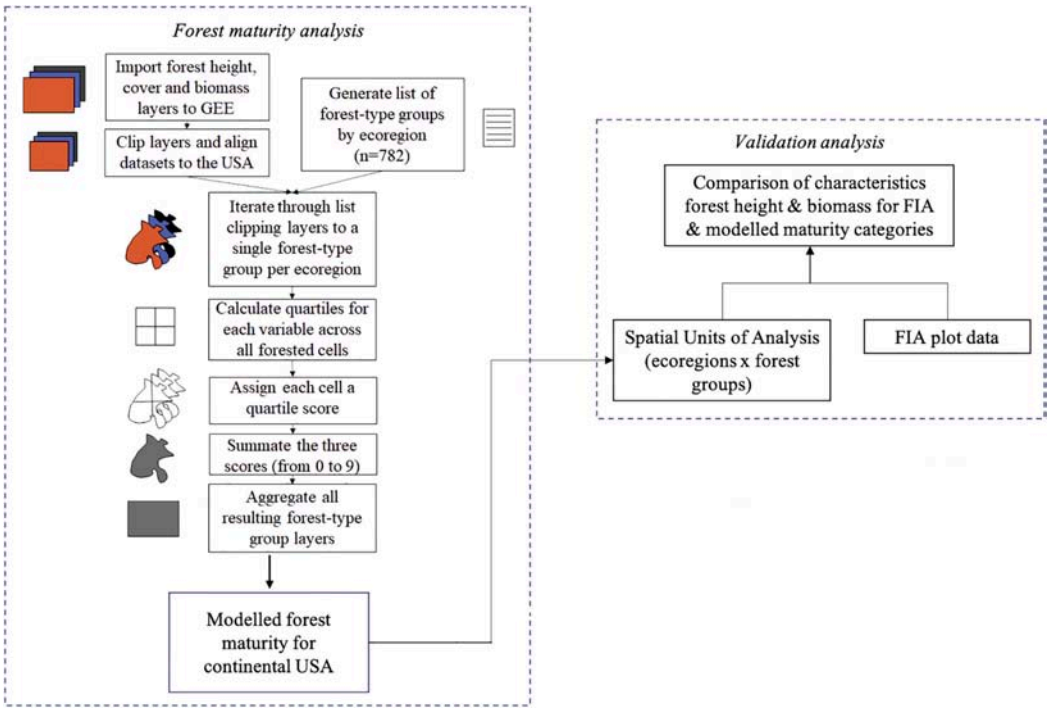

FIGURE 1
Workflow showing main steps in the calculation of the forest maturity structure model for conterminous United States, along with the validation analysis. The three 30-m resolution spatial data sets for forest cover, canopy height, and biomass were analyzed within 872 spatial units of analysis (SUA) defined by the intersection of ecoregions and major forest types. Forest Inventory Analysis (FIA, 2022) plot data were used for a validation analysis. Further details in **Supplementary Information**—Methods.

category was used as a mask to determine the extent of MOG within different tenures across the conterminous United States. The only additional aggregation made was the combination of the two FIA 41 categories, TIMO/REIT and private that were combined into a single masking layer. The Gap Analysis Project (GAP) management status codes (GAP1–4) was applied to MOG using the PAD-US Spatial Analysis Data provided by U.S. Geological Survey [USGS], and Gap Analysis Project [GAP] (2020). GAP 1 (e.g., Wilderness, National Parks) and GAP2 (e.g., National Monuments) were considered protected lands. GAP3 was multiple use management and GAP4 was no protection. The flattened version of the dataset was an important component of the analysis for determining the protected status of MOG. Inventoried roadless areas (IRAs) were filtered from the dataset and classified in our study as GAP2.5—that is—even though IRAs are given GAP3 status in the PAD-US dataset, we gave some credit to IRAs for administrative protections from most forms of logging. To ensure consistency among datasets, we compared the IRA layer to the 2001 Roadless Rule Feature layer provided by the USDA[5] for cross validation. We also assessed additional ownership and management of MOG including National Forests (National Forest System Land Units[6]), National Parks[7] and BLM (Derived from PAD-US[8]). The metadata[9] for landownerships did create some minor overlap problems where IRAs were inadvertently present in the dataset as within other ownerships even though this designation applies only to national forests. Those are recognized in each of the applicable tables as IRA misclassifications. The five western state regional example (79 M ha) that includes the Northern Rockies Ecosystem Protection Act was mapped after Bader (2000).

Biomass calculation

To determine the estimated amount of above-ground living biomass stored within MOG, spatial data produced by Harris et al. (2021) was used as an input layer. Calculating the

5 https://data.fs.usda.gov/geodata/edw/datasets.php?xmlKeyword=roadless

6 https://data.fs.usda.gov/geodata/edw/datasets.php

7 https://irma.nps.gov/DataStore/Reference/Profile/2224545?lnv=True

8 https://www.usgs.gov/programs/gap-analysis-project/science/pad-us-data-download

9 https://www.fs.usda.gov/rds/archive/products/RDS-2020-0044/_metadata_RDS-2020-0044.html

amount of biomass involved firstly warping the dataset to ensure a 30-m pixel size using GDAL and later masking to the extent of determined mature forest. The *R* program exactextractr was then utilized to sum the total amount of biomass within the forests. Due to the discrepancy between the input data being at a 30-m resolution and scaled to Mg/ha, the total value was then converted to produce overall biomass weight in tons.

At risk forest ecosystems and species

The IUCN Red List of Ecosystems (RLE) is an emerging global standard that integrates data and knowledge to document the relative risk status of ecosystem types. RLE criteria were used to assess 655 terrestrial ecosystems in temperate and tropical North America, including 182 forest and woodland ecosystem types in the conterminous United States using the U.S. National Vegetation Classification (Comer et al., 2022). We mapped these ecosystem types nationally using inter-agency LANDFIRE (2016) map products at 30-m pixel resolution with remote sensing data from approximately 2011. The RLE indicators that gauge the probability of range wide ecosystem collapse were measured for each criterion to address: trends in ecosystem extent (A); relative restricted nature of its distribution (B); extent and relative severity of environmental degradation (C); and extent and relative severity of disruption of biotic processes (D). Based on these measures, we categorized ecosystems as Collapsed, Critically Endangered, Endangered, Vulnerable, Near Threatened, Least Concern, Data Deficient, or Not Evaluated. Some 119 (65%) of the 182 United States forest ecosystem types were listed as threatened in some form (i.e., either Critically Endangered (CR) [6.5%], Endangered (EN) [24%], Vulnerable (VU) [24%], or Near Threatened (NT) [10%]).

We also overlaid our MOG map with the modeled distributions of the threatened forest and woodland types to quantify their relative representation within managed and protected lands.

At-risk forest-associated species

We used a database containing an analysis of the habitat requirements for species of conservation concern, including their co-occurrence with standard ecosystem classification units and vegetation structural attributes (Reid et al., 2016). This database includes over 6,000 plant and animal taxa known to occur throughout the conterminous United States. At-risk status was provided using both NatureServe conservation status ranks (Stein et al., 2000) and for listing status under the United States Endangered Species Act (i.e., for species listed as Threatened or Endangered, as well as Candidate or Proposed). We documented relationships through map overlays of species locations with mapped ecosystem type distributions. While incomplete, mapped distributions of forest types provide an initial indication of where MOG may support at-risk forest-associated species.

Drinking water source areas

The USDA Forest to Faucets assessment provides a relative index summarizing the importance of forested land for the provision of surface drinking water based on biophysical and demographic data (Mack et al., 2022). These data were available at the scale of subwatersheds delineated by the USGS, of which there were approximately 100,000 in the United States (USGS et al., 2013). We masked these data by the MOG pixels to provide a spatial layer showing the relative importance of MOG to surface drinking water. We also calculated MOG area for four classes representing each quartile of the relative importance to surface drinking water index and summarized by area for each GAP status and land tenure. Classes ranged from 1 (lowest importance, 0–25% relative importance) to 4 (highest importance, 76–100% relative importance) based on the relative importance to surface water index defined by the USDA Forest Service.

Results

Forest structure classes

Three categories of structural development were identified based on the ten ordinal i.e., ranked categorical classes: young—or least advanced structurally (scores of 1–3)—totaled 41.4 M ha (22.1%); intermediate (scores of 4–6) totaled 78.5 M ha (42.0%); and MOG –most advanced structurally (scores of 7–9)—totaled 67.2 M ha (35.9%) with a grand total of 187.0 M ha of mapped structural classes (**Supplementary Figure 1**). The percentage area of young, intermediate, and MOG within United States Ecoregions Level II is also detailed in **Supplementary Figure 2**. The comparisons of FIA plot based estimates of biomass, canopy height and relative structural maturity are provided in **Supplementary Figure 3** for the 41 spatial units of analysis were there were sufficient plot data.

Mature and old-growth forests spatial extent

The spatial distribution of MOG within the conterminous United States is shown at a national scale (**Figure 2**) and with a zoom-in to eight forested regions where these forests are widely scattered, including the Pacific Northwest (1), Pacific Southwest

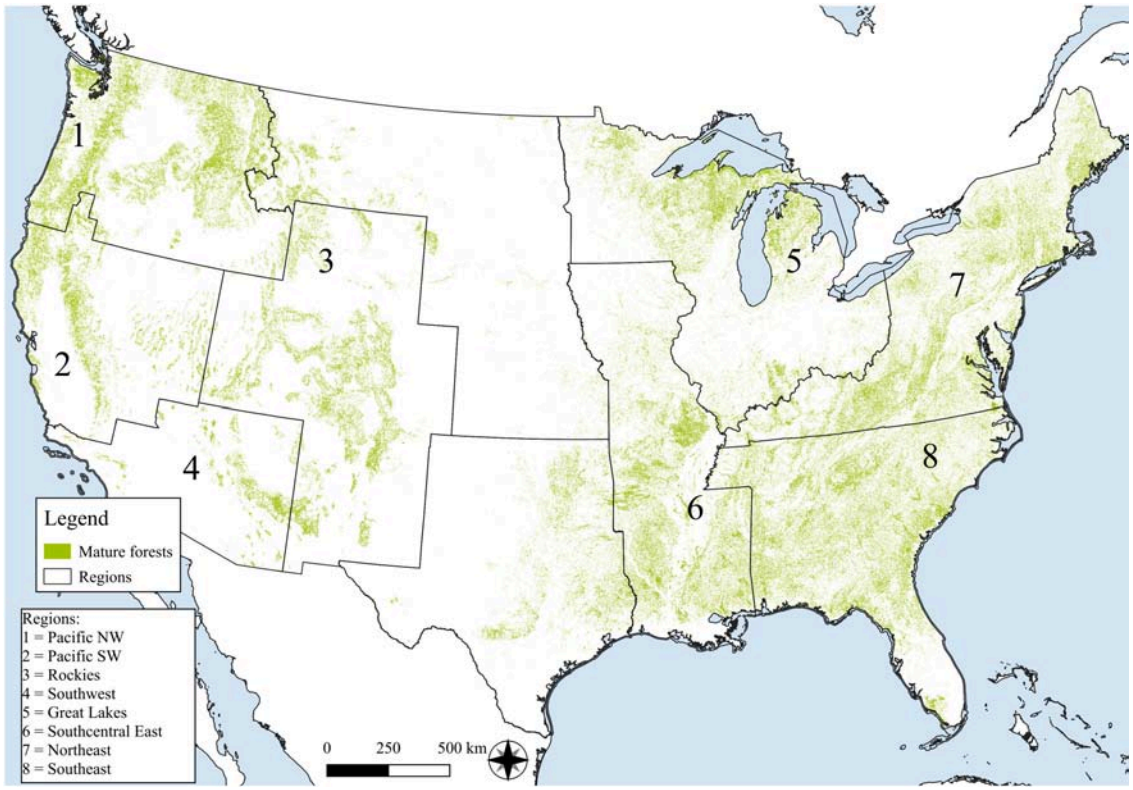

FIGURE 2
Distribution of modeled mature and old-growth forests (MOG) for the conterminous United States. Forest regions with MOG are numbered.

(2), Rockies (3), Southwest (4), Great Lakes (5), South Central (6), Northeast (7), and Southeast (8) (Figure 3).

Example photographs of general MOG structural features for major forest types of the conterminous United States illustrate anticipated variability in structural development of these forests (Figures 4A–F).

Using the western states regional MOG assessment example, MOG represent ∼7.60 M ha (9.6%) of the 79.1 M ha within the five-state area that includes the Northern Rockies Ecosystem Protection Act under consideration in the United States Congress (Figure 5). Only 20% of MOG are in GAP1 and 2 status with 30% in IRAs having intermediate protections (GAP 2.5) (Table 2), meaning the vast majority of MOG in this proposal is vulnerable to development pressures.

Mature and old-growth forests major forest types

Mature and old-growth forests were located within 22 forest groups spanning conifer and hardwood types in the conterminous United States (Table 3). Nearly all MOG types had their greatest percentages in unprotected status (GAP3, 4; no classifications) with only 14.7% overall in GAP1 and 2 and 7.1% in GAP2.5. Only two forest types, Fir (*Abies* sp.)/Spruce (*Picea* sp.)/Mountain Hemlock (*Tsuga mertensii*) (33.1%) and Other Western Softwoods (41.3%) met the lower bound (30%) target. Percentages would improve for several forest groups if IRAs (GAP2.5 status) received higher protection status. Importantly, FIA major forest classifications inappropriately lump longleaf (*Pinus palustris*) with slash pine (*Pinus elliottii*)-dominated communities as one equivalent forest type, thereby obscuring the imperiled conservation status and biodiversity of longleaf pine wiregrass (*Aristida stricta*) communities. For instance, there are five distinct longleaf pine ecosystem types mapped nationally and assessed under the IUCN Red Listing criteria (Comer et al., 2022), with two listed as Critically Endangered, and three as Endangered that do not show up on the FIA dataset.

Mature and old-growth forests land ownership and GAP analysis project status

Federal lands (36%) have the highest proportion of MOG, of which, National Forests have most (∼92%) of the federal total (Table 4). Approximately 24% of MOG on national forest lands

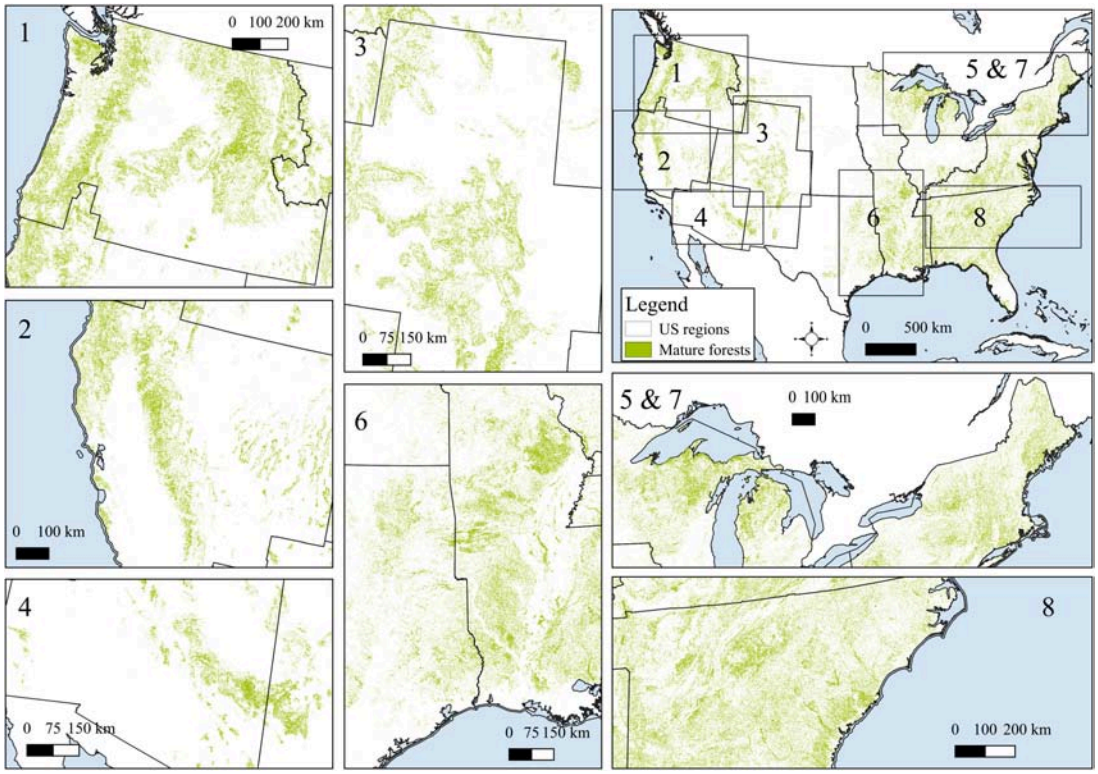

FIGURE 3
Regional zoom-ins of mature and old-growth forests of the conterminous United States. Panels show Pacific Northwest (1), Pacific Southwest (2), Rockies (3), Southwest (4), Great Lakes (5), South Central (6), Northeast (7), and Southeast (8).

are in GAP1 and 2 (Table 4). An additional 22% of MOG is within IRAs (GAP2.5). If IRAs received elevated conservation status, that would increase MOG protections in National Forests to 46%, which is within reach of the mid-level 50% target. Supplementary Table 1 has a breakdown of MOG by GAP status for every national forest.

The rest of MOG on federal lands are held by the National Parks (∼3%) and BLM (∼9%) (categories overlap some due to mapping errors in the datasets). BLM lands in particular are mostly non-forested with some notable exceptions such as in southwest Oregon. However, like National Forests, only ∼24% of MOG on BLM lands have GAP1 and 2 status (Table 4). Of non-federal lands, MOG were highest on family private (55%) and lowest on tribal (∼4%). Interestingly, state lands (41%) were the only non-federal category where a lower bound 30% target was met but they did not have much MOG overall. All other non-federal tenures were well below even the lowest 30% target.

Mature and old-growth forests above-ground living biomass

Aggregate above-ground living biomass values in MOG are by far highest on national forests, which contain 45% of the total above-ground living biomass for all ownerships (Table 5). For non-federal lands, family private has the most (52%) above-ground living biomass and tribal (4%) the least. The ratio of carbon to above-ground living biomass is typically taken to be 0.5 (i.e., about 50% of the dry weight of biomass is carbon) though globally the ratio can range from 0.4–0.6 (Keith et al., 2010).

Mature and old-growth forests red list of ecosystems

Of the 182 forest and woodland ecosystem types assessed with criteria from the IUCN RLE in the United States, 119 (65%) were categorized from near threatened (NT) to critically endangered (CR); collectively considered here as "threatened" (Figure 6). The 102 types categorized as vulnerable (VU) through critically endangered (CR) occurred on 38% of current forest area. Critically endangered and endangered forest ecosystems were concentrated in the eastern states; mostly in areas with the longest and most intensive land use histories. Types found there included Southeastern Interior Longleaf Pine Woodland, Atlantic Coastal Plain Fall-line Sandhills Longleaf Pine Woodland, and West Gulf Coastal Plain Sandhill Oak and

10.3389/ffgc.2022.979528

FIGURE 4
Examplary photographs of mature and old-growth forests in the United States. **(A)** Mixed-conifer forest, Sequoia National Park, CA, United States (B. Bryant). **(B)** Mature Eastern Hemlock (*Tsuga canadensis*) stand, Huron Mountain Club Upper Peninsula, MI, United States (B. Boucher). **(C)** Bottomland hardwood forest, Congaree National Park, SC, United States (J. Maloff, Old Growth Network). **(D)** North-Central Interior Dry-Mesic Oak Forest and Woodland (B.S. Slaughter). **(E)** Hardwood hammock forest, Starkey Park, FL, United States (D. DellaSala). **(F)** Top ten largest bald cypress (*Taxodium distichum*) in Florida, Upper Pithlachascotee River Preserve (D. DellaSala). Nearly all old growth cypress was logged in the 1930s.

Shortleaf Pine Forest and Woodland (**Supplementary Table 2**). Forest type descriptions are maintained for public access on NatureServe Explorer[10] (accessed September 4, 2022).

Large proportions of MOG under GAP1 to GAP 3 status include types categorized by the IUCN RLE as Least Concern (**Table 6**). About 39.4 M ha (394,000 km^2) of all at-risk (NT-CR) forests and woodlands occurred within area mapped as MOG. While current area of critically endangered forests was quite limited overall, most at-risk forest mapped as MOG was categorized as Near Threatened, Vulnerable, or Endangered. These were commonly located on either federal land, predominately national forests, or family private (**Table 6**). Importantly, ∼12.1 M ha (18%) of MOG with threatened status were located within GAP3 status

10 https://explorer.natureserve.org/

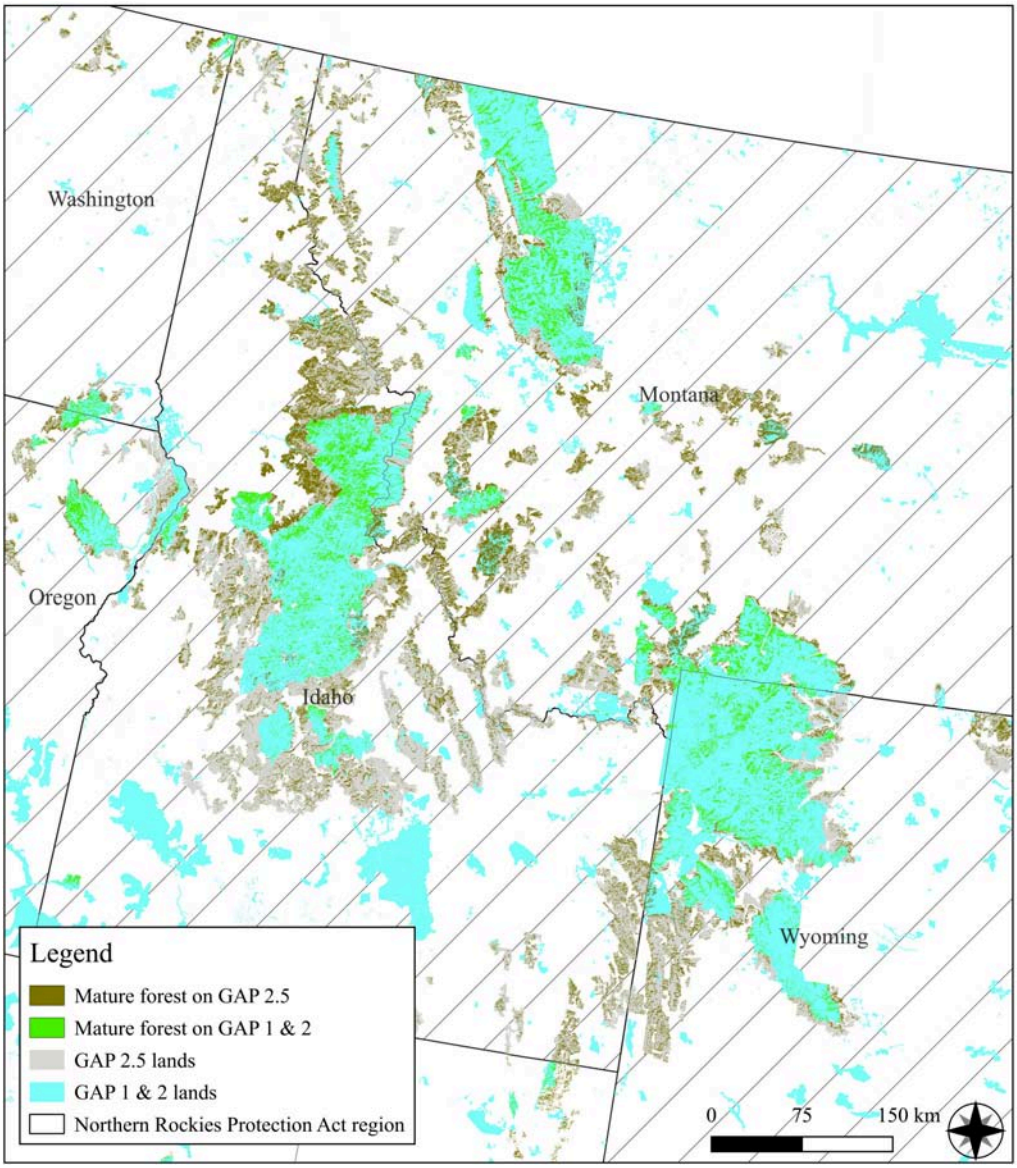

FIGURE 5
Distribution of mature and old-growth forests within the proposed five state protection area (OR, WA, ID, MT, and WY) including the Bader (2000) and Northern Rockies Ecosystem Protection Act (2021) by GAP classifications. GAP2.5 refers to Inventoried Roadless Areas (IRAs) that are not fully protected.

under multiple use management. These were, for example, North Pacific Maritime Mesic-Wet Douglas-fir (*Pseudotsuga menziesii*)-Western Hemlock (*Tsuga heterophylla*) Forest (VU) in the Pacific Northwest, and Southern Rocky Mountain Ponderosa Pine Woodland (VU) in the southern Rocky Mountains (**Figure 6**). The other large proportion of threatened MOG occurred on family private land, mostly throughout the eastern states (**Figure 6**). Examples included Ozark-Ouachita Dry Oak Woodland (EN), Allegheny-Cumberland Dry Oak Forest and Woodland (EN [VU-EN]), or Southern Piedmont Mesic Forest (EN [VU-EN]).

Mature and old-growth forests and at-risk species

Using documented relationships between species of concern and forests, there were 97 mapped forest ecosystem types known to support at-risk species (**Supplementary Table 2**) and the listed species are maintained for public access on the NatureServer Explorer (see text footnote 10; accessed September 5, 2022) under individual forest type summaries. MOG was present in 29.2 M ha of these mapped forest ecosystem types. Species considered "at-risk" within forest types using

TABLE 2 Mature and old-growth forests area (%) within the proposed five state protection area (OR, WA, ID, MT, and WY) that includes Northern Rockies Ecosystem Protection Act by GAP status.

GAP status	Area (ha)	Area (%)
GAP 1	1 174 117	15.4
GAP 2	342 516	4.5
GAP 2.5	2 331 074	30.7
GAP 3	5 033 750	66.2
GAP 4	295 733	3.9
Outside of GAP	755 909	9.9
Total area of mature forest	7 602 025	100
Total project area	79 173 694	–

Outside of GAP are areas with no GAP status, mostly on private lands.

NatureServe conservation status ranks included Vulnerable (G3), Imperiled (G2) or Critically Imperiled (G1) (Stein et al., 2000). From 1 to 64 of these at-risk species were associated with the 97 mapped forest types. Forest types with the most MOG that also included at-risk species were, for example, Laurentian-Acadian Northern Hardwood Forest (37,644 km^2 and 12 at-risk species), South-Central Interior Mesophytic Forest (16,046 km^2 and 50 at-risk species), and Southern Appalachian Oak Forest (10,190 km^2 and 48 at-risk species). Using United States Endangered Species Act (i.e., Threatened or Endangered, as well as Candidate or Proposed) as another measure of at-risk species status, 1 to 15 at-risk species were documented for their association with these 97 forest types. Among those supporting >1 at-risk species and with the extensive area in MOG were, for example, North Pacific Maritime Dry-Mesic Douglas-fir-Western Hemlock Forest (10,370 km^2 and 4 at-risk species), East Gulf Coastal Plain Large River Floodplain Forest (4,295 km^2 and 13 at-risk species), and Atlantic Coastal Plain Blackwater Stream Floodplain Forest (2,417 km^2 and 8 at-risk species).

Of the 97 forest ecosystem types with habitat relationships documented for at-risk species, 70 were considered threatened (IUCN NT, VU, EN, or CR) themselves. Threatened forest types support at-risk species (based here on NatureServe Conservation status ranks) with the most extensive area mapped as MOG in South-Central Interior Mesophytic Forest (EN) (16,046 km^2 and 50 at-risk species), Northeastern Interior Dry-Mesic Oak Forest (EN) (15, 327 km^2 and 12 at-risk species), and Southern Appalachian Oak Forest (VU) (10,190 km^2 and 48 at-risk species) (**Supplementary Table 2**).

TABLE 3 Area (×1000 hectares) and percent (%) of mature and old-growth forest within each Forest Inventory and Analysis (FIA) forest type group.

Forest type group	GAP 1	GAP 2	GAP 2.5	GAP 3	GAP 4	Outside of GAP	Total
Alder/Maple	1.1 (0.7)	5.9 (3.5)	0.8 (0.5)	46.3 (27.6)	7.9 (4.7)	106.4 (63.5)	167.6
Aspen/Birch	84.8 (2.5)	629.5 (18.9)	288.3 (8.7)	864.5 (26)	221.3 (6.6)	1 528.8 (45.9)	3 328.9
California Mixed Conifer	185.7 (13.8)	58.4 (4.3)	139.9 (10.4)	783.9 (58.3)	10.7 (0.8)	304.9 (22.7)	1 343.6
Douglas-fir	654.3 (11.1)	217.6 (3.7)	1 112.9 (18.9)	3 946.9 (67)	235.1 (4)	840 (14.3)	5 893.9
Elm/Ash/Cottonwood	11.7 (1.2)	139.9 (13.8)	1 (0.1)	46.1 (4.6)	75 (7.4)	738.9 (73)	1 011.6
Fir/Spruce/Mountain Hemlock	1 308.2 (29.6)	154.8 (3.5)	1 298.5 (29.4)	2 688.9 (60.8)	86.3 (2)	182.2 (4.1)	4 420.4
Hemlock/Sitka Spruce	127 (26.2)	15.8 (3.3)	55.3 (11.4)	287.6 (59.4)	12.5 (2.6)	41 (8.5)	483.9
Loblolly/Shortleaf Pine	41.5 (0.6)	555.8 (8.1)	9.7 (0.1)	562 (8.2)	229.3 (3.3)	5489 (79.8)	6 877.6
Lodgepole Pine	413.5 (22)	101.4 (5.4)	681.8 (36.3)	1 258.7 (67)	38.3 (2)	67.9 (3.6)	1 879.8
Longleaf/Slash Pine	19.3 (1)	90 (4.8)	3.2 (0.2)	308.7 (16.6)	72.7 (3.9)	1 365.5 (73.6)	1 856.2
Maple/Beech/Birch	65.6 (1.3)	868.6 (16.6)	29.2 (0.6)	523.7 (10)	302 (5.8)	3 484.3 (66.4)	5 244.2
Oak/Gum/Cypress	126.9 (4.1)	398.6 (13)	1.5 (0)	303.1 (9.9)	108.2 (3.5)	2138.7 (69.5)	3 075.5
Oak/Hickory	280.8 (1.6)	1173.9 (6.9)	153.2 (0.9)	1 810.3 (10.6)	1 363.4 (8)	12 421.7 (72.9)	17 050.1
Oak/Pine	23.1 (1.1)	147.6 (7)	7.1 (0.3)	167.6 (7.9)	66.3 (3.1)	1 711 (80.9)	2 115.6
Other Western Hardwoods	28.1 (23.4)	5.2 (4.4)	31.7 (26.4)	61.8 (51.5)	5.5 (4.6)	19.5 (16.2)	120.1
Other Western Softwood	86.9 (35.2)	15 (6.1)	102.1 (41.3)	119.3 (48.3)	16.7 (6.8)	9.1 (3.7)	247
Pinyon/Juniper	405.5 (10.5)	346 (9)	483.6 (12.5)	2 076.4 (53.7)	552.4 (14.3)	485.3 (12.6)	3 865.6
Ponderosa Pine	135.1 (4.2)	103 (3.2)	174.2 (5.4)	1817.3 (56.7)	412.6 (12.9)	738.2 (23)	3 206.2
Redwood	7.2 (9.4)	8.3 (10.9)	0.1 (0.1)	7 (9.2)	11.7 (15.3)	42.1 (55.2)	76.3
Spruce/Fir	31.4 (2)	312.7 (20.1)	16.9 (1.1)	264.5 (17)	153.6 (9.9)	790.9 (50.9)	1 553.1
Tanoak/Laurel	12 (5.9)	17.2 (8.4)	5.7 (2.8)	46.5 (22.6)	23.1 (11.2)	106.6 (51.9)	205.4
Tropical Hardwoods	1 (5)	4.7 (22.3)	0 (0)	7.4 (35.4)	0.3 (1.5)	7.5 (35.9)	20.9
Total	4 212.6	5 632.4	4 751	18 610.1	4 125.5	33 425.3	67 183

GAP2.5 refers to Inventoried Roadless Areas (IRAs). IRAs outside national forests are classification errors in the database. Outside of GAP are areas with no GAP status, mostly on private lands. Percentages are calculated by totaling each forest type group across rows.

TABLE 4 Total area of mature and old-growth forests (×1000 ha) and percent (parenthesis) for the conterminous United States by GAP and ownership.

Ownership and tenure	GAP 1	GAP 2	GAP 2.5	GAP 3	GAP 4	Total per owner
National Parks	822.3 (96.1)	24.5 (2.9)	0.7 (0.1)	3.3 (0.4)	4.4 (0.5)	855.6 (100)
National Forests	2 995.1 (13.7)	2 322.5 (10.6)	4 775.1 (21.9)	14 120.5 (64.7)	137.2 (0.6)	21 834.3 (100)
BLM	161.1 (7.1)	394.5 (17.4)	29.9 (1.3)	1 706.9 (75.4)	0.1 (0)	2262.6 (100)
State	11 5 (2.2)	2 086.3 (39)	4.9 (0.1)	2 054.9 (38.5)	430 (8)	5 343.7 (100)
Federal	4 014.9 (17.1)	2 906.7 (12.4)	4 756.2 (20.2)	15 731.6 (66.9)	402.4 (1.7)	23 514.5 (100)
Corporate private	13.5 (0.1)	215.4 (1.9)	3 (0)	232.4 (2.1)	645.2 (5.7)	11 223.5 (100)
Family private	32.5 (0.1)	296 (1.3)	5.2 (0)	350 (1.6)	1 067.7 (4.8)	22 467 (100)
Tribal	0.4 (0)	13.2 (0.8)	0.2 (0)	7.6 (0.5)	1 481.2 (94.6)	1 566 (100)
Total per GAP	4 239 (6.3)	5 686.8 (8.5)	4 784.2 (7.1)	18 736.3 (27.9)	4 198.1 (6.2)	67 183 (100)

Percentages are calculated across rows. GAP2.5 refers to Inventoried Roadless Areas (IRAs). IRAs outside national forests are classification errors of input datasets.

TABLE 5 Total-above ground living biomass within mature and old-growth forests (×1 M tons) by GAP and ownership.

Ownership and tenure	GAP 1	GAP 2	GAP 2.5	GAP 3	GAP 4	Total per owner
National Parks	281 (94.9)	10 (3.4)	0 (0)	1 (0.3)	3 (1)	296 (100)
National Forests	933 (15.7)	425 (7.1)	1 203 (20.2)	4 095 (68.8)	26 (0.4)	5 956 (100)
BLM	31 (5.3)	64 (11)	7 (1.2)	484 (83.4)	0 (0)	580 (100)
State	17 (1.9)	295 (33.4)	1 (0.1)	397 (45)	74 (8.4)	883 (100)
Federal	1 241 (19.3)	509 (7.9)	1203 (18.7)	4 539 (70.5)	60 (0.9)	6 441 (100)
Corporate private	3 (0.2)	35 (1.8)	0 (0)	42 (2.1)	89 (4.5)	1 970 (100)
Family private	6 (0.2)	47 (1.4)	0 (0)	56 (1.7)	123 (3.7)	3 325 (100)
Tribal	0 (0)	3 (1.1)	0 (0)	1 (0.4)	254 (93.4)	272 (100)
Total per GAP	1 285 (9.6)	920 (6.9)	1 203 (9)	5 091 (38.1)	626 (4.7)	13 351 (100)

Percentages (in brackets) are calculated across rows. GAP2.5 refers to Inventoried Roadless Areas (IRAs). IRAs outside national forests are classification errors of input datasets.

TABLE 6 Area of land (×1000 ha) and percentage area (parentheses) for each of the identified Red Listed Ecosystem (RLE) risk status by GAP and landowner.

	Not evaluated	Data deficient	Least concern	Near threatened	Vulnerable	Endangered	Critically endangered	Total by GAP
GAP status								
GAP 1	1.9 (0)	28.4 (0.5)	3 129.2 (60.3)	1 220.9 (23.5)	623 (12)	181.9 (3.5)	5.1 (0.1)	5 190.4 (100)
GAP 2	1.8 (0)	74.5 (1.5)	1 685.4 (35)	616.6 (12.8)	1 340.4 (27.9)	1 026.4 (21.3)	67.3 (1.4)	4 812.4 (100)
GAP 2.5	0 (0)	0.4 (0.1)	247.1 (81)	46.5 (15.2)	11.2 (3.7)	0 (0)	0 (0)	305.2 (100)
GAP 3	10.4 (0)	139 (0.6)	9 198.4 (42.9)	6 875.9 (32.1)	3 874.3 (18.1)	1 268.1 (5.9)	86.3 (0.4)	21 452.3 (100)
GAP 4	1.4 (0)	76.6 (1.8)	1 040.5 (24.2)	550.5 (12.8)	2 073.2 (48.3)	538.9 (12.5)	13.3 (0.3)	4 294.4 (100)
Landowner								
National Parks	1.5 (0.2)	8.3 (0.8)	558.4 (57.1)	195.2 (19.9)	200.1 (20.4)	15 (1.5)	0 (0)	978.6 (100)
National Forests	12 (0)	93.9 (0.4)	11 963.5 (46.6)	7 327.5 (28.5)	4 359.2 (17)	1 762.5 (6.9)	175.5 (0.7)	25 694 (100)
BLM	0 (0)	5.8 (0.2)	520.3 (19.9)	1 456.9 (55.7)	631.9 (24.1)	2.1 (0.1)	0 (0)	2 617.1 (100)
State	2.8 (0.1)	105.7 (2.6)	1 390.2 (34.4)	326 (8.1)	1 252.2 (30.9)	948.8 (23.5)	20.1 (0.5)	4 045.9 (100)
Federal	11.3 (0)	115 (0.4)	12 454.2 (45.1)	8 369 (30.3)	4 869.4 (17.6)	1 677.8 (6.1)	148.4 (0.5)	27 645.1 (100)
Corporate private	3.6 (0)	419.8 (5.3)	1 618 (20.3)	969.3 (12.1)	2 651.3 (33.2)	2 111.4 (26.4)	213.9 (2.7)	7 987.4 (100)
Family private	15 (0.1)	450.8 (2.7)	2 701.1 (16)	827.7 (4.9)	7 176.4 (42.5)	5 493.9 (32.5)	224.1 (1.3)	16 889 (100)
Tribal	0 (0)	16.4 (1)	738.3 (43.9)	447.1 (26.6)	457.4 (27.2)	21.2 (1.3)	0.2 (0)	1 680.6 (100)
Total by risk status	34.5 (0.1)	1 152.9 (1.9)	19 513.9 (32.4)	11 055 (18.4)	17 009.3 (28.3)	10 762.5 (17.9)	630 (1)	67 183 (100)

Percentages are calculated across rows. GAP2.5 refers to Inventoried Roadless Areas (IRAs). IRAs outside national forests are classification errors of input datasets.

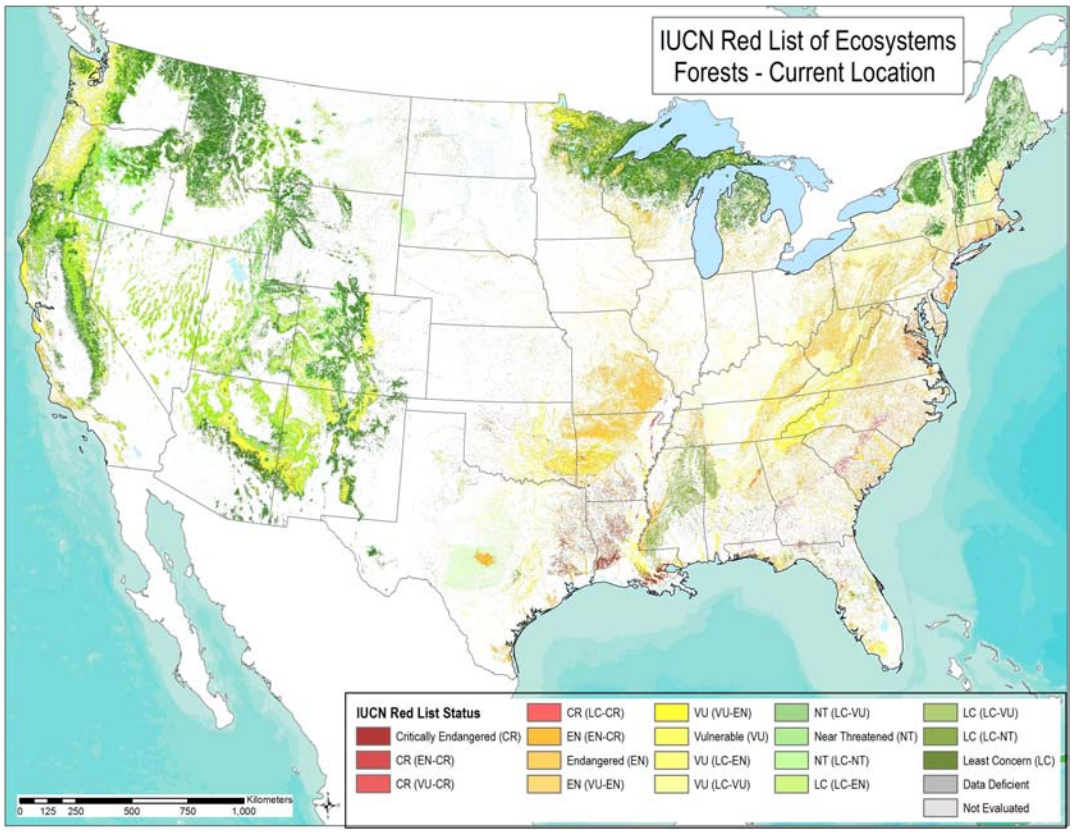

FIGURE 6
Current distribution of 182 forest and woodland ecosystem type categories under the IUCN Red List of Ecosystems (Comer et al., 2022). Nearly all these distributions include mature and old-growth forests (**Supplementary Table 2**).

TABLE 7 Mature forest area (ha) in each relative importance to surface drinking water class by GAP status and land tenure, with percentage of total mature and old-growth forest in the respective GAP/Tenure.

	Class 1 (0–25%)	Class 2 (26–50%)	Class 3 (51–75%)	Class 4 (76–100%)	Total
GAP Status					
GAP 1	1,188,095 (28.2)	1,021,604 (24.2)	1,218,859 (28.9)	790,612 (18.7)	4,219,170 (100)
GAP 2	1,804,722 (31.8)	915,163 (16.1)	1,541,173 (27.2)	1,411,752 (24.9)	5,672,810 (100)
GAP 2.5	1,646,869 (34.4)	1,220,674 (25.5)	1,355,166 (28.3)	561,520 (11.7)	4,784,229 (100)
GAP 3	5,922,561 (31.6)	4,494,644 (24)	4,720,470 (25.2)	3,598,512 (19.2)	18,736,188 (100)
GAP 4	1,178,791 (28.1)	773,969 (18.4)	1,370,386 (32.7)	873,587 (20.8)	4,196,733 (100)
Outside GAP	6,077,230 (20.6)	3,883,699 (13.2)	7,433,106 (25.2)	12,130,797 (41.1)	29,524,833 (100)
Land Tenure					
National Forests	5,713,619 (26.2)	5,498,207 (25.2)	6,119,473 (28)	4,501,227 (20.6)	21,832,525 (100)
National Parks	257,648 (30.1)	145,354 (17)	214,784 (25.1)	237,857 (27.8)	855,644 (100)
Federal Land	7,144,748 (30.4)	5,709,127 (24.3)	6,217,105 (26.5)	4,421,747 (18.8)	23,492,727 (100)
State Lands	1,704,860 (32.0)	803,361 (15.1)	1,360,235 (25.5)	1,463,130 (27.4)	5,331,587 (100)
Family Private Lands	4,381,601 (19.5)	3,208,018 (14.3)	6,200,135 (27.6)	8,666,291 (38.6)	22,456,045 (100)
Corporate Private Lands	3,081,796 (27.5)	1,815,543 (16.2)	2,672,084 (23.8)	3,653,002 (32.6)	11,222,425 (100)
Tribal Lands	611,203 (39)	384,502 (24.6)	517,106 (33)	53,000 (3.4)	1,565,810 (100)
BLM Lands	1,245,174 (55.6)	415,190 (18.5)	358,263 (16)	220,752 (9.9)	2,239,379 (100)
Total	17,818,269	12,309,753	17,639,160	19,366,781	67,133,962

Mature and old-growth forests and drinking water

Based on the USDA drinking water source area dataset, MOG with the highest drinking water value (Class 4) were mostly on Federal lands with surprising large areas on family private and corporate private (**Table 7**). Importantly, a substantial (4.5 M ha, >39%) amount of the highest quality drinking water comes from MOG within GAP3 and 4 status, and much more (12.1 M ha) is outside GAP status all together. Any loss of these forests due to logging and development would potentially impact drinking water supplies.

Discussion

Mature and old-growth forest structure and spatial analysis

Forest age and level of stand development are typically measured through tree ring analysis (e.g., core drill samples from living trees) and diameter distributions of dominant trees but can also be assessed using models based on measurements of forest structure—canopy height, canopy cover, biomass, as in our study. Other forest structural development characteristics indicative of the later stages of forest development include vertical vegetation layering and coarse woody debris (not measured in our study). Differences in the longevity, life history traits and niche requirements of tree species means that in many ecosystem types, the taxonomic composition of the dominant canopy species can reflect stages progressing from early to late seral. Gap-phase dynamics are diagnostic of the most structurally advanced old-growth. Furthermore, environmental factors that regulate plant growth, ecosystem processes rates and site productivity—thermal, moisture, radiation and nutrient regimes—result in variation within the ecosystem type of forest structure classes in terms of tree height, canopy density, and above-ground woody biomass.

Pan et al. (2011) used 2006 FIA plot data and remote sensing data at 1-km resolution to produce an age class distribution map in discrete age intervals of North American forests. Our inventory provides an updated and continuous-based structure map at 30-m resolution for tracking future changes in ecological development and management of MOG that can be updated as new datasets and advancements in monitoring technologies become available. We estimate 67.2 M (~36% of all structural classes) of MOG are scattered across eight geographic regions in the conterminous United States that provide options for stepped up national and regional conservation. With the exception of IRAs, MOG are mostly not large contiguous blocks as they are nested within a highly fragmented matrix that has contributed to edge effects and diminished ecosystem functions (see Heilman et al., 2002).

Federal lands

Combined federal lands represented ~35% of the total MOG structural classes with most (~92%) on national forests and a fraction managed by National Parks (~3%) and BLM (9%) (some overlap in mapping datasets). MOG on federal lands have the highest conservation values reflective of their above-ground living biomass, at-risk ecosystems and species, and drinking water source areas. However, only 24% of MOG on national forest and BLM lands each are fully protected, which is below even the lowest bound 30% target. Our analysis supports 100% of federal MOG for inclusion in protected areas based on their superior climate, water, and biodiversity associated values. We note that adding ~20.8 M ha of unprotected federal MOG to the United States protected areas network would still fall far short of the 30% target for all lands and waters given only 12% of all types are protected nationally. To achieve a near tripling of protections nationally on top of 20.8 M ha of proposed MOG protections would still require another 125 M ha of new protections from all types and landowners (National Geographic, 2021).

An alternative scenario is that the unprotected federal MOG in GAP2.5, 3, and 4 status is logged and then regrown. The consequences of this logging on exacerbating climate change can be assessed in terms of the projected emissions and their effect on the atmospheric CO_2 concentration. A comparison of protected vs. logged federal MOG allows the mitigation benefit of protecting MOG to be further evaluated in terms of carbon emissions avoided. The area of 20.8 M ha at-risk MOG on federal lands currently stores ~5.8 Gt of above-ground living biomass (Federal land GAP 2.5 + 3 + 4; **Table 5**), which is equivalent to 10.64 Gt CO_2. It is assumed that 50% of the carbon that had been stored in the biomass of logged MOG is emitted to the atmosphere due to combustion or decomposition of waste and short-lived wood products (Brown et al., 1997; Keith et al., 2014). This represents a carbon stock loss from the biosphere and a stock gain by the atmosphere. Logging emissions would remain in the atmosphere for decades and are partially removed by sinks. This can be calculated as the fraction of the airborne CO_2 from each pulse of emissions that decreases over time by removals from the natural land and ocean sinks and the regrowth of the forest (Keith et al., 2022). Carbon stock remaining in the atmosphere as the airborne fraction of the emissions was estimated for 2030 (after 8 years) and 2050 (after 28 years) to comply with global emissions reduction targets and for assessing the mitigation potential of full protection. By 2030, 74% of logging emissions would remain in the atmosphere, and by 2050, 54% would remain (Keith et al., 2022). This carbon stock remaining in the atmosphere also can be converted to parts per million by volume (ppm) as the common unit to express atmospheric CO_2 concentration (1 ppm = 7.8 Gt CO_2) (CIDAC, 1990). If 74% of the CO_2 emitted remains in the atmosphere by 2030, then 10.54 Gt CO_2 emissions are required to raise the atmospheric CO_2 concentration by 1 ppm. Logging emissions

would consequently result in 0.5 ppm increase in atmospheric CO_2 concentration by 2030 and 0.37 ppm by 2050.

The quantity of logging emissions also can be compared with the total United States emissions that were 5.8 Gt CO_{2e} in 2020[11] (accessed September 5, 2022), which would be 0.532 Gt CO_2 from MOG logging per year, the equivalent to 9.2% of the total annual United States emissions.

We note while such an accelerated increase in logging may be logistically unrealistic due to a number of factors (e.g., clearcut vs. selection logging, congressional appropriations, timber sale economics) not the least of which is accessibility of remaining MOG that becomes increasingly costly as easy to access sites are initially logged. However, the Trump administration issued an executive order in 2019 designed to greatly ramp up logging by 72% on national forests.[12] According to conservation groups, at least some of those sales under the Trump administration are ongoing[13] (accessed September 5, 2022). Additionally, legislation is routinely introduced in Congress to greatly increase federal lands logging at the expense of forest protections[14]. Logging unprotected MOG would also contribute to total United States emissions and make President Biden's stated goal of emissions reduction of 50–52% by 2030 far more difficult to achieve. Conversely, not logging these unprotected MOG would avoid the decadal logging equivalent of ∼0.5 ppm CO_2 (5.32 Gt CO_2) or ∼9% of United States total annual emissions, which would make a meaningful mitigation contribution to the world as natural climate solutions (Griscom et al., 2017; Moomaw et al., 2019; Keith et al., 2022). It is this current decade that is critical for mitigation actions to avoid emissions and not to add to the atmospheric CO_2 concentration, including those from the land-use sector.

The IRA component of MOG represents what remains of intact blocks on national forests. Elevating the conservation status of IRAs to GAP2 would increase MOG protections on national forests to that approaching the mid-bound (50%) target. However, that would take either an act of Congress or administrative changes that remove exemptions for logging and other development projects (e.g., hydroelectric development, mining) along with new regulations making it difficult to overturn roadless protections in general. The national roadless conservation rule has sustained 14 legal challenges upheld in appellate courts, was overturned twice on the Tongass National Forest in Alaska by pro-development administrations (i.e., George W Bush and Donald Trump), and was substantially changed by state petitions to the federal government in Idaho and Colorado. Increasing administrative or congressional IRA protections is key to elevating the conservation status of IRAs so they can be considered GAP2. While there is no comparable roadless policy for BLM lands, MOG could be nominated to the National Landscape Conservation System[15] (accessed May 15, 2022). The BLM oversees 14 M ha of mostly iconic lands and waterways designated by Congress or presidential executive order mainly for conservation purposes that includes national monuments and other protective designations.

Regional

Federal forests in the Eastern region are maturing from logging that eliminated all but a fraction (1–2%) of the old-growth forests over a century ago (Davis, 1996). Most mature forest types in this region lack protections, many are not on federal lands, and most are fragmented especially given that large IRAs are mostly in western regions. Additionally, the USDA Forest Service (2022) revised its 20-year forest management plans for the 416,000 ha Nantahala and Pisgah National Forest in western North Carolina claiming that they needed to log mature forests to create a diversity of seral stages even though classic old-growth forests are still well below historical levels (Davis, 1996). A combination of federal protections, improved forestry practices, and conservation incentives on non-federal lands are needed in this region to meet conservation targets for MOG.

Under the Trump administration, the USDA Forest Service removed protections for large diameter (>50 cm dbh, up to 150 years old) trees on national forests in eastern Oregon and Washington that were in place for over two decades, even though large trees remain below historical levels (Mildrexler et al., 2020). We recommend restoring those protections. The five state western proposal that includes the Northern Rockies Ecosystem Protection Act also contains nearly 11 M ha of MOG with only 20% in GAP1 and 2 status and another 30% in IRAs (GAP2.5). Recent policy and management decisions underscore the importance of increasing MOG protections in this region as well.

Non-federal lands

Family forest owners are a group of nearly 10 million families, trusts, and estates representing the largest landowner category in the United States with one-third of the total forest ownership (vonHedemann and Schultz, 2021). Substantial area of at-risk ecosystems, at-risk species, and drinking water also occur on these lands mostly in the eastern states where federal lands are scarce. Family landowners generally tend to manage their forests for aesthetics, wildlife, conservation, and family ownership legacy providing opportunities for conservation investments (Butler et al., 2016).

11 https://www.epa.gov/climate-indicators/climate-change-indicators-us-greenhouse-gas-emissions

12 https://www.usda.gov/sites/default/files/documents/usda-strategic-plan-2018-2022.pdf

13 https://www.climate-forests.org/worth-more-standing

14 https://www.congress.gov/bill/115th-congress/house-bill/2936/text/ih?overview=closed&format=txt

15 https://www.blm.gov/programs/national-conservation-lands

State lands are under state regulatory authorities and these vary widely in the extent to which they have as either policy or practice the protection of MOG. Aside from state parks, most forested states grant preference to intensive forest management over forest protections. Large corporate landowners manage forests mainly to maximize their return-on-investment by cutting trees when they approach culmination of mean annual increment (just before they reach maturity). MOG therefore are often looked at as a financial liability to be converted into fast growing monocultural plantations on short-timber rotation cycles. Many tribal lands also have timber objectives. In the Great Lakes, however, larger Indian reservations contain more MOG, higher biomass, and better sustain biodiversity than surrounding public lands (Waller and Reo, 2018).

In general, for all non-federal lands, a combination of regulatory improvements and incentives could retain more MOG (Dreiss and Malcolm, 2022). This might include conservation easements, fee-title acquisitions, and carbon offsets that result in verifiable conservation gains over *status quo* management. Our MOG assessment may also provide procurement guidance to the private sector regarding avoiding logging in older forests, as, for example, a recent shareholder resolution at the Home Depot chain to purchase wood not coming from old-growth forests[16] (accessed May 20, 2022).

Data and model limitations

A limitation of our modeled forest structural maturity is that it does not directly provide a measure of forest stand age. Such an effort would need to cross-walk our modeled MOG areas with on-the-ground forest plot metrics derived from the FIA dataset. However, our structural maturity levels (Young, Intermediate, and MOG) overlap well with the FIA Structural Stage Classification levels (Pole, Mature, and Late) and are reasonably indicative of forest age classes.

We assumed that for a given Forest Type Group in a given ecoregion, the level of maturity would be monotonically related to increasing canopy cover, canopy height and biomass. An initial visual inspection of the modeled forest maturity map identified two landscape settings where the forest was likely erroneously assigned a younger structural class. One was forests bordering the alpine zone that naturally have a sparser and shorter canopy and support lower biomass stocks compared to a similar type at a lower elevation. Less obviously, are forests in climatically drier ecoregions on exposed topographic positions that naturally would be sparser, shorter and have less biomass than similar forest types nearby with higher site productivity (McKenney and Pedlar, 2003). The Oak/Hickory Forest Type Group also had some anomalous results with lower-than-expected areas of Young forest. This is likely the result of substantial wildfire suppression in these fragmented forests across their range (Nowacki and Abrams, 2008).

The Forest Type Groups, stratified by United States Ecoregions Level III, were used to represent the major differences in forest ecosystems. However, as these Groups are only intended to indicate broad distribution patterns of forest cover in the United States, modeled with an overall accuracy of 65% (Ruefenacht et al., 2008). They represent a highly generalized level of ecological organization within which resides a rich forest biodiversity that encompasses a range of natural variability in tree growth rates due to local physical environmental conditions that means in some locations there can be a mismatch between stand development and forest structure.

Discretion should be taken when interpreting the MOG water overlay given the differing spatial scale of input datasets. The relative importance to surface drinking water dataset is provided at the scale of subwatersheds, which vary in size and shape as their bounds are largely determined by topographic and hydrologic features of the landscape (USGS et al., 2013). So, while we presented the water importance overlay at 30-m resolution, the masked values are from the coarser dataset, meaning there may be some fine-scale variation missed. There may also be some correlation between MOG area and areas highly valuable for surface drinking water, as the layer incorporates forest metrics including forest cover, forest ownership and insect and disease risk (Mack et al., 2022). Given that the index incorporates many other non-forest variables, the impact of this correlation is likely minimal.

Finally, we did not assess the critical landscape and climate refugia role that larger and more continuous MOG (e.g., IRAs) play in a rapidly changing climate, including enabling species movements (i.e., connectivity up and down elevation, northern latitudinal shifts) and providing minimum critical areas for apex predators and other area and climate sensitive species.

Conservation recommendations

President Biden's Executive Order (White House, 2022) for forests aims to "institutionalize climate-smart management and conservation strategies that address threats to mature and old-growth forests on Federal lands." Mature forests, which include the old-growth forest class, provide superior values compared to logged forests as natural climate solutions (Griscom et al., 2017; Moomaw et al., 2019) in meeting both White House (2021, 2022) executive orders. Moreover, the 30 × 30 executive order includes all lands and waters—and not just federal—that require a combination of conservation measures to achieve this target (e.g., in regions with little federal lands such as the eastern region). However, the current *status quo* management of MOG and low protection levels on all lands presents unacceptable risks at a time when the global community is seeking ways to reduce the rapidly accelerating biodiversity and climate

16 https://ir.homedepot.com/~/media/Files/H/HomeDepot-IR/2022/2022%20Proxy%20Statement%20-%20Final.pdf

crises (Ripple et al., 2021). While our analysis presented three target scenarios of 30, 50, and 100% protection, there are climate, biodiversity, and drinking water benefits for choosing the upper bound 100% target for MOG on federal lands with additional measures on non-federal lands to compliment a federal reserve system anchored in MOG. The IRA component of MOG includes remaining relatively intact forest blocks that would benefit from elevating the GAP status of IRAs through enhanced protective measures. One way to do this would be to introduce national rulemaking that protects all remaining federal MOG in and out of IRAs. We note that the White House (2022) also calls for prioritizing the restoration of old-growth forests as "climate-smart forest stewardship." In our view, this can include allowing mature forests to grow into old growth structurally over time as in the Eastern region in order to begin restoring the national and regional deficits in old-growth forests. It can also mean restoring the beneficial role of wildfires in maintaining diverse understories in fire-adapted older forests such as many dry mixed conifer, oak-hickory, and open pine systems (e.g., long-leaf pine wiregrass). Typically, MOG that have experienced severe natural disturbance are logged, including within administrative reserves (such as late-successional reserves under the Northwest Forest Plan in the Pacific Northwest) and even within IRAs. However, we recommend protections extend through post-disturbance successional stages to allow forests to recover carbon stocks (proforestation, Moomaw et al., 2019) and because most carbon in severe disturbances simply transfers from live to dead pools and soils (Law et al., 2021).

A large-scale effort to protect MOG nationwide, including all primary and old-growth forests within the highest end of the mature forest spectrum, would help the United States meet a range of multilateral commitments related to protecting and restoring ecosystem integrity. Ecosystem integrity has long been a bedrock principle in the United Nations, recognized in both the Rio Declaration and Agenda 21, and were agreed to in 1992 at the United Nations Conference on Environment and Development (UNCED) (the 'Earth Summit'). The UNFCCC's Paris Agreement (UNFCCC 1/CP.21), agreed in 2015, carried forward the concept of ecosystem integrity in its preamble, and more recently the Intergovernmental Panel on Climate Change's 6th Assessment Report made numerous references to the fundamental importance of primary forests, ecological restoration and ecosystem integrity (Intergovernmental Panel on Climate Change [IPCC], 2022). Similarly, the Convention on Biological Diversity also recognizes the importance of primary forests and ecosystem integrity *via* decisions 14/5 and 14/30 agreed in 2018 at its 14th Conference of the Parties. The United Nations Strategic Plan for Forests 2030 (ECOSOC Resolution 2017/4), which builds on the 2007 UN Forest Instrument (A/RES/62/98 and A/RES/70/199), emphasizes ending deforestation and preventing forest degradation as key globally priorities. The United Nations global decade on restoration was launched in 2021, following on the 2011 Bonn Challenge, with a target of 350 million ha of restoration, including a pledge of 15 million ha from the United States. The UN Sustainable Development Goals also has a goal of halting and reversing land degradation (United Nations, 2022). Finally, 95 nations, including the United States, recently agreed to support the 30 × 30 initiative as part of their COP15 Convention on Biological Diversity obligations in June 2022. Mature and old-growth forest inventories (White House, 2022) provide a foundation for introducing much needed policies that are based on the upper bound full protection for MOG, which would allow the United States to fulfill its international obligations as a leader in the global effort to end forest degradation and deforestation.

Data availability statement

The datasets presented in this study can be found in online repositories and on matureforests.org; accessed September 9, 2022. The names of the repository/repositories and accession number(s) can be found in the article/**Supplementary material**.

Ethics statement

Written informed consent was obtained from the individual(s) for the publication of any identifiable images or data included in this article.

Author contributions

BR contribute to the development of the article's methods that were added per reviewers request for more on the methodology – the methods were greatly expanded in the article and the online **Supplementary material**. All authors contributed to its completion.

Funding

This project was supported by a grant from One Earth to DD and BM and support from the Sweetgrass Foundation, Lisa & Douglas Goldman Fund, Weeden Foundation, Goatie Foundation, Wilburforce Foundation, and Forest-carbon Coalition to DD.

Acknowledgments

We thank Jim Strittholt for consult on databasin.org, and over 40 workshop participants in testing forest mapping methodologies.

Conflict of interest

The authors declare that the research was conducted in the absence of any commercial or financial relationships that could be construed as a potential conflict of interest.

Publisher's note

All claims expressed in this article are solely those of the authors and do not necessarily represent those of their affiliated organizations, or those of the publisher, the editors and the reviewers. Any product that may be evaluated in this article, or claim that may be made by its manufacturer, is not guaranteed or endorsed by the publisher.

Supplementary material

The Supplementary Material for this article can be found online at: https://www.frontiersin.org/articles/10.3389/ffgc.2022.979528/full#supplementary-material

References

Alverson, W. S., Kuhlmann, W., and Waller, D. M. (1994). *Wild Forests: Conservation Biology and Public Policy*. Washington, DC: Island Press.

Bader, M. (2000). Distribution of grizzly bears in the U.S. Northern Rockies. *Northwest Sci.* 74, 325–334.

Betts, M. G., Phalan, B., Rousseau, J. S., and Yang, Z. (2017). Old-growth forests buffer climate-sensitive bird populations from warming. *Divers. Distrib.* 24, 439–447. doi: 10.1111/ddi.12688

Brown, S., Schroeder, P., and Birdsey, R. (1997). Aboveground biomass distribution of US eastern hardwood forests and the use of large trees as an indicator of forest development. *For. Ecol. Manag.* 96, 37–47. doi: 10.1016/S0378-1127(97)00044-3

Butler, B. J., Hewes, J. H., Dickinson, B. J., Andrejczyk, K., Butler, S. M., and Markowski-Lindsay, M. (2016). Family forest ownerships of the United States, 2013: Findings from the USDA Forest Service's National Woodland Owner survey. *J. For.* 114, 638–647. doi: 10.5849/jof.15-099

Cannon, C. H., Piovesan, G., and Munné-Bosch, S. (2022). Old and ancient trees are life history lottery winners and vital evolutionary resources for long-term adaptive capacity. *Nat. Plants* 8, 136–145. doi: 10.1038/s41477-021-01088-5

Carleton, T. J. (2003). Old growth in the Great Lakes forest. *Environ. Rev.* 11:S115–S134. doi: 10.1139/a03-009

Carroll, C., and Noss, R. F. (2021). How percentage-protected targets can support positive biodiversity outcomes. *Conserv. Biol.* 36:e13869. doi: 10.1111/cobi.13869

Carroll, C., and Ray, J. C. (2021). Maximizing the effectiveness of national commitments to protected area expansion for conserving biodiversity and ecosystem carbon under climate change. *Glob. Change Biol.* 27, 3395–3414. doi: 10.1111/gcb.15645

CIDAC (1990). *Carbon Dioxide Information Analysis Center – Conversion Tables*. Available Online at: https://web.archive.org/web/20170118004650/http://cdiac.ornl.gov/pns/convert.html (accessed Sept 5, 2022).

Comer, P. J., Hak, J. C., and Seddon, E. (2022). Documenting at-risk status of terrestrial ecosystems in temperate and tropical North America. *Conserv. Sci. Pract.* 4:e603. doi: 10.1111/csp2.603

Crampe, E. A., Segura, C., and Jones, J. A. (2021). Fifty years of runoff response to conversion of old-growth forest to planted forest in the J.J. Andrews Forest, Oregon, USA. *Hydrol. Process.* doi: 10.1002/hyp.14168

Davis, M. B. (ed.) (1996). *Eastern old-Growth Forests. Prospects for Rediscovery and Recovery*. Washington, D.C: Island Press.

De Frenne, P., Rodríguez-Sánchez, F., Coomes, D. A., Baeten, L., and Verheyen, K. (2013). Microclimate moderates plant responses to macroclimate warming. *Proc. Natl. Acad. Sci. U.S.A.* 110, 18561–18565. doi: 10.1073/pnas.1311190110

DellaSala, D. A., Brandt, P., Koopman, M., Leonard, J., Meisch, C., Herzog, P., et al. (2015). "Climate Change May Trigger Broad Shifts in North America's Pacific Coastal Rainforests," in *Reference Module in Earth Systems and Environmental Sciences*, eds D. A. DellaSala and M. I. Goldstein (Amsterdam: Elsevier).

DellaSala, D. A. (ed.) (2011). *Temperate And Boreal Rainforests Of The World: Ecology And Conservation*. doi: 10.5822/978-1-61091-008-8 Washington, D.C: Island Press.

DellaSala, D. A., Gorelik, S. R., and Walker, W. S. (2022). The Tongass National Forest, southeast Alaska, USA: A natural climate solution of global significance. *Land* 11:717. doi: 10.3390/land11050717

DellaSala, D. A., Kormos, C., Keith, H., and Mackey, B. (2020). Primary forests are undervalued in the climate emergency. *Bioscience* 70, 445. doi: 10.1093/biosci/biaa030

Dinerstein, E., Vynne, C., Sala, E., Joshi, A. R., Fernando, S., Lovejoy, T. E., et al. (2019). A global deal for nature: Guiding principles, milestones, and targets. *Sci. Adv.* 5:eaaw2869. doi: 10.1126/sciadv.aaw2869

Dreiss, L. M., and Malcolm, J. W. (2022). Identifying key federal, stage, and private lands strategies for achieving 30 x 30 in the United States. *Conserv. Lett.* 15:e12849. doi: 10.1111/conl.12849

Ducey, M. J., Whitman, A. A., and Gunn, J. (2013). Late-successional and old-growth forests in the northeastern United States: Structure, dynamics, and prospects for restoration. *Forests* 4, 1055–1086.

FIA (2022). *Forest Inventory and Analysis (FIA) program of the USDA Forest Service. Research and Development Deputy Area of the U.S.* Available Online at: https://www.fia.fs.usda.gov/ (accessed Sep 5, 2022).

Franklin, J. F., and Van Pelt, R. (2004). Spatial aspects of structure complexity in old-growth forests. *J. For.* 102, 22–28.

Frey, S. J. K., Hadley, A. S., Johnson, S. L., Schulze, M., Jones, J. A., and Betts, M. G. (2016). Spatial models reveal the microclimatic buffering capacity of old-growth forests. *Sci. Adv.* 2016:e1501392. doi: 10.1126/sciadv.1501392

Gorelick, N., Hancher, M., Dixon, M., Ilyushchenko, S., Thaud, D., and Moore, R. (2017). Google Earth Engine: Planetary-scale geospatial analysis for everyone. *Remote Sens. Environ.* 202, 18–27. doi: 10.1016/j.rse.2017.06.031

Griscom, B. W., Adams, J., Ellis, P. W., Houghton, R. A., Lomax, G., Miteva, D. A., et al. (2017). Natural climate solutions. *Proc. Natl. Acad. Sci. U.S.A.* 114, 11645–11650. doi: 10.1073/pnas.1710465114

Gunn, J. S., Ducey, M. J., and Whitman, A. A. (2013). Late-successional and old-growth forest carbon temporal dynamics in the Northern Forest (Northeastern USA). *For. Ecol. Manag.* 312, 40–46. doi: 10.1016/j.foreco.2013.10.023

Hanberry, B. B., Brzuskek, R. F., Foster, H. T., and Schauwecker, F. J. (2018). Recalling open old growth forests in the southeastern mixed forest province of the United States. *Ecoscience.* 26, 1–12. doi: 10.1080/1195860.2018.1499282

Hansen, M. C., Potapov, P. V., Moore, R., Hancher, M., Turubanova, S. A., Tyukavina, A., et al. (2013). High-resolution global maps of 21st-century forest cover change. *Science* 342, 850–853. doi: 10.1126/science.1244693

Harris, N. L., Gibbs, D. A., Baccini, A., Birdsey, R. A., De Bruin, S., Farina, M., et al. (2021). Global maps of twenty-first century forest carbon fluxes. *Nat. Clim. Change* 11, 234–240. doi: 10.1038/s41558-020-00976-6

Heilman, G. E., Strittholt, J. R., Slosser, N. C., and DellaSala, D. A. (2002). Forest fragmentation of the conterminous United States: Assessing forest intactness through road density and spatial characteristics. *Bioscience* 52, 411–422. doi: 10.1641/0006-3568(2002)052[0411:FFOTCU]2.0.CO;2

Intergovernmental Panel on Climate Change [IPCC] (2022). *Climate Change 2022: Impacts, Adaptation And Vulnerability*. Available Online at: https://www.ipcc.ch/report/sixth-assessment-report-working-group-ii/ (accessed March 22, 2022).

IUCN (2020). *Policy On Primary Forests And Intact Forest Landscapes*. Available Online at: https://www.iucn.org/sites/dev/files/content/documents/iucn_pf-ifl_policy_2020_approved_version.pdf (accessed May 15, 2022).

Kauffman, M. R., Binkley, D., Fule, P. Z., Johnson, M., Stephens, S. L., and Swetnam, T. W. (2007). Defining old growth for fire-adapted forests of the western United States. *Ecol. Soc.* 12:15. doi: 10.5751/ES-02169-120215

Kauffman, M. R., Moir, W. H., and Bassett, R. L. (1992). *Old-growth forests in the southwest and Rocky Mountain Regions Proceedings of a Workshop*. Techn. Rept. RM-213, Washington, DC: USDA Forest Service Gen. doi: 10.2737/RM-GTR-213

Keith, H., Lindenmayer, D., Mackey, B., Blair, D., Carter, L., McBurney, L., et al. (2014). Managing temperate forests for carbon storage: Impacts of logging versus forest protection on carbon stocks. *Ecosphere* 5:75. doi: 10.1890/ES14-00051.1

Keith, H., Mackey, B., Berry, S., Lindenmayer, D., and Gibbons, P. (2010). Estimating carbon carrying capacity in natural forest ecosystems across heterogenous landscapes: Addressing sources of error. *Glob. Change Biol.* 16, 2971–2989. doi: 10.1111/j.1365-2486.2009.02146.x

Keith, H., Mackey, B., Kun, Z., Mikolas, M., Svitok, M., and Svoboda, M. (2022). Evaluating the mitigation effectectiveness of forests managed for conservation versus commodity production using an Australian example. *Conserv. Lett.* 2022:e12878. doi: 10.1111/conl.12878

Keith, H., Mackey, B. G., and Lindenmayer, D. B. (2009). Re-evaluation of forest biomass carbon stocks and lessons from the world's most carbon-dense forests. *Proc. Natl. Acad. Sci. U.S.A.* 106, 11635–11640. doi: 10.1073/pnas.0901970106

Krankina, O., DellaSala, D. A., Leonard, J., and Yatskov, M. (2014). High biomass forests of the Pacific Northwest: Who manages them and how much is protected? *Environ. Manag.* 54, 112–121. doi: 10.1007/s00267-014-0283-1

LANDFIRE (2016). *LF 2016 Maps*. Available Online at: https://landfire.gov/ (accessed May 15, 2022).

Law, B. E., Berner, L. T., Buotte, P. C., Mildrexler, D. J., and Ripple, W. J. (2021). Strategic forest reserves can protect biodiversity in the western United States and mitigate climate change. *Commun. Earth Environ.* 2:254. doi: 10.1038/s43247-021-00326-0

Law, B. E., Moomaw, W. R., Hudiburg, T. W., Schlesinger, W. H., Sternman, J. D., and Woodwell, G. M. (2022). Creating strategic reserves to protect forest carbon and reduce biodiversity losses in the United States. *Land* 2022:721. doi: 10.3390/land11050721

Lawrence, D., Coe, M., Walker, W., Verchot, L., and Vandecar, K. (2022). The unseen effects of deforestations: Biophysical effects on climate. *Front. For. Glob.* 5:756115. doi: 10.3389/ffgc.2022.756115

Leak, W. B., and Yamasaki, M. (2012). *Historical (1899) Age and Structural Characteristics of an Old-Growth Northern Hardwood Stand in New York State. Res. Note NRS-144*. Newtown Square, PA: U.S. Department of Agriculture. doi: 10.2737/NRS-RN-144

Lesmeister, D. B., Davis, R. J., Sovern, S. G., and Yang, Z. (2021). Northern spotted owl nesting forests as fire refugia: A 30-year synthesis of large wildfires. *Fire Ecol.* 17:32. doi: 10.1186/s42408-021-00118-z

Lindenmayer, D. B., Laurance, W. F., and Franklin, J. F. (2012). Global decline in large old trees. *Science* 338, 1305–1306. doi: 10.1126/science.1231070

Lindenmayer, D. B., Laurance, W. F., Franklin, J. F., Likens, G. E., Banks, S. C., Blanchard, W., et al. (2014). New policies for old trees: Averting a global crisis in a keystone ecological structure. *Conserv. Lett.* 7, 61–69. doi: 10.1111/conl.12013

Lutz, J. A., Furnis, T. J., Johnson, D. J., Davies, S. J., Allen, D., Alonson, A., et al. (2018). Global importance of large-diameter trees. *Glob. Ecol. Biogeogr.* 27, 849–864. doi: 10.1111/geb.12747

Luyssaert, S., Detlef Schulz, E., Borner, A., Knohl, A., Hessenmoller, D., Law, B. E., et al. (2008). Old-growth forests as global carbon sinks. *Nature* 455, 213–215. doi: 10.1038/nature07276

Mack, E., Lilja, R., Claggett, S., Sun, G., and Caldwell, P. (2022). *Forests To Faucets 2.0: Connecting Forests, Water And Communities*. Asheville: USDA Forest Service GTR Southern Research Station, doi: 10.2737/WO-GTR-99

Mackey, B., DellaSala, D. A., Kormos, C., Lindenmayer, D., Kumpel, N., Zimmerman, B., et al. (2014). Policy options for the world's primary forests in multilateral environmental agreements. *Conserv. Lett.* 8, 139–147. doi: 10.1111/conl.12120

Mayer, P., Prescott, C. E., Abaker, W. E. A., Augusto, L., Cécillon, L., Ferreira, G. W., et al. (2020). Tamm review: Influence of forest management activities on soil organic carbon stocks: A knowledge synthesis. *For. Ecol. Manag.* 466:118127. doi: 10.1016/j.foreco.2020.118127

McKenney, D. W., and Pedlar, J. H. (2003). Spatial models of site index based on climate and soil properties for two boreal tree species in Ontario, Canada. *For. Ecol. Manag.* 175, 497–507. doi: 10.1016/S0378-1127(02)00186-X

Mildrexler, D. J., Berner, L. T., Law, B. E., Birdsey, R. A., and Moomaw, W. R. (2020). Large trees dominate carbon storage in forests east of the Cascade Crest in the United States Pacific Northwest. *Front. For. Glob. Change* 3:594274. doi: 10.3389/ffgc.2020.594274

Moomaw, W. R., Masino, S. A., and Faison, E. K. (2019). Intact forests in the United States: Proforestation mitigates climate change and serves the greatest good. *Front. For. Glob. Change* 2:27. doi: 10.3389/ffgc.2019.00027

National Geographic (2021). *The U.S. Commits to Tripling its Protected lands. Here's how it Could be Done*. Available Online at: https://www.nationalgeographic.com/environment/article/biden-commits-to-30-by-2030-conservation-executive-orders#:~:text=DEFENDERS%20OF%\hbox{20WILDLIFE-,}Biden's%20commitment%20to%20conserve%2030%20percent%20of%20U.S.%20land%20by,30%20by%2030%20conservation%20goal (accessed Sep 5, 2022).

Northern Rockies Ecosystem Protection Act (2021). *S.1276-Northern Rockies Ecosystem Protection Act*. Available Online at: https://www.congress.gov/bill/117th-congress/senate-bill/1276/text (accessed April 15, 2022).

Noss, R. F., Dobson, A. P., Baldwin, R., Beier, P., Davis, C. R., DellaSala, D. A., et al. (2012). Bolder thinking for conservation. *Conserv. Biol.* 26, 1–4. doi: 10.1111/j.1523-1739.2011.01738.x

Nowacki, G. J., and Abrams, M. D. (2008). The demise of fire and "mesophication" of forests in the eastern United States. *Bioscience* 58, 123–138. doi: 10.1641/B580207

Omernik, J. M., and Griffith, G. E. (2014). Ecoregions of the conterminous United States: Evolution of a hierarchical spatial framework. *Environ. Manag.* 54, 1249–1266. doi: 10.1007/s00267-014-0364-1

Orians, G. H., and Schoen, J. W. (eds) (2012). *North Pacific Temperate Rainforests: ecology and conservation*. Seattle: University of Washington Press.

Pan, Y., Chen, J. M., Birdsey, R., McCullough, K., He, L., and Deng, F. (2011). Age structure and disturbance legacy of North American forests. *Biogeosciences* 8, 715–732. doi: 10.5194/bg-8-715-2011

Perry, T. D., and Jones, J. A. (2016). Summer streamflow deficits from regenerating Douglas-fir forest in the Pacific Northwest, USA. *Ecohydrology* 10:e1790. doi: 10.1002/eco.1790

Petersen, R., Goldman, E., Harris, N., Sargent, S., Aksenov, D., Manisha, A., et al. (2016). *Mapping Tree Plantations with Multispectral Imagery: Preliminary Results for Seven Tropical Countries*. Washington, DC: World Resources Institute.

Potapov, P., Li, X., Hernandez-Serna, A., Tyukavina, A., Hansen, M. C., Kommarddeddy, A., et al. (2021). Mapping global forest canopy height through integration of GEDI and Landsat data. *Remote Sens. Environ.* 253:112165. doi: 10.1016/j.rse.2020.112165

Reid, M., Harkness, M., Kittel, G., Schulz, K., and Comer, P. (2016). *Documenting Relationships Between Blms Special Status Species And Their Habitats*. Arlington VA: Bureau of Land Management by NatureServe. 35p + Appendices and Data Tables.

Ripple, W., Wolf, C., Newsome, T. M., Gregg, J. W., Lenton, T. M., Palomo, I., et al. (2021). World scientists' warning of a climate emergency. *Bioscience* 71, 894–898. doi: 10.1093/biosci/biab079

Ruefenacht, B., Finco, M. V., Nelson, M. D., Czaplewski, R., Helmer, E. H., Blackard, J. A., et al. (2008). Conterminous US and Alaska forest type mapping using forest inventory and analysis data. *Photogramm. Eng. Remote Sens.* 74, 1379–1388. doi: 10.14358/PERS.74.11.1379

Sass, E. M., Butler, B. J., and Markowski-Lindsay, M. A. (2020). *Forest Ownership In The Conterminous United States Circa 2017: Distribution Of Eight Ownership Types – Geospatial Dataset*. Fort Collins, CO: Forest Service Research Data Archive, doi: 10.2737/RDS-2020-0044

Shifley, S. R., Roovers, L. M., and Brookshire, B. L. (1995). "Structural and compositional differences between old-growth and mature second-growth forests in the Missouri Ozarks," in *Proceedings, 10th Central Hardwood Forest Conference*, eds K. W. Gottschalk, and S. L. C. Fosbroke (Radnor, PA: U.S. Department of Agriculture).

Spies, T. A. (2004). Ecological concepts and diversity of old-growth forests. *J. For.* 102, 14–20. doi: 10.1111/brv.12470

Stein, B. A., Kutner, L. S., and Adams, J. S. (eds) (2000). *Precious Heritage: The Status of Biodiversity in the United States*. New York, NY: Oxford University Press. doi: 10.1093/oso/9780195125191.001.0001

Stephenson, N. L. D. A. J., Condit, R., Russo, S. E., Baker, P. J., Beckman, N. G., Coomes, D. A., et al. (2014). Rate of tree carbon accumulation increases continuously with tree size. *Nature* 507, 90–93. doi: 10.1038/nature12914

Strittholt, J. R., DellaSala, D. A., and Jiang, H. (2006). Status of mature and old-growth forests in the Pacific Northwest. *Conserv. Biol.* 20, 363–374. doi: 10.1111/j.1523-1739.2006.00384.x

U.S. Geological Survey [USGS], and Gap Analysis Project [GAP] (2020). *Protected Areas Database of the United States (PAD-US) 2.1*. Reston: U.S. Geological Survey data release.

UNFCCC (2021). *United Nations Glasgow Climate Summit*. Available Online at: https://unfccc.int/process-and-meetings/conferences/glasgow-climate-change-conference-october-november-2021/outcomes-of-the-glasgow-climate-change-conference (accessed May 28, 2022).

United Nations (2022). *Sustainability Goal 15*. Available Online at: https://sdgs.un.org/goals/goal15 (accessed May 28, 2022).

United Nations Climate Change (2021). *Glasgow Leaders' Declaration on Forests and Land Use. (2021). UN 2104 Clim. Change Conf. COP26SEC—Glasg. 2021*. Available Online at: https://ukcop26.org/glasgow-leaders-declaration-on-forests-and-land-use/ (accessed on April 19, 2022).

USDA Forest Service (2022). *Nantahala and Pisgah National Forests. R8-MB-160*. Available Online at: https://www.fs.usda.gov/Internet/FSE_DOCUMENTS/fseprd987300.pdf (accessed May 15, 2022).

USGS, USDA, and NRCS (2013). *Federal Standards And Procedures For The National Watershed Boundary Dataset (Wbd)*. Lakewood: US Geological Survey Techniques and Methods.

vonHedemann, N., and Schultz, C. (2021). U.S. family forest owners' forest management for climate adaptation: Perspectives from extension and outreach specialists. *Front. Clim.* 3:674718. doi: 10.3389/fclim.2021.674718

Vynne, C., Dovichin, E., Fresco, N., Dawson, N., JoshL, A., Law, B. E., et al. (2021). The importance of Alaska for climate stabilization, resilience, and biodiversity conservation. *Front. For. Glob. Change* 4:701277. doi: 10.3389/ffgc.2021.701277

Waller, D. M., and Reo, N. J. (2018). First stewards: Ecological outcomes of forest and wildlife stewardship by indigenous peoples of Wisconsin, USA. *Ecol. Soc.* 23:45. doi: 10.5751/ES-09865-230145

White House (2021). *Executive Order on Catalyzing Clean Energy Industries and Jobs Through Federal Sustainability*. Available Online at: https://www.whitehouse.gov/briefing-room/presidential-actions/2021/12/08/executive-order-on-catalyzing-clean-energy-industries-and-jobs-through-federal-sustainability/ (accessed May 28, 2022).

White House (2022). *Executive Order on Strengthening the Nation's Forests, Communities, and Local Economies*. Available Online at: https://www.whitehouse.gov/briefing-room/presidential-actions/2022/04/22/executive-order-on-strengthening-the-nations-forests-communities-and-local-economies/ (accessed May 28, 2022).

Wilson, E. O. (2016). *Half-Earth: Our Planet's Fight For Life*. New York, NY: Liveright Publishing Corporation.

Have product substitution carbon benefits been overestimated? A sensitivity analysis of key assumptions

Environmental Research Letters

LETTER

Have product substitution carbon benefits been overestimated? A sensitivity analysis of key assumptions

Mark E Harmon

Department of Forest Ecosystems and Society, Oregon State University, Corvallis, OR 97331, United States of America

E-mail: Mark.Harmon@oregonstate.edu

OPEN ACCESS

RECEIVED
12 May 2017

REVISED
7 March 2019

ACCEPTED FOR PUBLICATION
1 May 2019

PUBLISHED
21 June 2019

Keywords: forest sector, carbon storage, forest management, climate mitigation, forest ecosystems

Supplementary material for this article is available online

Abstract

Substitution of wood for more fossil carbon intensive building materials has been projected to result in major climate mitigation benefits often exceeding those of the forests themselves. A reexamination of the fundamental assumptions underlying these projections indicates long-term mitigation benefits related to product substitution may have been overestimated 2- to 100-fold. This suggests that while product substitution has limited climate mitigation benefits, to be effective the value and duration of the fossil carbon displacement, the longevity of buildings, and the nature of the forest supplying building materials must be considered.

Introduction

Forest ecosystems represent important stores of global terrestrial carbon and are the focus of possible climate mitigation strategies [1–3]. Along with that stored in forest ecosystems, carbon can be stored in wood products in-use and after disposal [4, 5]. Another way forests could mitigate climate change is through product substitution, a process whereby products from the forest substitute for others (i.e. concrete and steel) which, if used, would result in more fossil carbon release to the atmosphere [6–16]. While wood-based building materials generally embody less fossil-derived energy in their manufacture than steel and concrete, resulting in a net displacement of fossil carbon, its effectiveness as a climate mitigation strategy depends on the amount of carbon displaced and its duration. Current estimates of climate mitigation benefits of product substitution are generally based on three critical, often unstated assumptions: (1) the carbon displacement value remains constant [8–16], (2) the displacement is permanent and therefore of infinite duration [12–16] which implies no losses via cross-sector leakage, and (3) there is no relationship between building longevity and substitution longevity [10]. Below, each of these assumptions is reviewed.

Although most analyses of product substitution benefits implicitly assume a constant displacement value over time [8–16], it is subject to change. Schlamadinger and Marland [12] hypothesized energy substitution displacement values increase over time because of increased efficiencies. For product substitution, I hypothesize it will likely move in the opposite direction for three reasons. First, changing manufacturing methods impact embodied energy: for example, as long as it is available, the addition of fly ash could lead to a 22%–38% reduction in embodied energy required for concrete reducing the displacement value [17]. At the same time, increased processing of wood to create materials suitable for taller buildings (e.g. cross laminated timbers) would likely lead to a lower displacement value given laminated beams have 63%–83% more embodied energy than sawn softwoods [9, 17]. Second, the increases in energy efficiency hypothesized by [12] related to rising energy costs and recycling [9, 18, 19] and as noted by [8, 16] would also result in a decrease in product substitution displacement because the key relationship involves the difference in emissions and not the ratio as in energy substitution [20] (see supplemental information is available online at stacks.iop.org/ERL/14/065008/mmedia for detailed analysis of the displacement formula). Finally, changing the mix of fossil fuels used to generate energy can also substantially change the amount of carbon released per unit energy consumed and if natural gas continues to increase relative

to coal, as has been observed [21], then the displacement value would likely decline in the future. The same is true if non-fossil energy sources such as solar, wind, or hydropower are increasingly used as projected [22].

One possible mechanism leading to permanent displacement is that fossil carbon not used by the building sector is also not used in any other sector in the future. However, this seems unlikely given carbon leakage [20, 23–25]. While the rate of product substitution-related leakage is difficult to estimate (in part because the form and location of the fossil carbon is not specifically known), it is unlikely to be zero given fossil carbon-based fuels are expected to be depleted in the next 107–235 years [26, 27] (see supplemental information). Even if these depletion time estimates are off by centuries, the duration of the displacement is not infinite and the claim that 'saved fossil emissions are forever' [12] is untenable. I hypothesize that without a mechanism to prevent its use, that fossil carbon displaced by product substitution will gradually be released by other sectors and will not be excluded from depletion as implied by [10, 12].

The key assumption of no relationship between product longevity and product substitution longevity has been asserted [10], but not fully explained. If there always is a preference for non-wood building materials, then avoiding their use avoids fossil carbon emissions, hence the displacement would continue to accumulate [20]. However, if wood is preferred then the use of wood does not necessarily increase cumulative displacement [20]. Despite differences in regional preferences for wood [28], most if not all assessments of product substitution tacitly assume wood is not preferred and that preferences never change. As a consequence, the product substitution store never saturates and implying there is no negative feedback in the net cumulative displacement. In all other forest-related carbon pools, a negative feedback exists between pool size and output (i.e. they are donor controlled systems): the larger the pool size, the larger the output flow. This causes these pools to saturate in time as long as the input remains constant. It is striking that this behavior is true for wood products, but not for product substitution (see supplemental information). In [12] product and energy substitution are treated the same. However, I believe they are quite different. In the case of energy, once energy is used it does not have a lifespan or store per se. However, in the case of wood products when the product lifespan is exceeded it has to be replaced with either wood-based or some other materials. If it is the former, the fossil carbon displacement continues, but does not necessarily increase [20] (see supplemental information). If it is the latter, the fossil carbon that was displaced is released to the atmosphere [20]. I therefore hypothesize that when wood is or becomes the preferred building material the product substitution pool has a negative feedback directly related to building longevity.

The objective of this study is a sensitivity analysis of these three assumptions and their impact on projected climate mitigation benefits. In addition to examining each assumption separately, I examined how they might work together to determine whether product substitution carbon benefits eventually become as large relative to the forest ecosystem and harvested materials as previous analyzes suggest [10–15]. To perform this analysis I used a relatively simple landscape model assuming an idealized, regulated system and focused on conditions in which product substitution benefits would be highest (i.e. clear-cut harvest, high manufacturing efficiency, and maximum use of products in buildings). The cases examined are therefore illustrative of the kinds of behavior the assumptions create, but not an exhaustive analysis of all forest ecosystems, management or manufacturing systems. Nor does the analysis try to identify the most likely values of displacement factors, carbon leakage, or product lifespans: e.g. [29, 30].

Methods

Each of the three assumptions was examined individually and then jointly for three contrasting initial conditions using a simple landscape model[1] that tracks the stores for the live, dead, and soil carbon pools in the forest ecosystem, the products in use and disposal, and the virtual carbon stores associated with product substitution. Each of these pools was modeled as a simple input–output, donor controlled sub-model following first order dynamics in which the output was regulated by a rate-constant describing the fraction lost per year. For product substitution, the fossil carbon displaced was the input, and losses were associated with use of fossil carbon by other sectors (hereafter called leakage losses) and those associated with the replacement of wooden buildings (hereafter called replacement losses). All simulations were conducted for a 300 year period as in [8] using a 50 year harvest cycle.

Displacement decline

In this set of simulations I assumed no losses associated with leakage or building replacement. The initial displacement value of 2.1 Mg C per 1 Mg C wood use [20] was reduced by 25%, 50% and 100% over either a 25, 50, or 100 year period. The 100% decline represents the possibility that fossil carbon will be completely replaced as a source of energy in the location of manufacture. As a control, the displacement value was assumed to not decline.

[1] A more complete description of the model and parameters are available as supplemental information online.

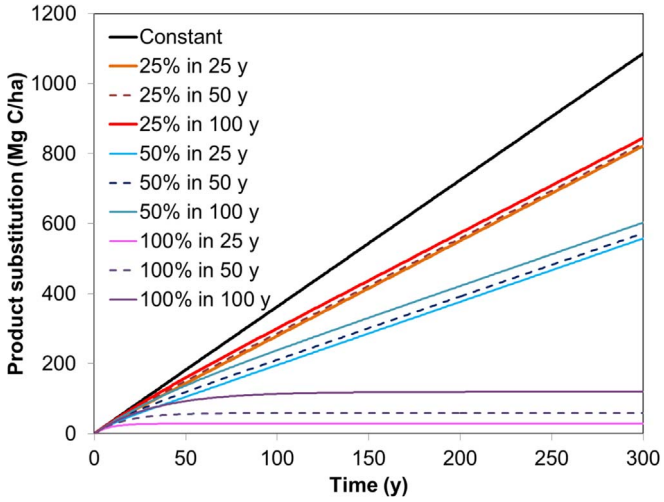

Figure 1. Accumulation of product substitution carbon when displacement is reduced 25%–100% over a 25–100 year period for a 50 year clear-cut harvest interval. For these simulations losses via leakage and replacement were zero[3].

Leakage losses

In this set of simulations I assumed the displacement value remained 2.1 Mg C per 1 Mg C wood use and there were no losses associated with building replacement. To examine the sensitivity of substitution benefits to cross-sector leakage, I simulated five possible scenarios: (1) no leakage, (2) 12%, (3) 6%, (4) 3%, (5) 1.5%, (6) 0.75, and (7) 0.375% yr^{-1}. In these scenarios leakage via other sectors was assumed to be continuous and not a one-time phenomenon. While expressed as a constant percentage lost per year, these values imply depletion times ranging between 25 and 800 years, which are 71%–340% of the currently estimated range of 35–235 years [26, 27].

Replacement losses

In this set of simulations I assumed the displacement value remained 2.1 Mg C per 1 Mg C wood use and there were no losses associated with cross-sector leakage. I varied the average building life-span to be 25, 50, 100, and 200 years, which bracket current estimates[2]. To provide a comparison to past studies, I reduced replacement losses to zero since this parameterization mimics the consequences of assuming no relationship between building longevity and product substitution longevity (see supplemental information).

Overall effect

To assess the overall effect of product substitution assumptions I examined a clear-cut system for three possible initial conditions: (1) an old-field planted to a production forest, (2) a production forest that originated from an old-growth forest landscape that began conversion 100 years ago, and (3) an old-growth forest converted to a production forest. In each case I assumed that 65% of the live carbon would be harvested, that 75% of that harvest would be converted into buildings. To explore the sensitivity of the assumptions on their overall impact I used the displacement and leakage loss parameter values that gave the minimum, median, and maximum effect based on the earlier simulations. In the case of replacement losses, I assumed an average building lifespan of either 50 years, 100 years, or an infinite number of years. The various combinations resulted in 47 simulations per initial condition. The model parameterization was based on a productive forest in the Pacific Northwest, a major source of wood building materials and US carbon stores [31].

Results

Displacement decline

There was a direct relationship to the total product substitution virtual store and the degree displacement declined, although the faster the decline in the displacement, the lower the final value (figure 1). For example, a 25% decline in 25, 50, and 100 years led to a final reduction in the product substitution virtual store of 24.3%, 23.6%, and 22.3%, respectively. This suggests that while the timing of the decline had an effect, the major response was to the level. The product substitution virtual store saturated only for the cases in which displacement went to zero and even if this took 100 years, product substitution stores estimates at 300 years were reduced by ≈89%.

[2] Estimates of housing longevity are highly variable with exponential rate-constants ranging from 0.0069/y to 0.03/y [12–16]. In some cases building longevity has been modeled as a step function, with rapid losses after 80 years [10–11]. These estimates give an average lifespan or turnover time of 33–144 years. I explored a range of 25 to 200 years to bracket this uncertainty. Note that the average lifespan is not the same as the maximum lifespan of buildings: for an average lifespan of 50 years, the maximum lifespan would be over 230 years.

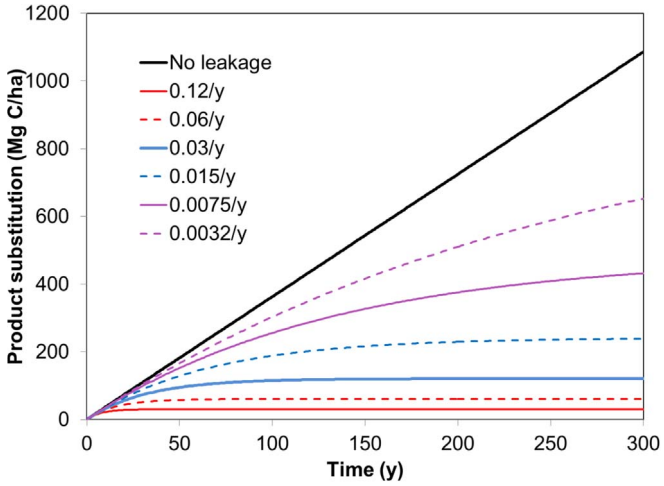

Figure 2. Accumulation of product substitution carbon when the time for displacement to be lost via leakage varies from 25 to 800 years for a 50 year clear-cut harvest interval. Displacement was assumed constant and replacement losses zero[3].

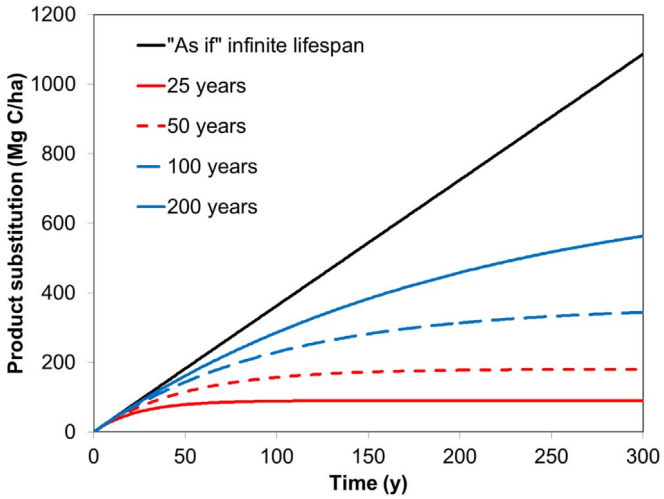

Figure 3. Accumulation of product substitution carbon when the average longevity of building varies for a 50 year clear-cut harvest interval. For these simulations displacement was constant and there were no leakage losses[3].

Leakage losses

Regardless of the time required for cross-sector leakage to occur, this process substantially limited the product substitution virtual store relative to the case without leakage (figure 2). With a leakage as low as 0.375% yr^{-1} (≈one-third the current estimate of the minimum depletion rate [27]) the store at 300 years was ≈40% lower than when there was no leakage. If the leakage rate-constant was 12% yr^{-1}, then ≈97% less would be stored relative to the no leakage scenario. Moreover, if the current range of depletion times (i.e. 35–235 years) is correct, then cross-sector leakage would reduce the estimates by 78%–96%. This indicates that leakage via other sectors may substantially undermine any attempt to displace fossil carbon using product substitution.

Replacement losses

For an average building longevity of 50 years the product substitution store at 300 years was ≈17% of that of the case in which product substitution behaved as if it had infinite lifespan (figure 3). Even when average building lifespan was 200 years, this store at 300 years was ≈52% that of when product substitutions behaved as if they had an infinite lifespan. This indicates that assuming no relationship between product substitution lifespan and building lifespan overestimates benefits.

Overall effect

Product substitution, estimated using past assumptions regarding displacement decline, leakage, and relationship to building longevity, increased for each initial condition; increasing the most when old-growth forests were harvested (figure 4). When alternative assumptions about product substitution were used, the shape of the product substitution accumulation curve varied: generally increasing for the old-field conversion to an asymptote, decreasing or increasing

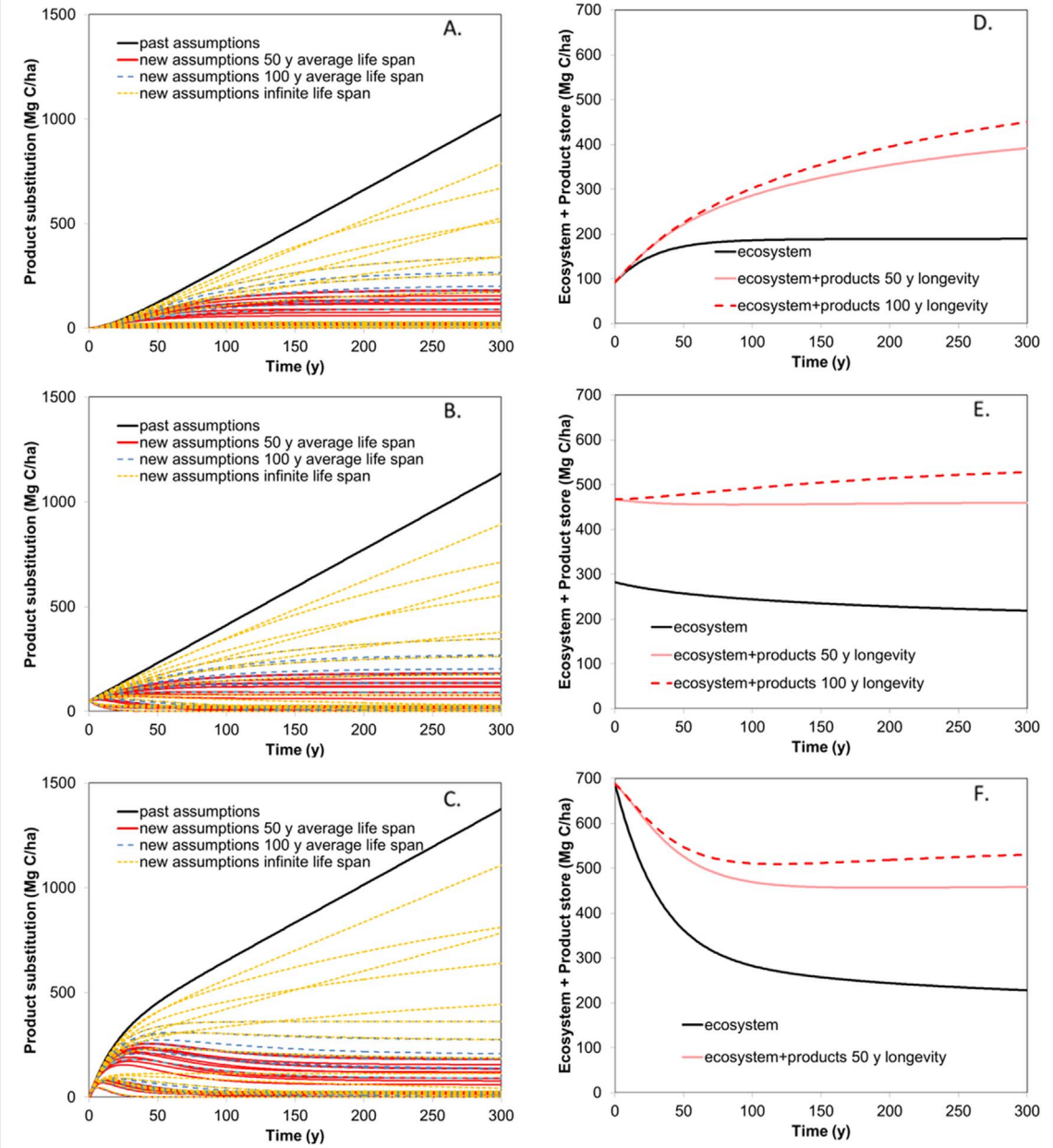

Figure 4. Accumulation of ecosystem, products in-use and disposed, and product substitution carbon stores for a 50 year clear-cut harvest interval in the Pacific Northwest for three possible scenarios: a plantation forest established on an agricultural field (A), (D); a production forest system that is continued (B), (E); an old-growth forest replaced by a forest plantation (C), (F). For past assumptions there was no decline in displacement value, there was no leakage, and buildings were assumed to have an infinite lifespan[3,4].

to an asymptote for the plantation system depending on replacement assumptions, and for most combinations reaching a peak at 10–40 years for the old-growth forest converted to a plantation scenario. This analysis indicates that to increase the overall amount of carbon stored in the system, that conversions of old-growth forests in the Pacific Northwest to plantations should be avoided, whereas creation of plantations on old-fields should be encouraged. Moreover, existing plantation systems are unlikely to increase their carbon stores unless building longevity is substantially increased (figure 4(e)).

Regardless of the initial conditions, product substitution was lower when alternative assumptions regarding displacement decline, leakage, and relationship to building lifespan were used, ranging from virtually zero to 80% of the past assumptions at year 300 depending on the parameter values assumed (tables S-2 to S-4). At the very least this suggests product substitution estimates are extremely uncertain. However, 85% of the 141 combinations examined were <50% than currently estimated. Those few exceeding 50% involved the assumption that substitution replacement losses were zero (i.e. an infinite lifespan) and had either an unrealistically low rate of

[3] See figures S-7 to S-10 for detailed view of the first 50 years.

[4] See supplemental text and figure for similar results for a productive Southeastern US forest.

leakage (i.e. less than one-third that indicated by the maximum depletion time) or a minimal decline in displacement. Moreover, although past assumptions would indicate product substitution forms a large share of carbon stores at year 300 (74%–80% depending on the initial conditions), 90% of the alternative combinations examined indicated it was less than 50%. The combinations in which product substitution stores comprise the majority share of stores assumed an infinite lifespan and either minimal displacement decline or extremely low cross-sector leakage rates (tables S-2 to S-4).

Discussion

Past analyses suggest product substitution benefits at the landscape level continue to increase at a constant rate into the future [6–16]. Moreover, they imply that while a carbon debt can be created in some situations (e.g. harvest of primary forests), that this debt is eventually paid back via product substitution [10, 12, 32]. While I examined only a few illustrative cases, in the case of product substitution, these debts would not be paid back if the displacement declines or there are losses via cross-sector leakage or related to product replacement. That is because negative feedbacks associated with losses can prevent product substitution from accumulating forever. These negative feedbacks could exist regardless of the forest ecosystem, the harvest system, and the efficiency of processing harvests into products as well as the proportion allocated to buildings. Thus, while I did not examine the effect on a wide range of ecosystems, or alternative harvest systems, or systems in which buildings are minor faction of harvested carbon, these underlying relationships would not be altered for these new situations[4].

The assumption that the product substitution benefit has no losses (e.g. [10]) results in at least two sets of untenable predictions: (1) if fossil fuel carbon is stored each time a wooden building is constructed, then theoretically it would be possible for fossil fuel carbon to be stored long after this carbon has been depleted by other sectors; hence this assumption may violate the conservation of mass; (2) this assumption also views the following as the same: (a) harvest that completely replaces wood building losses, (b) harvest that does not replace wood building losses, (c) harvest that exceeds wood building losses leading to more wood buildings, and (d) wood buildings that are not replaced. These cases clearly differ [20] (see supplemental information). This assumption also introduces a logical inconsistency: products appear to have different lifespans depending on whether their direct carbon (finite) or substitution carbon (infinite) effects are being considered (figure S-4).

Although displacement decline over time influences the accumulation of product substitution benefits, its effect is smaller than leakage or replacement losses. In contrast, leakage loss has as dramatic effect as longevity even if it occurs at a very slow rate implying the effect of product substitution is to delay eventual fossil carbon release, but not to stop it altogether. This may be important because it buys time, but this is not the same as the displaced fossil carbon never being released as suggested by [10, 12].

Collectively the past assumptions commonly used to assess the mitigation benefits of product substitution lead to a carbon pool that does not saturate causing the product substitution pool to eventually exceed the carbon stores in the forest ecosystem and in the associated wood products. Moreover, because there are no losses from the products substitution pool, its highest rate of increase occurs for the harvest interval providing the highest yield, typically a very young age relative to the forest ecosystem carbon maximum [32]. With no relationship to building longevity, there is no relationship to the size of the wood products pool despite the fact that more wooden buildings would imply more success in displacing fossil carbon. Finally, this set of assumptions makes product substitution benefits relatively insensitive to the initial conditions of the forest ecosystem because product substitution benefits always increase over time.

The alternative set of assumptions explored here suggests that the highest overall climate mitigation may not necessarily be achieved by maximizing the harvest yield using short rotation forestry [33]. Moreover, if product substitution is the primary climate mitigation strategy, wood building materials need to keep their carbon advantage by maintaining or increasing their displacement value. This suggests that while wood can be used in buildings taller than the general current practice, this may have less mitigation value than anticipated if these materials embody more fossil energy than current wood-based materials. Given the strong potential relationship between building and product substitution longevity, increasing the life-span of buildings or reusing building materials could potentially help meet future demand and increase mitigation benefits. Without a policy to assure that fossil carbon displaced by one sector is not used by another sector, product substitution benefits could be quite limited. While it is unlikely any policy could completely eliminate cross-sector leakage, designating long-term reserves might delay releases until their climate impacts are reduced to acceptable levels.

Conclusions

Despite its general and limited nature, this sensitivity analysis found that product substitution benefits

have likely been overestimated for many scenarios and are generally smaller than those related to the forest ecosystem and their derived products. This new analysis suggests that if product substitution is to be used as part of a climate mitigation strategy, then more attention will have to be paid to maintaining the amount of carbon displaced, reducing the rate of carbon cross-sector leakage, and increasing the longevity of buildings. This new analysis also suggests that the best strategy for forest-related climate mitigation for an important timber region, the Pacific Northwest, is largely determined by the initial conditions of the management system. Afforestation leads to an increase in carbon stores in the ecosystem, wood products, and substitution benefits for many decades. On existing production forests, substitution benefits could be maintained by continuing the current system or increased by harvesting more (but only as long as ecosystem carbon stores do not decline) and/or increasing the longevity of buildings. Conversion of older, high carbon stores forests to short rotation plantations would over the long-term likely lead to more carbon being added to the atmosphere despite some of the harvested carbon being stored and production substitution occurring [33].

Acknowledgments

This research was funded by the Kaye and Ward Richardson endowment to the College of Forestry, Oregon State University and grant from the National Science Foundation (DEB-0823380 and DEB-1440409) to the Andrews LTER. I thank Drs Darius Adams, Thomas C Maness and the anonymous reviewers for their valuable insights.

ORCID iDs

Mark E Harmon https://orcid.org/0000-0002-4195-8288

References

[1] Smith P *et al* 2014 Agriculture, forestry and other land use (AFOLU) *Climate Change 2014: Mitigation of Climate Change. Contribution of Working Group III to the Fifth Assessment Report of the Intergovernmental Panel on Climate Change* ed O R Edenhofer *et al* (Cambridge and New York, NY: Cambridge University Press)

[2] Birdsey R A, Plantinga A J and Heath L S 1993 Past and prospective carbon storage in United-States forests *Forest Ecol. Manage.* **58** 33–40

[3] McKinley D C *et al* 2011 A synthesis of current knowledge on forests and carbon storage in the United States *Ecol. Appl.* **21** 1902–24

[4] Skog K E 2008 Sequestration of carbon in harvested wood products for the United States *Forest Prod. J.* **58** 56–72

[5] Skog K E and Nicholson G A 1998 Carbon cycling through wood products: the role of wood and paper products in carbon sequestration *Forest Prod. J.* **48** 75–83

[6] Bethel J S and Schreuder G F 1976 Forest resources: an overview *Science* **191** 747–52

[7] Buchann A H and Levine S B 1999 Wood-based building materials and atmospheric carbon emissions *Environ. Sci. Policy* **2** 427–37

[8] Börjesson P and Gustavsson L 2000 Greenhouse gas balances in building construction: wood versus concrete from life-cycle and forest land-use perspectives *Energy Policy* **28** 575–88

[9] Glover J, White D O and Langrish T A G 2002 Wood versus concrete and steel in house construction *J. Forestry* **100** 34–41

[10] Lippke B, Oneil E, Harrison R, Skog K, Gustavsson L and Sathre R 2011 Life cycle impacts of forest management and wood utulization: knows and unknowns *Carbon Manage.* **2** 303–33

[11] Perez-Garcia J, Lippke B, Comnick J and Manriquez C 2005 An assessment of carbon pools, storage, and wood products market substitution using life-cycle analysis results *J. Wood Fiber Sci.* **37** 140–8

[12] Schlamadinger B and Marland G 1996 The role of forest and bioenergy strategies in the global carbon cycle *Biomass Bioenergy* **10** 275–300

[13] Hennigar C R, MacLean D A and Amos-Binks L J 2008 A novel approach to optimizing management strategies for carbon stored in both forests and wood products *Forest Ecol. Manage.* **256** 786–97

[14] Upton B, Miner R, Spinny M and Heath L S 2008 The greenhouse gas and energy impacts of using wood instead of alternative in residential construction in the United States *Biomass Bioenerg* **32** 1–10

[15] Eriksson E, Gillespie A R, Gustavsson L, Langvall O, Olsson M, Sathre R and Stendahl J 2007 Integrated carbon analysis of forest management practices and wood substitution *Can. J. For. Res.* **37** 671–81

[16] Gustavsson L, Pingoud K and Sathre R 2006 Carbon dioxide balance of wood substitution: comparing concrete-and wood-framed buildings *Mitig. Adapt. Strateg. Glob. Change* **11** 667–91

[17] Hammond G and Jones C 2008 Inventory of carbon and energy (ICE) Version 1.6a (https://doi.org/10.1680/ener.2008.161.2.87)

[18] Saghafi M and Teshnizi Z S H 2011 Recycling value of building materials in building assessment systems *Energy Build.* **43** 3181–8

[19] Tormark C 2002 A low energy building in a life cycle—its embodied energy, energy need for operation and recycling potential *Build. Environ.* **37** 429–35

[20] Sathre R and O'Connor J O 2010 Meta-analysis of greenhouse gas displacement factors of wood substitution *Environ. Sci. Policy* **13** 104–14

[21] Hayhoe K, Kheshgi H S, Jain A K and Wuebbles D J 2002 Substitution of natural gas for coal: climatic effects of utility sector emissions *Clim. Change* **54** 107–39

[22] US Energy Information Agency 2017 *Int. Energy Outlook 2017* (Washington, DC: USDOE Energy Information Administration, Office of Energy Analysis) (www.eia.gov/outlooks/ieo/pdf/0484(2017).pdf)

[23] Eichner T and Pethig R 2011 Carbon leakage, the green paradox, and perfect future markets *Int. Econ. Rev.* **52** 767–805

[24] Paltsev S V 2001 The Kyoto protocol: regional and sectoral contributions to the carbon leakage *Energy J.* **22** 53–80

[25] Babiker M H 2005 Climate change policy, market structure, and carbon leakage *J. Int. Econ.* **65** 421–45

[26] Shafiee S and Topal E 2009 When will fossil fuel reserves be diminished? *Energy Policy* **37** 181–9

[27] Mohr S H, Wang J, Ellem G, Ward J and Giurco D 2015 Projection of world fossil fuels by country *Fuel* **141** 120–35

[28] Gustavsson L, Madlener R, Hoen H F, Jungmeier G, Karjalainen T, Klöhn S, Mahapatra K, Pohjola J, Solberg B and Spelter H 2006 The role of wood material for greenhouse gas mitigation *Mitig. Adapt. Strateg. Glob. Change* **11** 1097–127

[29] Dymond C C 2012 Forest carbon in North America: annual storage and emissions from British Columbia's harvest, 1965–2065 *Carbon Bal. Manage.* **7** 1–8

[30] Dymond C C and Kamp A 2014 Fibre use, net calorific value, and consumption of forest-derived bioenergy in British Columbia, Canada *Biomass Bioenergy* **70** 217–24
[31] Birdsey R A 1992 Carbon storage and accumulation in United States forest ecosystems *Gen. Tech. Rep. WO-59* (Washington DC: U.S. Department of Agriculture, Forest Service, Washington Office) (https://doi.org/10.2737/WO-GTR-59)
[32] Oliver C D, Nassar N T, Lippke B R and McCarter J B 2014 Carbon, fossil fuel, and biodiversity mitigation with wood and forests *J. Sustain. For.* **33** 248–75
[33] Mackey B, Prentice I C, Steffen W, House J I, Lindenmayer D, Keith H and Berry S 2013 Untangling the confusion around land carbon science and climate change mitigation policy *Nat. Clim. Change* **3** 552–7

Meeting GHG reduction targets requires accounting for all forest sector emissions

Environmental Research Letters

LETTER

Meeting GHG reduction targets requires accounting for all forest sector emissions

Tara W Hudiburg[1,4], Beverly E Law[2], William R Moomaw[3], Mark E Harmon[2] and Jeffrey E Stenzel[1]

[1] Department of Forest, Rangeland and Fire Sciences, 875 Perimeter Dr MS 1133, University of Idaho, Moscow, ID 83844, United States of America
[2] Department of Forest Ecosystems and Society, 321 Richardson Hall, Oregon State University, Corvallis, OR 97333, United States of America
[3] Center for International Environment and Resource Policy, The Fletcher School, and Global Development and Environment Institute, Tufts University, Medford MA, United States of America
[4] Author to whom any correspondence should be addressed.

E-mail: thudiburg@uidaho

Keywords: carbon, forests, wood products, climate mitigation, GHG mandates

Supplementary material for this article is available online

OPEN ACCESS

RECEIVED
20 February 2019

REVISED
3 June 2019

ACCEPTED FOR PUBLICATION
11 June 2019

PUBLISHED
23 August 2019

Abstract

Atmospheric greenhouse gases (GHGs) must be reduced to avoid an unsustainable climate. Because carbon dioxide is removed from the atmosphere and sequestered in forests and wood products, mitigation strategies to sustain and increase forest carbon sequestration are being developed. These strategies require full accounting of forest sector GHG budgets. Here, we describe a rigorous approach using over one million observations from forest inventory data and a regionally calibrated life-cycle assessment for calculating cradle-to-grave forest sector emissions and sequestration. We find that Western US forests are net sinks because there is a positive net balance of forest carbon uptake exceeding losses due to harvesting, wood product use, and combustion by wildfire. However, over 100 years of wood product usage is reducing the potential annual sink by an average of 21%, suggesting forest carbon storage can become more effective in climate mitigation through reduction in harvest, longer rotations, or more efficient wood product usage. Of the ~10 700 million metric tonnes of carbon dioxide equivalents removed from west coast forests since 1900, 81% of it has been returned to the atmosphere or deposited in landfills. Moreover, state and federal reporting have erroneously excluded some product-related emissions, resulting in 25%–55% underestimation of state total CO_2 emissions. For states seeking to reach GHG reduction mandates by 2030, it is important that state CO_2 budgets are effectively determined or claimed reductions will be insufficient to mitigate climate change.

Introduction

Heat trapping greenhouse gases (GHGs) are being added to the atmosphere at an accelerating rate by fossil fuel combustion and land use change. Climate change consequences were recently described by the Intergovernmental Panel on Climate Change (IPCC) and the United States National Climate Assessment (USGCRP 2018). The IPCC Special Report (IPCC 2018), Global Warming of 1.5 °C, concludes that to keep global average temperature below 1.5 °C by 2100, it is essential to reduce fossil fuel emissions by 45% by 2030, while substantially increasing the removal of atmospheric CO_2. Both reports emphasize the need to increase atmospheric CO_2 removal strategies by forests in addition to sustaining current forest carbon uptake (Houghton and Nassikas 2018). Some states in the US have set targets for reducing GHGs that include forest climate mitigation options (Anderson *et al* 2017, Law *et al* 2018), yet consistent, rigorous accounting methods are required for evaluating options. Challenges include determining the extent that forests, harvest operations, and wood products affect GHG budgets and emissions accountability.

The most recent global carbon budget estimate indicates that land-based sinks remove 29% of anthropogenic emissions (including land use change) with a significant contribution from forests (Le Quéré *et al* 2018). However, none of the agreements or policies (IPCC 2006, NRCS 2010, Brown *et al* 2014, Doe 2017, EPA 2017, Duncan 2017) provides clear and consistent procedures for quantitatively assessing the extent forests and forest products are increasing or reducing carbon dioxide concentrations in the atmosphere. Assessments are challenging because they involve components that require multiple types of expertise and accounting methods (i.e. forest ecosystem processes, wood products, and inherently uncertain substitution credits). Methods are often in disagreement over the wood product Life Cycle Assessment (LCA) assumption of *a priori* carbon neutrality, where biogenic emissions from the combustion and decomposition of wood is ignored because the carbon released from wood is assumed to be replaced by subsequent tree growth in the following decades (EPA 2016). Despite a multitude of analyses that recognize that the assumption is fundamentally flawed (Harmon *et al* 1996, Gunn *et al* 2011, Haberl *et al* 2012, Schulze *et al* 2012, Buchholz *et al* 2016, Booth 2018), it continues to be used in mitigation analyses, particularly for wood bioenergy.

Forests are sustainable *net* sinks as long as forest carbon uptake from the atmosphere exceeds emissions from harvesting, wood product use and decomposition, and wildfire. Wood products ultimately release CO_2 to the atmosphere as they are manufactured, disposed of, and decompose or are burned. However, because of concerns about double-counting, significant emissions associated with harvest and wood product use have not been counted for any sector (EPA 2018). These emissions are often not included in state CO_2 budget estimates (Brown *et al* 2014, Oregon Global Warming Commission 2017), even when they are included in national budgets (EPA 2017) (table S1 is available online at stacks.iop.org/ERL/14/095005/mmedia). If US states intend to use forests for mitigation strategies, they must account for all contributing sources and sinks of forests and forest-derived products (Stockmann *et al* 2012, IPCC 2014).

By focusing on a region with sufficient information to conduct a meaningful LCA, we demonstrate how a quantitative assessment of forests, management practices and wood products can assess the actual role played by forests and forestry practices in managing atmospheric CO_2. We calculate the regional forest carbon balance (from 2001 to 2016) using observations from over 24 000 forest inventory plots in Washington, Oregon, and California (states with GHG reduction mandates). Net forest sector carbon balance is quantified using an improved LCA including harvest, transportation, manufacturing, wood product pool storage and decay, emissions associated with fire, and substitution for both building construction and energy production. We specifically consider global warming potential associated with carbon dioxide and do not include additional GHGs such as nitrous oxide and methane. Our aim is to provide an accurate cradle-to-grave, transparent and transferable accounting method of all forest-derived carbon for other states and countries with GHG reduction mandates (figure 1; box 1; figure S1; tables S2–S6).

Results

Western US forest ecosystem CO_2 balance (2001–2016)

Forest carbon uptake and release (net ecosystem production (NEP); figure 1(a)) controlled by ecosystem biological processes is calculated as the balance between forest carbon uptake (net primary production (NPP)) and forest carbon release through the decomposition of dead organic matter (heterotrophic respiration; R_h). In this study, a negative number indicates a net carbon sink (removal from the atmosphere) and a positive number indicates a net carbon source (addition to the atmosphere). The coastal Western US states together are a strong forest carbon sink with NEP of -292 ± 36 million metric tonnes (MMT) CO_2e per year (-857 g CO_2e m^{-2} yr^{-1}) (table 1; table S1), and account for approximately 60% of total Western US forest NEP (coastal, southwestern, and intermountain regions).

In addition to NEP, disturbances from harvest and wildfire influence estimates of net ecosystem carbon balance (NECB = NEP minus losses Chapin *et al* 2006; figure 1(a)). In the Western US states, the significant carbon losses from the forest are primarily from removals of wood through harvest, decomposition or burning of aboveground and belowground harvest residues, and wildfire (Law and Waring 2015). Significant harvest has been occurring in the western US since the early 20th century (figure S2). Up to 40% of the harvested wood does not become a product and the products themselves decay over time, resulting in product accumulation much smaller than the total amount harvested (figure 2(a); solid line) (Harmon *et al* 1996, Dymond 2012, Williams *et al* 2016, EPA 2017). Emissions include combustion of wood that does not become a product, combustion for energy, decomposition and/or combustion at end-of-life (table 1; rows 5, 6, 9, and 10). When these carbon losses are accounted for, these forests remain significant carbon sinks at -187 ± 33 MMT CO_2e per year (-551 g CO_2e m^{-2} yr^{-1}), with the largest sink in California (40%) followed by Oregon (33%) and Washington (27%). Despite California having twice the fire emissions of the other states (~10 versus ~5 MMT CO_2e yr^{-1} per state) the ranking is due to much lower harvest removals in California (~12 MMT CO_2e yr^{-1}) compared to almost double in

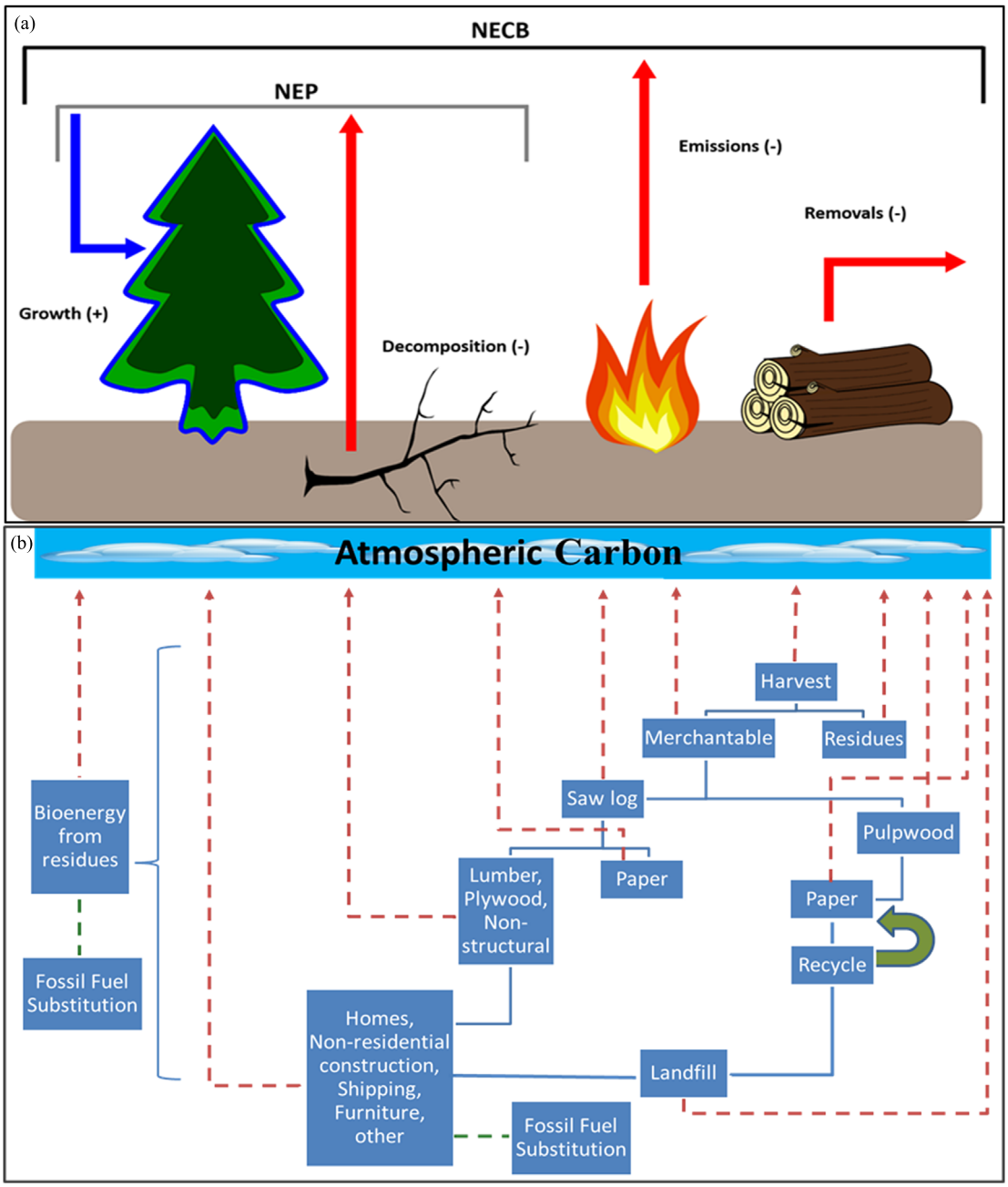

Figure 1. Conceptual diagram of Forest-GHG (a) describes the natural, land-based forest carbon sink where the net of growth and decomposition is net ecosystem production (NEP), and after accounting for removals from fire and harvest, the balance is net ecosystem carbon balance (NECB), (b) describes the cascade of wood products until eventual deposition in landfills or the atmosphere and shows the pathway of emissions.

Washington (~20 MMT $CO_2e\ yr^{-1}$) and triple in Oregon (~31 MMT $CO_2e\ yr^{-1}$). Fire emissions are a third of harvest removals region-wide.

Building on our earlier work (Harmon *et al* 1996, Hudiburg *et al* 2011, Law *et al* 2018), we developed a modified cradle-to-grave model (Forest-GHG) for combining the balance of carbon captured in forest ecosystems, wood product use, lifetime emissions, and eventual return to the atmosphere or long-term storage in landfills. Forest-GHG tracks emissions associated with harvest of wood and manufacturing, transport and use of wood products. Harvest removals result in immediate (combustion of residues on-site or as mill residues with and without energy recapture), fast (short-lived products such as paper), decadal (long-lived products such as wood) and centuries-long (older buildings and land-filled) timeframes before emissions are released back to the atmosphere (figures 1(b) and S1). Our model includes seven product pools and temporally dynamic recycling and landfill rates. Most importantly, we now include a more mechanistic representation of longer-term structural wood in buildings, by moving beyond a simple half-life with exponential decay (figure 3 and SI methods and SI tables 2–6). Our new building cohort-component method tracks decay of short- and

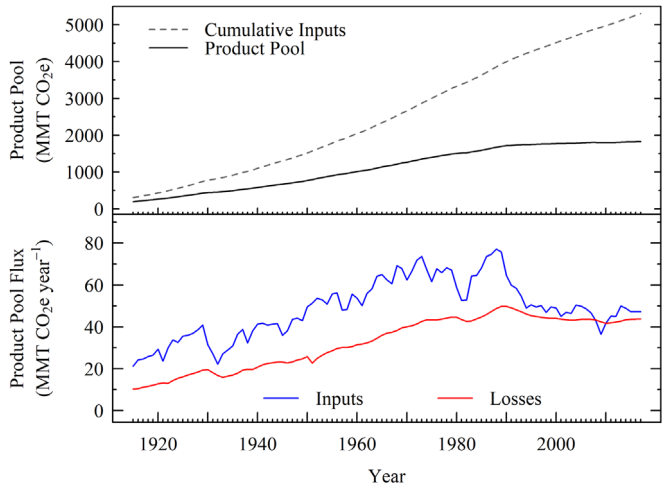

Figure 2. Wood product inputs and outputs from 1900 to 2016 for Washington, Oregon, and California. (A) Cumulative production in MMT CO_2e per year assuming no losses over time (dotted grey line) versus the realized in-use wood product pool over time after accounting for decay (losses). (B) Yearly product inputs over time (blue line) that represents the fraction of harvest (removed wood) that becomes a product versus the decay emissions from the pool over time (red line).

Table 1. Average annual total fluxes by state and region from 2001 to 2016. All units are in million MT CO_2e. Negative numbers indicate a carbon sink (CO_2 is being removed from the atmosphere). The more negative the number, the stronger the sink. Grey shading is used to indicate net values that represent carbon sink strength both before and after removals are accounted for.

Ecosystem	Washington	Oregon	California	Total
1. Forested area (million hectares)	9.7	12.4	11.9	34.0
2. Net ecosystem production (NEP)	**−89.9**	**−102.0**	**−99.8**	**−291.6**
3. Fire emissions	5.1	5.3	10.3	20.7
4. Harvest removals	18.5	30.5	11.5	60.5
Net ecosystem carbon balance (NECB) (sum of rows 1 through 4)	**− 66.4**	**−66.2**	**−78.0**	**−210.5**
Forest industry	**Washington**	**Oregon**	**California**	**Total**
5. Harvest residue combustion (onsite)	3.9	6.5	2.5	12.9
6. Harvest, transportation, manufacturing (FFE emissions)	2.8	4.6	1.6	9.0
7. Wood product pool annual inputs	−18.5	−30.5	−11.5	−60.5
8. Landfill annual inputs (from products)	−6.8	−11.9	−4.2	−22.9
9. Wood manufacturing losses	3.9	6.5	3.9	14.3
10. Wood product and landfill decomposition	21.4	36.2	13.3	71.0
Net forest sector carbon balance (NECB + sum of rows 5 through 10)	**−59.5**	**−54.7**	**−72.4**	**−186.6**
11. Wood product substitution (wood)	−3.0	−4.9	−1.6	−9.4
12. Wood product substitution (energy)	−1.8	−3.0	−1.8	−6.6
Net forest sector carbon balance (with credits; NECB + sum of rows 5 through 12)	**−64.3**	**−62.6**	**−75.8**	**−202.7**

long-lived building components annually, and the lag time associated with these losses (figure S3). Our wood bioenergy substitution credits (Sathre and O'Connor 2010) include wood waste from harvest, mill residues, and wood products displacement of more fossil fuel intensive materials.

Using our component tracking LCA, we found that of the ~10 700 MMT CO_2e of wood harvested in all three states since 1900 (figure 2), only 2028 MMT CO_2e are currently stored in wood products with half stored in Oregon (1043 MMT CO_2e). In just over 100 years, Oregon has removed the equivalent of all live trees in the state's Coast Range forests (Law *et al* 2018), and returned 65% to the atmosphere and transferred 16% to landfills. Even though these are some of the most productive and carbon dense forests in the world (Hudiburg *et al* 2009), the carbon accumulated in much of the removed biomass took up to 800 years to accumulate—and cannot be recovered if current management practices continue.

Forest harvest-related emissions have averaged 107 MMT CO_2e annually from 2001 to 2016 (table 1; row 5, 6, 9, and 10). Emissions are highest from decay of the wood product pool that has been accumulating for over 100 years (table 1 row 10; figures 3 and S3). This is after accounting for recycling and semi-permanent storage in landfills. Structural wood product decay for long- and short-term components (wood in buildings; figure 3) account for about 30%–35% of wood product and landfill decomposition while paper and non-building wood products account for about 65%–70%. Under this complete accounting, the

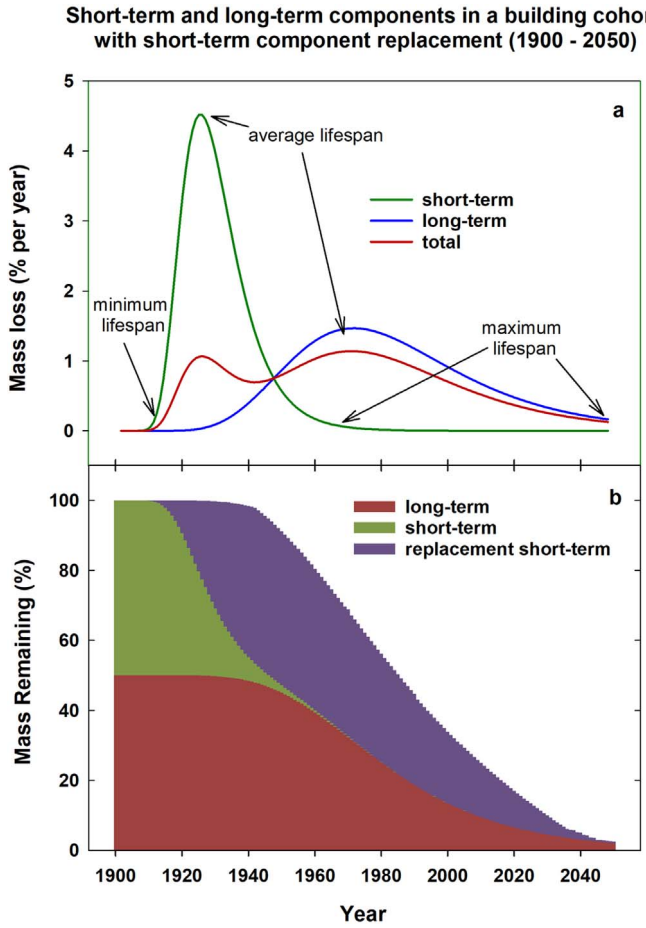

Figure 3. Conceptual models of the Forest-GHG cohort-component method for: (a) mass loss in a cohort of buildings with a 75 year average life span that accounts for the short and long-term portions of buildings and (b) mass remaining in a single building cohort over time (with replacement). Data presented is based on the 1900 cohort of single-family homes built in Oregon.

lowest contribution to overall emissions is from fossil fuel usage during harvest, transportation, and manufacturing, i.e. less than 10% of total wood product-related emissions in the three states.

We found that wood-related substitution for construction materials (0.54 fossil fuel carbon emissions avoided per unit carbon of wood; table 1 row 11) and energy (0.68 fossil fuel carbon emissions avoided; table 1 row 12) may offset 18% of forest industry emissions. This assumes 50% of wood-derived construction products are substituted for a non-wood product and that 75% of mill residues are substituted for fossil fuel energy (Berg *et al* 2016).

We varied the maximum average life spans of the wood products used in construction (e.g. buildings) to examine its effect on emissions estimates. Emissions are minimally reduced by 2%–4% in each state when a longer average maximum lifespan is used (100 years) for the long-term building components and minimally increased by 2%–3% when a shorter average maximum lifespan is used (50 years, which is the mean lifetime of buildings in the US EPA 2013).

Combined, the US west coast state forest sector (cradle-to-grave) is a net carbon sink, removing ~187 MMT CO_2e annually from the atmosphere and potentially reducing fossil fuel emissions by up to another 20 MMT CO_2e through product and energy substitution. Harvest-related emissions reduce the natural sink (NEP—Fire) by 34, 46, and 27% for Washington, Oregon, and California, respectively. When substitution credits are included, this changes to reductions of 27%, 37%, and 23%. Harvest rates have been highest in Oregon (table 1), contributing to increasing wood product emissions and the largest reductions to forest sink capacity.

Discussion

NECB is a good estimate of ecosystem carbon uptake, e.g. for carbon offsets programs (Anderson *et al* 2017), and can be compared spatially with changing environmental conditions or disturbances, but is an incomplete calculation of the entire forest sector emissions. It does not include emissions from wood products caused by machinery, transport, manufacturing and losses—emissions that can equal up to 85% of the total versus 15% from fire, insects, and land use change (Williams *et al* 2016). Nor does it account for the storage and subsequent release of carbon in varying

end uses with varied product lifetimes. Given that not all harvested wood is an immediate source to the atmosphere and very little harvested wood is stored in perpetuity, it is essential to track associated emissions over time. For state- or region-level carbon budgets, a cradle-to-grave carbon LCA should be combined with the ecosystem carbon balance (NEP and NECB) to account for how much the forestry sector is contributing to or offsetting total carbon emissions.

If wood buildings are replaced by wood buildings, substitution is not occurring, and because wood is preferred for construction of single-family housing in North America, some of our substitution values are overestimated (Sathre and O'Connor 2010). Wood products store carbon temporarily, and a larger wood product pool increases decomposition emissions over time (figure 3). This emphasizes that increasing the wood product carbon sink will require shifts in product allocation from short-term to long-term pools such as reclaimed (re-used) wood products from demolition of buildings, and reduction of product manufacturing losses (EPA 2016). Clearly, there is potential for climate mitigation by using forests to sequester carbon in biomass and reduce losses associated with the wood product chain (Law *et al* 2018).

It is argued that there may be reductions in fossil carbon emissions when wood is substituted for more fossil fuel intensive building materials (e.g. steel or concrete) or used as an alternative energy source (Butarbutar *et al* 2016). Substitution is a one-time credit in the year of the input. Studies have reported a range of substitution displacement factors (from negative to positive displacement; Sathre and O'Connor 2010, Smyth *et al* 2017), but we found no study that has tracked the actual amount of construction product substitution that is occurring or has occurred in the past in the United States. This makes substitution one of the most uncertain parts of this carbon budget. It may be more easily tracked in the fossil fuel sector through a decrease in emissions because of reduction in product supply, in which case it would be double counting to then include it as a credit for the forest sector. We show results with and without the substitution credit (a decrease in forest sector emissions) because it cannot be verified. We show the potential impact it has on the overall forest sector carbon sink, even though the displacement factor may be unrealistically high (Smyth *et al* 2017, Dugan *et al* 2018). For forest sector emissions assessments, the uncertainty suggests exclusion of the credit.

Currently, state's GHG accounting budgets are incorrect because they are not full cradle-to-grave estimates of all CO_2 emissions associated with forest natural processes and human influences. For accurate GHG accounting, these emissions should be included in the forestry sector as they are not accounted for by state's energy and transportation sectors (IPCC 2006) (table S1). The US EPA reported average fossil fuel CO_2 emissions of 491 MMT CO_2e yr^{-1} for the three states combined (2013–2016). Forest industry harvest, transportation, and manufacturing fossil fuel emissions are included in this total. However, it is unclear to what extent wood product decay and combustion emissions are also counted in state budgets. In Oregon, they are not included at all, resulting in state CO_2 emissions that have been underestimated by up to 55% (Oregon Global Warming Commission 2017, Law *et al* 2018). Washington includes combustion emissions from the current year's harvest (table 1; Manufacturing losses; row 9), but not from wood product decay, resulting in up to a 25% underestimation of state CO_2 emissions. Because California's emissions from other sectors are so high (76% of regional total), and harvest rates have been historically lower than in Oregon and Washington, the impact of not including these emissions is very small as a proportion of the total. Although fire in California has received much attention, it only accounts for 3% of the state's total fossil fuel CO_2 emissions.

These underestimates are especially alarming for Oregon where GHG reduction targets are to be 10% below 1990 levels by 2020 and at least 75% below 1990 levels by 2050 (Pietz and Gregor 2014). California and Washington emissions are to be reduced to 1990 levels by 2020 (Nunez 2006), and 80% and 50% below 1990 levels by 2050 (Washington State 2008), respectively.

In contrast, the US EPA reports emissions from wood product decay and landfills (EPA 2017) per the IPCC guidelines (IPCC 2006) (table S1). However, combustion emissions from logging and mill residues are not reported (EPA 2017). Moreover, ecosystem carbon losses are indirectly estimated through changes in biomass pools with measurement uncertainty that can be greater than the change (Ferster *et al* 2015). So even at the national level, emissions (as a fraction of fossil fuel emissions) would be underestimated by 10% and 24% in Washington and Oregon, respectively. Undoubtedly, there are implications for reduction mandates when the magnitude of emissions themselves are incorrect.

Conclusions

The goal for all societies and governments as stated in Article 2 of the *United Nations Framework Convention on Climate* Change (Oppenheimer and Petsonk 2005) should be '…stabilization of GHG concentrations in the atmosphere at a level that would prevent dangerous anthropogenic interference with the climate system.' The Paris Climate Agreement (UNFCCC 2015) aims to keep global average temperature from rising by no more than 2 °C above preindustrial levels, and if possible no more than 1.5 °C. Forests are identified as part of the strategy (UNFCCC 2015).

Although some US states have attempted to quantify a portion of forest-related emissions, improved estimates are essential to track emissions to meet

reduction goals. We identified the main components that should be part of the forest sector state estimates. We found that emissions have been underestimated by up to 55% in Oregon and 25% in Washington, and that at present, these emissions are not reported in state GHG reporting guidelines. The accuracy of forest sector emissions estimates can be improved with sub-regional data on residential and commercial building lifespans, recycling, verifiable substitution benefits and accurate monitoring of growth rates of forests. However, verifiable substitution of one material for another may be more readily quantified in the fossil fuel sector.

The 2006 IPCC GHG guidelines provide three different approaches for calculating emissions from harvested wood products (IPCC 2006) (including reporting 'zero') and reporting of this component is not required by UNFCCC. To complicate accounting further, several studies have shown that using the different recommended approaches results in emissions that differ by over 100% (Green *et al* 2006, Dias *et al* 2007). Moreover, according to IPCC and UNFCCC, emissions of CO_2 from forest bioenergy are to be counted under land use change and not counted in the energy sector to avoid double counting. However, this provides a 'loophole' leading to their not being counted at all.

The United States government currently requires all federal agencies to count forest bioenergy as carbon neutral because the EPA assumes replacement by future regrowth of forests somewhere that may take several decades or longer (EPA 2018). While it is theoretically possible that a replacement forest will grow and absorb a like amount of CO_2 to that emitted decades or a century before, there is no guarantee that this will happen, and the enforcement is transferred to future generations. In any rational economic analysis, a benefit in the distant future must be discounted against the immediate damage associated with emissions during combustion. Furthermore, the goal for climate protection is not climate neutrality, but rather reduction of net GHGs emissions to the atmosphere to avoid dangerous interference with the climate system. Allowing forests to reach their biological potential for growth and sequestration, maintaining large trees (Lutz *et al* 2018), reforesting recently cut lands, and afforestation of suitable areas will remove additional CO_2 from the atmosphere. Global vegetation stores of carbon are 50% of their potential including western forests because of harvest activities (Erb *et al* 2017). Clearly, western forests could do more to address climate change through carbon sequestration if allowed to grow longer.

Since it is now clear that both CO_2 emissions and removal rates are essential to meet temperature limitation goals and prevent irreversible climate change, each should be counted and reported. We recommend that international agreements and states utilize a consistent and transparent carbon LCA that explicitly accounts for all forest and wood product storage and emissions to determine compliance with goals to lower atmospheric GHGs. Only by using a full accounting of GHGs can the world manage its emissions of heat trapping gases to achieve concentrations in the atmosphere that will support a stable climate.

Materials and methods

We calculated the 2001 to 2016 average net forestry sector emissions from cradle-to-grave, accounting for all carbon captured in biomass and released through decomposition by forest ecosystems and wood products industry in Washington, Oregon, and California. Building on our previous work (Harmon *et al* 1996, Hudiburg *et al* 2011, Law *et al* 2013, Law *et al* 2018), we developed a modified and expanded LCA method to combine with our ecosystem carbon balance, now called Forest-GHG (version 1.0; figure 1 and box 1). We accounted for all carbon removed from forests through fire and harvest. All harvested carbon was tracked until it either was returned to the atmosphere through wood product decomposition/combustion or decomposition in landfills, minus the amount semi-permanently stored in landfills (buried). This required calculating the carbon removed by harvest operations starting in 1900 to present day because a portion of the wood removed in the past century is still in-use or decomposing. In addition to carbon in biomass, we also accounted for all carbon emissions associated with harvest (equipment fuel, transportation, manufacturing inputs). Moreover, our wood product life-cycle assessment includes pathways for recycling and deposition in landfills. Finally, we give substitution credits for not using more fossil fuel intensive materials than wood used in construction of buildings and energy production.

Observed carbon stocks and fluxes (ecosystem carbon balance)

Carbon stock and flux estimates were calculated from over 30 000 forest inventory plots (FIA) containing over 1 million tree records in the region following methods developed in previous studies (Law *et al* 2018) (SI Methods). Flux calculations include NPP (Clark *et al* 2001) NEP, and NECB. The NECB represents the net rate of carbon accumulation in or loss from ecosystems.

Off-site emissions associated with harvest (LCA)

Decomposition of wood through the product cycle was computed using a LCA (Harmon and Marks 2002, Law *et al* 2018). A 117 year wood products pool (1900–2016) was simulated using reported harvest rates from 1900 to 2016 for Oregon and Washington (Harmon *et al* 1996, DNR 2017, Oregon Department of Forestry 2017) and from the California State Board of Equalization (CA 2018). Harvest was converted to

Box 1. Terminology and Flux Definitions for table 1

1. Forest Area = sum of all forest area in each state derived from US Forest Service forest area map (30 m resolution). Includes all ownerships.

1. NEP = Net Primary Production—heterotrophic respiration; microbial respiration as they decompose dead organic matter in an ecosystem.

1. Fire emissions = the emissions associated with *combustion* of organic matter at the time of the fire. Most of what burns is fine surface fuels, averaging 5% of aboveground biomass in mixed severity fires of Oregon and Northern California.

1. Harvest removals = Wood actually removed from the forest (not the total aboveground biomass killed). Removals are not equal to emissions but are the removed carbon from the forests at the time of harvest. This is subtracted from NEP along with fire emissions to calculate the net forest carbon balance from the viewpoint of the forest ecosystem.

NECB = NEP + Fire Emissions + Harvest Removals. The term is the simplest expression of forest carbon balance without tracking wood through the product life cycle. Although not all of the harvest removals will result in instant or near-term emissions, NECB still captures the impact of the removed carbon on the forest ecosystem carbon balance, and is consistent with international agreements (REDD+, conservation).

1. Harvest Residue Combustion = the emissions associated with combustion of slash piles; the branches, foliage, and non-merchantable wood left after harvest operations (remains in the forest) and burned onsite (assumed to be 50% of slash).

1. Harvest, Transportation, Manufacturing (FFE emissions) = the fossil fuel emissions associated with harvest (skidding, sawing, etc), transportation of logs to mills, manufacturing of wood and paper products, and transportation of products to stores (see table S5 for coefficients).

1. Wood Product Pool Annual Inputs = Harvest removals

1. Landfill Annual Inputs (from products) = The amount of wood and paper that is sent to landfills at end of life. In Forest-GHG, this occurs incrementally from 1950 to 1960 and then in 1961 is assumed to be constant at the current rate.

1. Wood Manufacturing Losses = fraction of wood that is lost at the mill (sawdust, etc) and is assumed to be returned to the atmosphere within one year through combustion (with 75% energy recapture) or decomposition.

1. Wood Product and Landfill Decomposition = fraction of the total wood product and non-permanent landfill carbon pools that is returned to the atmosphere annually.

Net Forest Sector Carbon Balance = sum of NECB and rows 5 through 10. Emission sources are rows 5, 6, 9, and 10. Sinks are rows 7 and 8.

1. Wood product substitution (Wood) = carbon credits that account for the displaced fossil fuel emissions when wood is substituted for a fossil fuel derived product in buildings (e.g. concrete or steel). We assume 0.54 g C fossil fuel emissions avoided per g of C of wood biomass used.

Box 1. (Continued.)

1. Wood product substitution (Energy) = carbon credits that account for the displaced fossil fuel emissions when wood is substituted for energy. In the Oregon, Washington, and California this primarily a mix of natural gas and coal. We include the biogenic emissions from combustion of forest-derived woody biomass and include an energy substitution credit if it is combusted with energy recapture.

Net Forest Sector Carbon Balance (with substitution credit) = sum of NECB and rows 5 through 12.

total aboveground biomass using methods from (Law *et al* 2018). The carbon emissions to the atmosphere from harvest were calculated annually over the timeframe of the analysis (1900–2016).

The coefficients and sources for the Forest-GHG LCA (figures 1(b) and S1) are included in table S1 through S6 with all units expressed as a function of the wood biomass being cut, transported, manufactured, burned, etc. We accounted for the fossil fuel emissions that occur during harvest (fuel for equipment) and the fossil fuel emissions associated with transport of wood to mills. Then, we accounted for the fossil fuel emissions associated with manufacturing of products followed by a second transportation emission for delivery of products to stores and warehouses. Wood that is not made into a wood or paper product (e.g. waste) is assumed to be combusted onsite at the mill (with 50% energy recapture as combined heat and power) or used in a product that will return the carbon to the atmosphere within one year (table 1 and box 1; Wood Manufacturing Losses).

Wood products are divided into varying product pools and are then tracked through the wood product cascade until end of life (figure 1(b)). Wood products are split into seven product pools: single-family homes, multi-family homes, mobile homes, non-residential construction, furniture and manufacturing, shipping, and other wood. We simulated wood product storage and emissions to 2050 for display purposes in the figures assuming a constant harvest rate after 2016.

We estimate the carbon pools and fluxes associated with buildings by separating buildings into components with different life spans (figures 3 and S3). This allows components and buildings to have a lag time before significant losses occur, and recognizes the difference between building life span and the residence time of carbon in a building. This also allows capacity for Forest-GHG to have component and building life spans evolve over time as construction practices and the environment (including biophysical, economic, and social drivers) change.

In Forest-GHG, a fraction of each year's new harvest is allocated to residential (single-family, multi-family, and mobile homes) and non-residential construction (Smith *et al* 2006). This fraction is further divided into the short-term (23%) and long-term (77%) components. The

resulting pools are tracked independently, quantifying losses through decay and demolition from the year they start until then end of the simulation.

All the components created in a given year are considered a building cohort that is also tracked separately each year. All components are summed to give the total amount of building carbon remaining in a cohort at a given time (figure S3). For each year, the amount lost to the atmosphere or to the landfills through demolition, is simply the current year's total wood product carbon pool plus the current years inputs and minus last year's total wood product carbon pool.

Substitution

We calculated wood product substitution for fossil fuel derived products (concrete, steel and energy). The displacement value for product substitution was assumed to be 0.54 Mg fossil C/Mg C (Smyth *et al* 2017, Dugan *et al* 2018) wood use in long-term structures (Sathre and O'Connor 2010). Although the displacement value likely fluctuates over time, we assumed it was constant for the simulation period. We accounted for losses in product substitution associated with building replacement (Harmon *et al* 2009), but ignored the leakage effect related to fossil C use by other sectors. We assumed 75% of 'waste wood' was used for fuelwood in homes or at mills (wood manufacturing losses in table 1). We accounted for displacement of fossil fuel energy sources using a displacement factor of 0.68 assuming a mix of coal and natural gas replacement (Smyth *et al* 2017, Dugan *et al* 2018).

Uncertainty estimates and sensitivity analysis

We calculate a combined uncertainty estimate for NEP and NECB using the uncertainty in the observations and input datasets (climate, land cover, harvest amounts). For the biomass and NPP observations, we performed Monte Carlo simulations of the mean and standard deviations for NPP (Hudiburg *et al* 2011) derived for each plot using three alternative sets of allometric equations. Uncertainty in NECB was calculated as the combined uncertainty of NEP, fire emissions (10%), harvest removals (7%), and land cover estimates (10%) using the propagation of error approach. Sensitivity analysis was only used for the long-term wood product pool by varying the average life spans of buildings by $\pm$25 years in our new cohort component method. Our estimates varied by 7%. This was combined with the uncertainty in NECB to calculate total uncertainty on the net forest sector carbon balance.

Acknowledgments

This research was supported by the Agriculture and Food Research Initiative of the US National Institute of Food and Agriculture Grant 2013-67003-20652 and the National Science Foundation award number DEB-1553049.

ORCID iDs

Tara W Hudiburg https://orcid.org/0000-0003-4422-1510
William R Moomaw https://orcid.org/0000-0003-2690-2339
Mark E Harmon https://orcid.org/0000-0002-4195-8288
Jeffrey E Stenzel https://orcid.org/0000-0001-8881-0566

References

Anderson C M, Field C B and Mach K J 2017 Forest offsets partner climate-change mitigation with conservation *Frontiers Ecol. Environ.* **15** 359–65

Berg E, Morgan T and Simmons E 2016 *Timber Products Output (TPO): Forest Inventory, Timber Harvest, Mill and Logging Residue-Essential Feedstock Information Needed to Chracterize the NAPA Supply Chain* (Missoula, MT: University of Montana)

Booth M S 2018 Not carbon neutral: assessing the net emissions impact of residues burned for bioenergy *Environ. Res. Lett.* **13** 035001

Brown E G, Rodriquez M, Nichols M D and Corey R W 2014 First Update to the California Climate Change Scoping Plan (Sacramento, CA: California Environmental Protection Agency, Air Resources Board)

Buchholz T, Hurteau M D, Gunn J and Saah D 2016 A global meta-analysis of forest bioenergy greenhouse gas emission accounting studies *GCB Bioenergy* **8** 281–9

Butarbutar T, Köhl M and Neupane P R 2016 Harvested wood products and REDD+: looking beyond the forest border *Carbon Balance Manage.* **11** 4

CA 2018 *California Timber Harvest Statistics* ed Equalization C B O (Sacremento, CA: California Board of Equalization) (https://www.boe.ca.gov/proptaxes/pdf/harvyr2.pdf)

Chapin F *et al* 2006 Reconciling carbon-cycle concepts, terminology, and methods *Ecosystems* **9** 1041–50

Clark D A, Brown S, Kicklighter D W, Chambers J Q, Thomlinson J R and Ni J 2001 Measuring net primary production in forests: concepts and field methods *Ecol. Appl.* **11** 356–70

Department of Ecology (Washington) 2017 Washington Mandatory Greenhouse Gas Reporting Program—Reported Emissions for 2012–2015 *Report* (Olympia, WA: Washington Department of Ecology) (https://ecology.wa.gov/Air-Climate/Climate-change/Greenhouse-gas-reporting/Inventories)

Dias A C, Louro M, Arroja L and Capela I 2007 Carbon estimation in harvested wood products using a country-specific method: Portugal as a case study *Environ. Sci. Policy* **10** 250–9

DNR 2017 Washington Timber Harvest Reports (https://dnr.wa.gov/TimberHarvestReports) (Accessed: July 2017)

Dugan A J, Birdsey R, Mascorro V S, Magnan M, Smyth C E, Olguin M and Kurz W A 2018 A systems approach to assess climate change mitigation options in landscapes of the United States forest sector *Carbon Balance Manage.* **13** 13

Duncan A 2017 *Biennial Report to the Legislature* (Salem, OR: Oregon Global Warming Commission)

Dymond C C 2012 Forest carbon in North America: annual storage and emissions from British Columbia's harvest, 1965–2065 *Carbon Balance Manage.* **7** 8–8

EPA 2013 *Analysis of the Life Cycle Impacts and Potential for Avoided Impacts Associated with Single-Family Homes* (Washington DC: Environmental Protection Agency) (https://www.epa.gov/sites/production/files/2015-11/documents/sfhomes.pdf)

EPA 2016 *Documentation for Greenhouse Gas Emission and Energy Factors Used in the Waste Reduction Model (WARM)* (Washington DC: Environmental Protection Agency) (https://www.epa.gov/warm/documentation-chapters-greenhouse-gas-emission-and-energy-factors-used-waste-reduction-model)

EPA 2017 *Inventory of US Greenhouse Gas Emissions and Sinks: 1990–2016* (Washington, DC: Environmental Protection Agency)

EPA 2018 *EPA's Treatment of Biogenic Carbon Dioxide (CO_2) Emissions from Stationary Sources that Use Forest Biomass for Energy Production* (Washington DC: Environmental Protection Agency) (https://www.epa.gov/air-and-radiation/epas-treatment-biogenic-carbon-dioxide-emissions-stationary-sources-use-forest)

Erb K-H *et al* 2017 Unexpectedly large impact of forest management and grazing on global vegetation biomass *Nature* **553** 73

Ferster C J, Trofymow J T, Coops N C, Chen B and Black T A 2015 Comparison of carbon-stock changes, eddy-covariance carbon fluxes and model estimates in coastal Douglas-fir stands in British Columbia *Forest Ecosyst.* **2** 13

Green C, Avitabile V, Farrell E P and Byrne K A 2006 Reporting harvested wood products in national greenhouse gas inventories: Implications for Ireland *Biomass Bioenergy* **30** 105–14

Gunn J S, Ganz D J and Keeton W S 2011 Biogenic versus geologic carbon emissions and forest biomass energy production *GCB Bioenergy* **4** 239–42

Haberl H, Sprinz D, Bonazountas M, Cocco P, Desaubies Y, Henze M, Hertel O, Johnson R K, Kastrup U and Laconte P 2012 Correcting a fundamental error in greenhouse gas accounting related to bioenergy *Energy Policy* **45** 18–23

Harmon M E, Harmon J M, Ferrell W K and Brooks D 1996 Modeling carbon stores in Oregon and Washington forest products: 1900–1992 *Clim. Change* **33** 521–50

Harmon M E and Marks B 2002 Effects of silvicultural practices on carbon stores in Douglas-fir western hemlock forests in the Pacific Northwest, USA: results from a simulation model *Can. J. For. Res.* **32** 863–77

Harmon M E, Moreno A and Domingo J B 2009 Effects of partial harvest on the carbon stores in Douglas-fir/western hemlock forests: a simulation study *Ecosystems* **12** 777–91

Houghton R A and Nassikas A A 2018 Negative emissions from stopping deforestation and forest degradation, globally *Glob. Change Biol.* **24** 350–9

Hudiburg T, Law B, Turner D P, Campbell J, Donato D and Duane M 2009 Carbon dynamics of Oregon and Northern California forests and potential land-based carbon storage *Ecol. Appl.* **19** 163–80

Hudiburg T W, Law B E, Wirth C and Luyssaert S 2011 Regional carbon dioxide implications of forest bioenergy production *Nat. Clim. Change* **1** 419–23

IPCC 2006 *2006 IPCC Guidelines for National Greenhouse Gas Inventories, Prepared by the National Greenhouse Gas Inventories Programme* ed H S Eggleston (Japan: IGES, Intergovernmental Panel on Climate Change)

IPCC 2014 *Climate Change 2014: Impacts, Adaptation, and Vulnerability. Part A: Global and Sectoral Aspects. Contribution of Working Group II to the Fifth Assessment Report of the Intergovernmental Panel on Climate Change* ed C B Field (Cambridge and New York, NY: Cambridge University Press)

IPCC 2018 Global warming of 1.5°C *Summary for Policymakers* ed P Zhai (Geneva: World Meteorological Organization)

Law B E, Hudiburg T W, Berner L T, Kent J J, Buotte P C and Harmon M E 2018 Land use strategies to mitigate climate change in carbon dense temperate forests *Proc. Natl Acad. Sci.* **115** 3663–8

Law B E, Hudiburg T W and Luyssaert S 2013 Thinning effects on forest productivity: consequences of preserving old forests and mitigating impacts of fire and drought *Plant Ecol. Diversity* **6** 73–85

Law B E and Waring R H 2015 Carbon implications of current and future effects of drought, fire and management on Pacific Northwest forests *Forest Ecol. Manage.* **355** 4–14

Le Quéré *et al* 2018 Global carbon budget 2018 *Earth Syst. Sci. Data* **10** 2141–94

Lutz J A *et al* 2018 Global importance of large-diameter trees *Glob. Ecol. Biogeogr.* **27** 849–64

NRCS 2010 Soil Survey Staff, Natural Resources Conservation Service, United States Department of Agriculture (http://soildatamart.nrcs.usda.gov). Soil Survey Geographic (SSURGO) Database for Eastern US

Nunez F and Paveley F 2006 Assembly Bill 32: the California Global Warming Solutions Act of 2006 (Sacramento, CA: California State Assembly)

Oppenheimer M and Petsonk A 2005 Article 2 of the UNFCCC: historical origins, recent interpretations *Clim. Change* **73** 195–226

Oregon Department of Forestry 2017 Timber Harvest Data 1942–2016 (https://catalog.data.gov/dataset/timber-harvest-data-1942-2016)

Pietz A and Gregor B 2014 Oregon statewide transportation strategy: 2050 vision for greenhouse gas emission reduction *Transp. Res. Rec.* **2454** 45–52

Sathre R and O'Connor J 2010 Meta-analysis of greenhouse gas displacement factors of wood product substitution *Environ. Sci. Policy* **13** 104–14

Schulze E D, Körner C, Law B E, Haberl H and Luyssaert S 2012 Large-scale bioenergy from additional harvest of forest biomass is neither sustainable nor greenhouse gas neutral *GCB Bioenergy* **4** 611–6

Smith J E, Heath L, Skog K E and Birdsey R 2006 Methods for calculating forest ecosystem and harvested carbon with standard estimates for forest types of the United States Gen *Tech. Rep*. NE-343 Newtown Square, PA: US Department of Agriculture, Forest Service, Northeastern Research Station

Smyth C, Rampley G, Lemprière T C, Schwab O and Kurz W A 2017 Estimating product and energy substitution benefits in national-scale mitigation analyses for Canada *GCB Bioenergy* **9** 1071–84

Stockmann K D, Anderson N M, Skog K E, Healey S P, Loeffler D R, Jones G and Morrison J F 2012 Estimates of carbon stored in harvested wood products from the United States forest service northern region, 1906-2010 *Carbon Balance Manage.* **7** 1

UNFCCC 2015 *Article 5. Paris Agreement* (Paris, France)

USGCRP *Impacts, Risks, and Adaptation in the United States: Fourth National Climate Assessment* vol II ed D R Reidmiller *et al* 2018 (Washington DC: US Global Change Research Program)

Washington State 2008 Engrossed Second Substitute House Bill 2815, State of Washington, 60th Legislature 2008 Regular Session (http://lawfilesext.leg.wa.gov/biennium/2007-08/Pdf/Bills/House%20Bills/2815-S2.E.pdf)

Williams C A, Gu H, Maclean R, Masek J G and Collatz G J 2016 Disturbance and the carbon balance of US forests: a quantitative review of impacts from harvests, fires, insects, and droughts *Glob. Planet. Change* **143** 66–80

Land use strategies to mitigate climate change in carbon dense temperate forests

Beverly E. Law[a,1], Tara W. Hudiburg[b], Logan T. Berner[c], Jeffrey J. Kent[b], Polly C. Buotte[a], and Mark E. Harmon[a]

[a]Department of Forest Ecosystems and Society, Oregon State University, Corvallis, OR 97333; [b]Department of Forest, Rangeland, and Fire Sciences, University of Idaho, Moscow, ID 83844; and [c]EcoSpatial Services L.L.C., Flagstaff, AZ 86004

Edited by William H. Schlesinger, Duke University, Durham, NC, and approved January 22, 2018 (received for review November 16, 2017)

Strategies to mitigate carbon dioxide emissions through forestry activities have been proposed, but ecosystem process-based integration of climate change, enhanced CO_2, disturbance from fire, and management actions at regional scales are extremely limited. Here, we examine the relative merits of afforestation, reforestation, management changes, and harvest residue bioenergy use in the Pacific Northwest. This region represents some of the highest carbon density forests in the world, which can store carbon in trees for 800 y or more. Oregon's net ecosystem carbon balance (NECB) was equivalent to 72% of total emissions in 2011–2015. By 2100, simulations show increased net carbon uptake with little change in wildfires. Reforestation, afforestation, lengthened harvest cycles on private lands, and restricting harvest on public lands increase NECB 56% by 2100, with the latter two actions contributing the most. Resultant cobenefits included water availability and biodiversity, primarily from increased forest area, age, and species diversity. Converting 127,000 ha of irrigated grass crops to native forests could decrease irrigation demand by 233 billion $m^3 \cdot y^{-1}$. Utilizing harvest residues for bioenergy production instead of leaving them in forests to decompose increased emissions in the short-term (50 y), reducing mitigation effectiveness. Increasing forest carbon on public lands reduced emissions compared with storage in wood products because the residence time is more than twice that of wood products. Hence, temperate forests with high carbon densities and lower vulnerability to mortality have substantial potential for reducing forest sector emissions. Our analysis framework provides a template for assessments in other temperate regions.

forests | carbon balance | greenhouse gas emissions | climate mitigation

Strategies to mitigate carbon dioxide emissions through forestry activities have been proposed, but regional assessments to determine feasibility, timeliness, and effectiveness are limited and rarely account for the interactive effects of future climate, atmospheric CO_2 enrichment, nitrogen deposition, disturbance from wildfires, and management actions on forest processes. We examine the net effect of all of these factors and a suite of mitigation strategies at fine resolution (4-km grid). Proven strategies immediately available to mitigate carbon emissions from forest activities include the following: (*i*) reforestation (growing forests where they recently existed), (*ii*) afforestation (growing forests where they did not recently exist), (*iii*) increasing carbon density of existing forests, and (*iv*) reducing emissions from deforestation and degradation (1). Other proposed strategies include wood bioenergy production (2–4), bioenergy combined with carbon capture and storage (BECCS), and increasing wood product use in buildings. However, examples of commercial-scale BECCS are still scarce, and sustainability of wood sources remains controversial because of forgone ecosystem carbon storage and low environmental cobenefits (5, 6). Carbon stored in buildings generally outlives its usefulness or is replaced within decades (7) rather than the centuries possible in forests, and the factors influencing product substitution have yet to be fully explored (8). Our analysis of mitigation strategies focuses on the first four strategies, as well as bioenergy production, utilizing harvest residues only and without carbon capture and storage.

The appropriateness and effectiveness of mitigation strategies within regions vary depending on the current forest sink, competition with land-use and watershed protection, and environmental conditions affecting forest sustainability and resilience. Few process-based regional studies have quantified strategies that could actually be implemented, are low-risk, and do not depend on developing technologies. Our previous studies focused on regional modeling of the effects of forest thinning on net ecosystem carbon balance (NECB) and net emissions, as well as improving modeled drought sensitivity (9, 10), while this study focuses mainly on strategies to enhance forest carbon.

Our study region is Oregon in the Pacific Northwest, where coastal and montane forests have high biomass and carbon sequestration potential. They represent coastal forests from northern California to southeast Alaska, where trees live 800 y or more and biomass can exceed that of tropical forests (11) (Fig. S1). The semiarid ecoregions consist of woodlands that experience frequent fires (12). Land-use history is a major determinant of forest carbon balance. Harvest was the dominant cause of tree mortality (2003–2012) and accounted for fivefold as much mortality as that from fire and beetles combined (13). Forest land ownership is predominantly public (64%), and 76% of the biomass harvested is on private lands.

Significance

Regional quantification of feasibility and effectiveness of forest strategies to mitigate climate change should integrate observations and mechanistic ecosystem process models with future climate, CO_2, disturbances from fire, and management. Here, we demonstrate this approach in a high biomass region, and found that reforestation, afforestation, lengthened harvest cycles on private lands, and restricting harvest on public lands increased net ecosystem carbon balance by 56% by 2100, with the latter two actions contributing the most. Forest sector emissions tracked with our life cycle assessment model decreased by 17%, partially meeting emissions reduction goals. Harvest residue bioenergy use did not reduce short-term emissions. Cobenefits include increased water availability and biodiversity of forest species. Our improved analysis framework can be used in other temperate regions.

Author contributions: B.E.L. and T.W.H. designed research; B.E.L., T.W.H., and P.C.B. performed research; M.E.H. contributed new reagents/analytic tools; B.E.L., L.T.B., J.J.K., and P.C.B. analyzed data; B.E.L., T.W.H., L.T.B., and M.E.H. wrote the paper; and M.E.H. contributed the substitution model.

The authors declare no conflict of interest.

This article is a PNAS Direct Submission.

Data deposition: The CLM4.5 model data are available at Oregon State University (terraweb.forestry.oregonstate.edu/FMEC). Data from the >200 intensive plots on forest carbon are available at Oak Ridge National Laboratory (https://daac.ornl.gov/NACP/guides/NACP_TERRA-PNW.html), and FIA data are available at the USDA Forest Service (https://www.fia.fs.fed.us/tools-data/).

[1]To whom correspondence should be addressed. Email: bev.law@oregonstate.edu.

This article contains supporting information online at www.pnas.org/lookup/suppl/doi:10.1073/pnas.1720064115/-/DCSupplemental.

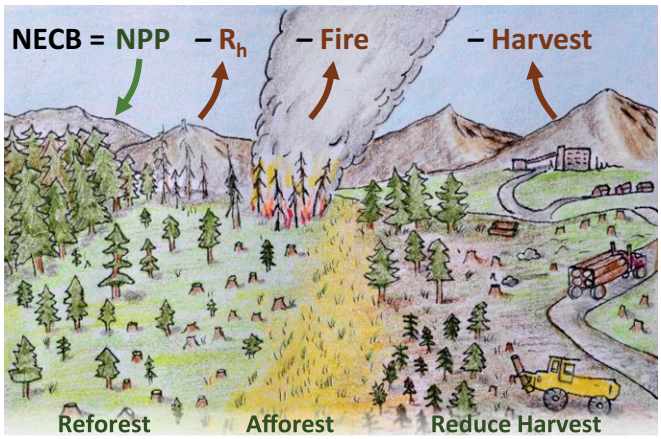

Fig. 1. Approach to assessing effects of mitigation strategies on forest carbon and forest sector emissions. NECB is productivity (NPP) minus Rh and losses from fire and harvest (red arrows). Harvest emissions include those associated with wood products and bioenergy.

Many US states, including Oregon (14), plan to reduce their greenhouse gas (GHG) emissions in accordance with the Paris Agreement. We evaluated strategies to address this question: How much carbon can the region's forests realistically remove from the atmosphere in the future, and which forest carbon strategies can reduce regional emissions by 2025, 2050, and 2100? We propose an integrated approach that combines observations with models and a life cycle assessment (LCA) to evaluate current and future effects of mitigation actions on forest carbon and forest sector emissions in temperate regions (Fig. 1). We estimated the recent carbon budget of Oregon's forests, and simulated the potential to increase the forest sink and decrease forest sector emissions under current and future climate conditions. We provide recommendations for regional assessments of mitigation strategies.

Results

Carbon stocks and fluxes are summarized for the observation cycles of 2001–2005, 2006–2010, and 2011–2015 (Table 1 and Tables S1 and S2). In 2011–2015, state-level forest carbon stocks totaled 3,036 Tg C (3 billion metric tons), with the coastal and montane ecoregions accounting for 57% of the live tree carbon (Tables S1 and S2). Net ecosystem production [NEP; net primary production (NPP) minus heterotrophic respiration (Rh)] averaged 28 teragrams carbon per year (Tg C y^{-1}) over all three periods. Fire emissions were unusually high at 8.69 million metric tons carbon dioxide equivalent ($tCO_2e\ y^{-1}$, i.e., 2.37 Tg C y^{-1}) in 2001–2005 due to the historic Biscuit Fire, but decreased to 3.56 million $tCO_2e\ y^{-1}$ (0.97 Tg C y^{-1}) in 2011–2015 (Table S4). Note that 1 million tCO_2e equals 3.667 Tg C.

Our LCA showed that in 2001–2005, Oregon's net wood product emissions were 32.61 million tCO_2e (Table S3), and 3.7-fold wildfire emissions in the period that included the record fire year (15) (Fig. 2). In 2011–2015, net wood product emissions were 34.45 million tCO_2e and almost 10-fold fire emissions, mostly due to lower fire emissions. The net wood product emissions are higher than fire emissions despite carbon benefits of storage in wood products and substitution for more fossil fuel-intensive products. Hence, combining fire and net wood product emissions, the forest sector emissions averaged 40 million $tCO_2e\ y^{-1}$ and accounted for about 39% of total emissions across all sectors (Fig. 2 and Table S4). NECB was calculated from NEP minus losses from fire emissions and harvest (Fig. 1). State NECB was equivalent to 60% and 70% of total emissions for 2001–2005 and 2011–2015, respectively (Fig. 2, Table 1, and Table S4). Fire emissions were only between 4% and 8% of total emissions from all sources (2011–2015 and 2001–2004, respectively). Oregon's forests play a larger role in meeting its GHG targets than US forests have in meeting the nation's targets (16, 17).

Historical disturbance regimes were simulated using stand age and disturbance history from remote sensing products. Comparisons of Community Land Model (CLM4.5) output with Forest Inventory and Analysis (FIA) aboveground tree biomass (>6,000 plots) were within 1 SD of the ecoregion means (Fig. S2). CLM4.5 estimates of cumulative burn area and emissions from 1990 to 2014 were 14% and 25% less than observed, respectively. The discrepancy was mostly due to the model missing an anomalously large fire in 2002 (Fig. S3*A*). When excluded, modeled versus observed fire emissions were in good agreement (r^2 = 0.62; Fig. S3*B*). A sensitivity test of a 14% underestimate of burn area did not affect our final results because predicted emissions would increase almost equally for business as usual (BAU) management and our scenarios, resulting in no proportional change in NECB. However, the ratio of harvest to fire emissions would be lower.

Projections show that under future climate, atmospheric carbon dioxide, and BAU management, an increase in net carbon uptake due to CO_2 fertilization and climate in the mesic ecoregions far outweighs losses from fire and drought in the semiarid ecoregions. There was not an increasing trend in fire. Carbon stocks increased by 2% and 7% and NEP increased by 12% and 40% by 2050 and 2100, respectively.

We evaluated emission reduction strategies in the forest sector: protecting existing forest carbon, lengthening harvest cycles, reforestation, afforestation, and bioenergy production with product substitution. The largest potential increase in forest carbon is in the mesic Coast Range and West Cascade ecoregions. These forests are buffered by the ocean, have high soil water-holding capacity, low risk of wildfire [fire intervals average 260–400 y (18)], long carbon residence time, and potential for high carbon density. They can attain biomass up to 520 Mg C ha^{-1} (12). Although Oregon has several protected areas, they account for only 9–15% of the total forest area, so we expect it may be feasible to add carbon-protected lands with cobenefits of water protection and biodiversity.

Reforestation of recently forested areas include those areas impacted by fire and beetles. Our simulations to 2100 assume regrowth of the same species and incorporate future fire responses to climate and cyclical beetle outbreaks [70–80 y (13)]. Reforestation has the potential to increase stocks by 315 Tg C by 2100, reducing forest sector net emissions by 5% by 2100 relative to BAU management (Fig. 3). The East and West Cascades ecoregions had the highest reforestation potential, accounting for 90% of the increase (Table S5).

Afforestation of old fields within forest boundaries and non-food/nonforage grass crops, hereafter referred to as "grass crops," had to meet minimum conditions for tree growth, and crop grid cells had to be partially forested (*SI Methods* and Table S6). These crops are not grazed or used for animal feed. Competing land uses may decrease the actual amount of area that can be afforested. We calculated the amount of irrigated grass crops (127,000 ha) that could be converted to forest, assuming success of carbon offset programs (19). By 2100, afforestation increased stocks by

Table 1. Forest carbon budget components used to compute NECB

Flux, Tg C·y^{-1}	2001–2005		2006–2010		2011–2015		2001–2015
NPP	73.64	7.59	73.57	7.58	73.57	7.58	73.60
Rh	45.67	5.11	45.38	5.07	45.19	5.05	45.41
NEP	27.97	9.15	28.19	9.12	28.39	9.11	28.18
Harvest removals	8.58	0.60	7.77	0.54	8.61	0.6	8.32
Fire emissions	2.37	0.27	1.79	0.2	0.97	0.11	1.71
NECB	17.02	9.17	18.63	9.14	18.81	9.13	18.15

Average annual values for each period, including uncertainty (95% confidence interval) in Tg C y^{-1} (multiply by 3.667 to get million tCO_2e).

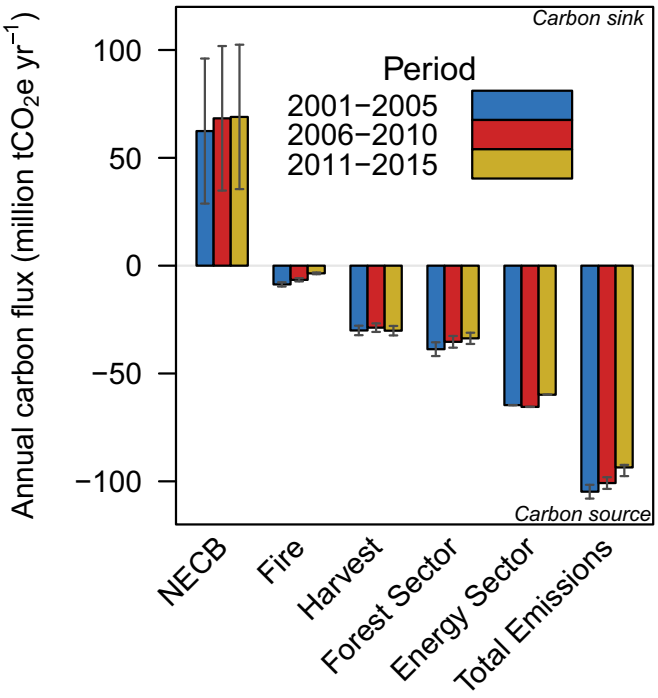

Fig. 2. Oregon's forest carbon sink and emissions from forest and energy sectors. Harvest emissions are computed by LCA. Fire and harvest emissions sum to forest sector emissions. Energy sector emissions are from the Oregon Global Warming Commission (14), minus forest-related emissions. Error bars are 95% confidence intervals (Monte Carlo analysis).

94 Tg C and cumulative NECB by 14 Tg C, and afforestation reduced forest sector GHG emissions by 1.3–1.4% in 2025, 2050, and 2100 (Fig. 3).

We quantified cobenefits of afforestation of irrigated grass crops on water availability based on data from hydrology and agricultural simulations of future grass crop area and related irrigation demand (20). Afforestation of 127,000 ha of grass cropland with Douglas fir could decrease irrigation demand by 222 and 233 billion $m^3 \cdot y^{-1}$ by 2050 and 2100, respectively. An independent estimate from measured precipitation and evapotranspiration (ET) at our mature Douglas fir and grass crop flux sites in the Willamette Valley shows the ET/precipitation fraction averaged 33% and 52%, respectively, and water balance (precipitation minus ET) averaged 910 $mm \cdot y^{-1}$ and 516 $mm \cdot y^{-1}$. Under current climate conditions, the observations suggest an increase in annual water availability of 260 billion $m^3 \cdot y^{-1}$ if 127,000 ha of the irrigated grass crops were converted to forest.

Harvest cycles in the mesic and montane forests have declined from over 120 y to 45 y despite the fact that these trees can live 500–1,000 y and net primary productivity peaks at 80–125 y (21). If harvest cycles were lengthened to 80 y on private lands and harvested area was reduced 50% on public lands, state-level stocks would increase by 17% to a total of ~3,600 Tg C and NECB would increase 2–3 Tg C y^{-1} by 2100. The lengthened harvest cycles reduced harvest by 2 Tg C y^{-1}, which contributed to higher NECB. Leakage (more harvest elsewhere) is difficult to quantify and could counter these carbon gains. However, because harvest on federal lands was reduced significantly since 1992 (NW Forest Plan), leakage has probably already occurred.

The four strategies together increased NECB by 64%, 82%, and 56% by 2025, 2050, and 2100, respectively. This reduced forest sector net emissions by 11%, 10%, and 17% over the same periods (Fig. 3). By 2050, potential increases in NECB were largest in the Coast Range (Table S5), East Cascades, and Klamath Mountains, accounting for 19%, 25%, and 42% of the total increase, whereas by 2100, they were most evident in the West Cascades, East Cascades, and Klamath Mountains.

We examined the potential for using existing harvest residue for electricity generation, where burning the harvest residue for energy emits carbon immediately (3) versus the BAU practice of leaving residues in forests to slowly decompose. Assuming half of forest residues from harvest practices could be used to replace natural gas or coal in distributed facilities across the state, they would provide an average supply of 0.75–1 Tg C y^{-1} to the year 2100 in the reduced harvest and BAU scenarios, respectively. Compared with BAU harvest practices, where residues are left to decompose, proposed bioenergy production would increase cumulative net emissions by up to 45 Tg C by 2100. Even at 50% use, residue collection and transport are not likely to be economically viable, given the distances (>200 km) to Oregon's facilities.

Discussion

Earth system models have the potential to bring terrestrial observations related to climate, vulnerability, impacts, adaptation,

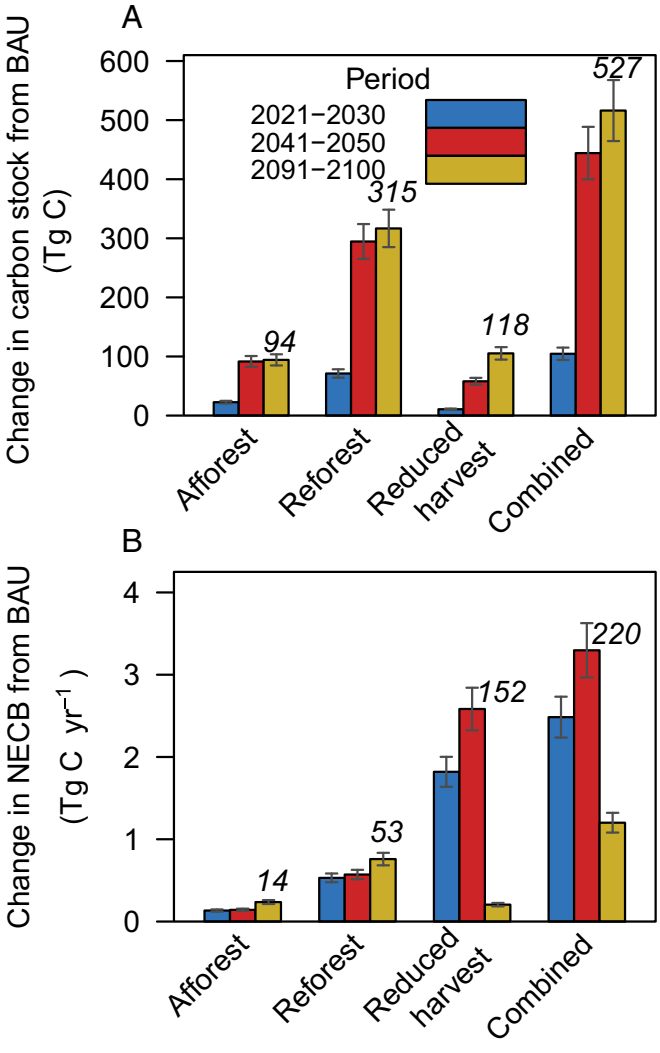

Fig. 3. Future change in carbon stocks and NECB with mitigation strategies relative to BAU management. The decadal average change in forest carbon stocks (*A*) and NECB relative to BAU (*B*) are shown. Italicized numbers over bars indicate mean forest carbon stocks in 2091–2100 (*A*) and cumulative change in NECB for 2015–2100 (*B*). Error bars are ±10%.

and mitigation into a common framework, melding biophysical with social components (22). We developed a framework to examine a suite of mitigation actions to increase forest carbon sequestration and reduce forest sector emissions under current and future environmental conditions.

Harvest-related emissions had a large impact on recent forest NECB, reducing it by an average of 34% from 2001 to 2015. By comparison, fire emissions were relatively small and reduced NECB by 12% in the Biscuit Fire year, but only reduced NECB 5–9% from 2006 to 2015. Thus, altered forest management has the potential to enhance the forest carbon balance and reduce emissions.

Future NEP increased because enhancement from atmospheric carbon dioxide outweighed the losses from fire. Lengthened harvest cycles on private lands to 80 y and restricting harvest to 50% of current rates on public lands increased NECB the most by 2100, accounting for 90% of total emissions reduction (Fig. 3 and Tables S5 and S6). Reduced harvest led to NECB increasing earlier than the other strategies (by 2050), suggesting this could be a priority for implementation.

Our afforestation estimates may be too conservative by limiting them to nonforest areas within current forest boundaries and 127,000 ha of irrigated grass cropland. There was a net loss of 367,000 ha of forest area in Oregon and Washington combined from 2001 to 2006 (23), and less than 1% of native habitat remains in the Willamette Valley due to urbanization and agriculture (24). Perhaps more of this area could be afforested.

The spatial variation in the potential for each mitigation option to improve carbon stocks and fluxes shows that the reforestation potential is highest in the Cascade Mountains, where fire and insects occur (Fig. 4). The potential to reduce harvest on public land is highest in the Cascade Mountains, and that to lengthen harvest cycles on private lands is highest in the Coast Range.

Although western Oregon is mesic with little expected change in precipitation, the afforestation cobenefits of increased water availability will be important. Urban demand for water is projected to increase, but agricultural irrigation will continue to consume much more water than urban use (25). Converting 127,000 ha of irrigated grass crops to native forests appears to be a win–win strategy, returning some of the area to forest land, providing habitat and connectivity for forest species, and easing irrigation demand. Because the afforested grass crop represents only 11% of the available grass cropland (1.18 million ha), it is not likely to result in leakage or indirect land use change. The two forest strategies combined are likely to be important contributors to water security.

Cobenefits with biodiversity were not assessed in our study. However, a recent study showed that in the mesic forests, cobenefits with biodiversity of forest species are largest on lands with harvest cycles longer than 80 y, and thus would be most pronounced on private lands (26). We selected 80 y for the harvest cycle mitigation strategy because productivity peaks at 80–125 y in this region, which coincides with the point at which cobenefits with wildlife habitat are substantial.

Habitat loss and climate change are the two greatest threats to biodiversity. Afforestation of areas that are currently grass crops would likely improve the habitat of forest species (27), as about 90% of the forests in these areas were replaced by agriculture. About 45 mammal species are at risk because of range contraction (28). Forests are more efficient at dissipating heat than grass and crop lands, and forest cover gains lead to net surface cooling in all regions south of about 45° latitude in North American and Europe (29). The cooler conditions can buffer climate-sensitive bird populations from approaching their thermal limits and provide more food and nest sites (30). Thus, the mitigation strategies of afforestation, protecting forests on public lands and lengthening harvest cycles to 80–125 y, would likely benefit forest-dependent species.

Oregon has a legislated mandate to reduce emissions, and is considering an offsets program that limits use of offsets to 8% of

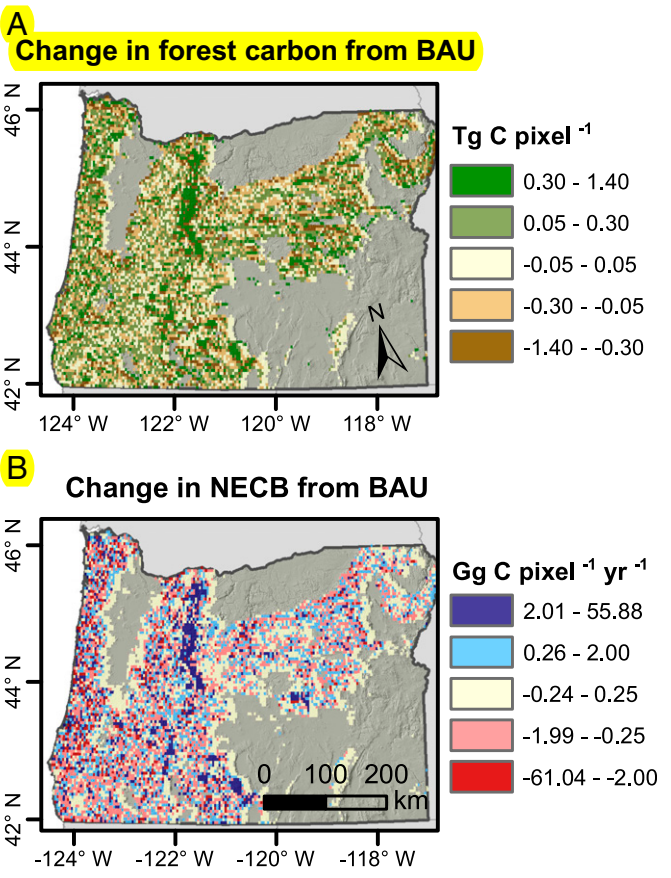

Fig. 4. Spatial patterns of forest carbon stocks and NECB by 2091–2100. The decadal average changes in forest carbon stocks (*A*) and NECB (*B*) due to afforestation, reforestation, protected areas, and lengthened harvest cycles relative to continued BAU forest management (red is increase in NECB) are shown.

the total emissions reduction to ensure that regulated entities substantially reduce their own emissions, similar to California's program (19). An offset becomes a net emissions reduction by increasing the forest carbon sink (NECB). If only 8% of the GHG reduction is allowed for forest offsets, the limits for forest offsets would be 2.1 and 8.4 million metric tCO_2e of total emissions by 2025 and 2050, respectively (Table S6). The combination of afforestation, reforestation, and reduced harvest would provide 13 million metric tCO_2e emissions reductions, and any one of the strategies or a portion of each could be applied. Thus, additionality beyond what would happen without the program is possible.

State-level reporting of GHG emissions includes the agriculture sector, but does not appear to include forest sector emissions, except for industrial fuel (i.e., utility fuel in Table S3) and, potentially, fire emissions. Harvest-related emissions should be quantified, as they are much larger than fire emissions in the western United States. Full accounting of forest sector emissions is necessary to meet climate mitigation goals.

Increased long-term storage in buildings and via product substitution has been suggested as a potential climate mitigation option. Pacific temperate forests can store carbon for many hundreds of years, which is much longer than is expected for buildings that are generally assumed to outlive their usefulness or be replaced within several decades (7). By 2035, about 75% of buildings in the United States will be replaced or renovated, based on new construction, demolition, and renovation trends (31, 32). Recent analysis suggests substitution benefits of using wood versus more fossil fuel-intensive materials have been overestimated by at

least an order of magnitude (33). Our LCA accounts for losses in product substitution stores (PSSs) associated with building life span, and thus are considerably lower than when no losses are assumed (4, 34). While product substitution reduces the overall forest sector emissions, it cannot offset the losses incurred by frequent harvest and losses associated with product transportation, manufacturing, use, disposal, and decay. Methods for calculating substitution benefits should be improved in other regional assessments.

Wood bioenergy production is interpreted as being carbon-neutral by assuming that trees regrow to replace those that burned. However, this does not account for reduced forest carbon stocks that took decades to centuries to sequester, degraded productive capacity, emissions from transportation and the production process, and biogenic/direct emissions at the facility (35). Increased harvest through proposed thinning practices in the region has been shown to elevate emissions for decades to centuries regardless of product end use (36). It is therefore unlikely that increased wood bioenergy production in this region would decrease overall forest sector emissions.

Conclusions

GHG reduction must happen quickly to avoid surpassing a 2 °C increase in temperature since preindustrial times. Alterations in forest management can contribute to increasing the land sink and decreasing emissions by keeping carbon in high biomass forests, extending harvest cycles, reforestation, and afforestation. Forests are carbon-ready and do not require new technologies or infrastructure for immediate mitigation of climate change. Growing forests for bioenergy production competes with forest carbon sequestration and does not reduce emissions in the next decades (10). BECCS requires new technology, and few locations have sufficient geological storage for CO_2 at power facilities with high-productivity forests nearby. Accurate accounting of forest carbon in trees and soils, NECB, and historic harvest rates, combined with transparent quantification of emissions from the wood product process, can ensure realistic reductions in forest sector emissions.

As states and regions take a larger role in implementing climate mitigation steps, robust forest sector assessments are urgently needed. Our integrated approach of combining observations, an LCA, and high-resolution process modeling (4-km grid vs. typical 200-km grid) of a suite of potential mitigation actions and their effects on forest carbon sequestration and emissions under changing climate and CO_2 provides an analysis framework that can be applied in other temperate regions.

Materials and Methods

Current Stocks and Fluxes. We quantified recent forest carbon stocks and fluxes using a combination of observations from FIA; Landsat products on forest type, land cover, and fire risk; 200 intensive plots in Oregon (37); and a wood decomposition database. Tree biomass was calculated from species-specific allometric equations and ecoregion-specific wood density. We estimated ecosystem carbon stocks, NEP (photosynthesis minus respiration), and NECB (NEP minus losses due to fire or harvest) using a mass-balance approach (36, 38) (Table 1 and *SI Materials and Methods*). Fire emissions were computed from the Monitoring Trends in Burn Severity database, biomass data, and region-specific combustion factors (15, 39) (*SI Materials and Methods*).

Future Projections and Model Description. Carbon stocks and NEP were quantified to the years 2025, 2050, and 2100 using CLM4.5 with physiological parameters for 10 major forest species, initial forest biomass (36), and future climate and atmospheric carbon dioxide as input (Institut Pierre Simon Laplace climate system model downscaled to 4 km × 4 km, representative concentration pathway 8.5). CLM4.5 uses 3-h climate data, ecophysiological characteristics, site physical characteristics, and site history to estimate the daily fluxes of carbon, nitrogen, and water between the atmosphere, plant state variables, and litter and soil state variables. Model components are biogeophysics, hydrological cycle, and biogeochemistry. This model version does not include a dynamic vegetation model to simulate resilience and establishment following disturbance. However, the effect of regeneration lags on forest carbon is not particularly strong for the long disturbance intervals in this study (40). Our plant functional type (PFT) parameterization for 10 major forest species rather than one significantly improves carbon modeling in the region (41).

Forest Management and Land Use Change Scenarios. Harvest cycles, reforestation, and afforestation were simulated to the year 2100. Carbon stocks and NEP were predicted for the current harvest cycle of 45 y compared with simulations extending it to 80 y. Reforestation potential was simulated over areas that recently suffered mortality from harvest, fire, and 12 species of beetles (13). We assumed the same vegetation regrew to the maximum potential, which is expected with the combination of natural regeneration and planting that commonly occurs after these events. Future BAU harvest files were constructed using current harvest rates, where county-specific average harvest and the actual amounts per ownership were used to guide grid cell selection. This resulted in the majority of harvest occurring on private land (70%) and in the mesic ecoregions. Beetle outbreaks were implemented using a modified mortality rate of the lodgepole pine PFT with 0.1% y^{-1} biomass mortality by 2100.

For afforestation potential, we identified areas that are within forest boundaries that are not currently forest and areas that are currently grass crops. We assumed no competition with conversion of irrigated grass crops to urban growth, given Oregon's land use laws for developing within urban growth boundaries. A separate study suggested that, on average, about 17% of all irrigated agricultural crops in the Willamette Valley could be converted to urban area under future climate; however, because 20% of total cropland is grass seed, it suggests little competition with urban growth (25).

Landsat observations (12,500 scenes) were processed to map changes in land cover from 1984 to 2012. Land cover types were separated with an unsupervised K-means clustering approach. Land cover classes were assigned to an existing forest type map (42). The CropScape Cropland Data Layer (CDL 2015, https://nassgeodata.gmu.edu/CropScape/) was used to distinguish nonforage grass crops from other grasses. For afforestation, we selected grass cropland with a minimum soil water-holding capacity of 150 mm and minimum precipitation of 500 mm that can support trees (43).

Afforestation Cobenefits. Modeled irrigation demand of grass seed crops under future climate conditions was previously conducted with hydrology and agricultural models, where ET is a function of climate, crop type, crop growth state, and soil-holding capacity (20) (Table S7). The simulations produced total land area, ET, and irrigation demand for each cover type. Current grass seed crop irrigation in the Willamette Valley is 413 billion $m^3 \cdot y^{-1}$ for 238,679 ha and is projected to be 412 and 405 billion m^3 in 2050 and 2100 (20) (Table S7). We used annual output from the simulations to estimate irrigation demand per unit area of grass seed crops (1.73, 1.75, and 1.84 million $m^3 \cdot ha^{-1}$ in 2015, 2050, and 2100, respectively), and applied it to the mapped irrigated crop area that met conditions necessary to support forests (Table S7).

LCA. Decomposition of wood through the product cycle was computed using an LCA (8, 10). Carbon emissions to the atmosphere from harvest were calculated annually over the time frame of the analysis (2001–2015). The net carbon emissions equal NECB plus total harvest minus wood lost during manufacturing and wood decomposed over time from product use. Wood industry fossil fuel emissions were computed for harvest, transportation, and manufacturing processes. Carbon credit was calculated for wood product storage, substitution, and internal mill recycling of wood losses for bioenergy.

Products were divided into sawtimber, pulpwood, and wood and paper products using published coefficients (44). Long-term and short-term products were assumed to decay at 2% and 10% per year, respectively (45). For product substitution, we focused on manufacturing for long-term structures (building life span >30 y). Because it is not clear when product substitution started in the Pacific Northwest, we evaluated it starting in 1970 since use of concrete and steel for housing was uncommon before 1965. The displacement value for product substitution was assumed to be 2.1 Mg fossil C/Mg C wood use in long-term structures (46), and although it likely fluctuates over time, we assumed it was constant. We accounted for losses in product substitution associated with building replacement (33) using a loss rate of 2% per year (33), but ignored leakage related to fossil C use by other sectors, which may result in more substitution benefit than will actually occur.

The general assumption for modern buildings, including cross-laminate timber, is they will outlive their usefulness and be replaced in about 30 y (7). By 2035, ~75% of buildings in the United States will be replaced or renovated, based on new construction, demolition, and renovation trends, resulting in threefold as many buildings as there are now [2005 baseline (31, 32)]. The loss of

the PSS is therefore PSS multiplied by the proportion of buildings lost per year (2% per year).

To compare the NECB equivalence to emissions, we calculated forest sector and energy sector emissions separately. Energy sector emissions ["in-boundary" state-quantified emissions by the Oregon Global Warming Commission (14)] include those from transportation, residential and commercial buildings, industry, and agriculture. The forest sector emissions are cradle-to-grave annual carbon emissions from harvest and product emissions, transportation, and utility fuels (Table S3). Forest sector utility fuels were subtracted from energy sector emissions to avoid double counting.

Uncertainty Estimates. For the observation-based analysis, Monte Carlo simulations were used to conduct an uncertainty analysis with the mean and SDs for NPP and Rh calculated using several approaches (36) (*SI Materials and Methods*). Uncertainty in NECB was calculated as the combined uncertainty of NEP, fire emissions (10%), harvest emissions (7%), and land cover estimates (10%) using the propagation of error approach. Uncertainty in CLM4.5 model simulations and LCA were quantified by combining the uncertainty in the observations used to evaluate the model, the uncertainty in input datasets (e.g., remote sensing), and the uncertainty in the LCA coefficients (41).

Model input data for physiological parameters and model evaluation data on stocks and fluxes are available online (37).

ACKNOWLEDGMENTS. We thank Dr. Thomas Hilker (deceased) for producing the grass data layer, and Carley Lowe for Fig. 1. This research was supported by the US Department of Energy (Grant DE-SC0012194) and Agriculture and Food Research Initiative of the US Department of Agriculture National Institute of Food and Agriculture (Grants 2013-67003-20652, 2014-67003-22065, and 2014-35100-22066) for our North American Carbon Program studies, "Carbon cycle dynamics within Oregon's urban-suburban-forested-agricultural landscapes," and "Forest die-off, climate change, and human intervention in western North America."

1. Canadell JG, Raupach MR (2008) Managing forests for climate change mitigation. *Science* 320:1456–1457.
2. Holtsmark B (2013) The outcome is in the assumptions: Analyzing the effects on atmospheric CO2 levels of increased use of bioenergy from forest biomass. *Glob Change Biol Bioenergy* 5:467–473.
3. Repo A, Tuomi M, Liski J (2011) Indirect carbon dioxide emissions from producing bioenergy from forest harvest residues. *Glob Change Biol Bioenergy* 3:107–115.
4. Schlamadinger B, Marland G (1996) The role of forest and bioenergy strategies in the global carbon cycle. *Biomass Bioenergy* 10:275–300.
5. Heck V, Gerten D, Lucht W, Popp A (2018) Biomass-based negative emissions difficult to reconcile with planetary boundaries. *Nat Clim Chang* 8:151–155.
6. Field CB, Mach KJ (2017) Rightsizing carbon dioxide removal. *Science* 356:706–707.
7. Tollefson J (2017) The wooden skyscrapers that could help to cool the planet. *Nature* 545:280–282.
8. Law BE, Harmon ME (2011) Forest sector carbon management, measurement and verification, and discussion of policy related to climate change. *Carbon Manag* 2: 73–84.
9. Law BE (2014) Regional analysis of drought and heat impacts on forests: Current and future science directions. *Glob Change Biol* 20:3595–3599.
10. Hudiburg TW, Luyssaert S, Thornton PE, Law BE (2013) Interactive effects of environmental change and management strategies on regional forest carbon emissions. *Environ Sci Technol* 47:13132–13140.
11. Keith H, Mackey BG, Lindenmayer DB (2009) Re-evaluation of forest biomass carbon stocks and lessons from the world's most carbon-dense forests. *Proc Natl Acad Sci USA* 106:11635–11640.
12. Law B, Waring R (2015) Carbon implications of current and future effects of drought, fire and management on Pacific Northwest forests. *For Ecol Manage* 355:4–14.
13. Berner LT, Law BE, Meddens AJ, Hicke JA (2017) Tree mortality from fires, bark beetles, and timber harvest during a hot and dry decade in the western United States (2003–2012). *Environ Res Lett* 12:065005.
14. Oregon Global Warming Commission (2017) Biennial Report to the Legislature (Oregon Global Warming Commission, Salem, OR).
15. Campbell J, Donato D, Azuma D, Law B (2007) Pyrogenic carbon emission from a large wildfire in Oregon, United States. *J Geophys Res Biogeosci* 112:G04014.
16. King AW, Hayes DJ, Huntzinger DN, West TO, Post WM (2012) North American carbon dioxide sources and sinks: Magnitude, attribution, and uncertainty. *Front Ecol Environ* 10:512–519.
17. Wilson BT, Woodall CW, Griffith DM (2013) Imputing forest carbon stock estimates from inventory plots to a nationally continuous coverage. *Carbon Balance Manag* 8:1.
18. Reilly MJ, et al. (2017) Contemporary patterns of fire extent and severity in forests of the Pacific Northwest, USA (1985–2010). *Ecosphere* 8:e01695.
19. Anderson CM, Field CB, Mach KJ (2017) Forest offsets partner climate-change mitigation with conservation. *Front Ecol Environ* 15:359–365.
20. Willamette Water 2100 Explorer (2017) Assessing water futures under alternative climate and management scenarios: Agricultural water demand, crop and irrigation decisions. Available at explorer.bee.oregonstate.edu/Topic/WW2100/AgSummaries.aspx. Accessed November 13, 2017.
21. Hudiburg T, et al. (2009) Carbon dynamics of Oregon and Northern California forests and potential land-based carbon storage. *Ecol Appl* 19:163–180.
22. Bonan GB, Doney SC (2018) Climate, ecosystems, and planetary futures: The challenge to predict life in Earth system models. *Science* 359:eaam8328.
23. Riitters KH, Wickham JD (2012) Decline of forest interior conditions in the conterminous United States. *Sci Rep* 2:653.
24. Noss RF, LaRoe ET, Scott JM (1995) *Endangered Ecosystems of the United States: A Preliminary Assessment of Loss and Degradation* (US Department of the Interior, National Biological Service, Washington, DC).
25. Jaeger W, Plantinga A, Langpap C, Bigelow D, Moore K (2017) *Water, Economics and Climate Change in the Willamette Basin* (Oregon State University Extension Service, Corvallis, OR).
26. Kline JD, et al. (2016) Evaluating carbon storage, timber harvest, and habitat possibilities for a Western Cascades (USA) forest landscape. *Ecol Appl* 26:2044–2059.
27. Matthews S, O'Connor R, Plantinga AJ (2002) Quantifying the impacts on biodiversity of policies for carbon sequestration in forests. *Ecol Econ* 40:71–87.
28. Arnold S, Kagan J, Taylor B (2000) Summary of current status of Oregon's biodiversity. *Oregon State of the Environment Report* (Oregon Progress Board, Salem, OR), pp 121–126.
29. Bright RM, et al. (2017) Local temperature response to land cover and management change driven by non-radiative processes. *Nat Clim Chang* 7:296–302.
30. Betts M, Phalan B, Frey S, Rousseau J, Yang Z (2017) Old-growth forests buffer climate-sensitive bird populations from warming. *Diversity Distrib*, 10.1111/ddi.12688.
31. Architecture 2030(2017) The 2030 Challenge. Available at architecture2030.org. Accessed October 23, 2017.
32. Oliver CD, Nassar NT, Lippke BR, McCarter JB (2014) Carbon, fossil fuel, and biodiversity mitigation with wood and forests. *J Sustain For* 33:248–275.
33. Harmon ME, Moreno A, Domingo JB (2009) Effects of partial harvest on the carbon stores in Douglas-fir/western hemlock forests: A simulation study. *Ecosystems (N Y)* 12:777–791.
34. Lippke B, et al. (2011) Life cycle impacts of forest management and wood utilization on carbon mitigation: Knowns and unknowns. *Carbon Manag* 2:303–333.
35. Gunn JS, Ganz DJ, Keeton WS (2011) Biogenic vs. geologic carbon emissions and forest biomass energy production. *GCB Bioenergy* 4:239–242.
36. Hudiburg TW, Law BE, Wirth C, Luyssaert S (2011) Regional carbon dioxide implications of forest bioenergy production. *Nat Clim Chang* 1:419–423.
37. Law BE, Berner LT (2015) *NACP TERRA-PNW: Forest Plant Traits, NPP, Biomass, and Soil Properties, 1999-2014* (ORNL DAAC, Oak Ridge, TN).
38. Law BE, Hudiburg TW, Luyssaert S (2013) Thinning effects on forest productivity: Consequences of preserving old forests and mitigating impacts of fire and drought. *Plant Ecol Divers* 6:73–85.
39. Meigs G, Donato D, Campbell J, Martin J, Law B (2009) Forest fire impacts on carbon uptake, storage, and emission: The role of burn severity in the Eastern Cascades, Oregon. *Ecosystems (N Y)* 12:1246–1267.
40. Harmon ME, Marks B (2002) Effects of silvicultural practices on carbon stores in Douglas-fir western hemlock forests in the Pacific Northwest, USA: Results from a simulation model. *Can J For Res* 32:863–877.
41. Hudiburg TW, Law BE, Thornton PE (2013) Evaluation and improvement of the community land model (CLM4) in Oregon forests. *Biogeosciences* 10:453–470.
42. Ruefenacht B, et al. (2008) Conterminous U.S. and Alaska forest type mapping using forest inventory and analysis data. *Photogramm Eng Remote Sens* 74:1379–1388.
43. Peterman W, Bachelet D, Ferschweiler K, Sheehan T (2014) Soil depth affects simulated carbon and water in the MC2 dynamic global vegetation model. *Ecol Modell* 294:84–93.
44. Smith JE, Heath L, Skog KE, Birdsey R (2006) Methods for calculating forest ecosystem and harvested carbon with standard estimates for forest types of the United States (US Department of Agriculture, Forest Service, Northeastern Research Station, Newtown Square, PA), General Technical Report NE-343.
45. Harmon ME, Harmon JM, Ferrell WK, Brooks D (1996) Modeling carbon stores in Oregon and Washington forest products: 1900–1992. *Clim Change* 33:521–550.
46. Sathre R, O'Connor J (2010) Meta-analysis of greenhouse gas displacement factors of wood product substitution. *Environ Sci Policy* 13:104–114.

Ecosystems
DOI: 10.1007/s10021-009-9285-x

ECOSYSTEMS

Forest Fire Impacts on Carbon Uptake, Storage, and Emission: The Role of Burn Severity in the Eastern Cascades, Oregon

Garrett W. Meigs,[1]* Daniel C. Donato,[2] John L. Campbell,[1] Jonathan G. Martin,[1] and Beverly E. Law[1]

[1]*Department of Forest Ecosystems and Society, Oregon State University, Corvallis, Oregon 97331, USA;* [2]*USDA Forest Service, Pacific Southwest Research Station, Institute of Pacific Islands Forestry, Hilo, Hawaii 96720, USA*

Abstract

This study quantifies the short-term effects of low-, moderate-, and high-severity fire on carbon pools and fluxes in the Eastern Cascades of Oregon. We surveyed 64 forest stands across four fires that burned 41,000 ha (35%) of the Metolius Watershed in 2002 and 2003, stratifying the landscape by burn severity (overstory tree mortality), forest type (ponderosa pine [PP] and mixed-conifer [MC]), and prefire biomass. Stand-scale C combustion ranged from 13 to 35% of prefire aboveground C pools (area − weighted mean = 22%). Across the sampled landscape, total estimated pyrogenic C emissions were equivalent to 2.5% of statewide anthropogenic CO_2 emissions from fossil fuel combustion and industrial processes for the same 2-year period. From low- to moderate- to high-severity ponderosa pine stands, average tree basal area mortality was 14, 49, and 100%, with parallel patterns in mixed-conifer stands (29, 58, 96%). Despite this decline in live aboveground C, total net primary productivity (NPP) was only 40% lower in high- versus low-severity stands, suggesting strong compensatory effects of non-tree vegetation on C uptake. Dead wood respiratory losses were small relative to total NPP (range: 10–35%), reflecting decomposition lags in this seasonally arid system. Although soil C, soil respiration, and fine root NPP were conserved across severity classes, net ecosystem production (NEP) declined with increasing severity, driven by trends in aboveground NPP. The high variability of C responses across this study underscores the need to account for landscape patterns of burn severity, particularly in regions such as the Pacific Northwest, where non-stand-replacement fire represents a large proportion of annual burned area.

Key words: carbon balance; Cascade Range; disturbance; fire emissions; heterotrophic respiration; mixed-severity fire regime; net ecosystem production; net primary productivity; *Pinus ponderosa*; wildfire.

Received 22 April 2009; accepted 10 August 2009

Author Contributions: G.M. contributed to the study design, conducted field work and data analysis, and wrote the manuscript. D.D., J.C., and J.M. contributed to the study design, field work, data analysis, and writing. B.L. conceived the study, guided design and methods, and contributed to data analysis and writing.

**Corresponding author; e-mail:* gmeigs@gmail.com

Published online: 30 October 2009

Introduction

Forest ecosystems play a vital role in the global carbon (C) cycle, and spatiotemporal variability due to disturbance remains an active frontier in C research (Goward and others 2008; Running 2008).

With increasing focus on forests in the context of climate change and potential mitigation strategies for anthropogenic C emissions (Birdsey and others 2007; IPCC 2007), it is important to quantify the impacts associated with anthropogenic and natural disturbance regimes, particularly wildfire. Although numerous studies have investigated the effects of fire on C dynamics, very few to date have analyzed the full gradient of burn severity and quantified pyrogenic C emission, C pools, and postfire C balance across multiple forest types in the first few years following disturbance.

Fire's role in the terrestrial C cycle has been studied extensively in the boreal zone (for example, Amiro and others 2001; Hicke and others 2003; Kurz and others 2008) and, to a lesser extent, in temperate forests (for example, Kashian and others 2006; Gough and others 2007; Irvine and others 2007), but many uncertainties remain. Like other disturbances (insects, pathogens, large storms), fire alters the distribution of live and dead C pools and associated C fluxes through mortality and regeneration, but fire also causes direct pyrogenic C emission through combustion (Amiro and others 2001; Campbell and others 2007; Bormann and others 2008). Depending on burn severity (defined here as overstory tree mortality), C transfer to the atmosphere, and from live to dead pools, can vary substantially. In some cases the amount of C released from necromass decomposition over decades can exceed the one-time emission from combustion (Wirth and others 2002; Hicke and others 2003). One key uncertainty is the magnitude of pyrogenic C emission and the relative combustion of different C pools (Campbell and others 2007). Another important uncertainty is the rate at which postfire vegetation net primary productivity (NPP) offsets the lagged decomposition of necromass pools and their effects on net C uptake (that is, net ecosystem production [NEP]; Wirth and others 2002; Chapin and others 2006). A third uncertainty is the dynamics of heterotrophic respiration (R_h) and soil C over the first few years postfire. Although fire might increase R_h or facilitate soil C loss, recent studies in Oregon and California have shown that both can be remarkably conserved following disturbance, buffering potential negative spikes in postfire NEP (that is, C source to atmosphere; Campbell and others 2004, 2009; Irvine and others 2007). A final uncertainty is the distribution and abundance of understory vegetation—shrubs, herbs, and regenerating trees—which influence both short-term NPP trends and C balance through succession. All of these ecosystem responses and uncertainties might diverge radically in high- versus low-severity stands, but most fire-carbon studies have been limited to stand-replacement events. For example, regional and continental C models typically ignore low-severity fire, largely due to remote-sensing detection limitations and assumed minor C impacts (Turner and others 2007), despite the inherent heterogeneity of fire effects across forest landscapes.

The area burned by wildfire has increased in recent decades across western North America due to an interaction of time since previous fire, forest management, and climate (Westerling and others 2006; Keane and others 2008). Recent fires have also exhibited increasing severity, but low- and moderate-severity fire effects remain an important component of nearly all large wildfires (Schwind 2008; Miller and others 2009). The mixed-severity fire regime, defined by a wide range and high variability of fire frequencies and effects (that is, high pyrodiversity; Martin and Sapsis 1991), is characteristic of many forest types (Schoennagel and others 2004; Lentile and others 2005; Hessburg and others 2007) and may represent a new fire regime in other types that historically burned with lower severity (Monsanto and Agee 2008). The widespread increase in burned area, combined with the intrinsic variability of mixed-severity fire regimes, represents a potentially dramatic and unpredictable shift in terrestrial C cycle processes. In addition, historically uncharacteristic fires in some systems, including ponderosa pine (*Pinus ponderosa* Douglas ex P. Lawson & C. Lawson) forests, can push vegetation into fundamentally different successional pathways and disturbance feedbacks (Savage and Mast 2005), which may lead to long-term reductions in terrestrial C storage (Dore and others 2008).

Since 2002, wildfires have burned approximately 65,000 ha in and around the Metolius River Watershed in the Eastern Cascades of Oregon (Figure 1). These fires generated a complex burn severity mosaic across multiple forest types and a wide range of prefire conditions. The extent and variability of these fires, coupled with robust existing datasets on C dynamics in unburned forests in the Metolius area (for example, Law and others 2001a, 2003), presented a unique opportunity to investigate wildfire impacts on the terrestrial C cycle. In this study, we measured forest ecosystem responses across four levels of burn severity and two forest types 4–5 years following fire. Our research objective was to quantify the effects of burn severity on:

1. Pyrogenic carbon emission (combustion);
2. Carbon pools (mortality, storage, and vegetation response);

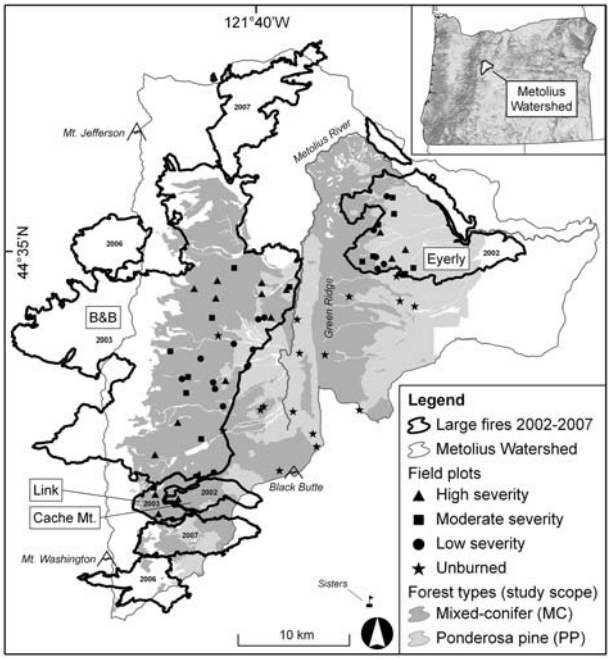

Figure 1. Metolius fire study area on the east slope of the Oregon Cascades. Point symbols denote survey plots (n = 64), labeled fires are the four surveyed (Table 2), and *shaded areas* are the sampled forest types. Other fires are outside the study scope and are labeled by fire year only. Forest type layer clipped to study scope: two types (MC and PP) on the Deschutes National Forest (DNF) within the Metolius Watershed. Other types (*unshaded area* within fires) include subalpine forests on the western margin, *Juniperus* woodlands to the east, riparian zones, and non-forest. Inset map shows study area location within Oregon elevation gradients. Fire perimeter and forest type GIS data from DNF. Other GIS data from archives at Oregon State University. Projection: UTM NAD 83.

3. Postfire carbon balance (biogenic C fluxes and NEP).

Here, we describe these three related response variables to elucidate the short-term fate of C pools and fluxes in the context of a highly heterogeneous postfire landscape.

Methods

Study Area

The Metolius Watershed is located NW of Sisters, OR, on the east slope of the Cascade Range (Figure 1). The postfire landscape is shaped by three important environmental gradients: forest type associated with climate, prefire biomass associated with past disturbance and management, and burn severity (overstory tree mortality) from recent fires.

Forest Type and Climate

The east slope is defined by one of the steepest precipitation gradients in western North America (Daly and others 2002; PRISM Group, Oregon St. Univ., http://prism.oregonstate.edu/). Within 25 km, vegetation transitions from subalpine forests (cool, wet) to *Juniperus* woodlands (warm, dry) and encompasses an unusual diversity of conifer species (Swedberg 1973). We focus on the two most prominent forest types—ponderosa pine (PP) and mixed-conifer (MC)—described by Franklin and Dyrness (1973) as the *Pinus ponderosa* and *Abies grandis* zones of Eastern Oregon. In general, the higher the elevation, mesic MC forest is more productive. Across the study area, ponderosa pine, grand fir (*Abies grandis* [Douglas ex D. Don] Lindl.), and Douglas-fir (*Pseudotsuga menziesii* [Mirb.] Franco) are the dominant tree species, and incense-cedar (*Calocedrus decurrens* [Torr.] Florin), western larch (*Larix occidentalis* Nutt.), and lodgepole pine (*Pinus contorta* Douglas ex Louden) are also abundant. Characteristic understory species include shrubs greenleaf manzanita (*Arctostaphylos patula* Greene), snowbrush (*Ceanothus velutinus* Douglas ex Hook.), and bitterbrush (*Purshia tridentata* [Pursh] DC.); forbs fireweed (*Epilobium angustifolium* L.), bracken fern (*Pteridium aquilinum* [L.] Kuhn), and American vetch (*Vicia americanum* Muhl. ex Willd.); and graminoids pinegrass (*Calamagrostis rubescens* Buckley), squirreltail grass (*Elymus elymoides* [Raf.] Swezey), and Idaho fescue (*Festuca idahoensis* Elmer). Study area elevation ranges from 600 to 2000 m, and slopes are generally gradual and east-facing. Mean annual precipitation ranges from 400 mm in eastern parts of the PP type to 2150 mm at high points in the MC type (Thornton and others 1997; DAYMET 2009). Summers are warm and dry; most precipitation falls as snow between October and June (Law and others 2001a). From W to E across the study area, average minimum January temperature ranges from −6 to −3.5°C and average maximum July temperature from 22 to 30°C (DAYMET 2009). Soils are volcanic in origin (vitricryands and vitrixerands), well-drained sandy loams/loamy sands. Additional study area characteristics are summarized in Table 1, and characteristic postfire stands are shown in Figure 2.

Historic Disturbance and Prefire Biomass

Historic fire return intervals ranged from 3 to 38 years in PP forests (Weaver 1959; Soeriaatmadhe 1966; Bork 1985; Fitzgerald 2005), from 9 to 53 years in the MC forest type (Bork 1985; Simon

Table 1. Metolius Watershed Study Area Characteristics

Forest type[1] Burn severity[2]	Number of plots	Burned area (ha) within study scope	Burned area %	Elevation (m) (mean, range)	Slope (°) (mean, range)	Total tree basal area (mean m^{-2} ha^{-1}, SE)[3]	Total tree density (mean trees ha^{-1}, SE)[3]	Tree % mortality (mean, SE)[4]
Mixed-conifer (MC)[1]	32	21,952	74	1160 (910–1558)	8.4 (1–22)	36 (3)	874 (103)	*61 (6)*
Unburned	8	na	na	1139 (910–1558)	4.9 (1–22)	35 (7)	911 (255)	13 (3)
Low severity	8	7236	25	1045 (972–1128)	6.8 (2–14)	40 (5)	1041 (252)	*29 (4)*
Moderate severity	8	4810	16	1155 (1068–1291)	10.5 (5–22)	35 (4)	1068 (142)	*58 (4)*
High severity	8	9906	33	1300 (1136–1479)	11.6 (8–14)	33 (7)	477 (81)	*96 (2)*
Ponderosa pine (PP)[1]	32	7821	26	1004 (862–1247)	5.2 (1–22)	21 (2)	643 (91)	*54 (8)*
Unburned	8	na	na	1035 (862–1247)	5.5 (1–17)	24 (4)	1020 (247)	6 (2)
Low severity	8	2371	8	977 (910–1074)	5.5 (1–22)	27 (5)	515 (122)	*14 (4)*
Moderate severity	8	2827	9	1046 (921–1092)	4.1 (1–7)	14 (3)	461 (122)	*49 (7)*
High severity	8	2623	9	957 (902–1063)	5.8 (1–15)	18 (5)	578 (168)	*100 (0)*
Overall	64	29,773	100	1082 (862–1558)	6.8 (1–22)	28 (2)	759 (70)	*58 (5)*

*Notes: Study scope was the area available for field sampling: Deschutes National Forest (DNF) non-wilderness land at least 50 m from roads, non-forest, and riparian areas. These area estimates also used for landscape scaling of pyrogenic C emission (Table 3). Note the uneven distribution of severity*type treatments across the sampled landscape.*

[1]*Determined from DNF plant association group GIS data. Forest type rows describe sum or mean values as applicable.*

[2]*Determined from DNF BARC burn severity GIS data.*

[3]*Mean basal area and density of all trees with DBH more than 1 cm, including live and dead. SE in parentheses.*

[4]*Mean% basal area mortality due to fire for burned stands (indicated by italics), mean% dead tree basal area for unburned plots. SE in parentheses.*

Figure 2. Characteristic forest stands across the Metolius Watershed study gradients. Clockwise from top-left: **A** unburned MC, **B** low-severity PP, **C** moderate-severity MC, **D** high-severity PP. Unburned stands contain heavy fuel accumulations and high tree and understory vegetation density; low-severity stands show partial bole scorching, high tree survivorship, and rapid recovery of surface litter; moderate-severity stands show increased bole scorch heights and overstory mortality; high-severity stands show near 100% tree mortality and generally thick understory vegetation (shrubs and herbs). Note that almost all fire-killed trees remain standing 4–5 years postfire.

1991), and up to 168 years in subalpine forests (Simon 1991). Given abundant lightning ignitions (Rorig and Ferguson 1999), it is likely that historic fires burned multiple forest types and exhibited the high spatiotemporal variability in fire behavior characteristic of mixed-severity fire regimes. During the twentieth century, fire suppression, grazing, timber harvest, and road construction resulted in fire exclusion. Dispersed patch clearcutting was the primary disturbance in recent decades, and most low biomass areas were young plantations (Deschutes National Forest [DNF] silvicultural GIS data). Anomalously dry, warm years (1985–1994, 2000–2005), contributed to regional drought stress (Figure 3; Thomas and others 2009). Beginning in 1986, an outbreak of western spruce budworm (*Choristoneura occidentalis*) and bark beetles (Family *Scolytidae*) killed trees across mid-to-high elevation MC forests (Franklin and others 1995). These interacting factors—time since previous fire, forest management, drought, and insect outbreaks—created fuel conditions conducive to large-scale wildfire.

Recent Large Wildfires

Since 2002, multiple large (>1000 ha) wildfires have affected half of the forested area in the watershed, burning across multiple forest types, land ownerships, and a wide range of fuel, weather, and topographic conditions. Surface, torching, and active crown fire behavior yielded a heterogeneous spatial pattern of burn severity (overstory tree mortality) at stand- and landscape-scales. This study focused on 4 major fires that burned approximately 35% of the watershed in 2002–2003 (Table 2, Figure 1).

Sampling Design and Scope

We measured postfire C pools and fluxes at 64 independent plots across the Metolius Watershed (Figure 1), sampling burned stands in 2007 (4–5 years postfire) and unburned stands in 2008. We employed a stratified random factorial sampling design with two factors—forest type and burn severity—and included prefire biomass as a covariate. We mapped forest type and burn severity

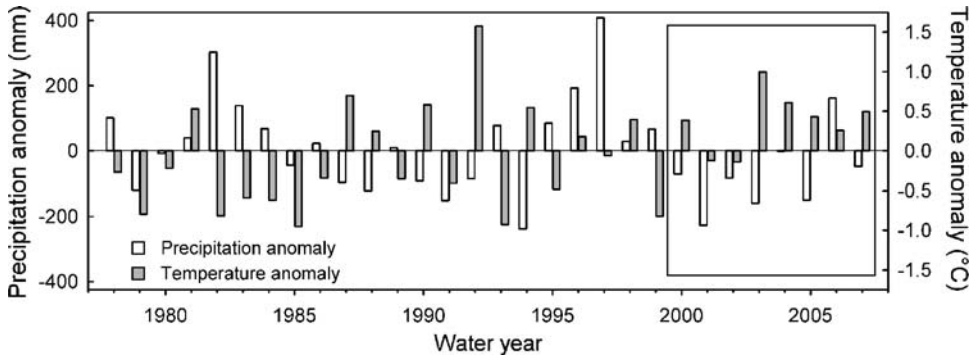

Figure 3. Climate anomalies in the Metolius Watershed. Anomalies in precipitation (mm) and temperature (°C) are in reference to the 30 year mean (1978-2007) from PRISM data (http://prism.oregonstate.edu/) extracted at a central location in the watershed (described by Thomas and others [2009]). Water year is defined as the 12-month period from October–September. The 2000 water year marked the beginning of an anomalously warm and dry period, coincident with a positive phase of the Pacific Decadal Oscillation (Thomas and others 2009). These anomalies contributed to drought stress and set the stage for wildfires and potentially harsh conifer regeneration conditions.

Table 2. Four Large Fires in the Metolius Watershed

Fire name	Fire size (ha) within watershed	Fire year	Ignition source
B&B Complex[1]	28,640	2003	Lightning
Eyerly Complex	9362	2002	Lightning
Link	1453	2003	Human
Cache Mt.	1376	2002	Lightning
Fire total	40,831		
Fire within MC and PP forest types (scope)	29,773		
Metolius Watershed area	115,869		

Note: [1]Booth and Bear Butte Complex: two large fires that merged into one.

classes from DNF GIS data. For forest type, we used a plant association group layer and combined wet and dry PP into one type and wet and dry MC into another. For burn severity, we used maps derived from the differenced normalized burn ratio (dNBR; Key and Benson 2006) classified as unburned, low, moderate, and high by DNF technicians following field assessment. Although the remotely sensed dNBR index has both known and unknown limitations (Roy and others 2006; French and others 2008), it is highly correlated with fire effects on vegetation and soil and has been used widely in conifer forests (Key and Benson 2006; Thompson and others 2007; Miller and others 2009). We defined plot-level burn severity as overstory tree basal area mortality (%), verified that plot-level mortality was consistent with the dNBR severity classes, and used the severity classes as a categorical variable (factor) in statistical analyses (described below). We used GIS to establish eight randomized survey plots within each combination of forest type and burn severity (hereafter 'type*severity treatment'; $n = 64$; Table 1, Figure 1). All plots were on DNF non-wilderness land at least 50 m from roads, non-forest, salvage-logged, and riparian areas. In addition, we used a live, aboveground biomass map from 2001 to sample the full range of prefire biomass and to ensure comparability among type*severity treatments. This biomass map was derived from regression tree analysis of Landsat spectral data and biophysical predictors (S. Powell, Univ. Montana, unpublished manuscript).

We used standard biometric methods described previously (Law and others 2001a, 2003; Campbell and others 2004; Irvine and others 2007). Below, we summarize these methods and provide specifics regarding postfire measurements, which are described in further detail by Meigs (2009). Each plot encompassed a 1 ha stand of structurally homogenous forest, which we sampled with a plot design similar to the USDA Forest Inventory and Analysis protocol (USDA 2003) enhanced for C budget measurements including tree increment, forest floor, fine and coarse woody detritus, and soil CO_2 effluxes (protocols in Law and others 2008). We scaled all measurements to slope-corrected areal units for comparison across study treatments.

Like other fire studies, this natural experiment lacked experimental control and detailed prefire data, but remotely sensed prefire biomass, GIS data, and plot attributes allowed us to account for preexisting differences. Because the forest type, burn severity, and prefire biomass were not randomly assigned, we limited statistical inference and

interpretations to the sampled forest types. To minimize potential confounding effects of spatial and temporal autocorrelation, we located plots at least 500 m apart, maximized interspersion within study area gradients, and sampled multiple fires from two different years. The experimental unit was the 1 ha plot.

Ecosystem Measurements

Aboveground C Pools, Productivity, and Heterotrophic Respiration

At each plot, we quantified aboveground C pools in four circular subplots (overstory trees, stumps, understory vegetation, forest floor) and along transects (coarse woody detritus [CWD], fine woody detritus [FWD]). We sampled overstory trees at various scales to account for different stem densities (10 m default subplot radius for trees 10.0–69.9 cm diameter at breast height [DBH; 1.37 m]). For all trees with DBH at least 1 cm, we recorded species, DBH, height, % bark and wood char, decay class (1–5; Maser and others 1979; Cline and others 1980), and whether or not trees were broken and/or dead prior to burning. We estimated CWD and FWD volume using line intercepts (Van Wagner 1968; Brown 1974; Harmon and Sexton 1996; Law and others 2008), recording diameter, decay class, and char class on four 75 m transects per plot. We sampled CWD (all pieces ≥7.62 cm diameter) along the full 300 m and FWD less than 0.64, 0.65–2.54, and 2.55–7.62 cm along 20, 60, and 120 m, respectively.

We sampled understory vegetation (tree seedlings [DBH < 1 cm], shrubs, forbs, graminoids), and ground cover in four 5 m radius subplots nested within overstory tree subplots. For tree seedlings, we recorded species, age, height, and live/dead status and identified seedlings established before fire. Based on seedling age and DNF GIS replanting data, we determined if seedlings were planted and excluded these from natural regeneration analyses. We calculated shrub volume from estimates of live shrub % cover in three height classes (0–0.5, 0.5–1.0, 1.0–2.0 m) and dead shrub stem number, length, and diameter. We estimated the % cover of forbs, graminoids, litter, woody detritus, cryptogams, rocks, and mineral soil.

We computed biomass with an allometry database of species-, ecoregion-, and decay class-specific volume equations and densities (Hudiburg 2008; Hudiburg and others 2009), adjusting tree, CWD, and FWD biomass estimates for char reduction (Donato and others 2009a), broken status, and severity-specific estimates of bark, wood, and foliage combustion after Campbell and others (2007). We used species-specific allometric equations to convert live shrub volume to mass and converted dead shrub volume to mass using the mean decay class 1 wood density of three locally abundant genera (*Acer*, *Alnus*, *Castanopsis*). We converted herbaceous cover to biomass using 0.25 m^2 clip plots of dominant species sampled across the study area. We assumed that the C content of all pools was 0.51 except for forest floor (assumed to be 0.40; Campbell and others 2007). We sampled forest floor (litter and duff) to mineral soil with 10.2 cm diameter pvc corers at 16 randomized locations per plot and oven-dried samples at 60°C for more than 72 h to determine mass.

We determined NPP and heterotrophic respiration (R_h) at the 48 burned plots. We estimated bolewood NPP from radial increment measurements of current and previous live tree biomass (Van Tuyl and others 2005; Hudiburg and others 2009), collecting increment cores at breast height from 20 representative live trees in each low- and moderate-severity plot. Although researchers typically average radial increment from the previous 5-10 y to account for climatic variability (for example, Law and others 2003), we used the last full year of radial growth (2006) to estimate bolewood NPP because we could not assume a steady state 4–5 years postfire. For live trees in high-severity stands (<0.5% of inventoried trees, n = 23 at 3 of 16 stands), we applied forest type averages of increment data from low- and moderate-severity stands. We calculated foliage NPP as the product of specific leaf mass per unit area (SLA), leaf retention time (LRT), and plot-level leaf area index (LAI). We estimated SLA and LRT from representative canopy shoots with full retention and measured LAI optically using a Sunfleck ceptometer (Decagon Devices, Inc., Pullman, WA) after Law and others (2001b) and Pierce and Running (1988). Because moderate- and high-severity fire substantially altered tree crowns through combustion and mortality, we scaled LAI measurements from low-severity plots using a regression of the positive relationship between LAI and live tree basal area ($LAI = 3.85 * [1 - e^{(-0.0311 * \text{live basal area})}]$, adj. R^2 = 0.54, n = 16; fitted using the exponential rise to maximum statistical program in SigmaPlot [Version 11.0, SPSS Science, IL]). We computed shrub wood and foliage NPP from annual radial increment and LRT (Law and Waring 1994; Hudiburg and others 2009). We assumed that herbaceous

mass equaled annual NPP and that annual mass loss was 50% (Irvine and others 2007).

We computed aboveground R_h of dead woody pools (R_{hWD}) as the product of necromass and decomposition constants from a regional CWD database (Harmon and others 2005). Because snags decay much more slowly than CWD in this seasonally moisture-limited system, we assumed that snag decomposition was 10% of CWD decomposition (Irvine and others 2007), but we used CWD decomposition rates for stumps, for which microbial decay processes are less moisture-limited (M. Harmon, Oregon St. Univ., 2009, personal communication). We estimated FWD decomposition after McIver and Ottmar (2007).

Belowground C Pools, Productivity, and Heterotrophic Soil Respiration

At the 48 burned plots, we collected soil and fine roots (FR: <2 mm diameter) at 16 randomized locations per plot using 7.3 cm diameter augers. Default sampling depth was 20 cm with one core up to 100 cm per plot. We used linear regression to scale C, N, and FR to 100 cm. We assumed that 49% (SD = 14) of soil C, 48% (SD = 17) of soil N, and 62% (SD = 20) of FR were in the top 20 cm, within the variation of the FR correction factor reported by Law and others (2003). All samples were sorted through 2 mm sieves, bench-dried, mixed by subplot, and analyzed for mass fraction of C and N (LECO CNS 2000 analyzer, Leco Corp., St. Joseph, MI), texture (hydrometer method), and pH (Oregon St. Univ. Central Analytical Laboratory). We calculated bulk density via stone displacement and separated FR and other organic matter. We combusted a representative FR subsample in a muffle furnace at 550°C for 5 h to determine organic content (74.24%), which we applied to all FR samples to estimate total organic matter. Based on published estimates of regional FR decomposition (Chen and others 2002) and mortality (Andersen and others 2008), we assumed that less than 40% of fire-killed FR remained when sampled, that far fewer were retained by 2 mm sieves, and that the vast majority of sampled FR was newly recruited postfire. We estimated that live roots were 61% of total FR mass in PP stands (Irvine and others 2007) and 87% of FR mass in MC stands (P. Schwarz, Oregon St. Univ., unpublished data). We computed FR NPP as the product of total organic FR mass and a root turnover index from rhizotron measurements in a nearby unburned PP forest (Andersen and others 2008). We estimated live and dead coarse root (CR: > 10 mm diameter) mass from the tree, snag, and stump surveys as a function of DBH (Santantonio and others 1977) and computed CR NPP from modeled current and previous live tree diameters (from increment cores). Because the median stump height was 30 cm, we applied a correction factor of 0.9 to account for bole taper to 1.37 m for stump CR estimates (adapted from D. Donato, unpublished data).

We measured soil CO_2 efflux and adjacent soil temperature at burned plots during the peak flux period (12 randomized locations; one set of manual measurements per plot in late June) using a Li-6400 infrared gas analyzer with Li-6000-9 soil chamber (Li-Cor Biosciences, Lincoln, NE) and established protocols (Law and others 1999; Campbell and Law 2005; Irvine and others 2007, 2008). We estimated annual soil respiration (R_{soil}) by matching plot measurements with concurrent, hourly, automated soil respiration measurements at a nearby unburned AmeriFlux PP tower site (Irvine and others 2008). The automated record consisted of hourly measurements spanning early May to mid November and was gap-filled using 16 cm soil temperature and 0–30 cm integrated soil moisture (see Irvine and others 2008 for model specifics). We scaled plot measurements to the annual dataset using plot-specific correction factors based on the ratio of mean soil respiration for a given plot divided by the concurrent automated rate. Correction factors ranged from 0.47 to 1.60 (range of type*severity means: 0.87–1.02). This approach sampled the spatial variability of R_{soil} within each plot to determine base rates and leveraged the long-term, intensive measurements of temperature- and moisture-driven variability. Similar automated measurements were made in 2002–2003 in a MC stand that subsequently burned in the B&B fire. A comparison of MC and PP continuous respiration datasets during the overlapping measurement period indicated near identical diel amplitudes and seasonal patterns between the two sites (data not shown). Given this similarity, we concluded that annual, plot-specific R_{soil} estimates based on the PP automated soil respiration would adequately represent the spatial and temporal variation within and among plots. We computed the heterotrophic fraction of soil respiration (R_{hsoil}) based on previous measurements at vegetation-excluded automated chambers at high-severity and unburned AmeriFlux tower sites within the study area (Irvine and others 2007).

Net Ecosystem Production

We estimated net ecosystem production (NEP: the difference between gross primary production and ecosystem respiration; Chapin and others 2006) using the mass balance approach (Law and others 2003; Campbell and others 2004; Irvine and others 2007):

$$\mathrm{NEP} = (\mathrm{NPP_A} - R_{\mathrm{hWD}}) + (\mathrm{NPP_B} - R_{\mathrm{hsoil}}) \quad (1)$$

where $\mathrm{NPP_A}$ is aboveground NPP, R_{hWD} is heterotrophic respiration of aboveground woody detritus, $\mathrm{NPP_B}$ is belowground NPP, and R_{hsoil} is heterotrophic soil surface CO_2 efflux (includes forest floor). NEP is the appropriate metric of C balance and uptake at the spatiotemporal scale of our measurements, whereas net ecosystem carbon balance (that is, net biome production) describes landscape- to regional-scale C balance and longer-term effects of fire and other fluxes (for example, erosion, leaching, timber harvest; Chapin and others 2006). Here, we assume these other fluxes to be negligible during the sampling period, and we account for combustion losses independently of NEP.

Pyrogenic C Emission from Combustion

Before-after measurement of C pools is the most certain method to measure pyrogenic C emission (Campbell and others 2007), but in this study, co-located prefire measurements were not available, and it was not possible to establish a paired plot for every burned condition across the study gradients. We estimated C loss from combustion using a standard simulation program (Consume 3.0; Prichard and others 2006), augmented with field estimates of tree consumption. Consume predicts aboveground fuel consumption, C emission, and heat release based on weather data, fuel moisture, and fuelbed inputs from the Fuel Characteristic Classification System (FCCS 2.0; Ottmar and others 2007); both models available at: www.fs.fed.us/pnw/fera/. We selected representative FCCS fuelbeds for PP and MC stands (Table 3) using GIS and modified these to develop custom fuelbeds based on field measurements at the 16 unburned plots. We simulated low-, moderate-, and high-severity fire by adjusting percent canopy consumption and fuel moisture content for woody fuels and duff (R. Ottmar, US Forest Service, 2009, personal communication). Because Consume 3.0 does not account for consumption of live tree stems and bark, we used field measurements to calculate the changes in mass and density due to charring (Donato and others 2009a). We assessed combustion at the stand-scale and scaled combustion to the sampled landscape with forest type and burn severity GIS data.

Statistical and Uncertainty Analysis

We used multiple linear regression and analysis of covariance to compare response variables across the study gradients. Because one- and two-way ANOVA (forest type and burn severity tested separately and combined) revealed a significant difference in prefire biomass between the two forest types ($P < 0.001$) but no significant prefire difference among burn severities within either forest type ($P > 0.5$), we conducted analyses separately by forest type. We derived test statistics (coefficients and standard errors) from a multiple linear regression model of the response variable as a function of prefire biomass (continuous) and burn severity (categorical) within a given forest type. Regression analysis showed no significant interactions among explanatory variables; coefficient estimates were calculated from additive models with an assumption of parallel lines among type*severity treatments. We log-transformed data when necessary to satisfy model assumptions. We accounted for multiple comparisons and reported statistical significance as the highest significant or lowest non-significant Tukey-adjusted P value ($\alpha = 0.05$) common to all groups (for example, severity classes) in a given comparison (PROC GLM lsmeans multiple comparisons; SAS 9.1, SAS Institute, Inc., Cary, NC).

We take a pragmatic view of uncertainty analysis after Irvine and others (2007). Many scaling assumptions are necessary to estimate plot-level metrics from components sampled at varying spatiotemporal scales. Further, given the wide range of sampled prefire biomass and variability across the postfire landscape, it is possible to commit Type II statistical errors when important differences exist but are confounded by additional factors. We thus focus on the trends and proportions across type*severity treatments rather than absolute magnitudes. To estimate NEP uncertainty, we used a Monte Carlo procedure with the four major fluxes described in equation (1) for each type*severity treatment (NEP uncertainty expressed as ± 1 SE after 10000 iterations based on the standard normal distribution with mean, standard deviation, and between-flux covariance in R [R Development Core Team 2009]).

Table 3. Pyrogenic C Emission (PE) from Consume 3.0 Simulations and Field Measurements of Consumption

FCCS fuelbed[1]	Forest type Burn severity[2]	Stand scale				Landscape scale	
		Total aboveground C (Mg C ha^{-1})[3]	Stand-scale PE (Mg C ha^{-1})[4]	% Consumption, aboveground C[5]	% Consumption, live tree stems[6]	Total PE (Tg C)[7]	Landscape % of total PE[7]
Grand fir–Douglas fir forest	Mixed-conifer						
(fire suppression) (SAF 213)	Unburned	132.6					
	Low severity		16.6	13	0.23	0.120	16
	Mod severity		25.3	19	0.71	0.122	16
	High severity		32.3	24	2.01	0.320	42
Pacific ponderosa pine forest	Ponderosa pine						
(fire suppression) (SAF 237)	Unburned	87.2					
	Low severity		19.7	23	0.27	0.047	6
	Mod severity		25.6	29	1.43	0.072	10
	High severity		30.2	35	2.77	0.079	10
Across sampled burn area (29,773 ha)			**25.5**[8]	**22**[8]	**1.24**[8]	**0.760**	100

Notes: [1]*Fuel Characteristic Classification System (FCCS) fuelbeds determined using GIS data and descriptions from US Forest Service FERA group: www.fs.fed.us/pnw/fera/. SAF codes are Society of American Foresters cover types (Eyre 1980).*
[2]*Severity classes derived by adjusting surface fuel moisture and canopy consumption (R. Ottmar, US Forest Service, 2009, personal communication).*
[3]*Total aboveground C from unburned stands, used for parameterizing FCCS fuelbed inputs for Consume modeling. Multiply by 2 for Mg ha^{-1} mass or by 100 for g C m^{-2}.*
[4]*Pyrogenic C emission (PE) computed from simulated biomass combustion in Consume and field measurements of bark and bole charring calculated after Donato and others (2009a) and Campbell and others (2007).*
[5]*% of unburned plot aboveground C (4th column).*
[6]*% of live tree bark and bole bark mass estimated from charring (mean, weighted by tree mass).*
[7]*Stand-scale PE scaled to the sampled landscape based on area of type*severity treatments (Table 1).*
[8]*Mean, weighted by area of type*severity treatments (Table 1).*

Results and Discussion

Pyrogenic C Emission (Combustion)

Simulated mean pyrogenic C emission (PE) was 25.5 Mg C ha^{-1} (range: 16.6–32.3 Mg C ha^{-1}) and was similar between forest types. The % consumed in PP stands was substantially higher (range: 23–35 vs. 13–24% for PP versus MC stands, respectively, Table 3). Stand-scale PE from low-severity fire was 51% and 65% of high-severity PE in MC and PP stands, respectively, indicating that the largest proportion of emissions was from combustion of surface and ground fuels. This result is consistent with Campbell and others (2007), who determined that greater than 60% of total combustion was from litter, foliage, and small downed wood, and that these high surface area:volume ratio pools were readily consumed (>50% combusted) in all burn severities in SW Oregon mixed-conifer forests. Our field-based estimate of live tree stem consumption was on average 1.24% (range: 0.23–2.77%) of live bark and bole mass, a trivial amount compared to other PE uncertainties. The largest remaining uncertainty is that the Consume 3.0 model does not account for belowground C loss due to combustion, erosion, or other fire effects, which can be substantial in some cases (Bormann and others 2008). Without detailed prefire measurements, we were unable to address this issue directly, but our soil C surveys did not show any significant C declines in high-severity stands (described below).

Scaled to the sampled landscape (approximately 30,000 ha of burned area), simulated total PE was 0.76 Tg C (Table 3). High-severity MC stands, with the largest per unit area emissions and landscape area, contributed a disproportionate amount of PE (42% of the total), whereas all PP forests combined released 26% of total PE. These proportions underscore the importance of incorporating landscape patterns of vegetation and fire effects (that is, the severity mosaic) into modeling and policy analyses. On a per unit area basis, PE from these fires was 33% higher than from the 200,000 ha Biscuit Fire (25.5 vs. 19 Mg C ha^{-1}; Campbell and others 2007). This C transfer represents a substantial pulse to the atmosphere relative to annual net C fluxes from unburned forest in the Metolius area (mean annual net C uptake at a mature PP site: 4.7 ± 0.4 Mg C ha^{-1} y^{-1}; Thomas and others 2009). Conversely, 0.76 Tg C is approximately 2.5% of Oregon statewide anthropogenic CO_2 emissions from fossil fuel combustion and industrial processes for the 2-year period 2002–2003 (30.62 Tg C equivalent; http://oregon.gov/energy/gblwrm/docs/ccigreport08web.pdf). It is important to note that the study scope burned area is less than half of the area burned in and around the Metolius Watershed since 2002 (>65,000 ha, 35,000 ha beyond this study scope) and that these were large fire years regionally. Thus, our study area represents a relatively small proportion of total wildfire PE. Although further refinements are possible, the current analysis provides a reasonable constraint for regional modeling efforts.

Carbon Pools (Mortality, Storage, and Vegetation Response)

Because large C pools (that is, live tree boles) were largely unaffected by combustion in all severities, fire-induced mortality was the most important overall C transformation, larger in magnitude than combustion. The distribution of live and dead C pools changed predictably with burn severity, dominated by the shift from live trees to dead wood mass (Table 4). Aboveground live tree and dead wood mass (g C m^{-2}) both exhibited wide ranges (live tree range: 0–9302, PP high severity to MC low severity; dead wood range: 924–6252, PP low severity to MC high severity), the latter range encompassing dead wood estimates from Washington East Cascades high-severity stands (approximately 3000; Monsanto and Agee 2008). Mean basal area mortality increased with burn severity classes, ranging from 14% in low-severity PP stands to 49% in moderate-severity and 100% in high-severity PP stands, with parallel patterns in MC stands (29, 58, 96%, respectively; Table 1, Figure 4A). Across both forest types, this mortality resulted in a significant reduction in live aboveground C in high- versus low-severity stands ($P < 0.005$), coupled with a near tripling of dead wood aboveground C (Table 4). In both forest types, forest floor mass showed the largest absolute and relative difference between burned and unburned stands (mean: 1588 and 232 g C m^{-2}, respectively), consistent with near-complete combustion of these pools. Whereas the difference between burned and unburned forest floor mass was highly significant (85% reduction; $P < 0.001$), there were no significant differences among low-, moderate-, and high-severity stands in either forest type ($P > 0.850$). Because of the decline in forest floor and high tree survival, low-severity stands exhibited lower aboveground necromass than unburned stands (Table 4).

Total aboveground C and total ecosystem C declined with increasing burn severity in both forest

Table 4. Carbon Pools of Forest Stands in the Metolius Watershed

Forest type[1] Burn severity	Aboveground					Belowground			
	Live tree mass	Non-tree live mass[2]	Dead wood mass[3]	FWD[4]	Forest floor[5]	Coarse root[6]	Fine root[7]	Soil C[8]	Ecosystem C[9]
Mixed-conifer[1]	5153 (807)	156 (12)	4080 (537)	171 (15)	610 (135)	3115 (232)	*185* (*34*)	*6556* (*348*)	***18,648*** (*1213*)
Unburned	$_{ab}$9302 (1146)	$_{ab}$140 (22)	2884 (1008)	205 (31)	$_{a}$1610 (180)	3588 (480)	na (na)	na (na)	**na** (na)
Low severity	$_{abc}$7268 (1147)	$_{a}$105 (22)	2813 (1009)	166 (31)	$_{b}$374 (180)	3162 (481)	172 (62)	5960 (611)	**20,414** (2189)
Mod severity	$_{bcd}$3071 (1140)	$_{ab}$181 (22)	4371 (1003)	162 (30)	$_{b}$289 (179)	2931 (478)	211 (61)	6434 (604)	**17,884** (2163)
High severity	$_{cd}$972 (1141)	$_{b}$200 (22)	6252 (1003)	153 (30)	$_{b}$169 (179)	2780 (478)	172 (61)	7225 (604)	**17,727** (2166)
Ponderosa pine[1]	3178 (538)	104 (9)	1898 (300)	112 (16)	531 (151)	1713 (142)	*135* (*10*)	*5903* (*195*)	***12,677*** (*648*)
Unburned	$_{w}$5110 (714)	$_{wxy}$78 (14)	$_{wx}$1517 (543)	$_{w}$179 (29)	$_{w}$1566 (219)	1842 (276)	na (na)	na (na)	**na** (na)
Low severity	$_{w}$5576 (716)	$_{wx}$67 (14)	$_{w}$924 (544)	$_{wx}$75 (29)	$_{x}$234 (219)	2131 (276)	128 (18)	6034 (353)	$_{w}$**15,244** (922)
Mod severity	$_{x}$2098 (724)	$_{xyz}$126 (14)	$_{wx}$1934 (551)	$_{wx}$130 (30)	$_{x}$258 (222)	1563 (280)	141 (18)	5899 (359)	$_{wx}$**12,089** (937)
High severity	$_{x}$0 (0)	$_{yz}$146 (14)	$_{x}$3218 (542)	$_{x}$64 (29)	$_{x}$67 (218)	1317 (275)	137 (18)	5775 (351)	$_{x}$**10,677** (918)

Notes: Values: mean C pools (g C m^{-2}). SE from ANCOVA in parentheses. Subscript letters indicate pairwise significant differences (Tukey-adjusted $P < 0.05$) between severities within each forest type. To convert values to Mg biomass ha^{-1}, divide by 50.

[1]*Forest type row: non-italics denote all stands (unburned and burned, n = 32); italics denote burned stands only (n = 24, unburned stands not surveyed [na]).*

[2]*Other live pools: shrubs, seedlings, graminoids, forbs.*

[3]*Dead wood mass: sum of snags, stumps, and CWD (dead down wood ≥ 7.63 cm diameter).*

[4]*FWD: all woody fuels less than 7.63 cm diameter.*

[5]*Forest floor: sum of litter and duff.*

[6]*Coarse roots at least 10 mm diameter (modeled from diameter of live and dead trees and stumps).*

[7]*Fine roots less than 2 mm diameter (live and dead), scaled from 20 cm depth (62% [SD = 20] of fine roots assumed in top 20 cm).*

[8]*Soil C to 100 cm depth, scaled from 20 cm depth (49% [SD = 14] of soil C assumed in top 20 cm).*

[9]*Ecosystem C: sum of all C pools. Includes dead shrubs (not included in other columns).*

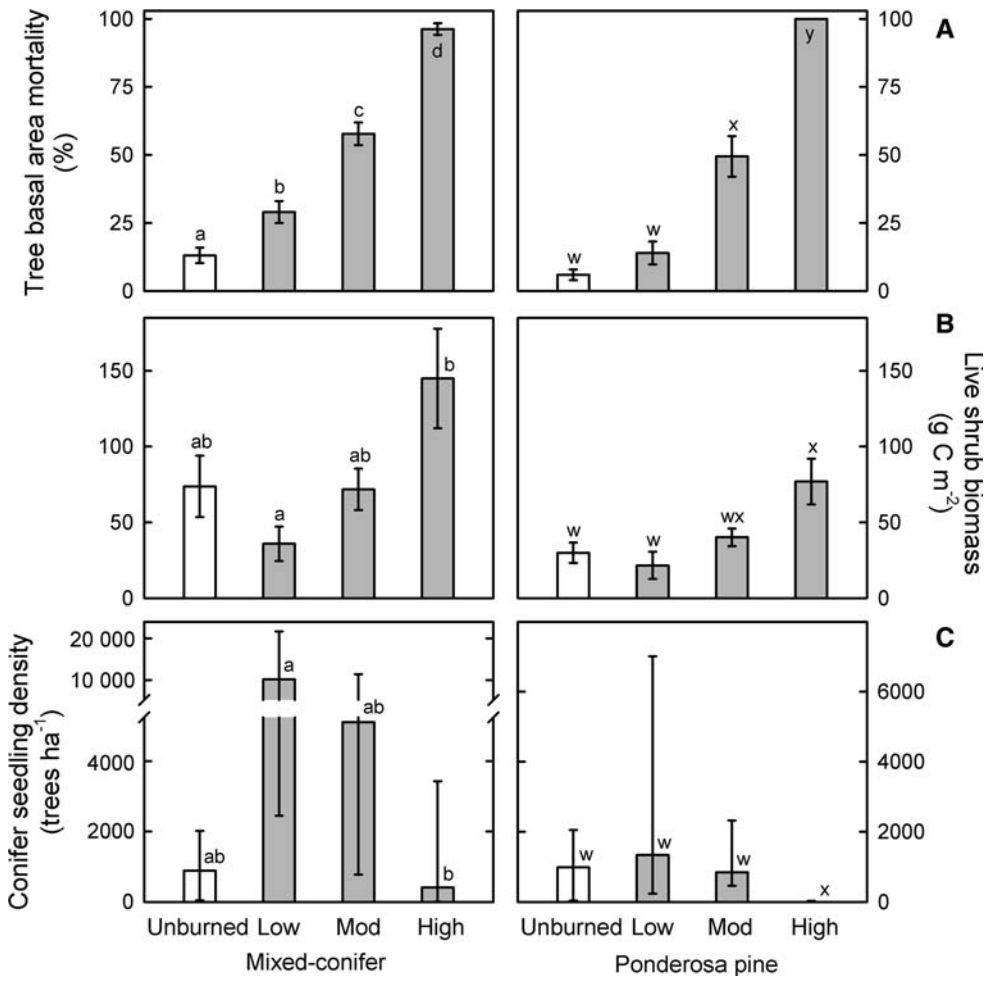

Figure 4. **A** Tree basal area (BA) mortality, **B** live shrub biomass, and **C** conifer seedling regeneration 4–5 years postfire by forest type and burn severity in the Metolius Watershed. Bars in **A** and **B** denote means; error bars denote ±1 SE from 8 plots in each forest type*burn severity treatment. Due to skewness, bars in **C** denote medians and error bars denote 25 and 75th percentile. Note the different scales between forest types above y-axis break in **C**. Tree mortality in **A** is % BA mortality due to fire in burned stands and total % dead BA in unburned stands. Lowercase letters denote statistically significant differences (Tukey-adjusted $P < 0.05$) among severities. Statistical tests for **A** used total % BA mortality, a metric common to all treatments. Statistical tests for **C** used $\log_e$-transformed data. **A** and **C** excluded the prefire biomass covariate. Seedlings are live, non-planted trees from the postfire time period only. Note that high-severity PP stands included 100% tree mortality in all 8 plots and a median seedling density of zero.

types (Table 4), although total ecosystem C was not significantly different among severities in MC forests ($P > 0.670$). In both types, fine root mass and soil C to 20 cm depth were not significantly different among severities ($P > 0.330$). Scaled to 100 cm, mean soil C stocks (±1 SE from regression) were 6556 ± 348 and 5903 ± 195 g C m^{-2} for burned MC and PP stands, respectively (Table 4). These values are similar to nearby unburned stands (7057 g C m^{-2}) and substantially lower than soil C in more mesic Oregon forests (14,244 and 36,174 g C m^{-2} in the West Cascades and Coast Range, respectively; Sun and others 2004). The lack of significant differences among severities furthers the evidence that soil C can be conserved with disturbance (Campbell and others 2009), including high-severity fire (Irvine and others 2007). Without site-specific prefire data we were unable to directly measure changes in soil C, and in applying a fixed-depth approach, a limitation of most postfire studies, we could not fully preclude the possibility of fire-induced soil C loss due to combustion, plume transport, or erosion (Bormann and others 2008). Unlike that study, in steep terrain experiencing stand-replacement fire (Bormann and others 2008), we did not observe severe erosion or changes in the soil surface between burned and unburned stands, and we detected no differences in

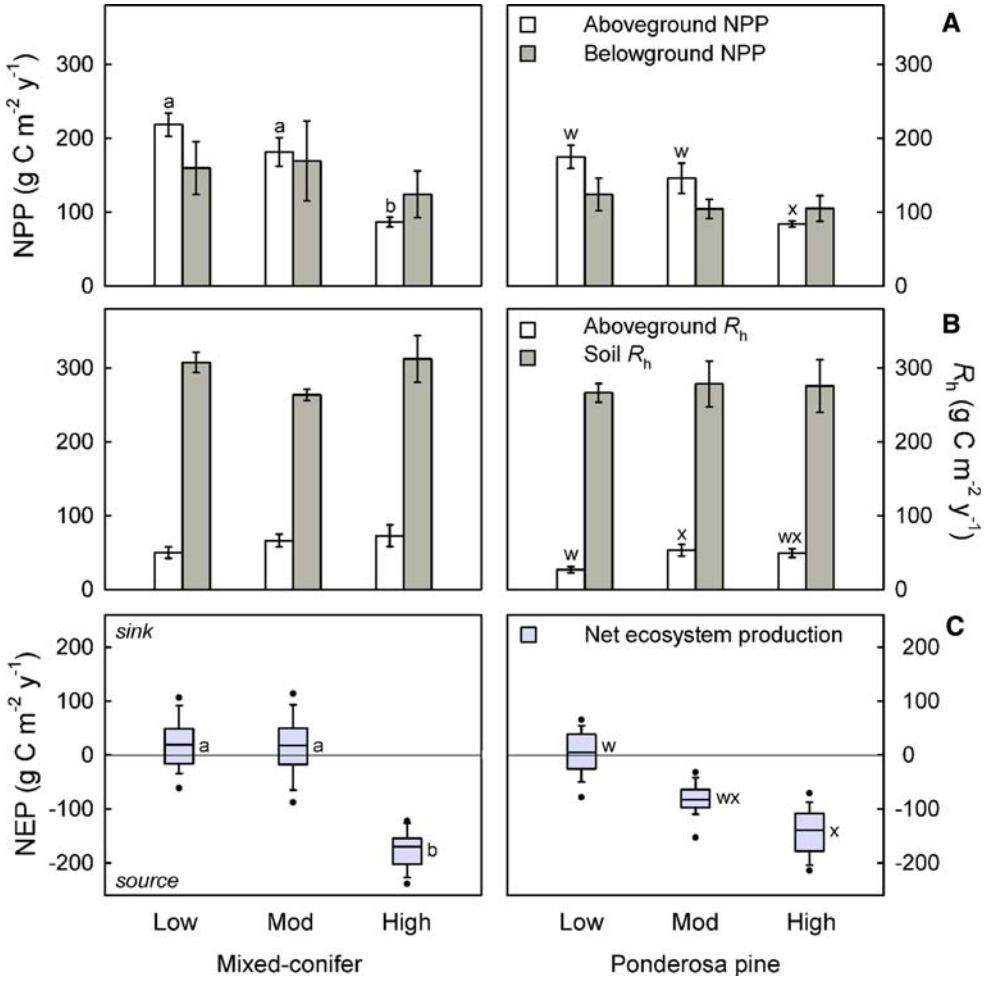

Figure 5. **A** Net primary productivity (NPP), **B** heterotrophic respiration (R_h), and **C** net ecosystem production (NEP) 4–5 years postfire by forest type and burn severity in the Metolius Watershed. Bars in **A** and **B** denote means; error bars denote ±1 SE from 8 plots in each forest type*burn severity treatment. Boxplots in **C** from Monte Carlo uncertainty propagation (see ''Methods''); line denotes median, box edges denote 25th and 75th percentiles, error bars denote 10th and 90th percentiles, and points denote 5th and 95th percentiles. Aboveground R_h includes all dead wood, shrubs, and herbaceous vegetation (Table 6). Soil R_h fractions from Irvine and others (2007). Lowercase letters denote statistically significant differences (Tukey-adjusted $P < 0.05$) among severities, tested with ANCOVA of each response variable given prefire biomass and burn severity.

mean or maximum soil depth among severities (Meigs 2009).

Our C pool estimates are consistent with previous estimates for PP in the Metolius area. Total aboveground C values for unburned and low-severity PP stands are similar to mature and young pine stands, respectively, whereas moderate- and high-severity stands fall between the values reported for initiation and young stands in a PP chronosequence (Law and others 2003). Our estimates of total ecosystem C in moderate- and high-severity PP stands are consistent with those reported by Irvine and others (2007). No analogous studies exist for the East Cascades MC forest type; the current study provides the first such estimates. The trends with burn severity were similar in both forest types, and the forest types differed consistently only in the magnitude of C pools. Total ecosystem C was 47% greater in MC forests than in PP forests (derived from Table 4).

Vegetation regeneration was generally robust but showed high variability and divergent responses of tree and non-tree functional types (Figure 4). Non-tree live biomass (that is, shrubs, forbs) was positively associated with burn severity, with significantly higher mass in high- versus low-severity stands ($P < 0.030$, Table 4, Figure 4). The strong shrub response—at or above prefire levels by 4–

5 years postfire—suggests important interactions with regenerating trees, which showed the opposite trend with burn severity. Tree seedling density (seedlings ha^{-1}) varied over 5 orders of magnitude (study wide range: 0–62,134) and, like shrub regeneration, was higher in MC than PP stands (Figure 4). This high variability is similar to studies of postfire conifer regeneration in the Klamath-Siskiyou and Rocky Mountain regions (5–6 orders of magnitude; Donato and others 2009b; Turner and others 2004), and the lack of PP regeneration in high-severity patches is consistent with previous studies reporting sparse regeneration beyond a generally short seed dispersal range (for example, Lentile and others 2005). Although regenerating vegetation represents a small C pool, it contributes to immediate postfire C uptake (described below) and sets the initial conditions for succession. The widespread presence of shrubs, particularly in high-severity stands, may initially reduce seedling growth through competition (Zavitkovski and Newton 1968), but over the long-term, understory shrubs play an important role in maintaining soil quality (C, N, microbial biomass C) in this ecoregion (Busse and others 1996). Because tree seedlings and shrubs were strongly correlated with overstory mortality, the burn severity mosaic could thus influence trajectories of C loss and accumulation for decades.

Postfire Carbon Balance (Biogenic C Fluxes and NEP)

Aboveground C Fluxes

Aboveground C fluxes followed the trends of live and dead C pools; NPP_A declined with increasing tree mortality (Figure 5A). In both forest types, NPP_A was significantly lower ($P < 0.015$) in high-severity versus moderate- and low-severity stands, which were not significantly different from each other ($P > 0.210$; overall range: 84–214 g C m^{-2} y^{-1}). Although NPP_A declined monotonically with burn severity, the sum of shrub and herbaceous NPP_A was about twofold higher in moderate- and high-severity versus low-severity stands, resulting in a dramatic increase in the non-tree proportion of NPP_A (Table 5). Thus, despite a reduction in live aboveground C of over 90% in both forest types in high-severity compared to low-severity stands, NPP_A was only 55% lower on average (Table 5). This trend, coupled with NPP_B (described below), resulted in a mean reduction of total NPP of about 40% from low- to high-severity, consistent with a strong compensatory effect of non-tree vegetation

Table 5. Annual Net Primary Productivity (NPP) of Burned Forest Stands in the Metolius Watershed

Forest type[1] / Burn severity	Aboveground				Belowground			Total NPP[7]	Non-tree[8] % of NPP_A	NPP_A:NPP_B ratio
	Tree[2]	Shrub	Herbaceous[3]	NPP_A[4]	Coarse root[2]	Fine root[5]	NPP_B[6]			
Mixed-conifer[1]	*93 (15)*	*20 (5)*	*46 (4)*	***159*** *(13)*	*18 (3)*	*132 (24)*	***150*** *(24)*	***309*** *(29)*	*42*	*1.06*
Low severity	$_{a}$173 (11)	8 (9)	33 (7)	$_{a}$**214** (15)	$_{a}$36 (3)	122 (44)	**159** (44)	**372** (47)	19	1.35
Mod severity	$_{b}$99 (11)	25 (9)	54 (7)	$_{a}$**178** (15)	$_{b}$18 (3)	151 (44)	**169** (43)	**347** (46)	44	1.05
High severity	$_{c}$12 (11)	27 (9)	51 (7)	$_{b}$**90** (15)	$_{c}$2 (3)	122 (44)	**125** (43)	**215** (46)	87	0.72
Ponderosa pine[1]	*68 (13)*	*10 (2)*	*57 (6)*	***135*** *(11)*	*10 (2)*	*96 (7)*	***107*** *(7)*	***242*** *(16)*	*50*	*1.26*
Low severity	$_{w}$135 (11)	3 (4)	$_{w}$34 (10)	$_{w}$**172** (15)	$_{w}$22 (2)	91 (13)	**113** (13)	$_{w}$**285** (24)	22	1.52
Mod severity	$_{x}$69 (12)	10 (4)	$_{x}$71 (10)	$_{w}$**151** (15)	$_{x}$9 (2)	101 (13)	**110** (13)	$_{wx}$**260** (24)	54	1.37
High severity	$_{y}$0 (0)	16 (4)	$_{wx}$68 (10)	$_{x}$**84** (15)	$_{y}$0 (0)	97 (13)	**97** (13)	$_{x}$**180** (24)	100	0.87

Notes: Values: mean NPP (g C m^{-2} y^{-1}). SE from ANCOVA in parentheses. Subscript letters indicate pairwise significant differences (Tukey-adjusted $P < 0.05$) between severities within each forest type. Summary fluxes bold.

[1] *Forest type row: italics denote values from burned stands only (n = 24; most NPP components not surveyed in unburned stands).*

[2] *Tree: sum of bole and foliage NPP_A. Coarse root NPP modeled from live tree DBH (6th column).*

[3] *Herbaceous: sum of graminoid and forb NPP_A, equal to dry mass.*

[4] *NPP_A: annual aboveground net primary productivity (bold, shown in Figure 4).*

[5] *Fine root NPP_B to 100 cm depth based on published turnover index (Andersen and others 2008) and total fine root mass scaled from 20 cm depth.*

[6] *NPP_B: annual belowground net primary productivity (bold, shown in Figure 4).*

[7] *Total NPP: sum of all above- and belowground fluxes entering the system (bold).*

[8] *Non-tree NPP_A: sum of shrub and herbaceous NPP_A.*

NPP_A. Previous studies in clearcut, thinned, and burned forests have shown the same pattern of rapid recolonization by non-trees contributing disproportionately to NPP (Campbell and others 2004; Gough and others 2007; Irvine and others 2007; Campbell and others 2009), and this study furthers the evidence across the severity gradient in two forest types. These findings suggest that fire studies focused solely on tree C pools (for example, Hurteau and others 2008) result in systematic biases and that C models and policies (for example, CCAR 2007) should encompass the full suite of ecosystem components and processes, including multiple vegetation functional types and rapid belowground recovery following disturbance.

Heterotrophic respiration of aboveground necromass (R_{hWD}), computed from C pools and decomposition constants, was a substantial component of C balance across both forest types but showed weak trends among severities (Figure 5B, Table 6). Despite the increase in dead wood mass with severity (Table 4), there were no significant differences in MC stands and only suggestive increases of R_{hWD} with severity in PP stands ($P = 0.031$–0.051). We attribute this surprising result to several factors: differing species- and decay class-specific constants and high variability among plots and severities; high retention and slow decomposition of snags; relatively high snag and dead shrub R_{hWD} in low-severity MC stands; relatively low CWD and dead shrub R_{hWD} in high-severity PP stands (Table 6). Although we expected that the immediate postfire period would exhibit maximum necromass over successional time (Wirth and others 2002; Hicke and others 2003), our R_{hWD} estimates were well less than both NPP_A and NPP_B ($R_{hWD} < 35\%$ of total NPP). In addition, R_{hWD} 4–5 years postfire constituted about 15% of total R_h across both forest types; R_{hsoil} (described below) accounted for approximately 85% (Table 6), demonstrating that belowground respiration processes are the predominant drivers of C loss.

Our range of R_{hWD} across the two forest types (28–75 g C m^{-2} y^{-1}; Table 6) is higher than estimates 2 years postfire in PP forest (Irvine and others 2007), similar to young PP stands in the Metolius area (Sun and others 2004) and an old-growth *Pseudotsuga-Tsuga* forest about 100 km away (Harmon and others 2004), and much less than untreated and thinned PP stands in Northern California (Campbell and others 2009). Our relatively low R_{hWD} estimates, particularly compared to C assimilation (NPP), illustrate the importance of decomposition lags in seasonally arid ecosystems, where microbial snag decomposition is moisture-limited. Other systems, such as sub-tropical humid zones where decomposition is not moisture- or temperature-limited and disturbance rapidly generates downed woody detritus (for example, hurricanes; Chambers and others 2007), may experience a more rapid pulse of C emission from necromass. The notion that fire-killed necromass represents a large, rapid C loss is unfounded, however, and warrants further investigation.

Woody detritus decomposition is a highly uncertain process, particularly in burned forests, where charring and snag fall play important, contrasting roles. For these R_{hWD} estimates, we used available decomposition constants derived from unburned forests. We believe that charring would likely reduce decomposition rates (DeLuca and Aplet 2008; Donato and others 2009a) but tested the sensitivity of our estimates by assuming snag decay rates equivalent to CWD. In this scenario, mean R_{hWD} would be approximately 125% and 50% higher in MC and PP stands, respectively, pushing low-severity stands into a net C source (negative NEP, although mean R_{hWD} would remain $<50\%$ of R_{hsoil} in both forest types). Our use of the 10% fraction is consistent with previous studies (Irvine and others 2007), and other studies have assumed zero snag decomposition (for example, Wirth and others 2002). Our short-term study precluded the assessment of snag fall, a stochastic process dependent on many factors (Russell and others 2006). The fall rates reported by Russell and others (2006)—snag half-lives for ponderosa pine and Douglas fir of 9–10 and 15–16 years, respectively—suggest that the majority of snags generated in the Metolius fires will stay standing for at least 10 years postfire. R_{hWD} may increase with accelerating snag fall (particularly in high-severity stands) but will remain small relative to R_{hsoil}, and NPP will likely increase over the same time period. Future studies are necessary to reduce the uncertainty of decomposition and snag dynamics in this area.

Belowground C Fluxes

Belowground C fluxes were by far the largest and most variable components of the annual C budget (NEP; Figure 5). Belowground NPP (NPP_B) was not significantly different across the entire study (overall mean: 284 g C m^{-2} y^{-1}; $P > 0.680$ in both forest types). Fine root NPP_B to 100 cm, based on total fine root mass and a constant turnover rate, accounted for about 90% of NPP_B, with increasing importance in high-severity stands, where very few live tree coarse roots survived. The apparent rapid establishment of fine roots in high-severity stands

Table 6. Annual Heterotrophic Respiration (R_h) and NEP of Forest Stands in the Metolius Watershed

Forest type[1] Burn severity	Aboveground (R_{hWD})						Belowground		Total R_h[7]	NEP[8]	NPP:R_h ratio[8]
	Snag[2]	Stump[2]	CWD[3]	Dead shrub	Herbaceous[4]	R_{hWD}[5]	R_{hsoil}[6]	R_{hsoil}:R_{soil} ratio[6]			
Mixed-conifer[1]	7 (1)	5 (1)	24 (4)	3 (2)	22 (2)	**61** (6)	*294* (*12*)	*na*	***357*** (*12*)	*−44* (*28*)	*0.87*
Unburned	3 (2)	7 (1)	29 (9)	1 (4)	19 (4)	**59** (12)	na (na)	na	**na** (na)	na (na)	na
Low severity	7 (2)	3 (1)	14 (9)	7 (4)	17 (4)	**47** (12)	305 (21)	0.48	**353** (20)	$_{a}$21 (48)	1.05
Mod severity	9 (2)	5 (1)	22 (9)	1 (4)	27 (4)	**64** (12)	261 (21)	0.52	**327** (19)	$_{a}$21 (55)	1.06
High severity	9 (2)	5 (1)	32 (9)	3 (4)	26 (4)	**75** (12)	314 (21)	0.56	**388** (19)	$_{b}$-174 (32)	0.55
Ponderosa pine[1]	2 (1)	3 (1)	9 (2)	2 (1)	26 (3)	**42** (3)	*274* (*15*)	*na*	***317*** (*17*)	*−76* (*20*)	*0.76*
Unburned	$_{w}$0 (1)	4 (1)	$_{w}$18 (3)	2 (2)	$_{w}$16 (4)	**$_{wx}$39** (6)	na (na)	na	**na** (na)	na (na)	na
Low severity	$_{wx}$1 (1)	3 (1)	$_{x}$5 (3)	2 (2)	$_{w}$17 (4)	**$_{w}$27** (6)	262 (28)	0.48	**290** (30)	$_{w}$0 (33)	0.98
Mod severity	$_{wx}$2 (1)	3 (1)	$_{wx}$8 (3)	4 (2)	$_{x}$36 (4)	**$_{x}$53** (6)	286 (28)	0.52	**338** (31)	$_{wx}$-87 (35)	0.77
High severity	$_{x}$5 (1)	3 (1)	$_{wx}$7 (3)	1 (2)	$_{x}$34 (4)	**$_{wx}$49** (6)	274 (28)	0.56	**324** (30)	$_{x}$-142 (37)	0.56

Notes: Values: mean R_h (g C m^{-2} y^{-1}). SE from ANCOVA in parentheses, except NEP SE from Monte Carlo. Subscript letters Indicate pairwise significant differences (Tukey-adjusted $P < 0.05$) between severities within each forest type. Summary fluxes bold.

[1]Forest type row: non-italics denote all stands (unburned and burned, n = 32); italics denote burned stands only (n = 24, unburned stands not surveyed [na]).

[2]Snag R_h uses 10% of CWD decay rate and stump R_h uses 100% of CWD decay rate.

[3]CWD R_h includes FWD R_h, which was less than 0.15% of CWD R_h in all treatments.

[4]Herbaceous: forb and graminoid combined (assumed 50% of dry mass).

[5]R_{hWD}: sum of aboveground components (bold). Includes herbaceous annual decomposition (50% of dry mass).

[6]R_{hsoil}: heterotrophic soil respiration, based on total soil efflux and heterotrophic fractions from Irvine and others (2007). Moderate severity fraction is mean of unburned and high severity fractions.

[7]Total R_h: sum of all above- and belowground fluxes from land to atmosphere (bold).

[8]Net ecosystem production: sum of NPP (Table 5) and R_h fluxes. SE from Monte Carlo uncertainty propagation. NPP:R_h ratio < 1 if negative NEP.

contributed to the strong NPP compensatory effect of non-tree vegetation (Table 5). NPP_B accounted for approximately 50% of total NPP averaged across all severities and forest types, but high-severity stands in both forest types exhibited higher NPP_B than NPP_A (NPP_B = 58 and 54% of total NPP in MC and PP, respectively), indicating belowground C allocation values between those reported for grasslands and shrublands (67 and 50%, respectively; Chapin and others 2002). These estimates of fine root NPP_B are very similar to those reported for moderate- and high-severity PP by Irvine and others (2007), even though that study accounted for fire-induced fine root mortality and computed fine root NPP from live rather than total fine root stocks. Our estimated FR NPP is higher than a thinned PP forest in Northern California (Campbell and others 2009) and lower than a mixed-deciduous forest in Michigan (Gough and others 2007). Our estimates of total NPP (approximately 200–400 g C m^{-2} y^{-1}) and NPP_A:NPP_B ratio (overall mean: 1.15; Table 5) are within the range of previous studies in the area (Law and others 2003; Campbell and others 2004) and consistent with the postfire C allocation patterns described by Irvine and others (2007).

Heterotrophic soil respiration (R_{hsoil}) was not significantly different among burn severities and forest types ($P > 0.200$; Figure 5B, Table 6), consistent with the trends of forest floor, fine roots, and soil C (Table 4). Mean annual R_{hsoil} (g C m^{-2} y^{-1}, ±1 SE from regression) was 294 ± 12 and 274 ± 15 in MC and PP stands, respectively, very similar to previous estimates in mature unburned PP stands (Law and others 2003; Sun and others 2004). The lack of R_{hsoil} differences among severity classes and similarity to unburned forest suggests that this flux is resistant to disturbance-induced changes in these forests and supports the findings of previous studies (Irvine and others 2007; Campbell and others 2009). R_{hsoil} chamber measurements 1 year postfire in a nearby high-severity PP site on the 2006 Black Crater fire (J. Martin, unpublished data) were similar to unburned PP forest (Irvine and others 2008) and the values in the current study, indicating the lack of a large R_{hsoil} pulse from 1–5 years postfire. Although we did not find evidence of this postfire pulse in the absolute magnitude of R_{hsoil}, the conservation of R_{hsoil} across severities, coupled with declines in NPP, resulted in a large decline of the NPP:R_h ratio (approximately 0.55 in high-severity stands, both forest types; Table 6). This increase in relative R_{hsoil} equated to a muted postfire pulse that is reflected in our NEP estimates.

Implications for NEP

In both forest types, NPP_A was the principal driver of NEP trends, whereas R_{hsoil} controlled NEP magnitudes (Figure 5, Table 6). NEP was significantly lower in high- versus low-severity stands in both forest types ($P < 0.035$). In MC stands, mean NEP (g C m^{-2} y^{-1}, ± 1 SE from Monte Carlo simulations) varied from a slight sink (21 ± 48 and 21 ± 55) in low- and moderate-severity stands to a substantial source in high-severity stands (−174 ± 32). In PP forest, mean NEP declined from C neutral in low-severity stands (0 ± 33) to an intermediate source in moderate-severity stands (−87 ± 35) and substantial source in high-severity stands (−142 ± 37). Thus, mean annual NEP was similar in high-severity stands of both forest types 4–5 years after fire. These results are consistent with previous estimates of NPP, R_h, and NEP in unburned, moderate-, and high-severity PP stands within the study area (Irvine and others 2007), although our NEP estimate for high-severity stands is lower.

Previous studies quantified a NEP recovery period to a net sink of 20–30 years in PP forest following stand-replacement clearcutting (Law and others 2003; Campbell and others 2004). Longer-term measurements are necessary to determine the NEP fate of these postfire stands, but less than 30 years seems appropriate for high-severity stands, which are already closer to zero than initiation stands described by Law and others (2003), despite the removal of necromass via timber harvest in that study and higher R_{hWD} estimates here. In both forest types, low-severity NEP was not significantly different from zero (error estimates include zero; Table 6, Figure 5), which may be explained by limited fire effects and/or relatively rapid recovery of NEP. Although not a large C source to the atmosphere, C neutral stands represent a substantial decline from prefire NEP (unburned PP mean ± 1 SE for a range of age classes: 50 ± 14 g C m^{-2} y^{-1}, Irvine and others 2007). Management actions that mimic low-severity fire via prescribed burning or thinning (thus removing C) will likely reduce short-term NEP and long-term average C storage (Campbell and others 2009; Mitchell and others 2009), although strategic fuels treatments may help stabilize large tree C pools (North and others 2009).

Conclusion

The 2002–2003 wildfires across the Metolius Watershed generated a heterogeneous landscape pattern of overstory tree mortality and associated transformations of C pools and fluxes. Our results

provide new constraints on short-term fire effects (4–5 years postfire) for regional C policy frameworks and underscore the importance of accounting for the full gradient of forest disturbance processes. Specifically, we found:

1. Stand-scale C combustion varied with burn severity from 13 to 35% of prefire aboveground C pools, with the largest emission proportion from combustion of surface/ground fuels and a study-wide average live tree stem consumption of 1.24%. Landscape-scale pyrogenic C emissions were equivalent to 2.5% of Oregon statewide anthropogenic CO_2 emissions from fossil fuel combustion and industrial processes for the same 2-year period.
2. Overstory live tree mass and seedling density decreased with increasing burn severity, whereas live shrub and herbaceous mass showed the opposite trend. From low- to moderate- to high-severity stands, average tree basal area mortality was 14, 49, and 100% in ponderosa pine, and 29, 58, and 96% in mixed-conifer forests.
3. Despite this decline in live aboveground C pools, total net primary productivity was only 40% lower in high- versus low-severity stands, reflecting a strong compensatory effect of nontree productivity. Thus, the rapid response of early successional vegetation offset declines in NPP and NEP, buffering potential fire impacts on stand and landscape C storage, particularly when combined with the protracted decomposition of dead mass and conservation of belowground components (soil C, R_{hsoil}, and NPP_B).

With predictions of accelerating climate change and increasing fire extent and severity in western North American forests (IPCC 2007; Balshi and others 2009; Miller and others 2009), long-term field measurements are essential to assess trends in C storage and net annual C uptake over the course of several fire cycles, as well as any potential for directional ecosystem responses over time (for example, state change). Because non-stand-replacement fire accounts for the majority of the annual burned area in the Pacific Northwest Region (Schwind 2008), studies that focus exclusively on high-severity patches systematically underestimate pyrogenic C emission, mortality, and reduced C uptake following fire, impacts that will likely play an increasingly important role in regional and global carbon cycling.

ACKNOWLEDGMENTS

This research was supported by the Office of Science (BER), U.S. Department of Energy, Grant No. DE-FG02-06ER64318 and the College of Forestry, Oregon State University. We thank A. Pfleeger, P. Bozarth-Dreher, L. Gupta, R. Gupta, C. Sodemann, and C. Hebel for field and lab assistance. We acknowledge the insightful reviews of W. Cohen, C. Dunn, F. Gonçalves, C. Hebel, P. Hessburg, J. Meigs, D. Turner, and two anonymous reviewers. M. Huso provided invaluable statistical assistance, and the OSU Central Analytical Laboratory performed thorough, efficient chemical analysis. M. Duane, K. Howell, T. Hudiburg, J. Irvine, R. Kennedy, R. Ottmar, S. Powell, S. Prichard, C. Sierra, C. Thomas, H. Zald, and the OSU Pyro-maniacs assisted with data analysis. G. Fiske and K. Olsen helped with Figure 1 cartography. We thank the Deschutes National Forest for GIS data and access to field sites.

REFERENCES

Amiro BD, Todd JB, Wotton BM, Logan KA, Flannigan MD, Stocks BJ, Mason JA, Martell DL, Hirsch KG. 2001. Direct carbon emissions from Canadian forest fires, 1959–1999. Can J For Res 31:512–25.

Andersen CP, Phillips DL, Rygiewicz PT, Storm MJ. 2008. Fine root growth and mortality in different-aged ponderosa pine stands. Can J For Res 38:1797–806.

Balshi MS, McGuire AD, Duffy P, Flannigan M, Walsh J, Melillo JM. 2009. Assessing the response of area burned to changing climate in western boreal North America using a Multivariate Adaptive Regression Splines (MARS) approach. Glob Change Biol 15:578–600.

Birdsey RA, Jenkins JC, Johnston M, Huber-Sannwald E, Amiro BD, de Jong B, Barra JDE, French NHF, Garcia-Oliva F, Harmon ME, Heath LS, Jaramillo VJ, Johnsen K, Law BE, Marín-Spiotta E, Masera O, Neilson R, Pan Y, Pregitzer KS. 2007. North American forests. In: King AW, Dilling L, Zimmerman GP, Fairman DM, Houghton RA, Marland G, Rose AZ, Wilbanks TJ, Eds. The first State of the Carbon Cycle Report (SOCCR): The North American carbon budget and implications for the global carbon cycle. A report by the U.S. Climate Change Science Program and the Subcommittee on Global Change Research. Asheville: National Oceanic and Atmospheric Administration National Climatic Data Center. p 117–26.

Bork BJ. 1985. Fire history in three vegetation types on the eastern side of the Oregon Cascades. PhD Thesis, Oregon State University. 94 p.

Bormann BT, Homann PS, Darbyshire RL, Morrissette BA. 2008. Intense forest wildfire sharply reduces mineral soil C and N: the first direct evidence. Can J For Res 38:2771–83.

Brown JK. 1974. Handbook for inventorying downed woods material. USDA Forest Service General Technical Report INT-GTR-16. Ogden.

Busse MD, Cochran PH, Barren JW. 1996. Changes in ponderosa pine site productivity following removal of understory vegetation. Soil Sci Soc Am J 60:1614–21.

Campbell JL, Alberti G, Martin JG, Law BE. 2009. Carbon dynamics of a ponderosa pine plantation following a thinning treatment in the northern Sierra Nevada. For Ecol Manag 257:453–63.

Campbell JL, Donato DC, Azuma DL, Law BE. 2007. Pyrogenic carbon emission from a large wildfire in Oregon, United States. J Geophys Res 112:G04014.

Campbell JL, Law BE. 2005. Forest soil respiration across three climatically distinct chronosequences in Oregon. Biogeochemistry 73:109–25.

Campbell JL, Sun OJ, Law BE. 2004. Disturbance and net ecosystem production across three climatically distinct forest landscapes. Glob Biogeochem Cycles 18.

CCAR. 2007. Forest sector protocol version 2.1. California Climate Action Registry (CCAR). http://www.climateregistry.org/tools/protocols/industry-specific-protocols.html.

Chambers JQ, Fisher JI, Zeng HC, Chapman EL, Baker DB, Hurtt GC. 2007. Hurricane Katrina's carbon footprint on U. S. Gulf Coast forests. Science 318:1107.

Chapin FSIII, Matson PA, Mooney HA. 2002. Principles of terrestrial ecosystem ecology. New York: Springer.

Chapin FSIII, Woodwell GM, Randerson JT, Rastetter EB, Lovett GM, Baldocchi DD, Clark DA, Harmon ME, Schimel DS, Valentini R, Wirth C, Aber JD, Cole JJ, Goulden ML, Harden JW, Heimann M, Howarth RW, Matson PA, McGuire AD, Melillo JM, Mooney HA, Neff JC, Houghton RA, Pace ML, Ryan MG, Running SW, Sala OE, Schlesinger WH, Schulze ED. 2006. Reconciling carbon-cycle concepts, terminology, and methods. Ecosystems 9:1041–50.

Chen H, Harmon ME, Sexton JM, Fasth B. 2002. Fine-root decomposition and N dynamics in coniferous forests of the Pacific Northwest, USA. Can J For Res 32:320–31.

Cline SP, Berg AB, Wight HM. 1980. Snag characteristics and dynamics in Douglas-fir forests, western Oregon. J Wildlife Manag 44:773–86.

Daly C, Gibson WP, Taylor GH, Johnson GL, Pasteris P. 2002. A knowledge-based approach to the statistical mapping of climate. Clim Res 22:99–113.

DAYMET. 2009. Distributed climate data, http://www.daymet.org/.

DeLuca TH, Aplet GH. 2008. Charcoal and carbon storage in forest soils of the Rocky Mountain West. Front Ecol Environ 6:18–24.

Donato DC, Campbell JL, Fontaine JB, Law BE. 2009a. Quantifying char in postfire woody detritus inventories. Fire Ecol 5(2):104–115.

Donato DC, Fontaine JB, Campbell JL, Robinson WD, Kauffman JB, Law BE. 2009b. Early conifer regeneration in stand-replacement portions of a large mixed-severity wildfire in the Siskiyou Mountains, Oregon. Can J For Res 39:823–38.

Dore S, Kolb TE, Montes-Helu M, Sullivan BW, Winslow WD, Hart SC, Kaye JP, Koch GW, Hungate BA. 2008. Long-term impact of a stand-replacing fire on ecosystem CO_2 exchange of a ponderosa pine forest. Glob Change Biol 14:1801–20.

Eyre FH, Eds.1980. Forest cover types of the United States and Canada. Society of American Foresters, Washington, DC.

Fitzgerald SA. 2005. Fire ecology of ponderosa pine and the rebuilding of fire-resilient ponderosa pine ecosystems. In: Proceedings of the symposium on ponderosa pine: issues, trends, and management. USDA Forest Service General Technical Report PSW-GTR-198, 18–21 October 2004, Klamath Falls, OR, Albany.

Franklin JF, Dyrness CT. 1973. Natural vegetation of Oregon and Washington. USDA Forest Service General Technical Report PNW-GTR-8. Portland.

Franklin SE, Waring RH, McCreight RW, Cohen WB, Fiorella M. 1995. Aerial and satellite sensor detection and classification of western spruce budworm defoliation in a subalpine forest. Can J Remote Sens 21:299–308.

French NHF, Kasischke ES, Hall RJ, Murphy KA, Verbyla DL, Hoy EE, Allen JL. 2008. Using Landsat data to assess fire and burn severity in the North American boreal forest region: an overview and summary of results. Int J Wildland Fire 17:443–62.

Goward SN, Masek JG, Cohen WB, Moisen G, Collatz GJ, Healey SP, Houghton RA, Huang C, Kennedy RE, Law BE, Powell SL, Turner DP, Wulder MA. 2008. Forest disturbance and North American carbon flux Eos, transactions. Am Geophys Union 89:105–16.

Gough CM, Vogel CS, Harrold KH, George K, Curtis PS. 2007. The legacy of harvest and fire on ecosystem carbon storage in a north temperate forest. Glob Change Biol 13:1935–49.

Harmon ME, Bible K, Ryan MG, Shaw DC, Chen H, Klopatek J, Li X. 2004. Production, respiration, and overall carbon balance in an old-growth *Pseudotsuga-tsuga* forest ecosystem. Ecosystems 7:498–512.

Harmon ME, Fasth B, Sexton JM. 2005. Bole decomposition rates of seventeen tree species in Western U.S.A.: a report prepared for the Pacific Northwest Experiment Station, the Joint Fire Sciences Program, and the Forest Management Service Center of WO Forest Management Staff. http://andrewsforest.oregonstate.edu/pubs/webdocs/reports/decomp/cwd_decomp_web.htm.

Harmon ME, Sexton JM. 1996. Guidelines for measurements of woody detritus in forest ecosystems. U.S. long term ecological research program network, vol. 20. Albuquerque.

Hessburg PF, Salter RB, James KM. 2007. Re-examining fire severity relations in pre-management era mixed conifer forests: inferences from landscape patterns of forest structure. Landsc Ecol 22:5–24.

Hicke JA, Asner GP, Kasischke ES, French NHF, Randerson JT, Collatz GJ, Stocks BJ, Tucker CJ, Los SO, Field CB. 2003. Postfire response of North American boreal forest net primary productivity analyzed with satellite observations. Glob Change Biol 9:1145–57.

Hudiburg T. 2008. Climate, management, and forest type influences on carbon dynamics of West-Coast US forests. M.S. Thesis, Oregon State University. 86 p.

Hudiburg T, Law BE, Turner DP, Campbell JL, Donato DC, Duane M. 2009. Carbon dynamics of Oregon and Northern California forests and potential land-based carbon storage. Ecol Appl 19:163–80.

Hurteau MD, Koch GW, Hungate BA. 2008. Carbon protection and fire risk reduction: toward a full accounting of forest carbon offsets. Front Ecol Environ 6:493–8.

IPCC. 2007. Climate change 2007: the physical science basis. In: Solomon S, Qin D, Manning M, Chen Z, Marquis M, Averyt KB, Tignor M, Miller HL, Eds. Contribution of working group I to the fourth assessment report of the intergovernmental panel on climate change (IPCC). Cambridge University Press, Cambridge, United Kingdom and New York. http://www.ipcc.ch.

Irvine J, Law BE, Hibbard KA. 2007. Postfire carbon pools and fluxes in semiarid ponderosa pine in Central Oregon. Glob Change Biol 13:1748–60.

Irvine J, Law BE, Martin JG, Vickers D. 2008. Interannual variation in soil CO_2 efflux and the response of root respiration to climate and canopy gas exchange in mature ponderosa pine. Glob Change Biol 14:2848–59.

Kashian DM, Romme WH, Tinker DB, Turner MG, Ryan MG. 2006. Carbon storage on landscapes with stand-replacing fires. Bioscience 56:598–606.

Keane RE, Agee JK, Fulé P, Keeley JE, Key C, Kitchen SG, Miller R, Schulte LA. 2008. Ecological effects of large fires on US landscapes: benefit or catastrophe? Int J Wildland Fire 17:696–712.

Key CH, Benson NC. 2006. Landscape assessment: Ground measure of severity, the Composite Burn Index; and remote sensing of severity, the Normalized Burn Ratio. In Lutes DC, et al, Eds. FIREMON: Fire effects monitoring and inventory system. USDA Forest Service General Technical Report RMRS-GTR-164-CD. Fort Collins.

Kurz WA, Stinson G, Rampley GJ, Dymond CC, Neilson ET. 2008. Risk of natural disturbances makes future contribution of Canada's forests to the global carbon cycle highly uncertain. Proc Natl Acad Sci USA 105:1551–5.

Law BE, Arkebauer T, Campbell JL, Chen J, Sun O, Schwartz M, van Ingen C, Verma S. 2008. Terrestrial carbon observations: Protocols for vegetation sampling and data submission. Report 55, Global Terrestrial Observing System. FAO, Rome. 87 pp.

Law BE, Ryan MG, Anthoni PM. 1999. Seasonal and annual respiration of a ponderosa pine ecosystem. Glob Change Biol 5:169–82.

Law BE, Sun OJ, Campbell JL, Van Tuyl S, Thornton PE. 2003. Changes in carbon storage and fluxes in a chronosequence of ponderosa pine. Glob Change Biol 9:510–24.

Law BE, Thornton PE, Irvine J, Anthoni PM, Van Tuyl S. 2001a. Carbon storage and fluxes in ponderosa pine forests at different developmental stages. Glob Change Biol 7:755–77.

Law BE, Van Tuyl S, Cescatti A, Baldocchi DD. 2001b. Estimation of leaf area index in open-canopy ponderosa pine forests at different successional stages and management regimes in Oregon. Agric For Meteorol 108:1–14.

Law BE, Waring RH. 1994. Combining remote sensing and climatic data to estimate net primary production across Oregon. Ecol Appl 4:717–28.

Lentile LB, Smith FW, Shepperd WD. 2005. Patch structure, fire-scar formation, and tree regeneration in a large mixed-severity fire in the South Dakota Black Hills, USA. Can J For Res 35:2875–85.

Martin RE, Sapsis DB. 1991. Fires as agents of biodiversity: pyrodiversity promotes biodiversity. In: Harris RR, Erman DE, Kerner HM (technical coordinators), Eds. Proceedings of the symposium on biodiversity of northwestern California. Santa Rosa, CA: Wildland Resources Center, pp. 150–7.

Maser C, Anderson RG, Cromack Jr K, Williams JT, Martin RE. 1979. Dead and down woody material. Wildlife habitats in managed forests of the Blue Mountains of Oregon and Washington, USDA Forest Service Agriculture Handbook No. 553.

McIver JD, Ottmar RD. 2007. Fuel mass and stand structure after post-fire logging of a severely burned ponderosa pine forest in northeastern Oregon. For Ecol Manag 238:268–79.

Meigs GW. 2009. Carbon dynamics following landscape fire: influence of burn severity, climate, and stand history in the Metolius Watershed, Oregon. M.S. Thesis, Oregon State University. 147 p.

Miller JD, Safford HD, Crimmins M, Thode AE. 2009. Quantitative evidence for increasing forest fire severity in the Sierra Nevada and Southern Cascade Mountains, California and Nevada, USA. Ecosystems 12:16–32.

Mitchell SR, Harmon ME, O'Connell KEB. 2009. Forest fuel reduction alters fire severity and long-term carbon storage in three Pacific Northwest ecosystems. Ecol Appl 19:643–55.

Monsanto PG, Agee JK. 2008. Long-term post-wildfire dynamics of coarse woody debris after salvage logging and implications for soil heating in dry forests of the eastern Cascades, Washington. For Ecol Manag 255:3952–61.

North M, Hurteau M, Innes J. 2009. Fire suppression and fuels treatment effects on mixed-conifer carbon stocks and emissions. Ecol Appl 19:1385–96.

Ottmar RD, Sandberg DV, Riccardi CL, Prichard SJ. 2007. An overview of the fuel characteristic classification system—quantifying, classifying, and creating fuelbeds for resource planning. Can J For Res 37:2383–93.

Pierce LL, Running SW. 1988. Rapid estimation of coniferous forest leaf-area index using a portable integrating radiometer. Ecology 69:1762–7.

Prichard SJ, Ottmar RD, Anderson GK. 2006. Consume 3.0 user's guide. Pacific Wildland Fire Sciences Laboratory, USDA Forest Service, Pacific Northwest Research Station. Seattle, WA. http://www.fs.fed.us/pnw/fera/research/smoke/consume/index.shtml.

Rorig ML, Ferguson SA. 1999. Characteristics of lightning and wildland fire ignition in the Pacific Northwest. J Appl Meteorol 38:1565–75.

Roy DR, Boschetti L, Trigg SN. 2006. Remote sensing of fire severity: assessing the performance of the normalized burn ratio. IEEE Geosci Remote Sens Lett 3:112–6.

Running SW. 2008. Ecosystem disturbance, carbon, and climate. Science 321:652–3.

Russell RE, Saab VA, Dudley JG, Rotella JJ. 2006. Snag longevity in relation to wildfire and postfire salvage logging. For Ecol Manag 232:179–87.

Santantonio D, Hermann RK, Overton WS. 1977. Root biomass studies in forest ecosystems. Pedobiologia 17:1–31.

Savage M, Mast JN. 2005. How resilient are southwestern ponderosa pine forests after crown fires? Can J For Res 35:967–77.

Schoennagel T, Veblen TT, Romme WH. 2004. The interaction of fire, fuels, and climate across Rocky Mountain forests. Bioscience 54:661–76.

Schwind B. 2008. Monitoring trends in burn severity: report on the Pacific Northwest and Pacific Southwest fires—1984 to 2005. Available online: http://mtbs.gov.

Simon SA. 1991. Fire history in the Jefferson Wilderness area of east of the Cascade Crest. A final report to the Deschutes National Forest Fire Staff.

Soeriaatmadhe RE. 1966. Fire history of the ponderosa pine forests of the Warm Springs Indian Reservation Oregon. PhD Thesis, Oregon State University.

Sun OJ, Campbell JL, Law BE, Wolf V. 2004. Dynamics of carbon stocks in soils and detritus across chronosequences of different forest types in the Pacific Northwest, USA. Glob Change Biol 10:1470–81.

Swedberg KC. 1973. A transition coniferous forest in the Cascade Mountains of Northern Oregon. Am Midl Nat 89:1–25.

Thomas CK, Law BE, Irvine J, Martin JG, Pettijohn JC, Davis KJ. 2009. Seasonal hydrology explains inter-annual and seasonal variation in carbon and water exchange in a semi-arid mature ponderosa pine forest in Central Oregon. J Geophys Res Biogeosci. doi:10.1029/2009JG001010.

Thompson JR, Spies TA, Ganio LM. 2007. Reburn severity in managed and unmanaged vegetation in a large wildfire. Proc Natl Acad Sci USA 104:10743–8.

Thornton PE, Running SW, White MA. 1997. Generating surfaces of daily meteorological variables over large regions of complex terrain. J Hydrol 190:214–51.

Turner DP, Ritts WD, Law BE, Cohen WB, Yang Z, Hudiburg T, Campbell JL, Duane M. 2007. Scaling net ecosystem production and net biome production over a heterogeneous region in the western United States. Biogeosciences 4:597–612.

Turner MG, Tinker DB, Romme WH, Kashian DM, Litton CM. 2004. Landscape patterns of sapling density, leaf area, and aboveground net primary production in postfire lodgepole pine forests, Yellowstone National Park (USA). Ecosystems 7:751–75.

USDA. 2003. Field instructions for the annual inventory of Washington, Oregon, and California Forest Inventory and Analysis Program. USDA Forest Service Pacific Northwest Research Station. Portland.

Van Tuyl S, Law BE, Turner DP, Gitelman AI. 2005. Variability in net primary production and carbon storage in biomass across Oregon forests: an assessment integrating data from forest inventories, intensive sites, and remote sensing. For Ecol Manag 209:273–91.

Van Wagner CE. 1968. The line intersect method in forest fuel sampling. For Sci 14:20–6.

Weaver H. 1959. Ecological changes in the ponderosa pine forest of the Warm Springs Indian Reservation in Oregon. J For 57:15–20.

Westerling AL, Hidalgo HG, Cayan DR, Swetnam TW. 2006. Warming and earlier spring increase western US forest wildfire activity. Science 313:940–3.

Wirth C, Czimczik CI, Schulze ED. 2002. Beyond annual budgets: carbon flux at different temporal scales in fire-prone Siberian Scots pine forests. Tellus B Chem Phys Meteorol 54:611–30.

Zavitkovski J, Newton M. 1968. Ecological importance of snowbrush *Ceanothus velutinus* in the Oregon Cascades. Ecology 49:1134–45.

ENVIRONMENTAL RESEARCH
CLIMATE

The drivers and predictability of wildfire re-burns in the western United States (US)

To cite this article before publication: Kurt C Solander *et al* 2023 *Environ. Res.: Climate* in press https://doi.org/10.1088/2752-5295/acb079

The drivers and predictability of wildfire re-burns in the western United States (US)

Solander, K.C.[1]*, Talsma, C.J.[1,2], Vesselinov, V.V.[1,2]

[1] Los Alamos National Laboratory, Los Alamos, NM 87545 USA

[2] Carbon Solutions LLC, Okemos, MI 48864, USA

*Corresponding author ksolander@lanl.gov

Keywords

Monitoring Trends in Burned Severity (MTBS), Wildland Urban Interface (WUI), Machine Learning (ML), wildfire re-burns

Abstract

Evidence is mounting that the effectiveness of using prescribed burns as a management tactic may be diminishing due to the higher incidence of wildfire re-burns. The development of predictive models of re-burns is thus essential to better understand their primary drivers so that forest management practices can be updated to account for these events. First, we assess the potential for human activity as a driver of re-burns by evaluating re-burn trends both within and outside of the Wildland Urban Interface (WUI) of the western US. Next, we investigate the predictability of re-burns through the application of both Random Forest and the explanatory Machine Learning (ML) Non-Negative Matrix Factorization using K-means clustering (NMFk) algorithms to predict re-burn occurrence over California based on a number of climate factors. Our findings indicate that while most states showed increasing trends within the WUI when trends were conducted over longer moving windows (e.g., 20 years), California was the only state where the rate of increase was consistently higher in the WUI, indicating a stronger

potential for human activity as a driver in that location. Furthermore, we find model performance was found to be robust over most of California (Testing F1 scores=0.688), although results were highly variable based on EPA level III ecoregion (F1 scores = 0.0-0.778). Insights provided from this study will lead to a better understanding of climate and human activity drivers of re-burns and how these vary at broad spatial scales so that improvements in forest management practices can be tuned according to the level of change that is expected for a given region.

Introduction

Wildfire re-burns can be thought of as the area of overlap between burn area perimeters of multiple wildfires that occurred over some time interval. In the western continental United States (US), re-burns have been found to be fairly widespread, with over 7.6% of wildland forests having burned multiple times between 1984 and 2016 (Buma et al., 2020). Over longer timescales (e.g., 10-25 years), re-burns have been found to be increasing just as rapidly as single-burn wildfires. The increased occurrence of re-burns as an agent of change across western US landscapes suggests that they will continue to be an important part of ecosystem functioning, and more work must be done to improve their understanding so forest management practices can be updated as appropriate.

Re-burns tend to have exacerbated impacts on ecosystem function relative to single burn wildfires due to the inability of vegetation and animal species to adapt to higher-frequency wildfires (Walker et al., 2018). For example, re-burns have caused an increase in conversion of forests to shrubs or grasslands in both the western US (Buma et al., 2020) and Patagonia (Paritsis et al., 2013) regions. The higher fire return intervals brought on by re-burns are expected to substantially change forest age structure and composition (Hart et al., 2018) as well as lead to failures in re-seeding (Buma et al., 2013; Bowman et al., 2014; Stevens-Rumann and Morgan,

2019). Given that the warmer and drier climate expected for much of the western US is already hampering the ability of trees to re-seed, re-burns will likely exacerbate these effects and further changes in forest structure and dynamics (Enright et al., 2015; Halofsky et al., 2020). Re-burns have reduced the capacity for tree regeneration, causing a delay in aboveground carbon stores and thus have the potential to result in additional major changes in forest structure and function. Already, the ability of trees to undergo epicormic or basal resprouting has been diminished due to re-burning, leading to greater forest structure vulnerabilities following a wildfire (Fairman et al., 2018).

Given the substantial number of impacts that re-burns have had on ecosystem structure and function, a number of studies have begun to investigate the primary vegetative and climatic drivers of re-burns. For instance, a Random Forest model identified mean daytime temperature, relative humidity and shrub cover as being the most important predictors of re-burn severity in forest plots located in northern California (Coppoletta et al., 2016). Vegetation was found to have a stronger control on re-burn severity than weather conditions at longer timescales (e.g., >19-years) for sites in the Klamath Mountains ecoregion of northern California (Grabinski et al., 2017). Extreme warm and dry months were found to be consistently associated with higher re-burn severity and maximum temperature was found to explain the greatest variance in re-burn severity for re-burns with shorter return intervals (e.g., 2-14 years, Parks et al., 2014). In addition, vegetation characteristics such as the occurrence of snags, logs and dense, low-lying shrubs were determined to provide ideal conditions for high re-burn severity.

Across larger spatial scales, different climatic and vegetative controls on fire return intervals likely play a role in the spatial variability of the occurrence of re-burns. For example, the highest concentration of re-burns was found to be located in southern California and the southwestern

desert mountains, as well as the northern Rocky Mountains of Idaho (Buma et al., 2020). However, the higher occurrence of re-burns in these regions may not be driven by the same features. The Idaho portion of the Rockies is characterized by the largest increase in area burned, where large burn years are typically preceded by months of drought; whereas large burn years in the hotter and drier southwest are often preceded by months of elevated moisture that promote the build-up of fine fuels (Littell et al., 2009). These spatial differences suggest that while re-burns in dry climates may be precipitated by a period of elevated moisture (e.g., fueled by an uptick in fuels), those in moist climates are precipitated by longer periods of drought (e.g., fueled by a drop in moisture). These spatial differences are known to play out in fire return intervals, which are strongly related to re-burns. For example, the fire return interval in the hot and dry southwest US is estimated at 15-years, while this number more than doubles to 33-years in Montana and boreal forests of Canada where conditions of elevated moisture tend to persist longer to prevent new fire ignitions (Parks et al., 2018). This finding points to how the immunity of the landscape to wildfires is much greater in forests where moisture limitations tend to be less frequent.

Although the aforementioned studies have investigated a number of possible drivers of re-burns and their spatial variability to quantify their importance for specific plots to the sub-region scale, there has been little research on quantifying the impact of multiple drivers to investigate their importance for re-burns over larger regions. First, to better understand the role of humans in the occurrence of re-burns, we investigate the difference in the magnitude of trends in re-burns throughout the western US and compare this with the same trends that occur within the Wildland Urban Interface (WUI). Although re-burn trends have been comprehensively explored in a previous study (e.g., Buma et al., 2020), this investigation only included re-burns that occurred in

wildland forests and thus the potential role of humans in these trends was largely omitted. Further consideration of the human component is necessary given the prevalence of human-caused wildfires in the western US (Balch, 2017). Next, we combine a gridded dataset of climate and environmental variables with machine learning (ML) techniques to investigate the importance of multiple climate variables as a predictor. Although numerous studies have explored the relationships between climate and wildfire over large areas (Litell, et al., 2009; Abatzoglou and Kolden, 2013; Williams et al., 2019) here, we strive to explore these relationships specifically for re-burns. The model is tested over California due to the higher frequency of re-burns observed in this state (Buma et al., 2020). Model performance is further tested over the US Environmental Protection Agency (EPA) Level III Ecoregions given the diversity of ecosystems and climate in this area that are likely to explain a high degree of differences in model performance.

Methods

Re-burns are calculated using the Landsat-based Monitoring Trends in Burn Severity (MTBS) data product, which is maintained and updated by the US Geological Survey Center for Earth Resources Observation and Science (EROS) and the USDA Forest Service Geospatial Technology and Applications Center (GTAC). The MTBS was established in 2006 to evaluate the location, extent and severity of wildfires using Landsat-based estimates of wildfire burn areas. Initially, MTBS was based exclusively on the differenced Normalized Burn Ratio (dNBR), but has since been expanded to include the Relativized dNBR, which is an estimate of the relative magnitude of change and removes the bias associated with pre-fire vegetation conditions (Miller and Thode, 2007). As of October 2019, the MTBS dataset included 22,969 fires. Within

the western United States, this dataset consists of only fires above 405 ha and does not include prescribed fires (Picotte et al., 2020).

Previous studies have indicated that errors due to the incorrect inclusion of pixels into MTBS that were not actually burned were found to be 15-18% of the total surface area, while errors of exclusion of pixels that were actually burned range anywhere from 0-45% of the total surface area (Piccote et al., 2020). These errors tend to result due to differences in the time since wildfire occurred versus the time when the satellite image was generated (Picotte and Robertson, 2010), terrain complexity (Kolden and Weisberg, 2007) and vegetation composition (Vanderhoof et al., 2017). In spite of these issues with misclassification, MTBS still represents the longest spatially comprehensive, high resolution, remote sensing-based fire history mapping dataset that is available for the western US (Buma et al., 2020). Given these characteristics, MTBS data were deemed to be ideal for training the ML models and conducting the trend analysis that was used in this study.

Re-burn areas were calculated for the 11 states that comprise the continental western US for each year by finding the intersection of wildfire burn perimeters obtained from MTBS during 1984-2018. The resulting data product displays the total wildfire re-burn perimeters across the western US. No distinction was made for how many times a given area re-burned (e.g., two times versus more than two times), given that areas that burn more than two times occur at a far lower rate than areas that burn only twice and thus would be difficult to extract meaningful information on climate drivers or trends for areas that burned greater than two times (Buma et al., 2020). As such, an area that burned multiple times was simply reported as a re-burn area.

The trend analysis was conducted by aggregating all the re-burn perimeter data by area per year for the 11 western US states. Data were then binned into 5- 10- and 20-year moving

windows and trends were estimated over the resulting data using the Mann-Kendall trend analysis for detecting monotonic trends (Mann, 1945; Kendall, 1975). The statistical significance ($p < 0.05$) of the trends for each of the three moving windows within each state was reported. For this calculation, the adjusted p-value based on an effective sample size to account for autocorrelation was used (Hamed and Rao, 1998). This sequence of steps was then repeated for only those re-burns that occurred within the Wildland Urban Interface (WUI) of each state, which was assumed to include both intermix and interface WUI. Intermix WUI is represented by those areas with a housing density greater than 6.17 houses per km^2 and at least 50% of the area is covered by wildland vegetation. Interface WUI represents areas with higher settlement densities and less than 50% wildland vegetation coverage that also lie within at least 2.4 km of heavily forested areas (e.g., areas with greater than 75% wildland vegetation covering more than 5 km^2) (Radeloff et al., 2018).

Climate drivers in California for use in the ML algorithms were derived using gridded, near-surface climate variables that included monthly and annual values of canopy moisture, soil moisture, precipitation, runoff, snow water equivalent (SWE), max temperature, min temperature, wind speed, and total evapotranspiration (Livneh et al., 2013). These data were derived from 20,000 National Oceanic and Atmospheric Administration (NOAA) Cooperative Observer (COOP) stations, as well as models and algorithms. The latest version of the data represents an update to an earlier version (Maurer et al., 2002) that includes increased spatial resolution to $1/16^{th}$ °, an extended period of analysis and an updated version of the Variable Infiltration Capacity (VIC) model to estimate hydrologic variables such as SWE. Comparisons of the two data products were found to be largely consistent, with main differences occurring over mountainous areas of the western United States. The data has been applied to a wide range of

studies used to assess water and energy budgets, droughts and climate change assessments (Livneh et al., 2013).

Additionally, we used historical Global Climate Model (GCM) output that was downscaled to 4-km using Multivariate Adaptive Constructed Analogs (MACA) (Abatzoglou and Brown, 2012). The GCM used in this simulated dataset consisted of the bcc-csm1-1m model (Taylor et al., 2012) from the CMIP5 suite of simulations (Zhou et al., 2014). This data included annual maximum temperature, minimum temperature, wind speed, and precipitation fields and was used given the potential to use projected climate data for future work. In recognition that there is no temporal correspondence between the GCM simulated data and re-burn occurrence and because we only attempted to predict the entire set of re-burns that occurred over the 1984-2018 observation period, annual means of these data were used to predict the occurrence of re-burns over the 35-year observation period. By including the historical simulated data from the GCM along with the meteorological station derived data that largely consisted of the same variables, our aim is to showcase the delta between the two. Prior to implementation in the NMFk algorithm, the MACA-derived GCM data was resampled to the larger spatial scale of the Livneh et al. (2013) dataset for use in this study. A summary of the data parameters, sources, and resolutions can be found in Table 1.

Prominent climate drivers contributing to re-burns were determined using the unsupervised machine learning algorithm Non-Negative Matrix Factorization using K-means clustering (NMFk) (Alexandrov and Vesselinov, 2014). NMFk is a blind source separation technique for the automated extraction of signals present in complex data. NMFk works through decomposing a data matrix X into a feature matrix W $\in R^{n \times k}$ and a mixing matrix $H \in R^{k \times m}$ such that $X = W \times H$. In our application m is the number of grid-cells and n is the number of

climate, hydrologic and wildfire-based input parameters we are using as inputs to NMFk. The matrix deconstruction process is able to extract an identifiable number of signals, *k*, within the data that can be used to reconstruct the original data when multiplied by the mixing matrix *H,* which provides weights to each parameter based on their importance to each signal. NMFk solves for different solutions sets for different values of k ranging from 2 to a user-defined value of d. K-means clustering is then used to determine how well a set of extracted features, *k,* is at accurately describing the original data based on several statistical measures. These measures include robustness, which is the degree to which a model performs as well when using new data versus training data; as well as the cluster silhouette, which measures how similar an object is to its own cluster. The solution clusters are obtained by executing the NMFk analyses with multiple random initial guesses, which was set to 1,000 for our purposes. One of the novelties of NMFk is the ability to automatically estimate the optimal number of signals (K^{opt}) present in the data using k-means clustering.

Here, we first apply NMFk to categorize the main climate and hydrologic signals present in California and how they relate to the re-burned areas as determined by the MTBS dataset. We include the MACA-derived climate data (temperature, precipitation, wind), the Livneh et al. (2013) climate and hydrologic data (Evapotranspiration, streamflow, runoff, rainfall, SWE, etc.), and the MTBS data as inputs to the NMFk algorithm. For this analysis, the MTBS re-burn data were resampled to a common $1/16^{th}$ ° resolution by calculating the percent area re-burn within the larger grid cell over the entire study period (e.g., 1984-2018), creating the parameter "mtbs_weights" discussed below. Additionally, we computed basic statistics (mean, maximum, minimum, standard deviation, quartiles) for each variable, which are then added to the input dataset along with the raw climate data. Each feature of the input data is normalized between 0

and 1 to enable the NMFk algorithm to decompose the input data into constituent signals, which are subsequently assigned weights for each input feature. The MTBS re-burn weights were enhanced by a factor of 7 to strengthen the separation of signals that are influenced by re-burns. Through iteration, we found that a factor of 7 was large enough to separate a distinct re-burn signal, but not so large that other factors were not included in that signal. This allows us to develop a re-burn signal that includes other input parameters that contribute to that signal as well as what climate and hydrologic signals are not seen as contributing to re-burns.

Next, the NMFk algorithm was applied to the climate dataset only in locations where re-burns have occurred according to the MTBS dataset. This allows determination of how climate drivers differ exclusively among re-burn events. Application of the NMFk algorithm to climate data co-located with re-burns proceeded in the same way in which it is described in the previous paragraph when applied to climate data over all of California.

In addition to the NMFk algorithm, a Random Forest classification model was used to predict re-burn areas across California over the entire study period (1984-2018) using the same climate datasets mentioned previously as inputs. Random Forest classification models work by partitioning model predictions into a series of decision trees, the depth and number of which are controlled by model hyperparameters, which are tuned prior to training the algorithm. Model outcomes are arrived at from taking the mean of output from individual trees. These outcomes are used to establish which features are the most important for model prediction. Random Forest models are effective at using complex data to model non-linearities and develop robust classification trees. Additionally, support vector machine models were used to classify the re-burned areas with limited success. Thus, we present only the Random Forest results for simplicity. The US Environmental Protection Agency (EPA) Level III Ecoregions of California

were used as additional inputs so the model performance could be evaluated across these subregions. Each region was one-hot encoded as a 1 or 0 for incorporation into the model input dataset. The model was trained using 70% of the California spatial data where the calculated MTBS re-burns (non-weighted) were used as the target variable. Unlike NMFk, which automatically detects the number of features present in the data, Random Forest imposes no such limits. However, we down-selected to the 200 most important features, which were used to train a new model on the same data to reduce overfitting. Additionally, model hyperparameters (e.g. number of estimators, minimum samples split, minimum sample leafs, maximum depth) were tuned by randomly selecting from an appropriate range of hyperparameters and then iteratively fitting the data using Kfold cross-validation with 3 folds within the training data. We performed 20 separate fits using different hyperparameter arrangements to determine the hyperparameter values based on the resulting F1-score. The F1-score was reported as the primary performance metric along with the sensitivity and precision scores.

Results

The 1984-2018 re-burns for the 11 western US states are shown in Figure 1. The total area covered by re-burns in the western US was 89,026 km^2, which represents 3.1% of the total land surface. The highest number of re-burns in terms of total area occurred in Idaho (16,703 km^2) and California (16,418 km^2), while the lowest number of re-burns in terms of total area occurred in Wyoming (1,840 km^2). The highest density of re-burns occurred in Idaho, where they comprised 7.7% of the total land surface, while the lowest density occurred in Montana, where they comprised only 0.6% of the total land surface.

Trends in re-burns for the 11 western US states over the 5-, 10- and 20-year moving windows are shown in Figure 2. Results indicate that when the longer 20-year moving windows are considered, trends tend to be stronger within the WUI where 7 of the 11 states had stronger trends indicated by the magnitude of the tau statistic. When the shorter 5-year and 10-year moving windows were considered, only 5 and 2 of the 11 states had stronger trends within the WUI, respectively. Trends were also more likely to be statistically significant ($p < 0.05$) over the longer 20-year moving windows, particularly in the WUI where 7 of the 11 states fell into this category. When shorter moving windows were considered, only 3 (5-year) and 2 (10-year) of the 11 states had statistically significant trends within the WUI. In both of these shorter time periods, there was a greater number of statistically significant trends that occurred when the analysis was conducted over the entire state than within the WUI. Decreasing trends only occurred within the WUI, which was true for 3 to 5 of the 11 states, depending on which moving window period was considered. However, the decreasing trends were only statistically significant for New Mexico over the 5-year period. California was the only state where trends were consistently stronger within the WUI for all three moving window periods that were considered, although none of these trends were statistically significant. Idaho was the only state that had decreasing trends of re-burns within the WUI for all three moving window periods, despite having the highest surface area and density of re-burns out of the 11 western states.

The extracted signals of the NMFk algorithm over the entire climate and re-burn dataset are shown over California in Figure 3. The top model weights for each signal are shown in Table 2. Here, larger parameter weights within a signal indicates that that parameter is important to constructing the signal (or pattern) identified by the NMFk algorithm. Spatially, a larger signal weight for a particular grid-cell indicates that that area is highly associated with the pattern

within the input data that is comprised of the input parameters that make up that signal. The optimal number of signals, as determined by the robustness measure of NMFk solutions, is six. Re-burns are represented in the model by the mtbs_weight feature. Of the optimal six signals that were identified, signal 2 is most associated with the re-burn perimeters, given that it was the only signal where mtbs_weights (e.g., re-burns) were included as one of the top features in Table 2 and had a normalized weight of 0.80. In addition, the spatial distribution of signal 2 was largely co-located with the MTBS re-burns (Figure 3), which was highest along the California coastal mountain and Sierra Nevada foothills regions. Signal 2 is most prominently associated with high evapotranspiration in May-July and moderately associated with high maximum January soil moisture. Re-burns were not determined to be one of the top features for all other signals, as listed in Table 2. Signal 1 is associated with both standard deviation in temperature and summer canopy moisture and is most prevalent in northeastern California. Signal 3 is associated with high wind speed, particularly in September and February-May, and is most prevalent in coastal California. Signal 4 is associated with high maximum temperature and is most prevalent in the California Central Valley and in the more arid desert regions of southern California. Signal 5 is associated with high minimum temperatures especially during the non-summer seasons. Signal 5 is most prevalent in the Central Valley, Southern California, and in coastal areas. Finally, signal 6 is associated with high evapotranspiration in July-September and is most prevalent in the high elevation areas of California.

The extracted signals of the NMFk algorithm for only the re-burned areas of California are shown in Figure 4. The top model weights for each signal are shown in Table 3. The optimal number of signals, as determined by the robustness measure of NMFk solutions, is six. Signal 1 is associated with high wind speed especially during the Spring and is most prevalent in coastal

areas of Southern California. Signal 2, which is primarily prevalent in mountainous areas of northwest California and the Sierra Nevada Mountains, is associated with high evapotranspiration in July-September and with the standard deviation of March SWE. Signal 3 is associated with high maximum and standard deviation in winter temperature and is strongest among re-burns located in southern California and in the foothills to the west of the Central Valley. Signal 4 is associated with high evapotranspiration in April-July and with high standard deviation in January soil moisture. Signal 4 is most prevalent among areas of the central California coast and in some areas of the foothills of the Cascades in northern California. Signal 5 is strongest only in mountainous regions of northwest California and is associated with high standard deviations in winter wind speed and with generally high annual wind speed values. Signal 6 is associated with high Summer SWE and runoff and is prevalent among re-burns in the higher elevation mountainous regions throughout California.

The results of the RF classifier model are shown in Figure 5, which shows the predicted and observed re-burns for the state of California, as well as the standard error for these predictions. The final RF model hyperparameters were determined to be 1000 estimators, a max depth of 7, a minimum samples split of 5, and a minimum samples leaf of 2. The model was able to achieve a testing F1 score of 0.596, although some overfitting did occur (training F1 score = 0.695). It is evident that the model over-predicted the size of re-burn perimeters, particularly along the southern and central coasts of California. However, we would not expect the model to capture the exact outlines of re-burn areas as the true perimeter could be related to factors extraneous to our input data such as vegetation cover, fire management, and the presence of natural or constructed fire-breaks.

The results of the RF classifier model are broken down by US EPA Level III Ecoregions in Table 4. The model performs poorly in some areas where re-burns are sparse, which is denoted by lower precision scores (e.g., <0.6) and are indicative of a high number of false positives relative to the total number of re-burns. These regions include the Coast Range and Cascades (no predicted re-burns), which had the third and fourth fewest re-burn pixels of the regions represented. However, the model does perform best in other areas where re-burns are less frequent, such as the Sonoran and Central Basin and Range Ecoregions, which had the fewest number of re-burn pixels of the regions represented. The model performs well (accuracy 0.87-0.92) in the Klamath Mountains, Central California Foothills, and Sierra Nevada, where re-burns are well-represented (precision score >0.6). In the Southern California Mountains and Southern California/Baja Coast where we see the highest percentage of reburns (34-43%), the precision score is low indicating many false positives and the recall score is high indicating a small number of false negatives. The maps provided in Figure 5 indicate that this is likely because the model is over-predicting re-burns in these areas. Again, the model has the skill to know that re-burns are occurring in this area, but the climate data alone does not appear to be sufficient to accurately represent the extent of the re-burn areas.

Discussion

Our findings related to the spatial variability of re-burn occurrence and trends are supported by several recent studies. For instance, the higher re-burn occurrence and/or densities observed within California and Idaho corroborate with the US EPA Level III Ecoregions that were identified as having higher re-burn percentages (Buma et al., 2020). Of the eight Level III Ecoregions with elevated re-burn percentages (e.g., >7%), five were at least partially located in

California or Idaho (Sierra Nevada = 7.7%, Central California Foothills and Coastal Mountains =13.2%, Idaho Batholith = 8.1%, Klamath Mountains =11.4%, and Sonoran Basin and Range = 16.7%). The consistently stronger increasing trends of re-burns that were found in the WUI only within California are perhaps related to the higher occurrence of human-caused wildfires within that state (85%). Contrastingly, in Idaho where the density of re-burns was still high, only decreasing trends were observed within the WUI possibly due to the lower incidence of human-caused wildfires (31%). This is supported by the discovery that the strongest increasing trends in lightning caused wildfires to have been detected in the North American Desert Ecoregion, which comprises a large portion of Idaho (Balch et al., 2017). In addition, the decreasing trends that occurred within the WUI in Idaho and elsewhere are perhaps related to the stronger fire suppression efforts that are more likely to take place there to protect critical infrastructure than in more remote locations. Fire suppression expenditures are reported to have increased by 250% from 2000-2013 relative to 1985-1999 and a main reason for this increase was the expansion of residential development within the WUI (Clark et al., 2016). The finding of more robust trends overall, particularly within the WUI, when the longer 20-year moving window is considered is supported by the lack of fuels following a burn that will decrease the likelihood of re-burns over shorter intervals (Buma et al., 2020). The protection against wildfire in the years following a burn due to the fuels limitation is reported to be particularly notable in the first 10-years after a wildfire (Hart et al., 2018).

Differences in regional climate and associated impacts on the fuels limitation have been identified as an important driver in the frequency of re-burns. For example, in the warm and dry climate of the southwestern US where the likelihood of wildfire re-burns is lower due to fuel limitations, the occurrence of re-burns has been strongly linked to periods of elevated moisture

that can boost fuel loads. Forests within these climate zones have been observed to have a short fire return interval of 9-15 years (Parks et al., 2016; Parks et al., 2018), perhaps because once the vegetation has regenerated following a wildfire, the persistence of elevated moisture over some time period can increase fuel loads above some tipping point that is necessary to carry fire. However, in cooler and more moist climates like the northwestern US where the likelihood of wildfire re-burns lower due to moisture limitations, decreases in moisture (e.g., droughts) will increase the probability of re-burns (Buma et al., 2020). Forests within these climates have been observed to have longer fire return intervals of 20-33 years (Parks et al., 2016; Parks et al., 2018) indicating that the moisture limitations to re-burns in these climate zones are generally stronger than the fuel limitations to re-burns in hot and dry climate zones.

Using NMFk for the analysis over all of California, we were able to derive which climate data is associated with a re-burn signal across all of the re-burned areas in California. ET was found to be a major driver of re-burns across all of California, especially in the late-Spring to early-Summer months. This was evident in signal 2 (Table 2), which was the only signal with a strong relationship to the occurrence of re-burns. Next, using only the re-burned areas of the state as inputs to the NMFk algorithm, we were able to disaggregate the re-burned areas to determine how climatic drivers differ spatially within re-burn areas of California. The NMFk results from only the areas of re-burn show that elevated ET in both the Summer and late Spring months comprise the bulk of the features in signals 2 and 4 (Table 3), respectively. The strong relationship between reburns and Spring and Summer ET highlights the importance of antecedent moisture conditions on re-burns given that wildfires typically occur later in the year in California (Swain, 2021). We also see strong signals associated with re-burn behavior based on raw wind speed, wind speed variability and seasonal wind speed. This is shown in signal 5 of

Figure 3, which is associated with re-burns located in northern California as well as signal 1 of Figure 3, which is associated with re-burns located in southern California. The strong signals associated with wind from these regions may be due to the Diablo and Santa Ana wind events, which are both strongly associated with wildfires (Smith et al., 2018). Both signal 1 and signal 5 share many of the same wind features. Signal 5, however, is more concerned with high variability in wind speed, while the top contributor of signal 1 is the raw wind speed indicating both are important features for re-burns. The wind speed standard deviation may be linked to the onset of these events, given that their presence is likely to increase the variability of wind speed in the season they occur. NMFk clearly shows that Fall and Winter minimum temperatures are also heavily associated with re-burns in signal 3, which covers re-burns in both northern and southern California, indicating that the high minimum temperatures brought on by the winds are also important. Snow and hydrology are also important for re-burns in high elevation areas, as evidenced by signal 6. These variables tended to be associated with the Summer and Fall months, which coincide with the peak fire season and underscores the importance of fuel moisture conditions.

The results of the RF classification model show some skill in predicting the general regions where re-burns are most prevalent for the entire study period from 1984 to 2018. However, the model overpredicts re-burn perimeters particularly in southern California likely due to the lack of representation of key features related to vegetation and fire management that are important drivers of reburns. Even still, because the model is proficient at identifying the general regions most impacted by re-burns (e.g., Southern and Central California Coast, Sierra Nevada Foothills and Northwest Mountains), the skill at properly identifying the general areas where re-burns occur based on climate data alone shows promise for future applications within a model. This

could include understanding how re-burn areas might expand or contract based on future climate change, which could have implications for changes in forest management practices to receive more regular fuel treatments.

As alluded to in the previous paragraph, several potentially important features were omitted from our ML model approaches at predicting re-burns in order to focus our predictors on climate. For example, vegetation characteristics such as composition and structure were shown to be important controls on re-burns at the local or Ecoregion scales (Coppoletta et al., 2016; Grabinski et al., 2017) Moreover, the productivity of fine fuels was found to be important at larger, more regional scales (Buma et al., 2020). Another important feature missing from the current study is the ability to test how human activity may drive re-burn occurrence within the existing ML model framework. Although this is tested through the trend analysis, doing so within our ML model approach would require estimates of WUI through time at a temporal resolution that was comparable to the climate drivers. To the best of our knowledge, this data was not available at the time of writing this manuscript. However, this information could be derived directly through analysis of optical imagery (e.g. Landsat or the Moderate Resolution Imaging Spectroradiometer [MODIS]) and/or approximated by evaluating changes in population growth from census data within the WUI. Both approaches were beyond the scope of this study, but could lay the foundation for future research on this topic.

Conclusion

The trend analysis of re-burn occurrence demonstrated that the strength of trends is generally higher within the WUI than outside this region particularly when trends were considered over longer time intervals (e.g., 20-years) due to the fuel limitation for shorter fire return intervals

(e.g., <10-years). California was the only state where fuel limitations were consistently stronger within the WUI over all time periods, possibly due to the much higher incidence of human-caused wildfires relative to other states. The applied unsupervised machine learning algorithm (NMFk) was able to highlight several important climatic features that are most strongly related to the occurrence of re-burns across a large area such as California. These include temperature, particularly during the Fall and Winter months, ET during the Spring and Summer months, raw and standard deviation of wind speed, as well as runoff and snow water equivalent (SWE) particularly during the peak fire season. The Random Forest classification model offered some skill at predicting general locations of re-burns based on climate data alone, although struggled with some false positives likely due to the lack of some important features related to vegetation or topography that were not incorporated into the model.

The results from this study have implications for the prioritization of fuel treatments such as thinning or prescribed burns by forest managers (Halofsky et al., 2020). Knowledge on the immunity of a landscape to fire can help managers determine the frequency of retreatments following fuel treatments. This is particularly important for areas treated with prescribed burns, which offer mixed results in effectiveness where mitigation in burn severity can range anywhere from 2- to 30-years post treatment (Prichard et al., 2017). Moreover, burn severities in re-burns have been found to not necessarily be lower, but generally reflective of the initial fire. These findings coupled with the results of this study suggest that prioritization of more regular treatment within the WUI of California than other states could be more effective in avoiding losses in structures or lives given the higher incidence of re-burns overall (Figure 1) and consistently stronger increasing trends in re-burns found in these locations than elsewhere in the state (Figure 2). Specific areas within the WUI to target could include those areas where seasonal

wind speed and evapotranspiration rates were shown to be strongly related to the occurrence of re-burns (Figures 3-4 and Table 4), as well as those areas that were shown to have generally higher re-burn densities according to the observations (Figure 1) and model (Figure 4). Future work could involve identifying areas of higher risk using this data, running the model using projected climate data to understand changes, the use of vegetation and topographic data to improve existing models, and testing separate ML models over the individual ecoregions to refine model predictions at a smaller scale that could be used as a supplement to the larger model.

Acknowledgements

Support for this research was made possible by a Los Alamos National Laboratory Information Science & Technology Institute (ISTI) FY21 research grant (XX8R00 RR2133KS). We would like to thank the US Geological Survey (USGS) and Environmental Protection Agency (EPA) for their continued support and updates to the MTBS and Level III Ecoregions data, respectively, which were both utilized in this research. The Livneh et al. (2013) climate dataset that was used in this study is available here (https://psl.noaa.gov/data/gridded/data.livneh.html). The Multivariate Adaptive Construct Analogs Dataset is available at https://climate.northwestknowledge.net/MACA/. NMFk is an open-source code and a part of the SmartTensors ML/AI framework (http://SmartTensors.com)

References

Abatzoglou, J.T., and Brown, T.J., 2012, A comparison of statistical downscaling methods suited for wildfire applications, Int. J. Clim., 32, 772-780.

Abatzoglou, J.T., and Kolden, C.A., 2013, Relationships between climate and macroscale area burned in the western United States, Int. J. Wildland Fire, 22, 1003-1020.

Alexandrov, B.S., and Vesselinov, V.V., 2014, Blind source separation for groundwater pressure analysis based on nonnegative matrix factorization, Water Resour. Res., 50, 7332-7347.

Balch, J.K., Bradley, B.A., Abatzoglou, J.T., Nagy, R.C., Fusco, E.J., Mahood, A.L., 2017, Proc. Nat. Acad. Sci., 114, 2946-2951, DOI: 10.1073/pnas.1617394114

Bowman, D.M., Murphy B.P., Neyland, D.L., Williamson, G.J. and Prior, L.D., 2014, Abrupt fire regime change may cause landscape-wide loss of mature obligate seeder forests Glob. Change Biol., 20, 1008–15.

Buma, B., Brown, C., Donato, D., Fontaine, J. and Johnstone, J., 2013, The impacts of changing disturbance regimes on serotinous plant populations and communities, Bioscience, 63, 866–76.

Buma, B., Weiss, S., Hayes, K., and Lucash, M., 2020, Wildland fire reburning trends across the US West suggest only short-term negative feedback and differing climatic effects, Environ. Res. Lett., 15, 034026.

Clark, A.M., and Coauthors, 2016, "The Impact of Residential Development Pattern on Wildland Fire Suppression Expenditures." Land Economics, vol. 92 no. 4, 2016, p. 656-678. Project MUSE muse.jhu.edu/article/631931.

Coppoletta, M., Merriam, K.E., and Collins, B.M., 2016, Post-fire vegetation and fuel development influences fire severity patterns in reburns, Ecol. Appl., 26, 686–99.

Enright, N.J., Fontaine J.B., Bowman, D.M., Bradstock, R.A., and Williams, R.J., 2015, Interval squeeze: altered fire regimes and demographic responses interact to threaten woody species persistence as climate changes, Front. Ecol. Environ. 13, 265–72.

Fairman, T.A., Bennett, L.T., and Nitschke, C.R., 2019, Short-interval wildfires increase likelihood of resprouting failure in fire tolerant trees, J. Environ. Manage., 231, 59–65.

Grabinski, Z.S., Sherriff, R.L., and Kane, J.M., 2017, Controls of reburn severity vary with fire interval in the Klamath Mountains, California, USA, Ecosphere, 8, e02012.

Halofsky, J.E., Peterson, D.L., and Harvey, B.J., 2020, Changing wildfire, changing forests: the effects of climate change on fire regimes and vegetation in the Pacific Northwest, USA. Fire ecol 16, 4, https://doi.org/10.1186/s42408-019-0062-8

Hamed, K.H., and Rao, A.R., 1998, A modified Mann-Kendall trend test for autocorrelated data, J. Hydrol, 204, 182-196.

Hart, S.J., Henkelman, J., McLoughlin, P.D., Nielsen S.E., Truchon-Savard, A., and Johnstone, J.F., 2019, Examining forest resilience to changing fire frequency in a fire-prone region of boreal forest, Glob. Change Biol., 25, 869–84.

Kendall, M. G. (1975). Rank Correlation Methods. New York, NY: Oxford University Press.

Kolden, C.A., and Weisberg, P.J., 2007, Assessing accuracy of manually-mapped wildfire perimeters in topographically dissected areas. Fire Ecol., 3, 22–31, https://doi.org/10.4996/fireecology.0301022.

Little, J.S., McKenzie, D., Peterson, D.L., and Westerling, A.L., 2009, Climate and wildfire area burned in western U.S. ecoprovinces, 1916-2003, Ecol. Appl., 19, 1003-1021.

Livneh, B., Rosenberg, E.A., Lin, C., Nijssen, B., Mishra, V., Andreadis, K.M., Maurer, E.P., and Lettenmaier, D.P., 2013: A Long-Term Hydrologically Based Dataset of Land Surface Fluxes and States for the Conterminous United States: Update and Extensions, J. Clim., 26, 9384–9392.

Lydersen, J.M., Collins, B.M., Coppoletta, M. et al., 2019, Fuel dynamics and reburn severity following high-severity fire in a Sierra Nevada, USA, mixed-conifer forest. Fire Ecol, 15, 43, https://doi.org/10.1186/s42408-019-0060-x

Mann, H. B.,1945, Nonparametric tests against trend. Econometrica, 13, 245–259. Doi: 10.2307/1907187

Maurer, E.P., Wood, A.W., Adam, J.C., Lettenmaier, D.P., and Nijssen, B., 2002: A long-term hydrologically based dataset of land surface fluxes and states for the conterminous United States, J. Clim. ,15, 3237–3251.

Parks, S.A., Miller, C., Holsinger, L.M., Baggett, L.S., and Bird, B.J., 2016, Wildland fire limits subsequent fire occurrence, Int. J. Wildland Fire, 25, 182–90.

Parks S.A., Parisien, M.A., Miller, C., Holsinger, L.M., and Baggett, L.S., 2018, Fine-scale spatial climate variation and drought mediate the likelihood of reburning, Ecol. Appl., 28, 573–86.

Paritsis, J., Veblen, T.T., and Holz, A., 2015 Positive fire feedbacks contribute to shifts from Nothofagus pumilio forests to fireprone shrublands in Patagonia, J. Vegetation Sci., 26, 89–101.

Picotte, J.J., and Robertson, K.M., 2010, Accuracy of remote sensing wildland fire burned area in southeastern U.S. Coastal Plain habitats, In Proceedings of the 24th Tall Timbers Fire Ecology Conference: The Future of Prescribed Fire: Public Awareness, Health, and Safety, ed. K.M. Robertson, K.E.M. Galley, and R.E. Masters, 86–93. Tallahassee: Tall Timbers Research Station.

Picotte, J.J., Bhattarai, K., Howard, D. and Coauthors, 2020, Changes to the Monitoring Trends in Burn Severity program mapping production procedures and data products. Fire Ecol., 16, 16, https://doi.org/10.1186/s42408-020-00076-y

Prichard, S. J., Stevens-Rumann, C.S., and Hessburg, P.F., 2017, Tamm review: shifting global fire regimes: lessons from reburns and research needs, For. Ecol. Manage., 396, 217-233.

Radeloff, V.C., and Coauthors, 2018, Rapid growth of the US wildland-urban interface raises wildfire risk, Proc. Nat. Acad. Sci., 115, 3314-3319; DOI: 10.1073/pnas.1718850115

Smith, C., Hatchett, B.J., and Kaplan, M., 2018, A surface observation based climatology of Diablo-like winds in California's Wine Country and Western Sierra Nevada, Fire, https://doi.org/10.3390/fire1020025.

Stevens-Rumann, C.S., and Morgan, P., 2019, Tree regeneration following wildfires in the western US: a review, Fire Ecol. 15, 15.

Swain, D.L., 2021, A shorter, sharper rainy season amplifies California wildfire risk, Geophys. Res. Lett., 48, https://doi.org/1029/2021GL092843.

Taylor, K. E., Stouffer, R. J., and Meehl, G. A. (2012). An overview of CMIP5 and the experiment design. *Bull. Am. Meteorol. Soc.* 93. doi: 10.1175/BAMS-D-11-00094.1.

Turner, M.G., Braziunas, K.H., Hansen, W.D., and Harvey, B.J., 2019, Short-interval severe fire erodes the resilience of subalpine lodgepole pine forests, Proc. Natl Acad. Sci., 116, 11319–28.

Vanderhoof, M.K., Fairaux, N., Beal, Y.-J.G., and Hawbaker, T.J., 2017, Validation of the USGS Landsat burned area essential climate variable (BAECV) across the conterminous United States. Rem. Sens. Environ., 198, 393–406, https://doi.org/10.1016/j.rse.2017.06.025.

Williams, A.P., and Coauthors, 2019, Observed impacts of anthropogenic climate change on wildfire in California, Earth's Future, 7, 892-910.

Zhou, T., Chen, X., Dong, L., Wu, B., Man, W., Zhang, L., et al. (2014). Chinese contribution to CMIP5: An overview of five Chinese models' performances. *J. Meteorol. Res.* 28. doi: 10.1007/s13351-014-4001-y.

Figures

Figure 1: 1984-2018 wildfire re-burn perimeters derived from the MTBS data for the 11 western US states. States are shaded according to a) total re-burn area and b) percent land area coverage that occurred within state boundaries.

Figure 2: Mann-Kendall tau statistic for trend analysis of re-burns for 11 western US states using a) 5-year, b) 10-year and c) 20-year moving windows. Trends are shown for all re-burns that occurred within each state (blue bars) and only re-burns that occurred within the WUI (orange bars).

Figure 3: NMFk output signals at the optimal six signals using the climate dataset over California. The first six panels show the individual signals output from NMFk, while the final panel shows the calculated fraction of the spatial cell that has re-burned.

Figure 4: NMFk output signals at the optimal six signals using the climate dataset for the calculated re-burned cells in California. The first six panels show the individual signals output from NMFk, while the final panel shows the calculated fraction of the spatial cell that has re-burned.

Figure 5: Observed MTBS Re-burns, predicted re-burns using a Random Forest Classification model, and the absolute error in model performance for the entire state of California. F1, sensitivity, and precision score are provided.

Tables

Table 1: Summary information for the climate drivers that were used in this study.

Table 2: The top nine features for each of the six NMFk outpus signals and their corresponding normalized weight for each signal over the entire state of California. The signals correspond to the signals shown in Figure 2.

Table 3: The top nine features for each of the six NMFk outpus signals and their corresponding weight for each signal using only the re-burned cells. The signals in correspond to the signals shown in Figure 3.

Table 4: Results statistics for the Random Forest classifier across the entire domain and for each US EPA Level III Ecoregion. Also included are the number of cells, number of burned cells and percent area burned within each ecoregion.

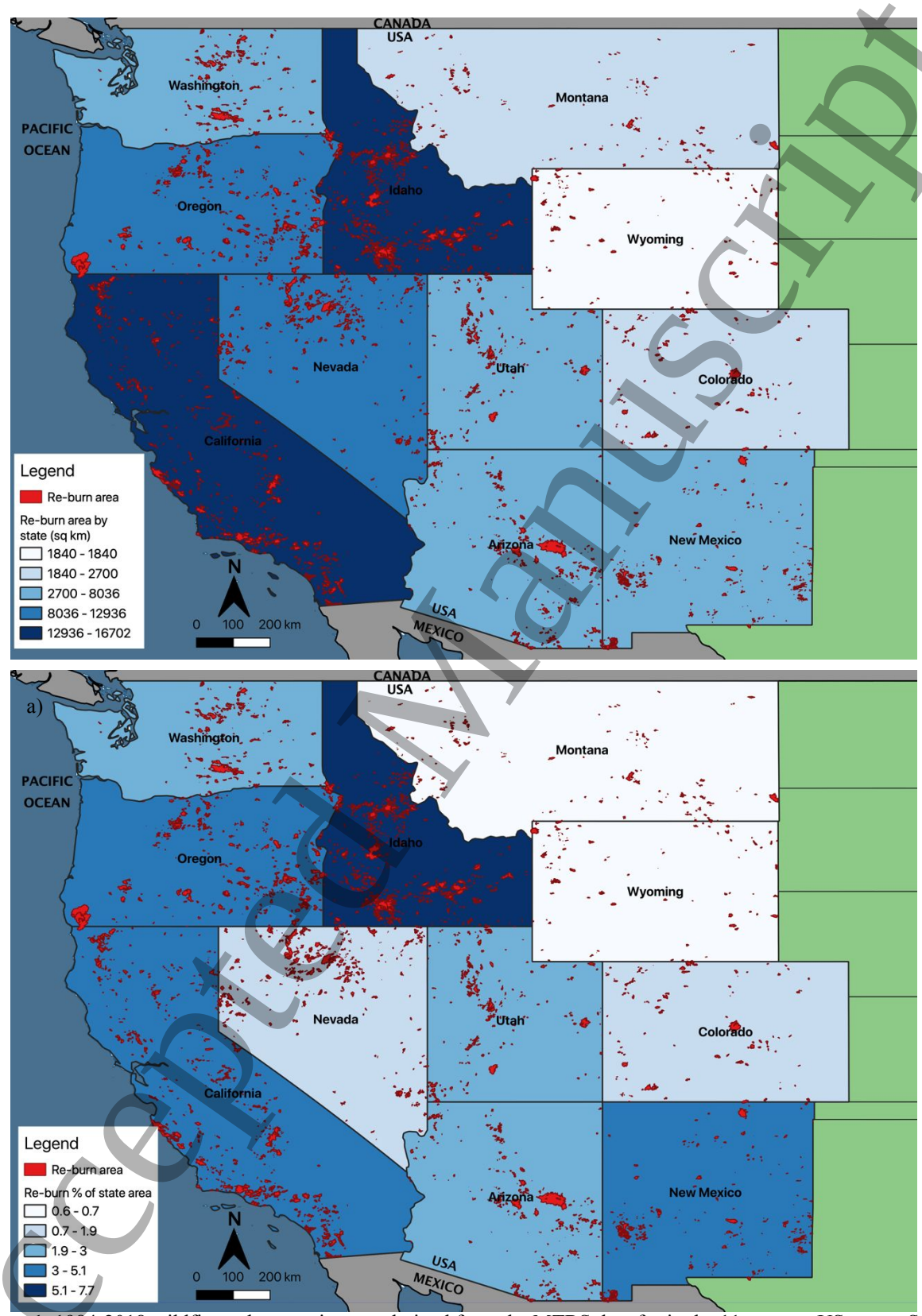

Figure 1: 1984-2018 wildfire re-burn perimeters derived from the MTBS data for in the 11 western US states. States are shaded according to a) total re-burn area and b) percent land area coverage that occurred within state boundaries.

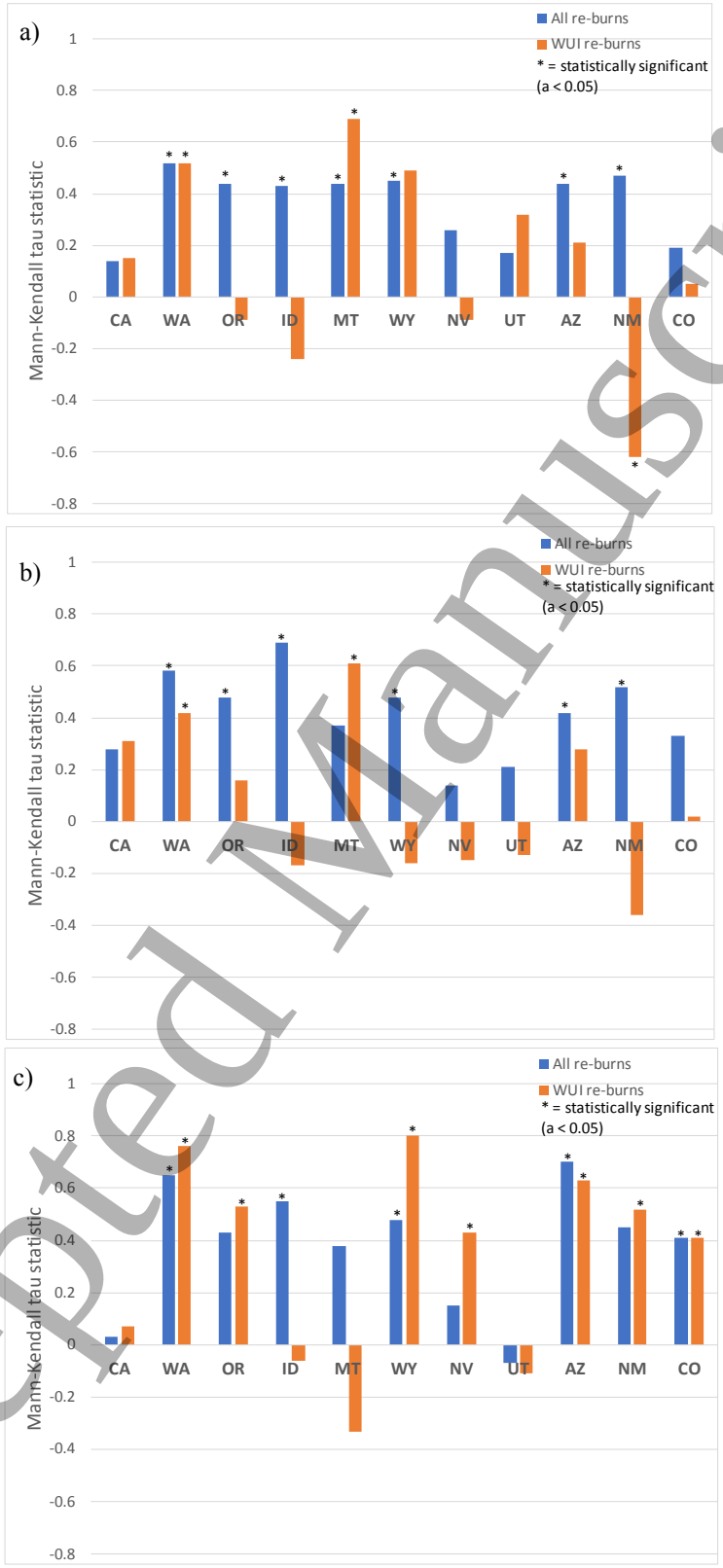

Figure 2: Mann-Kendall tau statistic for trend analysis of re-burns for 11 western US states using a) 5-year, b) 10-year and c) 20-year moving windows. Trends are shown for all re-burns that occurred within each state (blue bars) and only re-burns that occurred within the WUI (orange bars).

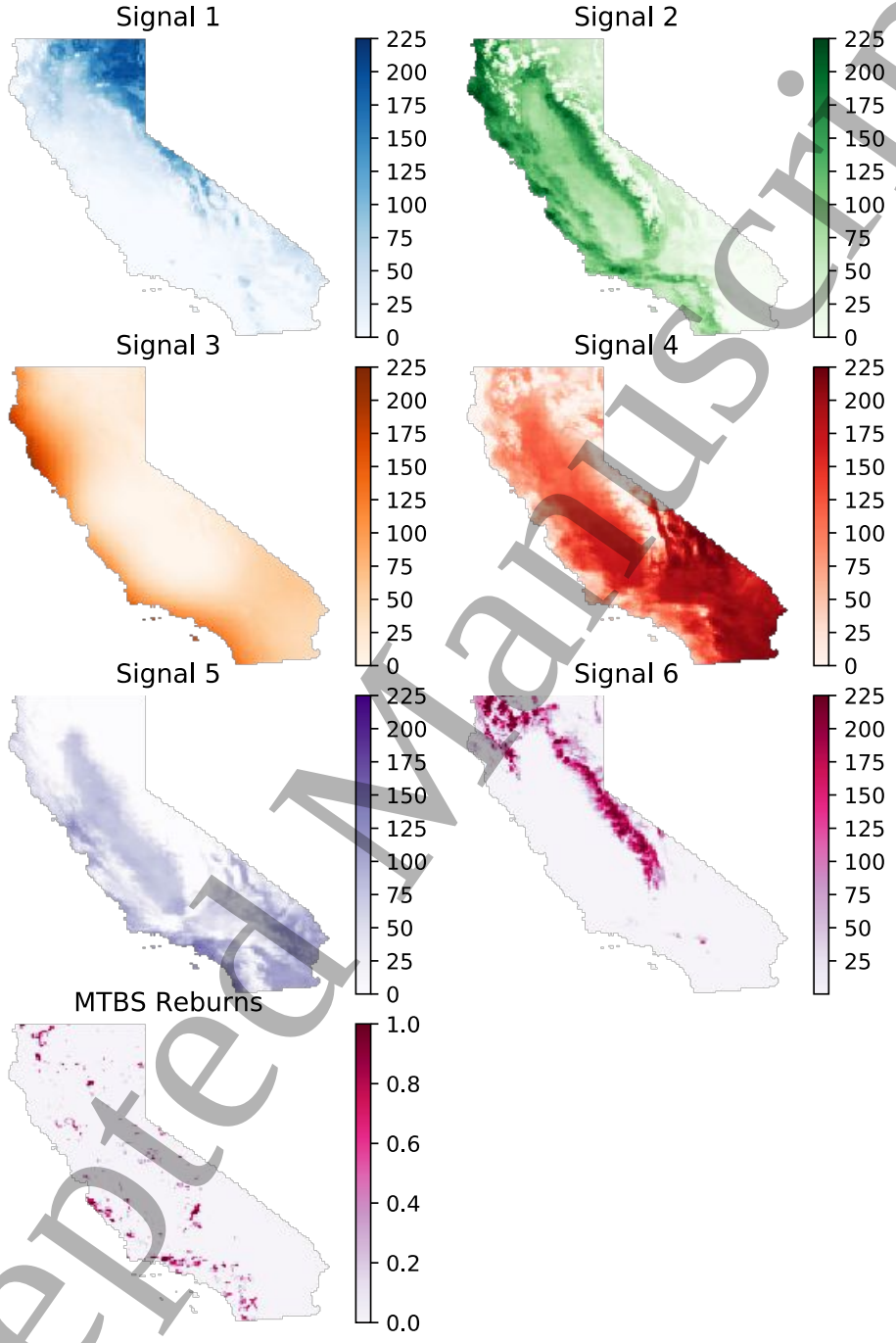

Figure 3: NMFk output signals at the optimal six signals using the climate dataset over California. The first six panels show the individual signals output from NMFk, while the final panel shows the calculated fraction of the spatial cell that has re-burned.

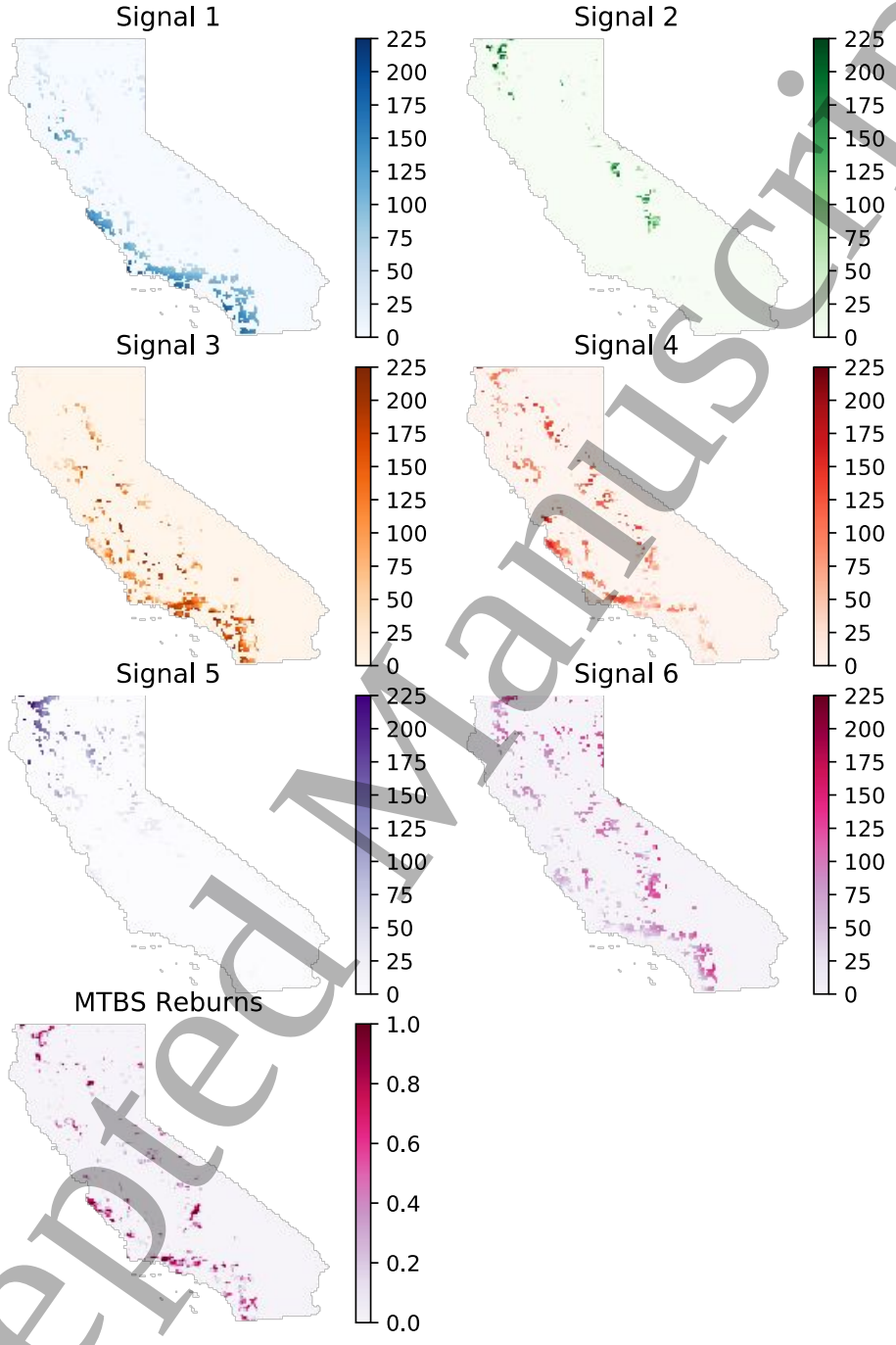

Figure 4: NMFk output signals at the optimal six signals using the climate dataset for the calculated re-burned cells in California. The first six panels show the individual signals output from NMFk, while the final panel shows the calculated fraction of the spatial cell that has re-burned.

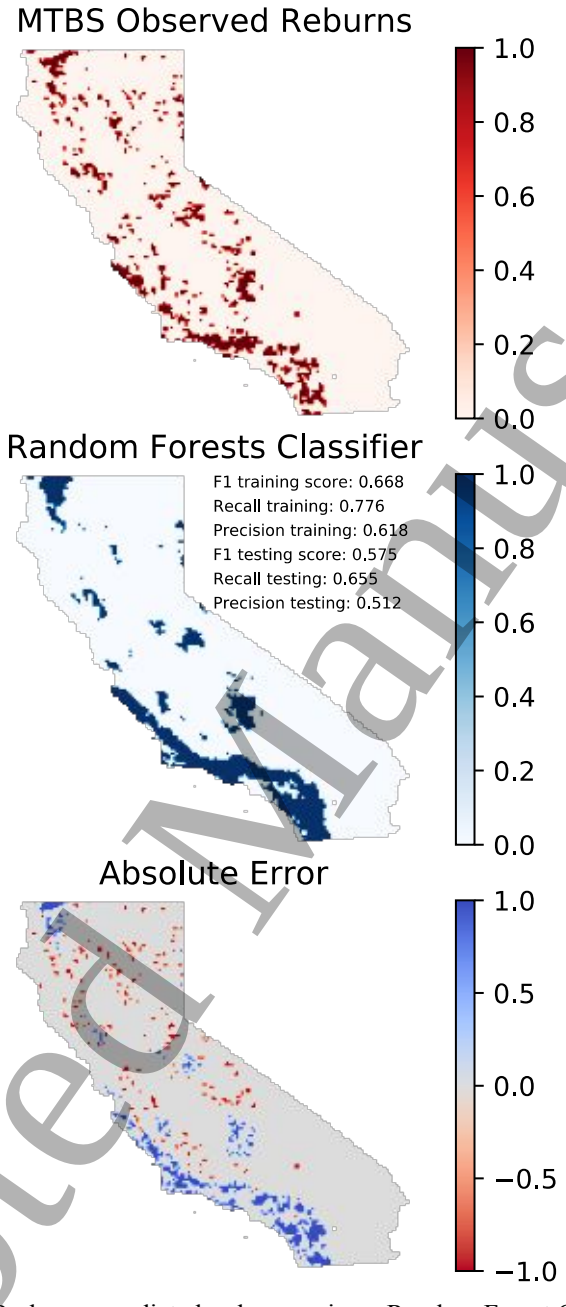

Figure 5: Observed MTBS Re-burns, predicted re-burns using a Random Forest Classification model, and the absolute error in model performance for the entire state of California. F1, sensitivity, and precision score are provided.

Table 1: Summary information for the climate drivers that were used in this study.

Variable	Temporal Range (Frequency)	Native Spatial Resolution	Source
Reburn Weights	1984-2018 (composite)	>405 ha	Monitoring trends in burn severity (MTBS)
Canopy Moisture	1950-2013 (monthly)	1/16º	Livneh et al., 2013 CONUS near-surface derived meteorology
Soil Moisture	1950-2013 (monthly)	1/16º	Livneh et al., 2013 CONUS near-surface derived meteorology
Precipitation	1950-2013 (monthly)	1/16º	Livneh et al., 2013 CONUS near-surface derived meteorology
Runoff	1950-2013 (monthly)	1/16º	Livneh et al., 2013 CONUS near-surface derived meteorology
Snow Water Equivalent	1950-2013 (monthly)	1/16º	Livneh et al., 2013 CONUS near-surface derived meteorology
Temperature (max)	1950-2013 (monthly)	1/16º	Livneh et al., 2013 CONUS near-surface derived meteorology
Temperature (min)	1950-2013 (monthly)	1/16º	Livneh et al., 2013 CONUS near-surface derived meteorology
Total Evapotranspiration	1950-2013 (monthly)	1/16º	Livneh et al., 2013 CONUS near-surface derived meteorology
Wind Speed	1950-2013 (monthly)	1/16º	Livneh et al., 2013 CONUS near-surface derived meteorology
Precipitation	1950-2020 (annual)	4 km	Abatzoglou and Brown, 2012 MACA downscaled global climate model
Temperature (min)	1950-2020 (annual)	4 km	Abatzoglou and Brown, 2012 MACA downscaled global climate model
Temperature (max)	1950-2020 (annual)	4 km	Abatzoglou and Brown, 2012 MACA downscaled global climate model
Wind Speed	1950-2020 (annual)	4 km	Abatzoglou and Brown, 2012 MACA downscaled global climate model

Table 2: The top nine features for each of the six NMFk outpus signals and their corresponding normalized weight for each signal over the entire state of California. The signals correspond to the signals shown in Figure 2. Abbreviations are defined in the table footer[a, b].

Signal 1		Signal 2		Signal 3		Signal 4		Signal 5		Signal 6	
Top Features	**Weights**	**Top Features**	**Weights**	**Top Features**	**Weights**	**Top Features**	**Weights**	**Top Features**	**Weights**	**Top Features**	**Weights**
Nov temp max std	1.00	May ET mean	1.00	Sep was 1st quartile	1.00	tmax 39	1.00	Feb temp min std	1.00	Jul ET 3rd quartile	1.00
Feb temp max std	0.91	May ET 1st quartile	0.94	wind 13	1.00	tmax 23	1.00	Mar temp min 3rd quartile	0.91	Jul ET mean	0.91
tmin std	0.88	May ET 3rd quartile	0.87	wind 65	0.97	tmax 4	0.99	Mar temp min max	0.86	Aug ET max	0.88
Jun canopy_moist std	0.87	Jun ET mean	0.87	Sep was mean	0.96	Jul temp max min	0.99	Oct temp min 1st quartile	0.86	Aug ET 3rd quartile	0.87
Sep canopy_moist max	0.86	ET mean	0.85	Mar was mean	0.96	tmax 51	0.99	Jan temp min std	0.85	Jul ET 1st quartile	0.86
May canopy_moist std	0.81	Jul ET max	0.82	Mar was 3rd quartile	0.96	tmax 71	0.99	Apr temp min 1st quartile	0.85	Jul ET max	0.81
Jun canopy_moist 3rd quartile	0.76	**mtbs_weights**	0.80	May was 1st quartile	0.95	tmax 31	0.98	Nov temp min max	0.85	Aug ET mean	0.76
Aug canopy_moist std	0.75	Jun ET 3rd quartile	0.78	Apr was 1st quartile	0.95	tmax 8	0.98	Oct temp min	0.85	Sep ET max	0.75
Jun canopy_moist mean	0.70	Jan soil_moist max	0.77	Feb was min	0.95	tmax 65	0.98	Jan temp max min	0.83	Sep ET 3rd quartile	0.70

[a] canopy_moist = Canopy Moisture; ET = Evapotranspiration; max = Maximum; min = Minimum; mtbs = Monitoring Trends in Burn Severity; soil_moist = Soil Moisture; std = Standard Deviation; tmax = Maximum Temperature; tmin = Minimum Temperature; was = Wind Speed

[b] tmax 51 = Maximum Temperature for the 51st year (e.g., 2000) of the time series from 1950 to 2020.

Table 3: The top nine features for each of the six NMFk outpus signals and their corresponding weight for each signal using only the re-burned cells. The signals in correspond to the signals shown in Figure 3. Abbreviations are defined in the table footer[a, b].

Signal 1		Signal 2		Signal 3		Signal 4		Signal 5		Signal 6	
Top Features	**Weights**	**Top Features**	**Weights**	**Top Features**	**Weights**	**Top Features**	**Weights**	**Top Features**	**Weights**	**Top Features**	**Weights**
wind 7	1.00	Jul ET 3rd quartile	1.00	Jan temp min std	1.00	Jun ET 3rd quartile	1.00	Nov was std	1.00	Oct SWE min	1.000
May was 1st quartile	0.96	Jul ET mean	0.90	Feb temp min std	0.92	May ET 1st quartile	0.94	wind std	0.98	Sep runoff min	1.000
wind 64	0.96	Jul ET max	0.83	Dec temp min std	0.91	May ET mean	0.88	wind 4	0.97	Jun SWE min	1.000
Apr was 1st quartile	0.94	Aug ET max	0.81	Feb temp min max	0.87	May ET 3rd quartile	0.88	Mar was std	0.96	Aug SWE 1st quartile	1.000
Apr was mean	0.94	Mar SWE std	0.81	Nov temp min max	0.85	Apr ET 1st quartile	0.84	Feb was std	0.94	Jul runoff min	1.000
Apr was 3rd quartile	0.94	Aug ET 3rd quartile	0.80	Nov temp min 3rd quartile	0.79	Jul ET max	0.79	wind 37	0.85	Sep SWE 1st quartile	1.000
wind 2	0.94	Jul ET 1st quartile	0.79	Mar temp min 3rd quartile	0.78	Jun ET mean	0.77	Dec was std	0.82	Jul SWE min	1.000
Mar was 1st quartile	0.93	Jun ET 3rd quartile	0.77	Feb temp min 3rd quartile	0.77	Apr ET min	0.75	wind 29	0.82	temp min	0.997
wind 15	0.93	Sep ET max	0.73	Dec temp min max	0.77	Jan soil_moist std	0.74	wind 68	0.82	Aug SWE min	0.997

[a] canopy_moist = Canopy Moisture; ET = Evapotranspiration; max = Maximum; min = Minimum; mtbs = Monitoring Trends in Burn Severity; std = Standard Deviation; SWE = Snow Water Equivalent; tmax = Maximum Temperature; tmin = Minimum Temperature; was = Wind Speed

[b] wind 64 = Wind Speed for the 64th year (e.g., 2013) of the time series from 1950 to 2020.

Table 4: Results statistics for the Random Forest classifier across the entire domain and for each US EPA Level III Ecoregion. Also included are the number of cells, number of burned cells and percent area burned within each ecoregion.

	Total	Coast Range	Central Basin and Range	Mojave Basin and Range	Cascades	Sierra Nevada	Central California Foothills and Coastal Mountains	Central California Valley	Klamath Mountains/ California High North Coast Range	Southern California Mountains	Northern Basin and Range		Southern California/ Northern Baja coast	Eastern Cascades Slopes and Foothills
F1 Score	0.660	0.308	0.703	0.615	0	0.671	0.673	0.435	0.653	0.675	0.778	0.71	0.694	0.261
Accuracy	0.916	0.977	0.967	0.992	0.945	0.92	0.873	0.979	0.883	0.584	0.963	0.987	0.698	0.965
Precision	0.592	0.286	0.929	0.571	0	0.729	0.619	0.833	0.616	0.513	0.875	0.55	0.535	1
Recall	0.747	0.333	0.565	0.667	0	0.621	0.736	0.294	0.695	0.983	0.7	1	0.988	0.15
N Burns	6	6	23	18	21	182	356	34	141	175	10	11	171	20
N Cells	10688	385	338	1905	383	1386	2011	1224	889	399	107	687	494	480
% Burn	0.06	1.56	6.80	0.94	5.48	13.13	17.70	2.78	15.86	43.86	9.35	1.60	34.62	4.17